Implication of capillary morphogenesis gene 2 (CMG2) in the disease progression and peritoneal metastasis of pancreatic cancer

By

Ziqian Fang

Cardiff China Medical Research Collaborative

School of Medicine, Cardiff University

Cardiff

September 2023

Supervisors: Dr Lin Ye, Professor Wen G. Jiang

Thesis submitted to Cardiff University for the degree of Doctor of Philosophy

Acknowledgements

This thesis shows the result of three years research during my PhD study. Many people helped me a lot during these years, I would like to express my heartfelt thanks to them. First of all, I would like to express my sincere gratitude to Dr Lin Ye, who is my supervisor. My supervisor gave me comprehensive and detailed guidance on the completion of my thesis, from the selection of the topic of the thesis, the formulation of the outline, and experiment technology to the completion of my thesis. With his help, I overcame a lot of difficulties during my scientific research.

I also want to express my sincere appreciation to my co-supervisor, Professor Wen G. Jiang. He is very kind and patient, who gave me a lot of support during my PhD study. Dr Jane and my teammate Yali Xu, helped me a lot during the PhD thesis proofreading. Mrs Fiona Ruge also helped me a lot in managing the working time during the Covid-19, and in maintaining a good and safe working area. Meanwhile, I would like to say thanks to all the other staff and students in CCMRC for their help to me during these 3 years. Including Dr Tracey A. Martin, Laijian Sui, Ming Liu, Jimmy Zeng, Hanson Gao, Yiming Yang, Wenxiao Ji, Xinguo Zhuang, Binbin Cong, Chuanliang Jia et.al.

My PhD study began during the Covid-19 pandemic and national lockdown, which really caused a lot of difficulties during my first year's research. However, under the support of COVID-19 officers of CCMRC, the School of Medicine and the University, I overcame these difficulties. The influence of it was limited to a minimum. I would like to express my sincere gratitude to my laboratories and supervisory team during this difficult period.

Full papers

1. Fang Z, Killick C, Halfpenny C, Frewer N, Frewer KA, Ruge F, Jiang WG, Ye L. Sex Hormone-regulated *CMG2* Is Involved in Breast and Prostate Cancer Progression. Cancer Genomics Proteomics. 2022 Nov-Dec;19(6):703-710. doi: 10.21873/cgp.20353. PMID: 36316045; PMCID: PMC9620450.

2. Fang Z, Zeng JJ, Yang Y, Ruge F, Lane J, Hargest R, Jiang WG. Expression of ALCAM in Clinical Colon Cancer and Relationship With Patients' Treatment Responses. In Vivo. 2023 May-Jun;37(3):1117-1128. doi: 10.21873/invivo.13187. PMID: 37103072; PMCID: PMC10188023.

3. Liu M, Sui L, Fang Z, Jiang WG, Ye L. Aberrant expression of bone morphogenetic proteins in the disease progression and metastasis of breast cancer. Front Oncol. 2023 Jun 2;13:1166955. doi: 10.3389/fonc.2023.1166955. PMID: 37333824; PMCID: PMC10272747.

Abstracts and conference presentations

1. Ziqian Fang, Paul Griffiths, Bilal Al-Sarireh, Wen G Jiang, Lin Ye, O1 Elevated expression level of capillary morphogenesis gene 2 in pancreatic ductal adenocarcinoma cell is associated with distant metastasis and poor prognosis, British Journal of Surgery, Volume 108, Issue Supplement_5, July 2021, znab282.006

2. Ziqian Fang, Jiang, W. and Ye, L. 2022. P-235 Elevated protein tyrosine phosphatase kappa expression is associated with disease progression and poor prognosis of pancreatic cancer. Annals of Oncology 33 (S4), S332-S332. 10.1016/j.annonc.2022.04.325

Summary

CMG2 (Capillary morphogenesis gene 2) has been implicated in certain cancers and tumour-associated angiogenesis. CMG2 acts as a tumour suppressor in endocrine-related cancers such as prostate cancer and breast cancer. In contrast, CMG2 can promote disease progression and distant metastasis in glioma and gastric cancer. The present study aimed to dissect the role of CMG2 in pancreatic cancer and disease-specific peritoneal metastasis.

CMG2 was found to be upregulated in pancreatic cancer tissues and associated with a poor prognosis. CMG2 was increased in metastatic lesions and those primary tumours which had distant metastases at the diagnosis of the disease. This suggests that CMG2 may promote the distant metastasis of pancreatic cancer. The influence of CMG2 on cellular functions was determined in pancreatic cancer cell lines, with CMG2 overexpression or knockdown. CMG2 promoted cell-matrix adhesion in PANC-1 and ASPC-1 cells, suggesting CMG2 can enhance cell-matrix adhesion. CMG2 enhanced cell aggregation of MiaPaCa-2 cells. CMG2 also facilitated adhesion of PANC-1 cells to mesothelial cells. CMG2-promoted adhesion of PANC-1 cells to mesothelial cells was partially blocked after treatment with soluble hyaluronic acid (HA). Furthermore, CMG2 promoted survival of disseminating pancreatic cancer cells, leading to evasion of *anoikis*. Proteomics analysis showed that the EGFR and focal adhesion pathways were activated in pancreatic cancer cells, with overexpression of CMG2. ICAM-1, VCAN and CD44 expression were also increased in pancreatic cancer cells with higher CMG2, which may be involved in CMG2 promoted cell-cell aggregation and cell-HA interaction.

In conclusion, CMG2 was upregulated in pancreatic cancer, which was associated with poor prognosis and distant metastasis. CMG2 promoted cell-matrix adhesion, cell-cell adhesion, cell HA interaction, viability and survival of suspended pancreatic cancer cells, may facilitate the dissemination of pancreatic cancer cells to the peritoneum, in which enhanced EGFR and FAK pathways were likely involved. Furthermore, the expression of integrins, tight junction proteins and HA interacting molecules were also enhanced by CMG2. Further study will shed light on the exact molecular mechanisms and therapeutic potential of targeting CMG2 in pancreatic cancer.

Contents

Chapter 1 General discussion

List of Figures

Chapter 1

Chapter 2

Chapter 3

Chapter 4

List of Tables

Aberrations

5-FU	Fluorouracil
ACC	Acinar cell carcinoma
ACTN1	Actinin Alpha 1
AFAP1L1	Actin Filament Associated Protein 1 Like 1
AFG3L2	AFG3 Like Matrix AAA Peptidase Subunit 2
AHNAK2	AHNAK Nucleoprotein 2
AJCC	American Joint Committee on Cancer
AKAP12	A-Kinase Anchoring Protein 12
AKT/PKB	Protein kinase B
AKT1	AKT Serine/Threonine Kinase 1
ALK	ALK Receptor Tyrosine Kinase
AMPK	5' adenosine monophosphate-activated protein kinase
APAF1	Apoptotic peptidase activating factor 1
ARAP3	ArfGAP With RhoGAP Domain, Ankyrin Repeat And PH Domain 3
ARHGEF11	Rho Guanine Nucleotide Exchange Factor 11
ARID1A	AT-rich interactive domain-containing protein 1A
ARID2	AT-rich interactive domain-containing protein 2
ARL4C	High ADP-ribosylation factor-like protein 4C
ARL4C	ADP-ribosylation factor-like protein 4C
ATM	Serine-protein kinase ATM
ATP	Adenosine triphosphate
BACH1	BTB and CNC homology 1
BACH1	BTB Domain And CNC Homolog 1
BAK	Bcl-2 homologous antagonist/killer
BASP1	Brain Abundant Membrane Attached Signal Protein 1
BAX	Bcl-2-associated X protein
Bcl-2	B-cell leukemia/lymphoma 2 protein
BCL2L1	BCL2 Like 1
BCL6	BCL6 Transcription Repressor
bFGF	basic fibroblast growth factor
BID	BH3 Interacting Domain Death Agonist
Bim	Bcl-2-like protein 11
Bmf	Bcl2 Modifying Factor

BRCA1	Breast Cancer gene 1
BRCA2	Breast cancer gene 2
CA19-9	Cancer Antigen 19-9
CA242	Cancer Antigen 242
CA50	Cancer Antigen 50
CA72-4	Cancer Antigen 72-4
CAFs	Cancer-associated fibroblasts
CALD1	Caldesmon 1
CAMK2D	Calcium/Calmodulin Dependent Protein Kinase II Delta
CANX	Calnexin
CARD	caspase recruitment domain
CAV1	Caveolin 1
CAVIN2	Caveolae Associated Protein 2
CCDC97	Coiled-Coil Domain Containing 97
CCL5	C-C chemokine ligand 5
CD109	CD109 Molecule
CD40	Cluster of differentiation 40
CD44	Cluster of differentiation 44
CDH4	Cadherin 4
CDHs	cadherins
CDK1	Cyclin Dependent Kinase 1
CDK5	Cyclin Dependent Kinase 5
CDKN3	Cyclin Dependent Kinase Inhibitor 3
CDKNA2A	cyclin-dependent kinase inhibitor 2A
CDX2	Caudal Type Homeobox 2
CEACAM1	CEA Cell Adhesion Molecule 1
CEP170B	Centrosomal Protein 170B
C-flip	Cellular FLICE-like Inhibitory Protein
CHM	CHM Rab Escort Protein
CKAP4	Cytoskeleton Associated Protein 4
CLDN1	claudin1
CLIP2	CAP-Gly Domain Containing Linker Protein 2
CLOCK	Clock Circadian Regulator
CMG2	Capillary morphogenesis gene 2

(ANTXR2)	
CREB	cAMP-response element binding protein
CSCs	cancer stem cells
CSF-1	colony stimulating factor 1
CSRP1	Cysteine And Glycine Rich Protein 1
CT	Computed Tomography Scan
CTLA4	cytotoxic T-lymphocyte–associated antigen 4
CTNNB1	β-catenin
CTSH	Cathepsin H
CTTN	Cortactin
CXCL12	C-X-C Motif Chemokine Ligand 12
CXCR4	C-X-C chemokine receptor type 4
DACH1	Dachshund Family Transcription Factor 1
DEPTOR	DEP Domain Containing MTOR Interacting Protein
DHX30	DExH-Box Helicase 30
DISC	disrupted in schizophrenia
DNAJB1	DnaJ Heat Shock Protein Family (Hsp40) Member B1
DOCK1	Dedicator Of Cytokinesis 1
DPC4	Deleted in Pancreatic Carcinoma Locus 4
(SMAD4)	
E2F1	E2F Transcription Factor 1
ECM	extracellular cellular matrix
EF	oedema factor
EGF	epidermal growth factor
EGFR	epidermal growth factor receptor
EIF4B	Eukaryotic Translation Initiation Factor 4B
ELAM1	Endothelial leukocyte adhesion molecule-1
EMT	Epithelial-mesenchymal transition
Enhanced	Abdominal Contrast Enhanced Ultrasound
USG	
EPC1	Enhancer of polycomb homolog 1
EPIC	early postoperative intraperitoneal chemotherapy
ERBB2	erythroblastic oncogene B2
ERCP	Endoscopic retrograde cholangiopancreatography

ERK	extracellular signal-regulated kinases
ESR1	Oestrogen Receptor 1
EUS	endoscopic ultrasonography
EUS-FNA	Endoscopic ultrasound guided fine needle aspiration biopsy
EZH2	Oestrogen Receptor 2
FAK	focal adhesion kinase
FAM83A	Family With Sequence Similarity 83 Member A
FAMMM	Familial Atypical Mole–Malignant Melanoma
FGF	Fibroblast growth factor
FHL3	Four And A Half LIM Domains 3
FLNB	Filamin B
FOLFIRINOX	FOL – folinic acid (also called leucovorin, calcium folinate or FA) F – fluorouracil (also called 5FU) Irin – irinotecan
FOSL1	FOS Like 1, AP-1 Transcription Factor Subunit
FOXO1	Forkhead Box O1
GAGs	glycosaminoglycans
GCSLCs	cancer stem-like cells
GIT1	GIT ArfGAP 1
GNAS	GNAS Complex Locus
GPD2	Glycerol-3-Phosphate Dehydrogenase 2
GPX1	Glutathione Peroxidase 1
HA	Hyaluronic acid
HADHA	Hydroxyacyl-CoA Dehydrogenase Trifunctional Multienzyme Complex Subunit Alpha
HAPLN	hyaluronan and proteoglycan link protein
HGF	Hepatocyte Growth Factor
HIF1α	heterodimeric transcription factor hypoxia-inducible factor 1
HIPEC	hyperthermic intraperitoneal chemotherapy
HMGB1	High mobility group box 1
HSP 70	Heat shock protein 70
HSP27	Heat shock protein 27
HSPA8	Heat Shock Protein Family A (Hsp70) Member 8
HSPH1	Heat Shock Protein Family H (Hsp110) Member 1
IAPs	Inhibitors of apoptosis proteins

ICAM-1	Intercellular Adhesion Molecule 1
ICK	Ciliogenesis Associated Kinase 1
IFP	interstitial fluid pressures
IGF	Insulin-like growth factor
IGFBP1	Insulin Like Growth Factor Binding Protein 1
IL-4	Interleukin 4
ILK	integrin-linked kinase
IMMT	Inner Membrane Mitochondrial Protein
IPMN	Intraductal papillary neoplasm
IQGAP1	IQ Motif Containing GTPase Activating Protein 1
ISH	infantile systemic hyalinosis
ITGA2	Integrin Subunit Alpha 2
ITGB3	Integrin Subunit Beta 3
ITPR2	Inositol 1,4,5-Trisphosphate Receptor Type 2
JAK	Janus tyrosine kinase
JHF	juvenile hyaline fibromatosis
JUN	Jun Proto-Oncogene, AP-1 Transcription Factor Subunit
KDM2B	Lysine Demethylase 2B
KIT	KIT Proto-Oncogene, Receptor Tyrosine Kinase
KLF5	KLF Transcription Factor 5
KRAS	Kirsten rat sarcoma viral oncogene homolog
KRT80	Keratin 80
LAD1	Ladinin 1
LAMP	Lysosomal-associated membrane protein 1
LEO1	LEO1 Homolog, Paf1/RNA Polymerase II Complex Component
LF	toxin lethal factor
LFA-1	lymphocyte function-associated antigen-1
LGR5	Leucine-rich repeat-containing G-protein coupled receptor 5
LIMCH1	LIM And Calponin Homology Domains 1
LKB1	liver kinase B1
LRP6	Low-density lipoprotein receptor-related protein 6
LYVE	Lymphatic Vessel Endothelial Hyaluronan Receptor 1
MAF	MAF BZIP Transcription Factor
MAGEA6	elanoma-associated antigen 6

MAP1B	Microtubule Associated Protein 1B
MAP3K2	Mitogen-Activated Protein Kinase Kinase Kinase 2
MAP3K7	Mitogen-Activated Protein Kinase Kinase Kinase 7
MCN	Mucinous cystic neoplasms
MEIS1	Meis Homeobox 1
MEK	Mitogen-activated protein kinase kinase
MET	Mesenchymal Epithelial Transition
MGMT	O-6-Methylguanine-DNA Methyltransferase
MIC-1	macrophage inhibitory cytokine 1
MICs	metastasis-initiating cells
MIF	Macrophage migration inhibitory factor
MISP	Mitotic Spindle Positioning
MKK4	Mitogen-activated protein kinase kinase 4
MLL3	mixed-lineage leukaemia protein 3
MMPs	matrix metalloproteinase
MMT	mesothelial-to-mesenchymal transition
MPHOSPH8	M-Phase Phosphoprotein 8
MRI	Magnetic resonance imaging
MSCs	mesenchymal stem cells
MSN	Moesin
MTDH	Metadherin
MYC	MYC Proto-Oncogene
MYH9	Myosin Heavy Chain 9
MYO1B	Myosin IB
MYO1C	Myosin IC
NADPH	nicotinamide adenine dinucleotide phosphate oxidase
NALCN	Sodium leak channel NALCN
NANOG	Nanog Homeobox
NASP	Nuclear Autoantigenic Sperm Protein
NCAM1	Neural Cell Adhesion Molecule 1
NCOR	Nuclear Receptor Corepressor 1
NF2	Neurofibromin 2
NFKB	Nuclear factor-κB
NFKB1	Nuclear Factor Kappa B Subunit 1

NIPS	neoadjuvant systemic and intraperitoneal chemotherapy
NNMT	Nicotinamide N-Methyltransferase
NOSIP	Nitric Oxide Synthase Interacting Protein
NOTCH	Neurogenic locus notch homolog protein 1
Noxa (PMAIP1)	Phorbol-12-myristate-13-acetate-induced protein 1
NRP2	Neuropilin 2
NSUN2	NOP2/Sun RNA Methyltransferase 2
OLIG2	Oligodendrocyte Transcription Factor 2
OXCT	3-Oxoacid CoA-Transferase 1
P16	cyclin-dependent kinase inhibitor 2A
PA	protective antigen
PAK1	P21 (RAC1) Activated Kinase 1
PanIN	Pancreatic intraepithelial neoplasm
PanNEN	Pancreatic neuroendocrine neoplasm
PCCs	pancreatic cancer cells
PD1	Programmed cell death 1
PDAC	pancreatic ductal adenocarcinoma
PDGF	platelet-derived growth factor
PDIA6	Protein Disulfide Isomerase Family A Member 6
PECAM-1	platelet-endothelial cell adhesion molecule-1
PET CT	Positron emission tomography scan CT
PFKL	Phosphofructokinase, Liver Type
PFN3	Profilin 3
PGK1	Phosphoglycerate Kinase 1
PI3K	phosphoinositide 3-kinase
PI3K	phosphoinositide-3-kinase
PICALM	Phosphatidylinositol Binding Clathrin Assembly Protein
PIPAC	pressurized intraperitoneal aerosolized chemotherapy
PKB/AKT	Protein kinase B
PKM	Pyruvate Kinase M1/2
PLEC	Plectin
PODXL	Podocalyxin Like
POU5F1	POU Class 5 Homeobox 1

PPME1	Protein Phosphatase Methylesterase 1
PPP1CC	Protein Phosphatase 1 Catalytic Subunit Gamma
PPP4C	Protein Phosphatase 4 Catalytic Subunit
PRKAB1	Protein Kinase AMP-Activated Non-Catalytic Subunit Beta 1
PSAP	Prosaposin
PSCs	pancreatic stellate cells
PTEN	Phosphatase and tensin homolog
PTGIS	Prostaglandin I2 Synthase
PTK2	Protein Tyrosine Kinase 2
Puma	p53 upregulated modulator of apoptosis
PXN	Paxillin
QPRT	Quinolinate Phosphoribosyltransferase
RACK7	Zinc Finger MYND-Type Containing 8
RAF	Rapidly accelerated fibrosarcoma kinase
RAF1	Raf-1 Proto-Oncogene, Serine/Threonine Kinase
RAI14	Retinoic Acid Induced 14
RALA	Ras-related protein Ral-A
RALGDS	Ral guanine nucleotide dissociation stimulator
RB	retinoblastoma protein
RELA	RELA Proto-Oncogene, NF-KB Subunit
RHO	Ras homologous
RIP	receptor‐interacting proteins
ROS	reactive oxygen species
RPL18A	Ribosomal Protein L18a
RTN4	Reticulon 4
S100A4	S100 Calcium Binding Protein A4
SAMD2	Sterile Alpha And TIR Motif Containing 1
SCA	Serous cystadenoma
SCL	TAL BHLH Transcription Factor 1, Erythroid Differentiation Factor
SDF-1	Stromal cell-derived factor 1
SFXN3	Sideroflexin 3
Sip1	Smad Interacting Protein 1
SIPC	sequential intraperitoneal chemotherapy

SLC16A1	Solute Carrier Family 16 Member 1
SLC16A4	Solute carrier 16A4
Smac	Second mitochondria-derived activator of caspase
SMAD3	SMAD Family Member 3
SMAD4	Mothers against decapentaplegic homolog 4
SMC3	Structural Maintenance Of Chromosomes 3
SMN1	Survival Of Motor Neuron 1, Telomeric
SMN2	Survival Of Motor Neuron 2, Centromeric
SOD2	Superoxide Dismutase 2
SORL1	Sortilin Related Receptor 1
SOX17	SRY-Box Transcription Factor 17
SOX9	SRY-Box Transcription Factor 9
SPIRE1	Spire Type Actin Nucleation Factor 1
SPTAN1	Spectrin Alpha, Non-Erythrocytic 1
SPTBN1	Spectrin Beta, Non-Erythrocytic 1
SQSTM1	Sequestosome 1
SRC	SRC Proto-Oncogene, Non-Receptor Tyrosine Kinase
SRRM1	Serine And Arginine Repetitive Matrix 1
SRRM2	Serine/Arginine Repetitive Matrix 2
STAT	signal transducer and activators of transcription
STAT1	Signal Transducer And Activator Of Transcription 1
STAT3	Signal Transducer And Activator Of Transcription 3
STAT5B	Signal Transducer And Activator Of Transcription 5B
STAT6	Signal Transducer And Activator Of Transcription 6
STEAP1	six-transmembrane epithelial antigen of prostate member 1
STMN1	Stathmin 1
TALDO1	Transaldolase 1
TARS1	Threonyl-TRNA Synthetase 1
TAU	Microtubule Associated Protein Tau
TCF21	Transcription Factor 21
TEM8 (ANTXR1)	Anthrax toxin receptor 1
TFAP2A	Transcription Factor AP-2 Alpha
TGFBR2	TGF-beta receptor type-2

TGF-β	Transforming growth factor beta
TJP1	Tight Junction Protein 1
TJP2	Tight Junction Protein 2
TLN1	Talin 1
TNFα	Tumour Necrosis Factor α
TNKS1BP1	Tankyrase 1 Binding Protein 1
TP53	Cellular tumour antigen p53
TPD52L2	TPD52 Like 2
TPM3	Tropomyosin 3
TRADD	TNFR-associated death domain
TRIO	Trio Rho Guanine Nucleotide Exchange Factor
TSP-1	Thrombospondin-1
TWIST1	Twist-related protein 1
TYMP	Thymidine Phosphorylase
UBE2E3	Ubiquitin Conjugating Enzyme E2 E3
UNC13D	Unc-13 Homolog D
uPA	Urokinase-Type plasminogen activator
uPAR	uPA receptor
VASH2	Vasohibin 2
VCAM-1	vascular adhesion molecule-1
VCL	Vinculin
VEGF	Vascular endothelial growth factor
VEGFR	Vascular endothelial growth factor receptor
VIM	Vimentin
VLA	integrins
WT1	WT1 Transcription Factor
XIAP	X-Linked Inhibitor of Apoptosis
XPO6	Exportin 6
YAP	yes-associated protein 1
YWHAZ	Tyrosine 3-Monooxygenase/Tryptophan 5-Monooxygenase Activation Protein Zeta
ZIM2	Zinc finger imprinted 2
ZNF185	Zinc Finger Protein 185 With LIM Domain

ZNF217	Zinc Finger Protein 217
ZYX	Zyxin

Chapter 1

General Introduction

1.1 Pancreatic cancer

Pancreatic cancer is one of the deadliest cancers. Globally, 495,773 people were diagnosed with pancreatic cancer in 2020, and 466,003 related deaths were reported (Sung et al. 2021). The morbidity and the number of deaths caused by pancreatic tumours have been gradually rising, although mortality and incidence, in particular for advanced diseases of various cancers, have been declining radically over the last few decades (Vincent et al. 2011). From 2015 to 2019, approximately 9710 people died of exocrine pancreatic adenocarcinoma in the United Kingdom, and the 10-year overall survival ratio is 5% (Sunagawa et al. 2020), making it one cancer type with poorest survivals amongst all the cancer types. There are some hereditary syndromes which are associated with the onset of pancreatic cancer, including familial atypical multiple mole melanoma (FAMMM), hereditary pancreatitis (HP), Peutz-Jeghers syndrome (PJS), familial adenomatous polyposis (FAP), Lynch syndrome (LS) and hereditary breast and ovarian cancer syndrome (HBOC) (Syngal et al. 2015). There are still no established screening procedures for these high-risk patients (Ohmoto et al. 2019). Lack of early detection, except for screening trials for those with family history, poor response to standard chemotherapy and radiotherapy and lack of target therapy, are amongst the key contributing factors to the poor clinical outcome and remain as challenges which provoke more intensive and extensive research of pancreatic cancer to shed light on the molecular and cellular machinery to tackle its disease-specific lethal threat.

Over the years, a huge effort has been made globally to develop new therapies for this cancer type, including new drugs, new combinational chemoradiotherapies and radiation therapies. Unfortunately, pancreatic cancer responds poorly to most chemotherapy agents. There are many reasons for this, including those stated earlier including absence of obvious and specific symptoms at early stages, making the diagnosis difficult. Lack of early detection, except for screening trials for those with family history, poor response to standard chemotherapy and radiotherapy and lack of target therapy, all lead to poor outcomes.

1.1.1 Anatomy of the pancreas

The human pancreas comprises three different parts: the head, the body and the tail.

The pancreas is both an exocrine and endocrine organ which lies in the upper left part of the enterocoelia, behind the stomach. The exocrine part accounts for 96%- 99% of total pancreas volume (Saito et al. 1978; Rahier et al. 1981), including acinar and ductal cells. Acinar cells secrete enzymes that play an important role in digestion, such as trypsin, chymotrypsin and pancreatic lipase. Ductal cells are responsible for the secretion of mucous and bicarbonate. The endocrine part accounts for about 1% to 4% of the pancreas (Saito et al. 1978; Rahier et al. 1981), and is constructed of many small cell clusters, which are referred as Langerhans' islet comprising α, β, γ and δ-cells. The α- and β-cells are profound in regulating the metabolism of glucose, via the production of insulin and glucagon. Pancreatic polypeptides and somatostatin are secreted by γ- and δ-cells to modulate the secretion of other cells in the pancreas.

The blood supply of the pancreas account for nearly 1% of the cardiac output (Lewis et al. 1998). The majority of the arterial blood is derived from the celiac and the superior mesenteric artery (Bertelli et al. 1995; Ito et al. 2019). The arteries which supply the head of the pancreas are the branches of the superior pancreaticoduodenal artery, which is derived from the celiac artery (Bertelli et al. 1998).

1.1.2 Pathology of pancreatic cancers

All the histological variants of pancreatic neoplasms are shown in Table1. Pancreatic cancer can be divided into two large groups: non-endocrine pancreatic tumours and endocrine pancreatic tumours. Non-endocrine pancreatic tumours can be further divided into benign and malignant. The benign group contains cystadenoma, lipoma, adenoma, fibroma, haemangioma, neuroma and lymphangioma, whilst the ductal adenocarcinoma, cystadenocarcinoma, and sarcoma are malignant tumours (Wolfgang et al. 2013). Prior to becoming malignant tumours, pancreatic cancer precursors may occur, which includes (Goral 2015): Pancreatic intraepithelial neoplasm (PanIN), Mucinous cystic neoplasms (MCN) and Intraductal papillary neoplasm (IPMN). PanIN is usually located at the small pancreatic duct. It is a microscopic epithelial neoplasm which is confined within the basement membrane and therefore is referred as a carcinoma *in situ* or non-invasive tumour. Based on the stage, this tumour type can be further divided into PanIN1A (flat type minimal atypia), PanIN1B (papillary type atypia), PanIN2 and PanIN3

(both are limited atypia). These lesions can be detected with an examination of endoscopic ultrasonography (EUS) (Gnoni et al. 2013). MCN is a rare tumour that has a fibrotic wall, the diameter varies from 5 to 35cm which usually develop over a long period without any symptom. However, in some circumstances, it can lead to weight loss, back pain and nausea. As in most other cancers, pancreatic cancer can also induce cachexia, which is a malnutrition induced by chronic diseases including chronic heart failure, cancer, chronic renal failure etc., (Nishikawa et al. 2021). Cachexia can also be induced by anorexia, increased energy expenditure, metabolic aberrations, immunological and neurological abnormalities (Tisdale 2003; Fearon et al. 2012; Petruzzelli and Wagner 2016). Back pain is an indication of the invasive expansion of pancreatic tumour to celiac plexus (Coveler et al. 2021). A MCN tumour usually locates at the pancreatic head and tail. In some cases, after further mutation, it can become a malignant form with gene mutations and the 5-years overall survival is about 20%-60% (Gnoni et al. 2013). IPMN is usually a very small and asymptomatic tumour. It seems that people who smoke have a higher risk of this disease. This type of tumours is able to secrete mucin as it derives from the main pancreatic duct (IPMN-MD) or branch ducts (IPMN-BD) (Gnoni et al. 2013).

The pancreatic malignancies are of several types. While pancreatic ductal adenocarcinoma (PDAC) accounts for the vast majority of pancreatic cancer (over 85%) (Mostafa et al. 2017), so the term “pancreatic cancer” is commonly used interchangeably with PDAC. Apart from PDAC, there are other different histomorphological variants, which are less well defined and require further research to clarify their clinical and pathological significance (Verbeke 2016). Other than histological types, pancreatic cancers are also grouped based on the anatomical location of pancreatic cancers, frequently referred to as pancreatic head carcinoma, pancreatic body carcinoma and pancreatic tail carcinoma or mixed locations. Each of these subtypes has a different prognosis and clinical symptoms.

Table 1.1 Histologic variants of pancreatic neoplasms (Mostafa et al. 2017)

Benign tumours	Serous cystadenoma (SCA)
	Intraductal papillary mucinous neoplasm (IPMN)
	Intraductal tubulopapillary neoplasm (ITPN)
	Mucinous cystic neoplasm (MCN)
Malignant neoplasms	
Ductal origin	Pancreatic ductal adenocarcinoma (PDAC)
	PDAC associated carcinomas
	Adenosquamous carcinoma
	Osteoclastic giant cell carcinoma
	Colloid carcinoma
	Medullary carcinoma
	Carcinomas arising in tumoral intraepithelial neoplasms
	IPMN with associated invasive carcinoma
	IPTN with associated invasive carcinoma
	MCN with associated invasive carcinoma
Neoplasms of non-ductal origin	Acinar cell carcinoma (ACC)
	Pancreatoblastoma
	Pancreatic neuroendocrine neoplasm (PanNEN)
	Solid pseudopapillary neoplasm

1.1.3 Epidemiology of pancreatic cancer

Globally in 2012, there were approximately 33,800 patients diagnosed with pancreatic cancer, making it the 11th most common cancer (Ilic and Ilic 2016). From 2015 to 2019, adenocarcinoma of the exocrine pancreas caused approximately 9,710 deaths every year in the United Kingdom, with a survival rate of only 5% for 5 to 10 years (www.cancerresearchuk.org, 2021). In different populations, the morbidity is different. For example, the risk of pancreatic cancer is low in the first three and four decades of life but increases significantly after age 50 years, with most patients diagnosed between 60 and 80 years (Gold and Goldin 1998).

Diabetes mellitus is associated with a higher risk of pancreatic cancer (Chow et al. 1995). Abnormal glucose metabolism may be associated with elevated risk of cancer, in which high insulin concentration can contribute to malignant transformation (Gapstur et al. 2000; Michaud et al. 2001).

There is a close relationship between chronic pancreatitis and the development of pancreatic cancer (Ammann et al. 1984), while alcohol and smoking play an important role in the association between pancreatitis and cancer [15]. The risk of adenocarcinoma is more likely to be increased in patients with hereditary pancreatitis (Viscardi et al. 2019). Furthermore, mutations in the cationic trypsinogen gene play an important role in pancreatitis thus with a higher risk of transformation to cancer. Trypsin normally remains in an inactivated form, called trypsinogen, until it reaches the duodenum. Mutated trypsinogen gene can result in pre-matured trypsin activation in the pancreatic duct which will then induce persistent stimulation to the surrounding tissue, inducing chronic pancreatitis, being considered as a risk factor of pancreatic cancer (Gorry et al. 1997; Kirkegard et al. 2017).

Some other cancers have a similar gene mutations with pancreatic cancer (Solomon et al. 2012). One of these cancers is hereditary breast-ovarian cancer syndrome, which has mutations in BRCA1 or BRCA2. BRCA2 mutations are associated with an up to 10 times greater risk of pancreatic cancer than exists in the general population (Klein et al. 2001). Additionally, Peutz-Jeghers syndrome (Su et al. 1999) and familial atypical multiple-mol melanoma syndrome (Lynch et al. 2002), are also considered as risk factors of pancreatic cancer.

Smoking is one of an evidently confirmed risk factor for pancreatic cancer (Coughlin et al. 2000; Lin et al. 2002). Diet is also a risk factor of pancreatic cancer, for example, higher intake of fat or meat presents a higher risk of pancreatic cancer, whereas more fruits and vegetables can reduce the risk (Howe and Burch 1996; Woutersen et al. 1999). Similarly, limonene, a component in citrus fruits, is a potent inhibitor of the KRAS oncoprotein, can help to reduce the risk of pancreatic cancer (Gelb et al. 1995).

1.1.4 TNM staging of pancreatic cancer

Pancreatic cancers are routinely evaluated according to TMN staging system from both the American Joint Committee on Cancer (AJCC) and the International Union Against Cancer (Table 1.2).

Table 1.2 Pathologic Staging of pancreatic cancer (Shin and Kim 2020)

Primary tumour			
T0	No evidence of primary tumour		
Tis	Carcinoma *in situ*		
T1	Tumour is confined in pancreas with a greatest dimension ≤2cm. Limited to pancreas		
T2	Tumour is localised in pancreas with a greatest dimension > 2cm.		
T3	Tumour extends beyond the pancreas but without involvement of celiac axis and/or superior mesenteric artery.		
T4	Tumour invades and expands to the celiac axis and/or superior mesenteric artery. Unresectable primary tumour		
TX	Primary tumour cannot be assessed		
Regional lymph nodes			
Nx	Regional lymph nodes cannot be assessed		
N0	No regional lymph nodes metastasis		
N1	With regional lymph nodes metastasis		
Distant metastasis			
M0	Without distant metastasis		
M1	With distant metastasis		
Pancreatic cancer stage			
0	Tis	N0	M0
IA	T1	N0	M0
IB	T2	N0	M0
IIA	T3	N0	M0
IIB	T1-3	N1	M0
III	T4	N0/1	M0
IV	T1-4	N0/1	M1

1.1.5 Diagnose and early detection of pancreatic cancer

A variety of approaches are commonly used in the diagnosis of pancreatic cancer, including ultrasonography, endoscopic ultrasound (EUS), Computed Tomography Scan (CT), Endoscopic Retrograde Cholangiopancreatography (ERCP), Magnetic resonance imaging (MRI), fine needle aspiration (FNA), Positron Emission Tomography- Computed Tomography Scan (PET-CT) and enhanced ultrasound (USG). ERCP is usually employed to guide a biopsy of tumours at the head of the pancreas. It is also used for a liquid biopsy for collecting pancreatic fluid. Furthermore, PET-CT is frequently used to examine extra-pancreatic involvement, i.e., distant metastases. (Chu et al. 2017). In PET-CT, a radioactive glucose will be injected into a vein which will enrich in the cancer lesions, due to a high consumption of glucose by cancer cells, in comparison with normal tissues (Giesel et al. 2021).

Multidetector computed tomography (MDCT), is the most widely used technique for detecting pancreatic cancer (Al-Hawary et al. 2014). Pancreatic cancer lesions usually present a weak enhancement in comparison with the adjacent normal tissue. This method has a good sensitivity of 89% with a 90% specificity (Treadwell et al. 2016). In addition to the MDCT, CT is often used to evaluate whether a tumour is resectable (Wong and Lu 2008). Moreover, CT is also employed to detect abdominal and lung metastasis, though it lacks, accuracy in detecting vascular invasion (Yang et al. 2014).

MRI is capable of detecting a pancreatic cancer lesion at an earlier stage, since it has a higher resolution and a better presentation of morphological alteration. Despite this, the sensitivity and specificity of MRI is very similar to CT (Treadwell et al. 2016). Since the cost of MRI examination is higher, MRI is more often recommended for patients with renal dysfunction, who cannot discharge the radioactive regent timely. In addition to its capability of detecting small tumours with a diameter less than 2 cm, another advantage of MRI is its ability to detect a pancreatic tumour from a mass-forming pancreatitis (Fattahi et al. 2009).

EUS is often used to examine a suspicious lesion of less than 2cm in the pancreas, which has an advantage of detecting primary tumour and disease staging compared with the CT (Agarwal et al. 2004). To date, the EUS is the best method for detecting vascular invasion in pancreatic cancer (Buchs et al. 2007). EUS is used in

combination with fine needle aspiration (EUS-FNA) for an on-site cytopathologic examination, so that the accuracy and sensitivity of detecting a malignant tumour can be increased significantly (Klapman et al. 2003; Buchs et al. 2007). Furthermore, contrast-enhanced EUS can be helpful in the detection of pancreatic ductal adenocarcinoma (PDAC), lymphoma, neuroendocrine tumours and metastatic lesions derived from a primary tumour other than pancreas. However, the CE-EUS is not suitable for patients with unstable angina (Zhang et al. 2018).

Although ERCP is less frequently used in detecting pancreatic cancer, it has an advantage of showing the structure of the pancreatic duct to detect any abnormality (Chu et al. 2017).

To date, there is still no reliable biomarker for early detection of pancreatic cancer, though a good number of biomarkers have been evaluated (Chu et al. 2017). Carbohydrate antigen 19-9 (CA 19-9) is one which has been studied more extensively. Moreover, CA19-9 has been recommended as a biomarker for assessing disease prognosis and recurrence.

In addition to the aforementioned techniques, confocal laser endomicroscopy (Napoleon et al. 2015) is a novel technique which can be further evaluated for its application in detecting and assessing the disease. Certain biomarkers appear to be promising, as a novel approach for the early detection in combination with EUS-FNA. For example, Kirsten rat sarcoma viral oncogene homolog (KRAS) mutation test, combined with the EUS-FNA, showed an increase in the accuracy of diagnosis (Bournet et al. 2015).

In addition, tumour biomarkers, including CA19-9, CA50, CA72-4, and CA242, have been applied in diagnosing pancreatic cancer for decades. To date, emerging new cancer markers hold promise for detecting pancreatic cancer. For instance, CEACAM1, MIC-1, lumican, gelsolin, apolipoprotein E, HSP70, HSP27 and HMGB1 CD40 (Chu et al. 2017).

1.1.6 Treatment of pancreatic cancer

Pancreaticoduodenectomy is the most widely used technique for treating pancreatic cancer located at the pancreatic head or body, while delayed gastric emptying and

infection are common complications. Surgical treatment is usually combined with chemoradiotherapy to improve the overall survival of patients (Khorana et al. 2019). Several drugs have been applied in the treatment of pancreatic cancer. 5-FU is one of the most extensively evaluated approaches used as a treatment for advanced pancreatic cancer (Carter and Comis 1975; Kelsen 1994). It has no effect on advanced pancreatic cancer when it is given as a bolus injection (Burris et al. 1997), while prolonged use of 5-FU and some other fluorinated pyrimidines may have some effect (Maisey et al. 2002). Long term intake of 5-FU has a reproducible effect against advanced pancreatic cancer (Casper et al. 1994; Carmichael et al. 1996; Burris et al. 1997).

In addition to this, the effect of camptothecins analogues, which can inhibit topoisomerase I, have also been evaluated, including irinotecan, topotecan and 9-nitro camptothecin. Supportive evidence for the effect of irinotecan and 9-nitro camptothecin in pancreatic cancer is still not enough, while topotecan does not appear to have any effect in the treatment of pancreatic cancer (Zarkavelis et al. 2019).

Although the modified combinational regime, FOLFIRINOX has been applied to the treatment of pancreatic cancer with some improvement in the prognosis, and a reduction in the tumour size, but the clinical outcome remains poor. The decreased tumour size may be a result of death of peri-tumoral inflammatory cells rather than cancer cells (McGuigan et al. 2018) .

Neoadjuvant therapy is another way to improve the treatment of pancreatic cancer, which is usually applied for the treatment of locally advanced and resectable tumours. It can be applied in patients before surgical treatment to reduce the tumour burden, which can increase the possibility of a surgical resection (Khorana et al. 2019). Furthermore, neoadjuvant therapy can also increase patients' disease-free survival and reduce number of lymph nodes in the regional invovlement (Bailey et al. 2016).

Immune checkpoint therapy has been evaluated in many cancers, and some agents, such as PD-1 and CTLA-4, are already being applied in clinical treatment. In contrast, these therapies are less effective in treating pancreatic cancer (Royal et al. 2010; Torphy et al. 2018).

1.2 Molecular and cellular biology of pancreatic cancer

Poor prognosis of the disease is partially due to the lack of early detection and effective treatment. On the other hand, laparotomy is usually applied to resect pancreatic cancer, which has a high risk of various perioperative and postoperative complications. Indeed, perioperative morbidity rate of laparotomy for pancreatic cancer treatment ranges between 40-50% (Torphy et al. 2020). Laparoscopic distal pancreatectomy is also used to treat pancreatic cancer with less perioperative complication (Bauman et al. 2018). Peritoneal metastasis may occur in one-third of the patients who had a curative resection (Hishinuma et al. 2006). In addition, the intrinsic factors of the tumour are of great importance. Insight into the molecular and cellular biology of pancreatic cancer will provide better knowledge of the intrinsic and vital factors and opportunities for developing a novel therapy.

1.2.1 Mutations of oncogenes and tumour suppressor genes in pancreatic cancer

To date, a number of mutated oncogenes have been identified in pancreatic cancer and may be associated with the development of the cancer type, including *SMAD4, KRAS, TP53, CDKNA2A, TGFBR2, ARID1A, MAGEA6, CC, EPC1, ARID2, ZIM2, ATM, MAP2K4, NALCN, SLC16A4* and *MLL3* (Hezel et al. 2006; Avila and Kissil 2013; Fang et al. 2013; Gnoni et al. 2013; Wood 2013). On the other hand, the deletion or mutation of tumour suppressor genes such as *p53, DPC4, LKB1* and *MKK4* have also been reported in pancreatic cancer (Su and Kern 2000). The mutation of *DPC4* can promote metastases in pancreatic cancer, whilst LKB1 (Liver Kinase B1, also called STK11, Serine/Threonine Kinase 11) gene mutation is associated with the Peutz-Jeghers syndrome, which is accompanied with a high risk of pancreatic cancer (Goral 2015).

In general, the imbalanced expression and function between oncogenes and tumour suppressor genes plays an important role in the development of a malignant tumour. Oncogenes can promote cell growth and proliferation, while the tumour suppressor gene shows an antagonistic effect when the oncogene is abnormally activated. During the process of neoplasia, the mutation of oncogene and tumour suppressor may both occur. For instance, oncogenic mutations of RAS can

permanently activate the RAS protein, even without a stimulation from upstream signalling, which ultimately leads to onset of a cancer with deregulated cell proliferation, differentiation and survival (Hanahan and Weinberg 2011).

As a key molecule in the PI3K/Akt (phosphoinositide-3-kinase–protein kinase B/Akt) pathway, mTOR can be targeted with an inhibitor. However, as a result of this inhibition, increased activity of PI3K and its effector Akt/PKB (AKT Serine/Threonine Kinase 1 /Protein kinase B) may consequently weaken the antiproliferative effect of the mTOR (Mechanistic Target Of Rapamycin Kinase) inhibition (Sudarsanam and Johnson 2010).

Early studies of the oncogenic action raised a notion that the increased expression of the oncogenes can promote cancer cell proliferation and tumour growth (Hanahan and Weinberg 2011). However, it has been revealed that excessively elevated signalling by oncogenic proteins such as RAS (rat sarcoma viral oncogene), MYC (MYC Proto-Oncogene), and RAF (rapidly accelerated fibrosarcoma kinases) can also induce cell senescence (Coghlin and Murray 2010). Acting as a negative and intrinsic regulatory mechanism, tumour suppressor genes can limit the oncogene-induced abnormal cell proliferation and tumour growth. There are two prototypical tumour suppressors, RB (retinoblastoma-associated) and Tumour Protein P53 (TP53) (Hanahan and Weinberg 2011).

The RB protein integrates extracellular and intracellular signalling to instruct a cell for entry into the next growth-and-division cycle (Sherr and DePinho 2000; Deshpande et al. 2005; Burkhart and Sage 2008). Aberrant RB pathway can impair a critical checkpoint in the cell-cycle progression in cancer cells (Hanahan and Weinberg 2011).

Unlike RB, TP53 can receive stimuli signals from stress sensors operating within the cell. For instance, when damage of the genome reaches a severe level, it will halt the cell-cycle progression until the damaged-DNA has been repaired. If the genome damage is overwhelming, TP53 can trigger apoptosis instead of a repair (Hanahan and Weinberg 2011).

Each of these two tumour suppressors operates as a part of a more extensively orchestrated network that is wired for functional redundancy (Hanahan and Weinberg 2011). An individual cell may not present an abnormality of proliferation, though it lacks

a functional Rb gene. Similarly, TP53 null mice usually develop and grow with essential and proper cell and tissue homeostasis but develop abnormalities later in their life span (Ghebranious and Donehower 1998).

1.2.1.1 The KRAS oncogene

KRAS (Kirsten rat sarcoma viral oncogene homolog) is a member of the RAS superfamily of small GTPases. Upon activation GTPase exchange factors (GEFs), it can regulate a variety of biological behaviours of a cell, including enhancing the survival and proliferation (Campbell et al. 1998; Malumbres and Barbacid 2003). In about 30% of early neoplasms, the mutation of KRAS was detected, when it come to the advanced PDAC, this frequency goes up to 100% (Klimstra and Longnecker 1994). The mutation of KRAS usually induces its insensitivity to the GAPs, and will then be a constitutively activated molecule (Wittinghofer et al. 1997). Mutated KRAS can promote cancer progression mainly in three signal pathways: RAF/ERK (Extracellular signal-regulated kinase) pathway, PI3K pathway and RalGDS (Ral guanine nucleotide dissociation stimulator) pathway.

KRAS is the most critical mutation in pancreatic cancer, detected in 90% of pancreatic cancer patients. It can activate many signalling pathways, especially the PI3K-AKT pathway, which promotes cell proliferation, apoptosis and migration. The KRAS also promotes cell proliferation, differentiation and cell apoptosis by activating the NOTCH pathway. Furthermore, KRAS also enhances the metastasis by activating the Hedgehog pathway (Goral 2015). There are a number of molecules and pathways regulated by KRAS which include RAFs (rapidly accelerated fibrosarcoma kinases), PI3K, RAL-GTPase, RHO and NFKB (Nuclear factor kappa B) etc.

The RAF family is a group of serine/threonine kinases. RAFs play an important role in relaying signals from KRAS to the downstream MEK/ERK pathway, which subsequently regulates cell proliferation, differentiation and survival (Baccarini 2005). Targeting RAS, MEKK1 and ERK can reduce survival of PDAC cells (Hirano et al. 2002). The PI3K pathway can be activated by the KRAS protein (Rodriguez-Viciana et al. 1996), which leads to uncontrolled cell proliferation and survival. An uncontrolled activated PI3K pathway can maintain a neoplasm even if the upstream signal inducing

KRAS is inhibited (Lim et al. 2016). PDAC cells may have a higher sensitivity to the chemotherapy when the PI3K pathway is blocked (Ng et al. 2000; Shah et al. 2001).

RAS related protein (RAL) GTPase is a member of the RAS family, and it is located downstream of KRAS. Moreover, activated RAL can enhance the effect of KRAS and promote oncogenic transformation towards a cancerous cell and subsequent tumourigenesis (Urano et al. 1996; Lu et al. 2000). Activation of RAL A has been evident in tumourigenesis of PDAC, whilst knockdown of RAL A in pancreatic cancer cell lines suppressed cell proliferation and malignant transformation (Lim et al. 2005).

NFKB is a transcription factor which can be activated by the KRAS pathway in PDAC (Dong et al. 2002), which can promote angiogenesis and tumour invasion (Orlowski and Baldwin 2002). Compared with the normal pancreatic tissues, significantly elevated NFKB activity has also been observed in PDAC tumours (Chandler et al. 2004).

RHO is another subfamily of the RAS superfamily, in addition to its promotive role in cell proliferation and survival, it is also involved in the rearrangement of cytoskeletal distribution, adhesion and migration of a cell (Wennerberg et al. 2005). Suwa et al. have found that RHO-C, a subtype of the RHO family, is implicated in the distant metastasis of PDAC (Suwa et al. 1998).

1.2.1.2 INK4A (CDKN2A, Cyclin Dependent Kinase Inhibitor 2A) tumour suppressor

The INK4 gene is located on 9p21. INK4A encodes, a critical tumour suppressor, P16INK4A. P16INK4A can arrest the phosphorylation of RB by inhibiting CDK4/6 activity, thereby governing the entry of the S phase in a cell cycle. Loss-of-function mutation of the INK4 gene has been found in 80% to 90% of PDAC (Bartsch et al. 2002), and the mutation usually happens in conjunction with the mutation of the KRAS gene. If the activation of KRAS is out of control, the expression of INK4 will be inhibited, which induces cell senescence (Serrano et al. 1997; Brookes et al. 2002). Therefore, both activated RAS and the loss of INK4A function coherently contribute to the tumourigenesis of PDAC (Aguirre et al. 2003). The loss-of-function mutation of INK4A is also observed in FAMMM syndrome (Goldstein et al. 1995) and it can also enhance the

ability of a cell to tackle the telomerase erosion (van Heek et al. 2002). Both FAMMM and deregulated responses to telomerase erosion are also evident with a higher risk of pancreatic cancer (Soura et al. 2016; Vinagre et al. 2016)

1.2.1.3 P53 tumour suppressor

Tumour protein 53 (P53), DPC4, LKB1, INK4a, and MKK4 are the most common tumour suppressors which present mutations or deletion in pancreatic cancer patients (Goral 2015). For instance, *P53* gene mutations are evident in over 50% of PDAC cases (Rozenblum et al. 1997). P53 helps to block the cell cycle if there is a chromosomal aberration. If it does not work well, the aberration can accumulate and eventually induce a malignant tumour. *INK4a*, also known as Cyclin Dependent Kinase Inhibitor 2A (CDKN2A /ARF) is a gene located on the 9p21, which encodes a tumour suppressor, p19ARF. The degradation of the p53 protein can be inhibited by p19ARF. In human PDAC, mutations of *p53* and *ARF* coexist in nearly 40% of cases (Pomerantz et al. 1998).

1.2.2 Other tumour suppressor genes

Contact inhibition is one mechanism by which cell proliferation is regulated and inhibited in normal tissue, thus to keep the appropriate homeostasis. Under normal physiological conditions, once the cell density is high enough and cells make contact with each other, further cell proliferation is suppressed (Hanahan and Weinberg 2011). This mechanism can prevent the unlimited cell proliferation. This regulating mechanism is lost or destroyed in many different cancers. One mechanism is induced by the mutation of the *NF2* (Merlin) gene, which is a known tumour suppressor. The NF2 coding protein, Merlin (moesin-ezrin-radixin-like protein) orchestrates contact inhibition through coupling cell-surface adhesion molecules to transmembrane receptors, a function known for its related ERM protein including Ezrin, Radixin and Moesin (Curto et al. 2007). The Serine/Threonine Kinase 11 gene (STK) epithelial polarity protein plays a central role in another mechanism, mediating contact inhibition. LKB1 organizes epithelial structure and helps maintain tissue integrity (Curto et al. 2007). LKB1 encodes a serine/threonine kinase, which is implicated in metabolism. Peutz-Jeghers syndrome is a disease which

is associated with mutated *LKB1*, and a patient with this disease has a higher risk of PDAC (over 40-fold) (Giardiello et al. 2000)

Transforming Growth Factor Beta (TGF-β) is well known for its antiproliferative effects. In many late-stage tumours, TGF-β signalling is redirected away from suppressing cell proliferation (Hanahan and Weinberg 2011).

Breast Cancer gene 2 (*BRCA2*) is a tumour suppressor which is mutated in about 17% of familial pancreatic cancer (Murphy et al. 2002). It plays a pivotal role in regulating the homologous recombination-based DNA repair. Loss of BRCA2 is also evident in high grade pancreatic intraepithelial neoplasm (PanIN), but not those low grade PanINs (Goggins et al. 2000).

1.2.3 Pancreatic cancer cell invasion and metastasis

Distant metastasis is the hall mark of advanced pancreatic cancer, which occurs in approximately 70% of pancreatic cancer patients and cannot be eliminated with a surgical procedure (Chen et al. 2021). The distant metastasis is a multiple-step process: i) dissemination of cancer cells from the primary tumour to a distant tissue. ii) Colonization and formation of a metastatic lesion. Furthermore, cancer stem like cells (CSCs) play an important role in distant metastasis by promoting cell motility, invasiveness and evasion of apoptosis (Charafe-Jauffret et al. 2009; Pang et al. 2010; Marcato et al. 2011). Several genes have been implicated in the distant metastasis of pancreatic cancer, including Smad4, KRAS, INK4Aand TP53 (Ichikawa et al. 1997; Callery et al. 2009; Karasawa et al. 2017; Cheng et al. 2019). EMT, upregulation of specific miRNAs, immune suppression and pre-metastatic niche formation in microenvironment are also involved in distant metastasis (Lamouille et al. 2014; Sefrioui et al. 2017; Kunovsky et al. 2018; Kamyabi et al. 2019; Zhu et al. 2020).

1.2.3.1 Angiogenesis in pancreatic cancer

Blood circulation is an important route for the systemic metastasis of cancer cells in the body. Tumours have a high demand on the blood supply to obtain nutrition and to evacuate metabolic waste. Pro-angiogenic factors can be activated in response to some stimuli, such as wound healing and chronic hypoxia (Sorg et al. 2017; de Heer et al.

2020). If the diameter of a solid tumour is less than 2-3mm, the tumour cells can still acquire nutrients and oxygen through diffusion. In larger tumours, hypoxia and stress can induce expression of pro-angiogenic factors and consequently promote formation of new vasculature, to bring in sufficient oxygen and nutrients leading to an explosive tumour growth (Holmgren et al. 1995).

The angiogenesis is coordinated by certain angiogenic factor and angiogenesis inhibitors, including vascular endothelial growth factor (VEGF), matrix metalloproteinase (MMPs), interleukin and thrombospondin-1 (TSP-1, or THBS1) (Taraboletti and Margosio 2001; Hanahan and Weinberg 2011). VEGF can be upregulated in tumours upon stimulation of hypoxia and oncogenic signalling (Mac Gabhann and Popel 2008; Ferrara 2009). For instance, hypoxia induced factor (HIF) released from the cancer cells under stress and hypoxia can induce expression of VEGFs in both cancer cells and stromal cells, which subsequently promote growth and migration of nearby vascular endothelial cells to form new vasculature (neovasculature). There are three receptor tyrosine kinases (VEGFR 1–3), mediating signalling for VEGFs. VEGFR1 and 2 are expressed mainly by vascular endothelial cells whilst VEGFR3 is expressed by lymphatic endothelial cells. VEGFR2 presents the strongest ability in promoting angiogenesis and to some degree lymphangiogenesis (Melincovici et al. 2018).

On the other hand, TSP-1 is a critical counterbalance molecule in the angiogenic switch. Upon binding to its receptors which include the Reelin receptors, VLDLR and ApoER2, TSP-1 evokes suppressive signals that can counteract the proangiogenic stimuli in vascular endothelial cells (Kazerounian et al. 2008). A recent study showed that TSP-1 can inhibit angiogenesis in intrahepatic cholangiocarcinoma (Carpino et al. 2021).

PDAC is different from many other cancers, which is characterized by an intense fibroinflammatory response, which can result in an extraordinarily high interstitial fluid pressure (IFP). The high IFP can interrupt the blood supply via small blood vessels and diffusion of the small molecules in the tumour (Provenzano et al. 2012). As a result, many molecules secreted by pancreatic cancer or stroma cell can be upregulated to promote angiogenesis. For instance, PDAC tumours present a high expression of TGF-β and connective tissue growth factor, which can promote angiogenesis (Masamune et

al. 2008). Other tumour released proangiogenic factors including VEGF, MMP-9, interleukin-8, and fibroblast growth factor-2, can also be upregulated (Burris et al. 1997). In contrast to PDAC tumours, pancreatic neuroendocrine carcinomas are highly angiogenic and densely vascularized, partially as a result of mild and less intense fibroinflammatory response in those tumours (Turner et al. 2003; Olive et al. 2009; Zee et al. 2010).

1.2.3.2 Cadherins and epithelial mesenchymal transition (EMT) in distant metastasis

E-Cadherin (Cadherin-1) is a key cell-to-cell adhesion molecule, which is well known as an epithelial cell marker and elicits an inhibitory effect on invasion and metastasis of cancerous cells. In human cancers, E-cadherin and its related molecules are frequently reduced or absent (Cavallaro and Christofori 2004; Berx and van Roy 2009).

N-cadherin (Cadherin-2) is another adhesion molecule that plays an important role in disease progression and is referred as a marker for epithelial mesenchymal transition (EMT). Elevated expression of N-cadherin has been observed in migrating neurons, mesenchymal cells during organogenesis and invasive cancerous cells (Cavallaro and Christofori 2004).

EMT is a crucial step through which cancer cells acquire aggressive and invasive traits to invade, disseminate and evasion from apoptosis (Klymkowsky and Savagner 2009). In addition to N- and E-cadherin, several biomarkers are positively correlated with EMT, including Snail, Slug, Twist, and Zeb1/2. In addition to orchestrating EMT in cancer, they also play an important role in cell differentiation and migratory processes during embryogenesis (Schmalhofer et al. 2009; Micalizzi et al. 2010).

1.2.3.3 Crosstalk between cancer cells and stroma is involved in invasive growth and metastasis

The communication between cancer cells and stromal tissue in a tumour plays a profound role in distant dissemination of cancer cells. For example, upon a stimulus from cancer cells via a paracrine pathway, mesenchymal stem cells (MSCs) in the tumour stroma can secrete C-C chemokine ligand 5 (CCL5), which reciprocally acts on

the cancer cells in the mode of chemotaxis and chemokinesis, to facilitate their invasiveness (Karnoub et al. 2007). Macrophages in the tumour, or peripheral area, can foster local invasion by supplying matrix-degrading enzymes, such as the matrix metalloproteinases. The macrophages can be activated by Interleukin 4 (IL-4) released from the cancer cells (Joyce and Pollard 2009; Gocheva et al. 2010; Kessenbrock et al. 2010).

It has been shown, in breast cancer, that tumour-associated macrophages act as an additional resource to provide epidermal growth factor (EGF) to cancer cells, which reciprocally stimulate the macrophages with CSF-1 (Wyckoff et al. 2007; Qian and Pollard 2010). A noteworthy finding is that, in the absence of ongoing exposure to contextual signals, carcinoma cells may undergo a process of mesenchymal epithelial transition (MET) in their new homes which is a process that is in contrast to EMT, to acquire a dormancy and noninvasive state (Hugo et al. 2007).

1.2.3.4 Metastatic cancer cells and role of fibroblasts in metastasis

Tumours consist of heterogeneous cancer cells, which include cancer stem cells (CSCs), though the concept remains controversial. Metastasis-initiating cells (MICs) are a subpopulation of CSCs which can promote metastasis (Brabletz et al. 2005; Hermann et al. 2007; Rosen and Jordan 2009). In pancreatic cancer, MICs play an important role in lymphatic metastasis， especially CD133+ MICs, which present a significant association with lymphatic metastasis (Li et al. 2007; Maeda et al. 2008; Ishizawa et al. 2010).

Cancer-associated fibroblasts (CAFs) also play a pivotal role in the disease progression of PDAC by fostering a niche to facilitate the development and progression of pancreatic cancer (Hussain et al. 2010). On the other hand, cancer cell secreted growth factors, such as platelet-derived growth factor (PDGF) and Transforming growth factor beta (TGF-beta), can act on the fibroblasts to further enhance the vicious reciprocal interactions (Xiao et al. 2014).

1.2.3.5 Gene alteration and aberrant signalling in metastases of pancreatic cancer

Matrix metalloproteinase 14 (MMP14), MMP24, Macrophage migration inhibitory factor

(MIF), R-rat sarcoma viral oncogene homolog (R-RAS) and Adhesion Regulating Molecule 1 (ADRM1) are highly expressed in the metastatic lymph nodes of pancreatic cancer, in comparison with their expression in primary tumours (Long et al. 2012). KRAS and *P53* mutations are also implicated in distant metastasis (Aguirre et al. 2003; Hingorani et al. 2005; Morton et al. 2010).

Certain signaling pathways are pivotal in distant metastasis of pancreatic cancer. For instance, TGF-β promotes invasion and metastasis by inducing EMT-associated gene expression and upregulating MMPs (Hosotani et al. 2002; Desgrosellier et al. 2009; Kabashima et al. 2009). Sonic Hedgehog (Shh) can also accelerate the progression of EMT to thus facilitate distant metastases in PDAC (Dai et al. 2011; Eberl et al. 2012).

The overexpression of notch-1, which is a receptor to ligands Delta-like and Jagged, can induce EMT, increase the vitality of CSCs and modulate metastasis-associated miRNA (Bao et al. 2011; Sureban et al. 2011). On the other hand, notch-1 also exhibits an anti-tumour effect in KRAS induced PDAC (Hanlon et al. 2010).

The SDF-1/CXCR-4 axis plays a critical role in lymph angiogenesis, proliferation, metastasis and chemoresistance in a variety of cancers (Zhou et al. 2019). This was also evident in the lymph node metastasis of PDAC (Mimeault and Batra 2008; Thomas et al. 2008; Singh et al. 2010; Li et al. 2012b).

VEGF-C and VEGF-D and their receptors, vascular endothelial growth factor receptor 2/3 (VEGFR-2/3), can promote lymph angiogenesis. Both VEGF-C and -D are positively correlated with lymph node metastasis, including PDAC (Stacker et al. 1999; Kurahara et al. 2004). VEGFR3, expressed on the lymphatic epithelium, can be activated by VEGFC or D, secreted by the pancreatic cancer cells, to facilitate lymphangiogenesis and consequently a high likelihood of lymph node metastasis (Tang et al. 2001; Kurahara et al. 2004).

1.2.3.6 Micro RNA and metastasis

Micro RNA (miRNA), which usually acts as a post-transcription regulator, has also been found to have pro and anti-tumour effects in PDAC, some are involved in the distant metastasis of pancreatic cancer (Long et al. 2012). MiRNA 196a, miRNA 186,

miRNA200b, miRNA190, miRNA15b, miRNA21, miRNA155, miRNA221, and miRNA222 play an important role in the development and distant metastasis of pancreatic cancer, by coordinating KRAS, Ras-responsive element-binding protein, Bcl-2 and Notch1/2 (Choudhury et al. 2004; Kent et al. 2010; Srivastava et al. 2011; Tavano et al. 2012).

1.2.4 Telomerase in tumour formation

Abnormal expression of the telomerase is associated with tumourigenesis (Hahn et al. 1999). Telomerase in premalignant lesions is characterised by telomere shortening and aberrations in chromosomal structure (Raynaud et al. 2010). The mutation of p53 can also promote the shortening of telomeres; thus, the dysfunction of telomeres and p53 can cooperate to promote the formation of tumours in different tissues (Chin et al. 1999). Shortened telomeres were also evident in low-grade PanINs (van Heek et al. 2002).The premalignant tumour usually express telomerase at a non-significant level, while mature malignant tumours express high level telomerase together with the fixation of telomeres. (Hanahan and Weinberg 2011). This means that the delayed acquisition of telomerase function serves to generate tumour-promoting mutations in premalignant tumours, and its subsequent activation can stabilize the mutant genome in malignant tumours (Hanahan and Weinberg 2011). The shortening of the telomere, or telomere erosion, which happened before the telomerase activation, plays a vital role in the initiation of PDAC. What is more, telomere erosion usually happens in older adults or patients with chronic pancreatitis, which may explain why these two groups of patients have a higher risk of developing PDAC (Vinagre et al. 2016; Lardy et al. 2017). The telomerase activation can also promote disease progression after the telomere erosion (Calcagnile and Gisselsson 2007).

1.3 Peritoneum and peritoneal metastasis

The peritoneum is the largest serous membrane in the human body, with a surface area around 1.8 m^2. It can promote the physiological movement of the organs in the abdominal cavity and is implicated in some diseases, such as inflammation and tumour metastasis. Once the malignant tumour cells are disseminated to the peritoneum, it is

difficult to treat with a surgical approach due to the extent and number of small miliary metastatic tumours formed in the abdominal cavity. The peritoneum is the second most common site of pancreatic cancer metastasis (Yachida and Iacobuzio-Donahue 2009).

1.3.1 Biology of the peritoneum

The peritoneum includes two portions, the parietal peritoneum and the visceral peritoneum. The former forms the liner of the abdominal wall, while the latter fuse with the serosal layers of visceral organs.

The blood supply of the visceral peritoneum mainly comes from the coeliac, visceral pelvic and coeliac arteries, and the pelvic parietal arteries, together with other arteries of the abdominal wall, support the parietal peritoneum (Khanna 2009).

The thoracoabdominal, subcostal, lumbosacral, and phrenic nerves govern the upper abdominal parietal peritoneum, and the obturator nerve innervates the pelvic portion. The nerves which control the visceral peritoneum were not clearly identified until 2017, while the mesenteric plexus, the splanchnic nerves, and the coeliac plexus may be implicated in it. (Aguirre and Abensur 2014; van Baal et al. 2017).

The visceral and parietal peritoneum structure is similar, consisting of 3 layers: the mesothelial layer, basal lamina and the submesothelial stroma. In different areas of the peritoneum, there is a significant difference in the thickness of the submesothelial stroma (van Baal et al. 2017).

In a normal human body, the peritoneal cavity contains about 5-20 ml of fluid, which contributes to lubrication and immunity. It derives from the transudate and macrophage secretion, while in women also contains exudate from ovarian and tubal fluid (Oral et al. 1996). This fluid also contains different types of immune cells, including natural killer cells, macrophages, eosinophils, mesothelial cells, mast cells and lymphocytes (Gazvani and Templeton 2002). The ascites can be induced by some diseases, such as inflammation and tumour metastasis, which disturb the balance between the formation and absorption of this fluid.

The mesothelial cells form a monolayer structure, which is called mesothelium, and it is the innermost layer of the peritoneum (van Baal et al. 2017). These cells connect each other through tight junctions, gap junctions and desmosomes (Ito et al.

2000) and have a well-developed intracellular vesical system, which means that they have a strong capability in secretion (Obradovic et al. 2001). These cells also contain lamellar bodies, which are made up of lipid membranes and surfactant proteins. They are organelles with secretory and storage functions and play an important role in lubrication and immunoregulation (Kishore et al. 2005; Michailova and Usunoff 2006; Qaseem et al. 2013). On the extracellular surface of these cell is a stagnant fluid layer, which contains proteoglycans and glycosaminoglycans (GAGs), and can protect the cells from friction damage (Dobbie and Anderson 1996; Mutsaers 2004).

Basal lamina lies under the mesothelium and supports it. Between the basal lamina and the mesothelium is a layer of the extracellular matrix, mainly composed of collagen type IV and laminin. Laminin is connected with the mesothelial cells through β1 integrins, and collagen type IV fibres interact with each other, forming a network together and help to stabilize the basal lamina (Yurchenco 2011).

The submesothelial stroma comprises connective tissue, especially the collagen fibres (Witz et al. 2001), which support the mesothelium and the basal lamina. Many immune cells inhabit this stroma, which are in a dormant stage in physical conditions. Under some pathological circumstances, these cells can be activated, inducing inflammation and angiogenesis (Witz et al. 2001).

1.3.2 Peritoneal metastasis of pancreatic cancer

The peritoneum plays an important role in cancer metastases, which is a preferred localization for metastases of certain cancers such as ovarian, colon or gastric carcinomas, and it is also the second most common site of distant metastasis of pancreatic cancer (Siegel et al. 2020). Peritoneal metastasis, also referred to as peritoneal carcinomatosis, is usually associated with a poor prognosis. Even a micro-metastasis can also cause a dismal outcome and these patients cannot benefit from the local treatments (Makary et al. 1998). About 9% PDAC patients present peritoneal metastasis at the time of diagnosis (Thomassen et al. 2013). Even following potentially curative resection, peritoneal metastasis can still happen in one-third of the patients (Hishinuma et al. 2006). During the progression of pancreatic cancer, some detached tumour cells can penetrate the peritoneal cavity directly, a phenomenon found in about

20-30% patients (Jayne 2007; Yachida and Iacobuzio-Donahue 2009). A study showed that, once peritoneal metastasis has occurred, the patients who do not receive systematic treatment had a median survival of 6 weeks (Thomassen et al. 2013). Peritoneal metastasis usually starts from tumour cell exfoliation, followed by the invasion into the peritoneum (Jayne 2007). An interesting finding is that pancreatic tumour cells, which have an advantage in haematogenous metastasis, are unsuitable for peritoneal metastasis (Nishimori et al. 2002)

Once peritoneal carcinomatosis happens, the prognosis is usually not good. Peritoneal metastasis involves the spread of tumour cells in the peritoneal cavity and the adhesion to the abdominal organs. The tumour metastasis to the peritoneum begins from the detachment of the tumour cells from the primary lesions. The first procedure can be promoted by EMT and the function of matrix metalloproteinase (MMPs), which can dissolve the extracellular matrix and make the invasion and metastasis easier. When the cells leave the primary tumour and enter the peritoneal cavity, it was once thought that the spread of these individuals or clusters of tumour cells go through a random diffusion process (Sugarbaker 1996). More and more researchers have pointed out that the direction and ultimate destination of these cells are dependent on the anatomic site of the primary tumour, the biological properties of the disseminating cells and the peritoneal fluid circulation, which can be affected by many different factors including respiration, bowel peristalsis, gravity and so on (Carmignani et al. 2003; Hugen et al. 2014; Wasnik et al. 2015; Lemoine et al. 2016). However, molecular machinery underlying the metastatic process and interaction between cancer cells and the peritoneum hold clues for a better understanding and therapeutic opportunity.

1.3.3 Moleculear mechanism in peritoneal carcinomatosis

There are two steps for peritoneal metastasis: single cell or cell clusters exfoliate from primary cancer and enter the peritoneal cavity following which, seeding occurs, the omental milky spots are the preferable area for seeding. Furthermore, accidental peritoneal metastasis can also happen during the surgical resection process (Miao et al. 2014; Weidle et al. 2016; Hoskovec et al. 2019). It has been revealed, in ovarian cancer, that cancer cells in the peritoneal metastatic lesion have a different gene expression

profile, with an elevated proliferation in comparison with the primary tumours (Lancaster et al. 2006; Brodsky et al. 2014). Several pathways have been implicated in ovarian cancer metastasis, including the p53 and JAK/STAT pathway (Lancaster et al. 2006; Malek et al. 2012). Gastric cancer is another cancer with a high frequency of peritoneal metastasis. Similar to ovarian cancer, examination of the ascites from peritoneal metastasis showed that several genes including STEAP1(Six Transmembrane epithelial antigen of the prostate 1), S100A4 (S100 calcium binding protein A4) and CTNNB1 (Catenin beta 1) are upregulated in peritoneal metastatic lesions from gastric cancer, compared with their expression in the primary tumours (Hippo et al. 2001; Sakakura et al. 2002; Bai et al. 2012; Wu et al. 2018)

There is a family of adhesion molecules called integrins, which are widely expressed on the cell membrane in many different type of cancer cells (van Baal et al. 2017). These transmembrane proteins are essential for cell-matrix adhesions and can bind to the fibronectin and matrix proteins expressed by the mesothelial cells (Witz et al. 2001; Slack-Davis et al. 2009). The binding, whilst conferring cancer-matrix adhesion, may also lead to the release of inflammatory factors by mesothelial cells. Once the inflammatory response is activated, the expression level and the activity of fibronectin and integrins are upregulated, which forms a positive-feedback loop (Kenny et al. 2014). Furthermore, the inflammation can promote angiogenesis, which makes it easier for the colonisation of the cancer cells.

In addition to malignant tumour cells, a tumour also contains other components which provide physical and biological support to tumour cells. These components are called tumour mesenchyme including fibroblasts, immune cells, blood vessels and the extracellular matrix (Kobayashi et al. 2019). In the tumour stroma, cancer-associated fibroblasts (CAFs) foster a favourable niche for the tumour growth, invasion and progression. CAF can also induce angiogenesis through the production of growth factors and other components of the extracellular matrix (Orimo and Weinberg 2006). CAFs in peritoneal metastases can be originated from mesothelial cells, through a progression called mesothelial-to-mesenchymal transition (MMT). MMT is a transformation of mesothelial cells from a normal, benign stage into a malignant, invasive and migratory stage through progressive loss of the mesothelial phenotype and

intercellular adhesion (Yanez-Mo et al. 2003). MMT is also implicated in the fibrosis of the peritoneum following the surgical treatment or inflammation (van Baal et al. 2017). These transformed mesothelial cells can promote tumour progression through a remodelling of the ECM and an upregulation of (VEGF), to stimulate angiogenesis (Sandoval et al. 2013; Rynne-Vidal et al. 2015). Furthermore, MMT can also accelerate the progression of peritoneal carcinomatosis by enhancing the integrin-dependent adhesion between tumour and mesothelial cells.

The mesothelial cells also express certain cell adhesion molecules, including intercellular adhesion molecule-1 (ICAM-1), vascular adhesion molecule-1 (VCAM-1) and platelet-endothelial cell adhesion molecule-1 (PECAM-1), which belong to the immunoglobulin superfamily (Jonjic et al. 1992; Klein et al. 1995) and CD44. These adhesion molecules can enhance the physical connection between mesothelial cells in the peritoneum. The postoperative inflammation, or inflammation induced by cytokines released from tumour cells, can induce both ICAM-1 and VCAM-1 in peritoneal mesothelial cells, which facilitate contraction of the mesothelial cells. The contraction of mesothelial cells reduces the size of the mesothelial cell layer, making it unable to cover the basement membrane (Jayne et al. 1999). The exposed basement membrane can be easily bound with the tumour cell through integrin β1 subunit (Takatsuki et al. 2004; van Grevenstein et al. 2007). The tumour not only binds to the basement membrane but can also bind with the mesothelial cells directly. Mesothelial cells can secrete glycosaminoglycan and hyaluronan and, these two molecules can then combine together to form the pericellular coat (Heldin and Pertoft 1993), which can protect the peritoneum from infections. On the other hand, this liquid coat is also involved in the adhesion between the tumour and mesothelial cells, with assistance from CD44. CD44 is a glycoprotein located on the cell membrane which promotes cell adhesion (Weidle et al. 2016).

1.3.4 Peritoneal metastasis process

Peritoneal metastasis undergoes five steps, including detachment, floating, adhesion, tumour cell invasion and metastatic deposit establishment (Jayne 2003; Jayne 2007; Mikula-Pietrasik et al. 2018). The cancer cells first detach from the primary tumour and

float in the peritoneal cavity following the peritoneal fluid cycle (Jayne 2007). Some floating cancer cells can avoid *anoikis* (a programmed cell death induced after a loss of anchorage to matrix) and adhere to the peritoneum mesothelial cells with subsequent invasion (Simpson et al. 2008). Once the cancer cells invade into the connective tissue, they stimulate the formation of a metastatic niche (Jayne 2003; Jayne 2007; Mikula-Pietrasik et al. 2018).

During the detachment period, the attenuation of E-cadherin plays an important role, for the downregulation of E-cadherin promotes cell motility through activating the Rho pathway, further reorganizing the cytoskeleton (Furuyama et al. 2000; Fukata and Kaibuchi 2001; O'Connor and Chen 2013; Kourtidis et al. 2017; Hu et al. 2018). During this period, some other genes and pathways which are associated with the Rho pathway are also activated, including the EGF pathway and ARL4C (ADP-ribosylation factor-like protein 4C) (Matsumoto et al. 2014; Chen et al. 2016b; Hu et al. 2018). In pancreatic adenocarcinoma, BACH1 (BTB Domain And CNC Homolog 1) is another gene which may be associated with detachment. It can inhibit E-cadherin and promote the EMT process to facilitate detachment (Sato et al. 2020). HGF (Hepatocyte growth factor) and its receptor c-Met can promote EMT, which has also been implicated in the peritoneal dissemination of pancreatic cancer cells (Takiguchi et al. 2017)

Once cancer cells detach from the primary lesion, they need to overcome *anoikis*. X-linked inhibitor of apoptosis (XIAP) and survivin can promote cell survival, by inhibiting the apoptosis protein family (Li et al. 2000; Cheng et al. 2002). Another way to enhance cell survival is to remain in the mesenchymal state, which is associated with a high expression of Sip1/ZEB2 (Zinc finger E-box binding homeobox 2) molecule (Rogers et al. 2013). The abdominal cavity is hypoxic, and the glucose concentration is meagre, so the cancer cells require a modification of their metabolism to overcome this. HIF1α is an important molecule which can help cancer cells to adapt to the hypoxic environment, which was found to be upregulated in PDAC (Zhong et al. 1999). HIF-1α can also promote the expression of ANGPTL4 (Angiopoietin like 4), as a secreted protein, it can enhance resistance to *anoikis* in cancer cells (Baba et al. 2017). Activation of other pathways including PI3K-Akt, PTEN-PI3K-NFκB-FAK and CXCL12-CXCR4 pathways can also promote cell survival during dissemination (Davies et al.

1999; Altomare and Testa 2005; Avizienyte and Frame 2005). Ascites arise after the peritoneal metastasis and can further promote the metastatic progression. Moreover, the dispatched cells, suspended in the ascites, can form clusters to support each other for an evasion from the *anoikis* process (Mikula-Pietrasik et al. 2018). It has shown that HGF and c-Met expressed in ovarian cancer can retain cell aggregation ability (Corps et al. 1997; Burleson et al. 2004). During this period, as well as the molecules expressed by cancer cells, cancer associated fibroblasts, activated mesothelial cells and tumour-associated macrophages can also assist the disseminating cancer cells with evasion from the immune system.

During the reattachment procedure, in a healthy peritoneum, the mesothelial cell layer has the ability to inhibit the attachment of cancer cells, as it can secret mucus-like substrates, which make the adhesion difficult (Barbolina 2018), while in a damaged or senescent layer cancer cells are more likely to attach (Wilson et al. 2019). Furthermore, cancer cell secreted TGF-β can promote mesothelial cells to express more fibronectin through the TGF-βRI-RAC1-SMAD pathway, which can enhance the attachment of cancer cells to the peritoneum (Lv et al. 2010; Kenny et al. 2014). Another interesting finding is that E-cadherin, whose deregulation is associated with EMT, can inhibit cancer cell detachment. On the other hand, it can also promote reattachment during distant metastasis, by promoting α5-integrin expression (Sawada et al. 2008). Despite this, when some cancer cells attach to the mesothelium, they will promote mesothelial cells to secrete MMPs, which is helpful for cancer invasion (Ahmed et al. 2002; Kenny et al. 2008). CD44 is a membrane protein expressed by both cancer and mesothelial cells. The interaction between CD44 and HA can mediate the adhesion of cancer cells to mesothelial cells (Weidle et al. 2016). Some other molecules can also promote the cancer-mesothelial cell adhesion such as IL-1, β/ β1 integrin interaction, ICAM-1 (Ziprin et al. 2004; Watanabe et al. 2012) and MSLN-MUC6 interaction (Kaneko et al. 2009).

Following the attachment, cancer cells can invade the connective tissue under the mesothelial cell layer to form a metastatic lesion. The first step is called mesothelial clearance, during which the mesothelial cells are pushed apart, which gives way to cancer cell invasion (Barbolina 2018). The RAC1-SMAD pathway can induce the mesenchymal transition of mesothelial cells, which promotes mesothelial cell clearance

by releasing cytokines, ECM components and growth factors (Barbolina 2018). HGF secreted by peritoneal fibroblasts can also promote peritoneal invasion. Targeting HGF with NK-4 can inhibit distant metastasis of gastric cancer cells in mice (Matsumoto et al. 2011). MMPs are also implicated in this metastatic process, especially MMP1, 2 and 9. The secretion of MMP9 can be promoted by CD44, and its expression can also be enhanced by eukaryotic translation elongation factor 1 alpha 2 (eEF1A2) (Kenny et al. 2008; Xu et al. 2013). Both MMP2 and MMP9 can also be upregulated by Discoidin domain receptor tyrosine kinase 1 (DDR1) and transmembrane 4 L six family member 1 (TM4SF1) (Yang et al. 2017).

After invasion, metastatic deposit formation is necessary for tumour cells to adapt to the new environment. A previous study showed that the interaction between pancreatic cancer cells and mesothelial cells can promote the formation of the deposits (Mitra et al. 2015). During this process, cancer cells can foster a tumour stroma to support themselves, which includes cancer-associated fibroblast cells, endothelial cells, immune cells and ECMs (Jayne 2007). The fibroblasts play a pivotal role in the formation of the tumour stroma, which can promote tumour cell proliferation, migration and invasion. The decreasing of miR-214 and miR-31 is associated with the transformation of these cells (Ozdemir et al. 2015; Ligorio et al. 2019). Cancer can also interact with the immune cells, including the tumour-associated macrophages, ly6G+ and CD11b et al (Acharyya et al. 2012; Pittet et al. 2022; Jaeger et al. 2023). These immune cells can promote cell migration and proliferation by activating the MEK, hedgehog and EGFR pathways (Yin et al. 2016; Gu et al. 2018). Cancer cells also promote lipolysis of the adipocytes located on the omental, which can be utilised by cancer cells as a nutrition supplement (Nieman et al. 2011; Xiang et al. 2017). Furthermore, the adipocytes also facilitate cancer cell invasion by activating the PI3K-Akt pathway (Xiang et al. 2017). In addition to that, omental fat cells secrete factors to promote proliferation and invasion of pancreatic cancer cells, which may be induced by the activation of the SDF1-CXCR4 pathway (Ji et al. 2013).

Angiogenesis is indispensable during the colonisation and growth of metastatic tumours, in which VEGF, integrin β3, PDGF, FGFs, HGF, VASH2 and angiopoietins are implicated (Connolly et al. 1989; Li et al. 2008; Gavalas et al. 2013; Takiguchi et al.

2017; Iida-Norita et al. 2019). Fibroblast growth factor (FGFs) can activate the Akt pathway and promote VEGF expression (Sako et al. 2003; Forough et al. 2005). Vasohibin 2 (VASH2) is another gene that can promote the tumour cell migration and angiogenesis (Iida-Norita et al. 2019). As for the cancer micro-environment, the dendritic cell, together with the SDF1-CXCL12 axis, can induce angiogenesis by promoting the expression of TNF-α and IL8 (Curiel et al. 2004). For pancreatic cancer treatment, once the peritoneum metastasis has occurred, radical surgical excision is usually impossible. At this stage, systemic chemotherapy is commonly considered. Two common chemotherapy regimens for metastatic pancreatic cancer are FOLFIRINOX (oxaliplatin + irinotecan + 5-FU + leucovorin) and AG (gemcitabine + albumin-binding paclitaxel).

Several new treatment strategies targeting peritoneal metastatic lesions have already been applied. Hyperthermic intraperitoneal chemotherapy (HIPEC) is one, which was proven to be efficient in gastric and colorectal cancer treatment (van Stein et al. 2021; Zeng et al. 2022). Despite this, PIPAC (pressurized intraperitoneal aerosolized chemotherapy), EPIC (early postoperative intraperitoneal chemotherapy), NIPS (neoadjuvant systemic and intraperitoneal chemotherapy) and SIPC (sequential intraperitoneal chemotherapy) are also applied to treat peritoneum metastases (Behrenbruch et al. 2017; Prabhu et al. 2022).

HIPEC can directly act on abdominal metastases through regional chemotherapy, hyperthermia and mechanical lavage of large-volume fluid. It is one of the treatment methods for peritoneal metastases of various malignant tumours. For prophylaxis, HIPEC was reported to significantly reduce the risk of peritoneal metastasis in gastric cancer (Desiderio et al. 2017; Yarema et al. 2019).

In gastric cancer, the intraperitoneal use of chemotherapy has also been evaluated. According to the results of a study in Japan, compared with the intravenous chemotherapy group, there was no statistically significant difference in the long-term survival of the patients treated with both intravenous chemotherapy and intraperitoneal chemotherapy (15.5months vs 17.7 months, P = 0.080). However, with the addition of oral S-1, the combination treatment significantly extended the long-term survival in gastric cancer patients with peritoneal metastasis (3-year survival rate: 21.9% vs. 6.0%)

(Ishigami et al. 2018).

1.4 *Anoikis* resistance during metastasis

Anoikis it is a term initially used by Frisch and Francis in 1994, which means 'homeless'. It is an important barrier to inhibit the metastasis of tumours, including pancreatic cancer. Once a normal cell is detached from the extracellular matrix, it will become 'without a home' and enter the progression of apoptosis. ECM contains a variety of different cytokines, which is essential for the survival of a cell, without these factors, cells cannot survive.

1.4.1 Cell death

Cell death mainly takes two forms: necrosis (uncontrolled cell death) and apoptosis (programmed cell death). Necrosis is usually induced by external injury such as radiation, chemicals and heat et al. It is an energy-independent process. Between necrosis and apoptosis there is another intermediate stage called necroptosis, which means regulated necrotic death (Degterev et al. 2005).

Apoptosis is a process whereby a cell stops growing and enters a programmed death. During this progress, caspases are involved, which are divided mainly into two parts: the initiator and the executioner (Elmore 2007). Caspases 8 and 9 are initiators, which activate the executioners (caspases 3) from the procaspases, once the unrepairable damage has occurred. Executioner caspases then induce the activation of endonucleases which destroy the DNA. They can also cause the destruction of other proteins, including nuclear proteins and cytoskeletal proteins etc. (Martinvalet et al. 2005). During apoptosis, the apoptotic bodies are formed, which can be phagocytosed by macrophages to prevent damage to surrounding cells. Apoptosis can be initiated by the damaged cell itself, which is called the intrinsic pathway. If apoptosis is initiated by the interaction between damaged cells and immune cells, it is termed the extrinsic pathway (Sica et al. 1990; Oppenheim et al. 2001). A balance between proliferation and apoptosis is crucial for maintaining tissue homeostasis. Once this balance is interrupted for example, in Alzheimer's disease, there is thought to be an association with excessive apoptosis of neuronal cells (Dickson 2004), while cancer is usually caused by

uncontrolled growth and insufficient apoptosis. The intrinsic pathway is also called the mitochondrial pathway, which can be activated by extrinsic stimulation. One mechanism can be initiated by the decrease of some molecules in the nearby microenvironment, including the cytokines, hormones and growth factors. The absence of these molecules will induce the disinhibition of pro-apoptotic proteins inside the cell. Some other environmental factors, including hypoxia, radiation and toxins can also induce apoptosis (Brenner and Mak 2009). The intrinsic pathway is initiated by the interaction between caspase 9 and Apoptotic peptidase activating factor 1 (ARAF1). Both molecules contain a caspase recruitment domain (CARD), and the CARD on APAF is blocked and unable to be bound. When the apoptosis is initiated, pores are opened on the mitochondrial membrane, so cytochrome c, HtrA serine peptidase 2 (HtrA2) and Diablo IAP-binding mitochondrial protein (Smac) will leak from the mitochondria. These molecules can activate the process of apoptosis. The interaction of cytochrome c with APAF1 can induce a conformational change, then CARD and oligomerization domains on APAF1 can be exposed. These APAF1s can combine together to form apoptosomes (Acehan et al. 2002) . The CARD domains on apoptosomes will recruit and activate procaspase 9. Caspase 9 can then activate caspase 3 leading to subsequent apoptosis. Other molecules leaked from mitochondria can inhibit the IAPs (inhibitors of apoptosis proteins), to promote apoptosis synergistically (Ekert and Vaux 2005).

The extrinsic pathway is usually triggered by natural killer cells and macrophages. Once the death ligands produced by the immune cells bind to the death receptors (DRs), which belong to the tumour necrosis factor (TNF) family on the target cells (Bossen et al. 2006), procaspase 8 will be recruited and bind with the death-inducing signalling complex (DISC) located on the cell membrane (Kim et al. 2004). After procaspase 8 binds to the DISC this forms a dimer and is simultaneously activated. The mechanism of caspase 8 inducing apoptosis differs in different cells (Samraj et al. 2006), which can be divided into type I and type II cells. In type I cells, caspase 8 directly activates the executioner caspases, while in type II cells IAPs inhibit the activation of the caspases downstream signal. This effect can be interrupted by pro-apoptotic molecules released by mitochondria (Spencer et al. 2009).

Apoptosis is usually thought to be non-harmful to surrounding tissue. However, a

particular form of apoptosis has also been detected, that even in the cell undergoing a programmed death, it also causes inflammation, which is called pyroptosis (Fink and Cookson 2005). This process is associated with caspase 1. When its precursor protein is activated, it can induce the formation of pores on the cell membrane, ions can pass through these pores, leading to a decreased osmotic pressure in the cell. Excessive water enters the cell, causing swelling and lysis. During this process, the pro-apoptotic molecules in the dead cells can be released into the microenvironment, which can induce inflammation (Hersh et al. 1999).

Sometime cells can be damaged, but not to a severe level, so autophagy can be triggered. During this process, some proteins or organelles are moved into the lysosomes and digested, then the components can be reused to synthesise other proteins (Shintani and Klionsky 2004). Autophagy is usually applied to recycle the organelles, while some senescent and early cancer cells are also removed in this way (Mizushima et al. 2008). There are three forms of autophagy: micro-autophagy, macro-autophagy and selective-autophagy (Cuervo 2004). Micro-autophagy is a specific form of autophagy through which the damaged organelles are fused with lysosomes. During macro-autophagy, a portion of cytoplasm in a cell is enclosed into a vesicle with subsequent fusion with the lysosome (Li et al. 2012a). As for selective autophagy, target proteins can be bound with a cytosolic chaperone which will then be carried into the lysosome, which is mediated by the receptor located on the lysosome membrane: LAMP-2A (Dice 2007).

Necrosis is an uncontrolled cell death, which is associated with inflammation (Elmore 2007). The contents in necrotic cells will be released into the surrounding tissues resulting in damage. Necrosis is an energy-independent process.

Necroptosis is a controlled necrosis, which is regulated by RIP1 and RIP3 (receptor-interacting proteins 1 and 3). It is usually activated by death receptors (DRs) (Oliveira et al. 2018). When activated by its ligand, TNFR1 is one of the DRs that can promote the formation of pro-survival complex I, which includes TNFR-associated death domain (TRADD), several ubiquitin E3 ligases and RIP1. Once the RIP1 is deubiquitinated, it can induce the formation of complex IIa and complex IIb. Complex IIa will activate apoptosis by activating caspase 8, while complex IIb can initiate

necroptosis (Wang et al. 2014).

Oncosis is another pathway that induces cell death, characterized by the swelling of cells and organelles. During this process, the energy supply for the cell is interrupted, causing the dysfunction of ionic pumps on the cell membrane (Majno and Joris 1995). During this process, the cell debris would leak out which will induce inflammation. During apoptosis, the ATP which supplies the energy may be used up, that can induce necrosis, so-called secondary necrosis.

1.4.2 *Anoikis*

In healthy people, the cells usually grow at the right location, and apoptosis usually happens when they are detached from the primary location. This is *anoikis*. The survival signals maintained by the ECM are necessary for cell growth, and *anoikis* is usually induced by detaching from the ECM (Frisch and Francis 1994; Douma et al. 2004). It was clarified that the integrins are necessary for inhibiting *anoikis*, and the anti-integrin antibody can promote cell apoptosis (Park et al. 2006; Wang et al. 2021). Bcl-2 is another gene that can inhibit *anoikis* (Douma et al. 2004). The ECM not only gives physical support for the tumour cell, the interaction between the ECM and cell adhesion can also activate many signal pathways which play important roles in maintaining the cell viability. Only the correct ECM which contains the suitable surface molecules can support the target cells. For example, epithelial cells can be supported by the interaction between laminin and integrin α6/β1, while collagen I with an interaction with integrin α2/β1 cannot prevent the cell from *anoikis* (Boudreau et al. 1995; Pullan et al. 1996). There are at least four different integrins which can interact with the ECM and support cells: α1β1, α5β1, α6β1 and αvβ3 (Zhang et al. 1995; O'Brien et al. 1996; Matter et al. 1998). These integrins can help increase cell viability by activating focal adhesion kinase (FAK) signalling (Frisch et al. 1996b), ILK (integrin-linked kinase) (Bottcher et al. 2009), Src kinase (Parsons and Parsons 2004) and the PI3K-Akt pathway (Khwaja et al. 1997).FAK is a crucial molecule in the focal adhesion pathway, which is activated by integrins and can promote cell survival, proliferation, and motility. FAK can also activate the PI3K-Akt and MAPK pathways, further enhancing cell survival. Akt can suppress the leakage of cytochrome c, promote Bcl-2 release and inhibit caspase 9 by initiating

phosphorylation (Datta et al. 1997; Schaller 2001). Bim and Bad are two proteins in the BCL-2 family, which can promote cell apoptosis. Activated MAPK1 and 2 can phosphorylate Bim, promoting its ubiquitination and can also inhibit its expression (Marani et al. 2004; Ley et al. 2005). MAPK can also phosphorylate Bad and inhibit its promotive effect in apoptosis (Bonni et al. 1999; Datta et al. 2000; Virdee et al. 2000). Another mechanism involves the MAPK pathway which can upregulate the expression of BCL-2 and BcL-XL which protect cells from apoptosis (Schlaepfer et al. 1999). ILK is another molecule which can prevent cells from undergoing *anoikis*, it can be activated by integrin receptors, and further activates the PKB-AKT signal pathway to improve cell viability (Wu 2001). For metastasis to be successful, evasion from *anoikis* is vital for the cancer cells which can be operated through following four mechanisms: 1) modifications of their integrins to adapt to the new microenvironment; 2) constitutive activation of the pro-survival signal pathway; 3) EMT can help cells to avoid *anoikis*; 4) alteration of metabolism through Warburg metabolism or autophagy mechanism.

The ECM can support normal melanocytes around the cells to modify the surface adhesion proteins, including integrins. In contrast, the collagen in the dermis does not support it because melanocytes do not express integrins, which bind with these collagens. When the malignant transformation happens, the integrin α5/β3 on the cell membrane will be upregulated, which enable the melanoma cells to receive support from the dermis during the invasion (Montgomery et al. 1994). Integrins can prevent *anoikis* through pathways including the PI3K pathway, ERK pathway and some MAPK pathways (Giancotti 2000). Integrins $\alpha 1\beta 1$, $\alpha 5\beta 1$ and $\alpha V\beta 3$ recruited FAK can suppress *anoikis* by regulating the PI3K pathway, MAPK pathway tyrosine kinases and small GTPases (Hungerford et al. 1996; Parsons 2003). *Anoikis* induced by p53 can be suppressed by FAK (Almeida et al. 2000). For pro-survival pathways, the PI3K-AKT pathway is one of the most important pathways that maintains the cell viability being the most common mechanism for the evasion of *anoikis* (Davies et al. 1999; Chen et al. 2001; Altomare and Testa 2005). Akt suppresses the function of some pro-apoptotic molecules such as Bad and procaspase 9, and it can also upregulate inhibitor of nuclear factor kappa B kinase (IKK), which is an anti-apoptosis gene (Semenza et al. 1996; Royer et al. 2000; Yu et al. 2000; Chen et al. 2001). Furthermore, sustained activation

of Akt can promote the progress of EMT. Activation of Src kinases is another means for cells to avoid *anoikis*: Src can enhance EMT, and promote the PI3K-Akt pathway by phosphorylating FAK. In addition, caspases can be inhibited by Src (Avizienyte and Frame 2005; Bouchard et al. 2007).

During the progress of EMT, the expression of several genes is modified, including the deregulation of E-cadherin and upregulation of Snail, N-cadherin, TWIST and ZEB1. The decrease of E-cadherin can enhance cell viability by upregulating β-catenin, which can activate the MAPK pathway (Orford et al. 1999). TWIST and Snail promote cell survival by upregulating the expression of Bcl-2 (Blanco et al. 2002; Yang et al. 2004). ZEB1 was found to be implicated in the anchorage-independent survival of lung cancer cells, which can activate the Akt pathway and increase the *anoikis* resistance (Takeyama et al. 2010).

To avoid *anoikis*, cell metabolism also needs to be modified. In normal cells, once they detach from the ECM, there will be a reduction of ATP and NADPH, inducing insufficient energy and increased ROS can induce apoptosis. ERBB2 overexpression can help cells to confront this by inducing PI3K-Akt pathway activation, which can increase the glucose uptake, and ERBB2 can also promote NADPH production and ROS quenching (Schafer et al. 2009; Cairns et al. 2011). Compared with normal cells, cancer cells uptake more glucose; most of them are not consumed by aerobic respiration but are metabolized into lactate (Jeon et al. 2012). Other molecules involved in metabolism modification are HIF-1, c-Myc, PTEN and p53 (Stambolic et al. 2001; Matoba et al. 2006; Feng et al. 2007).

Despite the support from the ECM, the cell shape is also important in maintaining the phenotype of cells. A special structure of the cancer cell derived from epithelial cell can suppress its apoptosis, and rearrangement of the cytoskeletal epithelial cells can help breast cancer cells to avoid *anoikis* (Weaver et al. 2002). Furthermore, overexpression of the neurotrophic receptor tyrosine kinase 2 (TrkB/NTRK2) gene, induces cell shape change, causing cell rounding and improving the resistance to *anoikis*.

Growth factor receptors (GFRs) are regulated by the interaction between integrins and the ECM, further promoting cell proliferation (Giancotti and Ruoslahti

1999). In neuro system, the cross-talk between integrins and GFRs is important for cell survival, through activating the ERK pathway (Colognato et al. 2002). Furthermore, IGF-1 in epithelial cells can be activated by the adhesion to lamina (Lee and Streuli 1999), and it can suppress apoptosis by activating the PI3K pathway.

All the pathways inducing anoikis terminally come together into the caspases, and the BcL2 family plays an important role in these pathways, which include the anti-apoptotic proteins (BCL-2, BcL-XL), pro-apoptosis proteins (Bax, Bak) and BH3 only proteins (Bid, Bad, Bim, Bmf etc.). The BH3-only protein plays an important role. In the intrinsic pathway, pro-apoptotic molecules in mitochondria need to penetrate out to activate caspase 8 and Bcl-2 can suppress this process (Frisch et al. 1996a; Almeida et al. 2000), while extracellular death receptor inhibitors do not interrupt *anoikis*. In addition, the interaction between epithelial cells and ECM can promote the expression of c-Flip, which suppress caspase 8 (Almeida et al. 2000). Bax and Bak are implicated in the intrinsic pathway of apoptosis. During this process, they are moved to the mitochondria, inducing the leakage of pro-apoptosis protein within 30 minutes after detachment from the ECM (Valentijn et al. 2003). How Bax and Bak are activated is yet to be discovered and the Bcl-2 may be implicated in the activation (Bouillet and Strasser 2002). Some other BH3- only proteins are found to be implicated in *anoikis* in different cells. Noxa and Puma can promote the *anoikis* of fibroblasts (Shibue et al. 2003), whilst Bad and Bim are controlled by the PI3K and ERK pathways (Gilley et al. 2003; Ley et al. 2003). Bid is cleaved when the death receptor is activated and induces *anoikis*. While it has also been found that the non-cleaved Bid can be translocated to the mitochondrial membrane directly in MEC cells detached from the ECM, which means it can mediate *anoikis* to bypass the death receptor pathway (Shimamura et al. 2000; Valentijn and Gilmore 2004). Bmf is another BH3-only protein, which is also associated with *anoikis* through its interaction with the myosin V motor complex (Puthalakath et al. 2001). Other BH3-only proteins are yet to be examined for their role in *anoikis*. Bad, Bik, Bmf, Noxa, Puma and Hrk can increase the sensitivity to *anoikis* (Vander Heiden et al. 1997; Belzacq et al. 2002; Idogawa et al. 2003; Kuwana et al. 2005). Mitochondrial protein Bit1 is implicated in promoting *anoikis*. Once cells are detached from the ECM, Bit1 is then released into the cytoplasm and mediates apoptosis by the caspase 8 independent

pathway (Jan et al. 2004; Jenning et al. 2013).

1.5 Key molecules in peritoneal metastasis

Adhesion molecules are implicated in tumour metastasis and invasion. These molecules can bind with other cells or ECM molecules during dissemination (Table 1.3)

Table 1.3 Adhesion molecules involved in cancer cell metastasis (2023b).

Gene name	CD Nomenclature	Ligand
Integrins		
Integrin alpha L	CD11a	ICAM-1, 2 and 3
Integrin alpha M	CD11b	ICAM-1, fibrinogen, and Mac-1
Integrin alpha X	CD11c	ICAM-1, fibrinogen, iC3b
Integrin beta 2	CD18	ICAM-1, 2 and 3
Integrin beta 1	CD29	VLA-1 to 6
Integrin alpha 2b	CD41	fibrinogen, fibronectin, thrombin and von Willebrand factor
Integrin alpha 1	CD49a	collagen IV
Integrin alpha 2	CD49b	collagen and laminin
Integrin alpha 3	CD49c	collagen, laminin and fibronectin
Integrin alpha 4	CD49d	fibronectin, VCAM and MadCAM
Integrin alpha 5	CD49e	fibronectin
Integrin alpha 6	CD49f	laminin
Integrin alpha v	CD51	fibronectin, vitronectin, fibrinogen, von Willebrand factor, thrombospondin and CD31
Integrin beta 3	CD61	Binds fibrinogen, fibronectin, thrombin and von Willebrand factor
Integrin alpha e	CD103	Binds E-Cadherin by dimerizing with integrin beta 7
Integrin beta 4	CD104	laminin
Integrin alpha 4 beta 7	LPAM-1	fibronectin, VCAM and MadCAM
Alpha 7 integrin		laminin
Alpha 9 beta 1 integrin		VCAM-1 and osteopontin
Alpha v beta 5 integrin		vitronectin
Non-Integrin Cell Adhesion Molecules		
PECAM-1	CD31	Homophilic interaction
CD34		L-Selectin
ICAM-1	CD54	LFA-1 or Mac-1
E-Selectin	CD62E	ESL-1 and PSGL-1
L-Selectin	CD62L	GlyCAM-1, MadCAM-1 and CD34

P-Selectin	CD62P	Binds to PSGL-1 on lymphocytes
CD99		Homophilic interaction
ICAM-2	CD102	LFA-1
VCAM	CD106	LPAM-1
Basigin	CD147	integrins
JAM-1	CD321	homophilic binding, LFA1
JAM-2	CD322	JAM-C, VLA-4
JAM-C	CD323	homophilic binding, Mac-1
MadCAM-1		LPAM-1, VLA-4 and L-Selectin
LAMP-2 (MAC-3)	CD107b	Lysosomal associated membrane protein and galectin
Gene name	CD Nomenclature	Ligand
Integrins		
Integrin alpha L	CD11a	ICAM-1, 2 and 3
Integrin alpha M	CD11b	ICAM-1, fibrinogen, and Mac-1
Integrin alpha X	CD11c	ICAM-1, fibrinogen, iC3b
Integrin beta 2	CD18	ICAM-1, 2 and 3
Integrin beta 1	CD29	VLA-1 to 6
Integrin alpha 2b	CD41	fibrinogen, fibronectin, thrombin and von Willebrand factor
Integrin alpha 1	CD49a	collagen IV
Integrin alpha 2	CD49b	collagen and laminin
Integrin alpha 3	CD49c	collagen, laminin and fibronectin
Integrin alpha 4	CD49d	fibronectin, VCAM and MadCAM
Integrin alpha 5	CD49e	fibronectin
Integrin alpha 6	CD49f	laminin
Integrin alpha v	CD51	fibronectin, vitronectin, fibrinogen, von Willebrand factor, thrombospondin and CD31
Integrin beta 3	CD61	Binds fibrinogen, fibronectin, thrombin and von Willebrand factor
Integrin alpha e	CD103	Binds E-Cadherin by dimerizing with integrin beta 7
Integrin beta 4	CD104	laminin
Integrin alpha 4 beta 7	LPAM-1	fibronectin, VCAM and MadCAM
Alpha 7 integrin		laminin
Alpha 9 beta 1 integrin		VCAM-1 and osteopontin
Alpha v beta 5 integrin		vitronectin
Non-Integrin Cell Adhesion Molecules		
PECAM-1	CD31	Homophilic interaction
CD34		L-Selectin
ICAM-1	CD54	LFA-1 or Mac-1
E-Selectin	CD62E	ESL-1 and PSGL-1

L-Selectin	CD62L	GlyCAM-1, MadCAM-1 and CD34
P-Selectin	CD62P	Binds to PSGL-1 on lymphocytes
CD99		Homophilic interaction
ICAM-2	CD102	LFA-1
VCAM	CD106	LPAM-1
Basigin	CD147	integrins
JAM-1	CD321	homophilic binding, LFA1
JAM-2	CD322	JAM-C, VLA-4
JAM-C	CD323	homophilic binding, Mac-1
MadCAM-1		LPAM-1, VLA-4 and L-Selectin
LAMP-2 (MAC-3)	CD107b	Lysosomal associated membrane protein and galectin

Cancer metastasis usually starts from the detachment of cancer cells from the primary lesion; during this step, the biological function of cadherin is usually interrupted. The interaction between tumour cells and the nearby tissue is disrupted, so that the cancerous cells can leave the initial lesion and enter the blood or lymph circulation (Takeichi et al. 2000). For example, E-cadherin expression is usually deregulated during EMT and is associated with poor prognosis and further promoting distant metastasis. In addition to cadherins, neural cell adhesion molecule 1 (N-CAM) is a member of the immunoglobulin superfamily, the decrease of which was shown to be associated with an enhanced metastatic ability in glioma (Andersson et al. 1991).

During dissemination, some cell adhesion molecules promote the homotypic aggregation between cancer cells, to support each other and avoid *anoikis*. These molecules include galactoside-specific lectin, LFA-1, CD44, ICAM-1 and cadherin etc. (Oppenheimer 1975; Raz and Lotan 1981; Mentzer et al. 1985; Wolf et al. 1987; Birch et al. 1991).

Following dissemination, tumour cells can bind with endothelial cells, during hematogenous metastasis, or to mesothelial cells during peritoneal metastasis. Several studies found that cytokines IL-1 and TNF promote the expression of ICAM-1, ELAM-1 and VCAM-1 in endothelial cells, which can promote cell-cell adhesion (Bevilacqua et al. 1987; Pober et al. 1987; Osborn et al. 1989). This means that cytokines may mediate the adhesion of tumour cells in a similar mechanism as in recruiting leukocytes. Furthermore, it was also found that the inter-glycolipid interaction can enhance cell

motility (Kojima and Hakomori 1991). The overexpression of CD44, which is a receptor detected on lymphocytes, fibroblasts and epithelial cells, can promote the distant metastasis of pancreatic cancer (Hofmann et al. 1991; Faassen et al. 1992).

After the tumour cells bind with endothelial or mesothelial cells, they need to invade through the layer of cellular barrier to enter the tissue, during which the integrins (VLAs) play an important role (Hynes 1987). ITGA2 overexpression in lung cancer can induce a significant increase in the cell adhesion ability to collagen and laminin (Chan et al. 1991).

1.5.1 CD44

CD44 is a well-characterized hyaluronic acid receptor, the standard isoform of which is called CD44s.It consists of 363 amino acids and has three domains: cytoplasmic domain, transmembrane domain and extracellular domain. The HA binding domain is located in the extracellular domain, and it is highly conserved, which is also called the link module of the CLP domain (Kohda et al. 1996) (Figure 1.1).

It was found that all CD44 isotopes contain the HA binding domains. However, not all cells respond to HA binding, since CD44 isoforms present a variety of formats following post-translation modifications: active, inducible or inactive patterns on the cell membrane (Lesley et al. 1995).

Apart from CD44 itself, some other molecules also bind with the CD44, and osteopontin is one of them. It is a cytokine which can be secreted by several different cells and has a chemotactic effect (Weber et al. 1996). It binds with CD44 specifically to promote cancer cell metastasis (Ue et al. 1998), which can be competitively inhibited by HA (Ue et al. 1998). Other molecules which can bind with the CD44 include collagen, laminin and fibronectin (Faassen et al. 1992; Jalkanen and Jalkanen 1992), suggesting that CD44 can also enhance cell adhesion to the ECM.

CD44 can interact with other cell membrane proteins, especially the Her2 (ERBB2) cell surface protein (Xu et al. 1997). Both the expression and the function of CD44 are coupled with Her2. In breast cancer, heregulin is a ligand of Her2 which can increase cell adhesion and invasion, by upregulating CD44. The pro-invasion function of heregulin can be partially blocked by CD44 antibody (Xu et al. 1997). Furthermore, once the Her2 expression is repressed, the CD44s expression and the adhesion mediated by

CD44 are also significantly inhibited (Bourguignon et al. 1997).

For CD44 in cancer cells, it has been described that the cells can migrate across the HA, which means the CD44 and HA interaction can mediate cell movement. It was also found that CD44 has an altered expression in many cancers and its upregulation is associated with a more aggressive cancer type (Birch et al. 1991; Sy et al. 1991). Furthermore, the interaction between CD44 and hyaluronic can promote cancer cell development (Sy et al. 1992; Zawadzki et al. 1998), once this interaction is inhibited, the formation of metastatic lesions can be suppressed (Bartolazzi et al. 1994; Zeng et al. 1998). In addition to that, the competitive inhibition of CD44 can even promote apoptosis (Yu et al. 1997). For cancer metastasis, compared with CD44s, CD44v (another isotope of CD44) may play a more important role (Birch et al. 1991; Sy et al. 1991), which may promote metastasis by enhancing cell viability (Driessens et al. 1995).

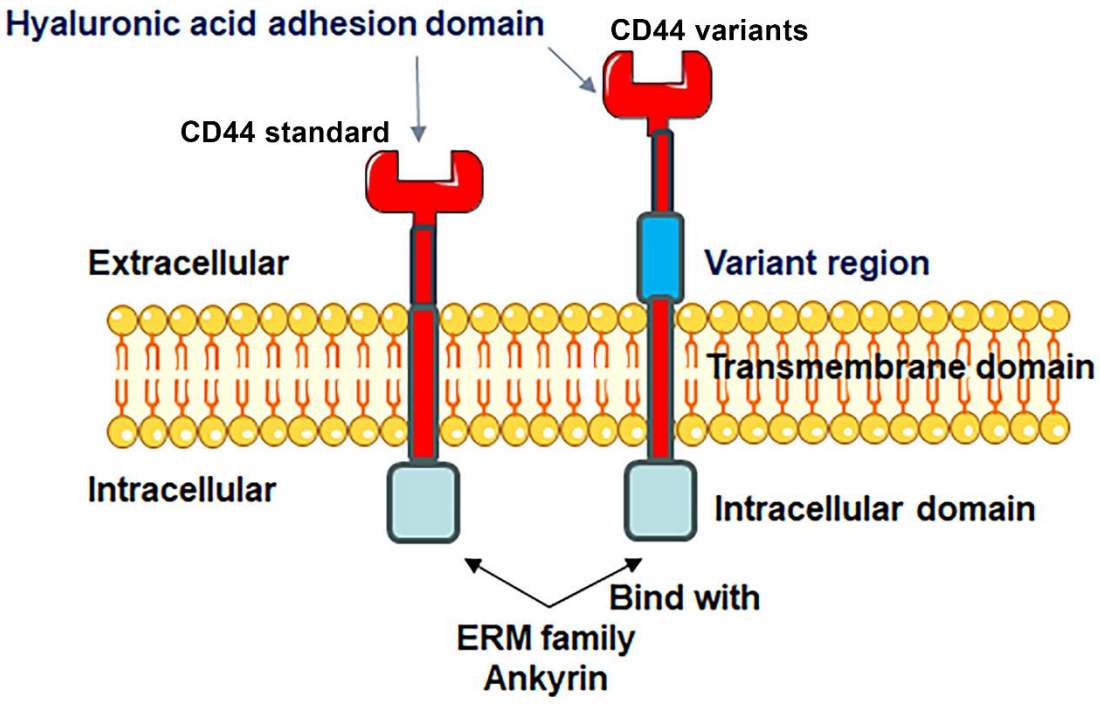

Figure 1.1 The structures of both CD44s and CD44v. Compared with CD44s, CD44v contains a variant region. Both of them contain a hyaluronic acid adhesion domain. The intracellular domain interacts with the cytoskeleton through binding with ankyrin and the ERM family (ezrin, radixin, moesin) (Kohda et al. 1996).

1.5.2 LYVE-1

LYVE1 (Lymphatic vessel endothelial hyaluronan receptor 1) structure is similar to that of CD44 (Figure 1.2), which has a HA binding domain and a transmembrane region. Its interaction with HA can enhance the cell adhesion ability to the ECM. Both of them can bind with soluble and immobilised HA (Jackson et al. 2001). For CD44, the HA binding domain is normally inactivated, and it can be activated by inflammatory factors (Lesley et al. 1993; Kincade et al. 1997). To date, the default status of LYVE1 is still unknown.

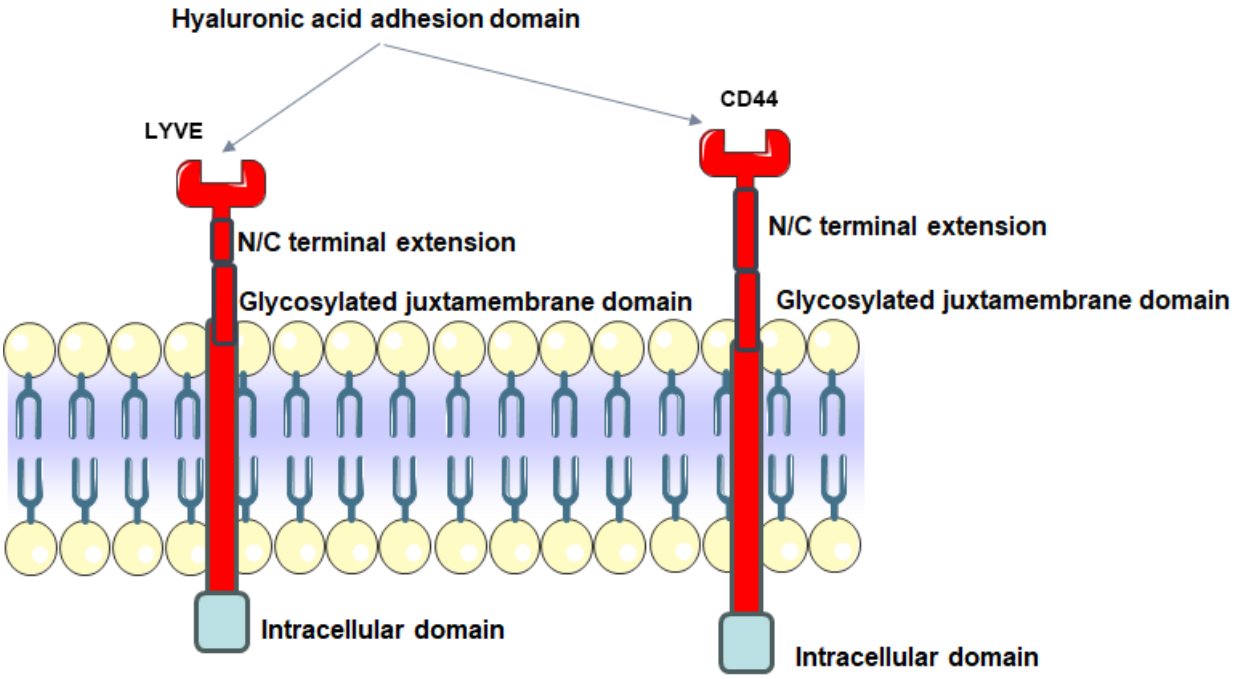

Figure 1.2 The structure of LYVE and CD44 are similar, both contain the hyaluronic acid, N/C terminal extension domain and glycosylated juxta-membrane domain (Jackson et al. 2001).

As for the bio-function of LYVE-1 it can transport HA across the lymphatic wall and it also mediates the uptake of HA. LYVE-1 is located both on the luminal and abluminal faces of the lymphatic vessel, so there is a hypothesis that LYVE-1 can shuttle across the lymphatic vessel wall and transport HA (Mandriota et al. 2001; Prevo et al. 2001). Furthermore, the interaction between HA and LYVE-1 can enhance the migration of lymphocytes, since HA bound to LYVE-1 might promote cell adhesion and mitosis of CD44+ lymphatic cells. In cancers, high density of LYVE-1^{+} vessels is positively associated with lymph node metastasis (Jackson et al. 2001).

1.5.3 Integrins

Integrins are a family of proteins located on the cell membrane which mediate the interaction between cells and the ECM, the expression of which is altered in numerous types of cancer (Seguin et al. 2015; Hamidi et al. 2016). Despite the expression regulation, many additional mechanisms are applied to adjust integrins' activity in cells. Integrins are implicated in nearly every step of cancer development, including initiation, invasion, escaping *anoikis* and promoting metastatic niche formation. Cancer metastasis usually starts from invasion through the basement membrane, during which MMPs play an important role, while the integrins can promote the expression of MMPs (Munshi and Stack 2006). During invasion, cancer-associated fibroblasts can promote this progression, through the interaction with integrins and the ECM, which can induce the deposal of the fibronectin (Attieh and Vignjevic 2016) and generate tracks in the ECM, making cell migration easier (Gaggioli et al. 2007). Once cancer cells enter the blood, integrins can also help them to avoid *anoikis* (Strilic and Offermanns 2017). At the end of circulation, cancer cells aggregate and recruit fibronectin to activate the integrins, which can help cells to extravasate from the blood vessels (Malik et al. 2010; Knowles et al. 2013). Furthermore, once cells enter the tissue, integration between integrins and the ECM will determine whether the proliferation can start or dormancy is more feasible (Lambert et al. 2017).

It was reported that cell motility is important to tumour growth, invasion and metastasis, as *in vitro* study shows integrins can interact with the ECM and propel the cell to move forward, by converting the actin polymerisation, which can significantly increase cell migration (Mitchison and Kirschner 1988; Chan and Odde 2008; Gardel et al. 2008). In breast cancer and PDAC, the degradation of collagen in the tumour stroma is usually associated with a worse prognosis (Provenzano et al. 2006; Laklai et al. 2016). Collagen-binding integrins can also mediate the removal of collagen. In addition to that, in colon cancer, the αvβ3 integrin on CAFs can promote the invasion by promoting the clearance of fibronectin (Attieh and Vignjevic 2016). In recent research, it has been found that AMPK inhibition can induce the activation of integrins and the removal of fibronectin (Georgiadou and Ivaska 2017; Georgiadou et al. 2017).

The balance between cell-cell interaction and cell-ECM interaction regulates cell

migration. The interactions between integrins and the ECM can interrupt the intracellular adhesion mediated by E-cadherin (Borghi et al. 2010) while the reintroduction of integrin β1 into integrin β1-null epithelial cells can induce the loss of cell-cell adhesion (Gimond et al. 1999). The integrin traffic inside the cell is also implicated in tumour invasion, by promoting the remodelling of actin and membrane protrusion (Paul et al. 2015). It was found that the mutation of p53 can promote the invasion and metastasis of cancer cells (Adorno et al. 2009; Muller et al. 2009; Morton et al. 2010), also the mutant p53 can promote the recycling of α5β1 integrin, which is positively associated with cell invasion in a fibronectin-rich 3D model driven by RHO (Jacquemet et al. 2013). Furthermore, integrins can help stabilize filopodia, by regulating the activity of calcium channels and the downstream signalling of integrin itself, which is important for cancer cell migration (Jacquemet et al. 2017).

In addition to the function of integrins in regulating focal adhesion pathways, they have also been proven to be associated with pathways that can help cancer escape from *anoikis*. As aforementioned, integrins can recruit the focal adhesion pathway protein to support cancer cells. Despite this, integrins can also support cancer cells in a ligand-independent manner. The MET pathway can be activated by HGF (hepatocyte growth factor), following which, the β1 integrins can be endocytosed (Mai et al. 2014; Barrow-McGee et al. 2016). The endocytosed β1 integrins cannot be degraded, leading to a prolonged activation of the MET pathway and ERKs. This mechanism is profound for the MET pathway to help cancer cells in evasion of *anoikis* (Barrow-McGee et al. 2016). More interestingly, in breast cancer cells and glioblastoma, MET protein can replace the α5 integrin which binds with β1 integrin to form a MET- β1 complex, while its function is still unrevealed (Barrow-McGee et al. 2016). Integrin αvβ3 also recruits SRC protein inducing the activation of SRC, which can support cells survival (Desgrosellier et al. 2009).

During metastasis, extravasation is another important step. Integrin α5 can interact with NRP2 (neuropilin 2) to promote extravasation (Cao et al. 2013). Integrin β1 has been implicated in the metastatic foci formation in both breast cancer and PDAC, though the exact mechanism is yet to be elucidated (Huck et al. 2010; Grzesiak et al.

2011). One possible mechanism is that the integration between β1 integrins and ECM plays a critical role in the initial formation and stabilizing of the metastatic foci (Chen et al. 2016a). Procedures which are regulated by integrins during cancer metastasis were shown in Figure 1.3

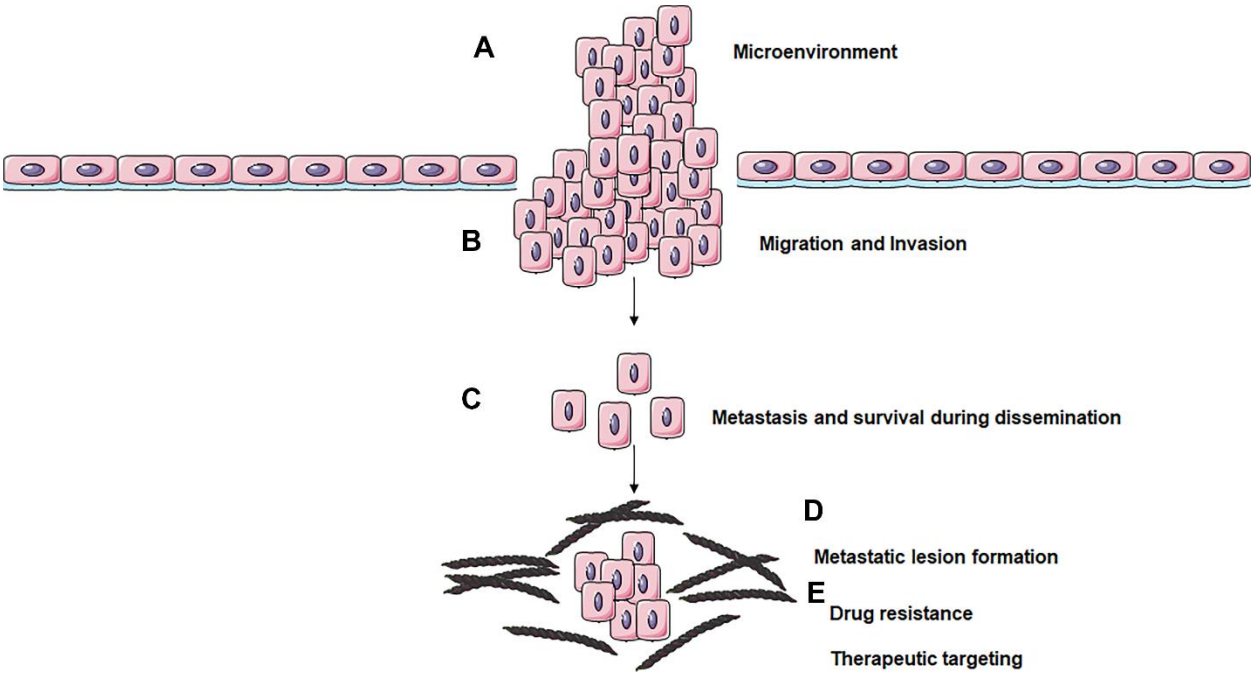

Figure 1.3 Integrins are implicated in distant metastasis (A) Integrins are upregulated in the tumour microenvironment, which can enhance the outside-in signalling pathway and cooperate with RTKs and other oncogenes. (B) During migration and invasion, higher integrins are associated with the activation of proteases. Integrins are implicated in the metastasis guided by CAFs. (C) Higher integrin levels can enhance cell viability by contacting with endothelium or mesothelium. Endosomal integrins can aid cancer cells to avoid *anoikis*. (D) Integrins can promote the formation of metastatic lesions by activating cancer from dormancy. (E) Integrins are implicated in drug resistance. Integrins are also target molecules which can be blocked during cancer treatment. (Hamidi and Ivaska 2018)

1.5.4 Cadherins

Cadherins are a large superfamily of transmembrane proteins and 12 main variants are involved in the development of human cancer (Table 1.4). Cadherin 1 (CDH1), also known as E-cadherin, is recognised as a tumour suppressor, by regulating cell adhesion

and inhibiting the oncogene β-catenin and EGFR. It can also promote cell survival and metastasis in invasive breast carcinoma (Padmanaban et al. 2019). CDH1 is classified as a paradigmatic classical cadherin, which has five extracellular cadherin repeats, a transmembrane domain and an intracellular domain, which has a high affinity with p120-catenin (van Roy 2014). Both CDH1 and cadherin 2 (CDH2) belong to type I cadherins; compared with CDH1, CDH2 is usually distributed in non-epithelial cells. In cancer, during the progress of EMT, one characteristic is that CDH2 can replace DH1, so CDH2 is usually recognised as a pro-metastasis factor (Thiery et al. 2009; De Craene and Berx 2013). CDH2 (Cadherin-2/ N-cadherin) has its unique function compared with CDH1, it can stimulate the activation of fibroblast growth factor receptor 1 (FGFR1), to further promote the malignancy of tumours (Suyama et al. 2002; Sanchez-Heras et al. 2006).

CDH3 and CDH4 are two other type-I cadherins which are well-studied. The distribution of CDH3 overlaps with CDH1 in basal, suprabasal and simple epithelia (van Roy 2014). In cancer CDH3 can repress the expression of CDH1 and promote CDH2 (Vieira and Paredes 2015). In contrast to this finding, CDH3 also plays a similar role as CDH1 in malignant melanoma and Merkel cell carcinoma, with an inhibition of invasion (Van Marck et al. 2005; Jacobs et al. 2011; Werling et al. 2011; Vlahova et al. 2012). While in colon cancer, compared with normal tissue, the CDH3 increases very early during the malignant transformation. In many epithelial tumour cells, overexpression of CDH3 was observed to promote invasion via regulation of MMPs (Ribeiro et al. 2010). In addition to this, it has also been found that the co-expression of CDH1 and CDH3 can promote the localization of p120- catenin, which is associated with poor survival.

Unlike CDH 1, CDH2 and CDH3, CDH11 is a type II cadherin. Type II cadherins still belong to the classical cadherin family, which has a phylogenetic branch. CDH11 is also known as the osteoblast cadherin and is widely distributed in the human body. It was reported that it is upregulated in prostate cancer and is associated with bone metastasis (Tomita et al. 2000; Chu et al. 2008). It is also upregulated in highly malignant glioblastoma multiforme compared with the normal tissue. CDH11 knockdown can reduce the migrating ability of tumour cells (Kaur et al. 2012).

Table 1.4 Cadherin subtypes in cadherin superfamily (van Roy 2014).

Classical types	Representative member(s)
Classical type I	CDH1
Classical type II	CDH11
Desmosome	DSG2
7D cadherin	CDH16
Truncated cadherin	CDH13
Clustered protocadherin	PCDHα6
Non-clustered protocadherin	PCDH1, PCDH8
Cadherin related proteins	FAT4, FAT1, CDH23, CDHR5

1.6 CMG2

CMG-2 (capillary morphogenesis gene 2), is also known as Anthrax Toxin Receptor-2 or ANTXR2. CMG2 is encoded by the *ANTXR2* gene which located on chromosome 4q of the human genome (Bell et al. 2001). It was originally identified as a gene that has an elevated level in human umbilical vein endothelial cells, that were induced to form capillaries (Bukowski et al. 1983). In 2003, scientists found that this gene encodes proteins that function as a receptor to anthrax and can mediate the internalization of the anthrax toxin (Scobie et al. 2003). It is also called anthrax toxin receptor-2 (ANTXR-2), which is similar to another molecule, anthrax toxin receptor-1 (ANTXR-1, also known as Tumour Endothelial Marker-8 or TEM-8). CMG-2 is also implicated in the tumour formation and development (Cryan and Rogers 2011b).

1.6.1 Structure and distribution of CMG2

CMG-2 was originally described as a 386 amino acid protein with an extracellular, transmembrane and cytoplasmic domain (Bell et al. 2001). It has three other isoforms: CMG2 (488), CMG2 (322) and CMG2 (489) (Scobie et al. 2003). Both CMG-2 and TEM-8 (also called ANTXR-1) are type I transmembrane proteins, containing extracellular von Willebrand Factor A (vWA) domains (Cryan and Rogers 2011b). The vWA domain is widespread in the human body and plays an important role in protein-protein junctions. The protein structure of vWA in TEM8 and CMG2 shares a high

similarity (Fu et al. 2010), which can bind to the PA subunit of anthrax (Cryan and Rogers 2011b). The vWA domain also has an important physiological function, by providing an anchor for the protein-to-protein connection between CMG2 and the extracellular matrix, including collagen IV and laminin, as well as other cell adhesion receptors (Cryan and Rogers 2011b). The structure of CMG2 is shown in Figure 1.4. The transmembrane domain of TEM8 may combine together to form a polymer (Go et al. 2006), with CMG2 possibly having the same characteristics (Deuquet et al. 2012). CMG2 is an intrinsically disordered protein (IDPs), making its intracellular tail structure easily modified under physiological stimulilation. CMG2 intracellular tail is easily modified and binds to numerous different molecules. This may play an important role in regulating the subsequent signal pathway (Dyson and Wright 2005), the half-life of the receptor, and the anthrax toxin uptake (Cryan and Rogers 2011b). CMG2 expression has been evident in gastric mucosa, smooth muscle, stomal cell of endometrium, Achilles tendon, myometrium, gall bladder, urinary bladder, synovial joint, seminal vescicles and rectum (2023a).

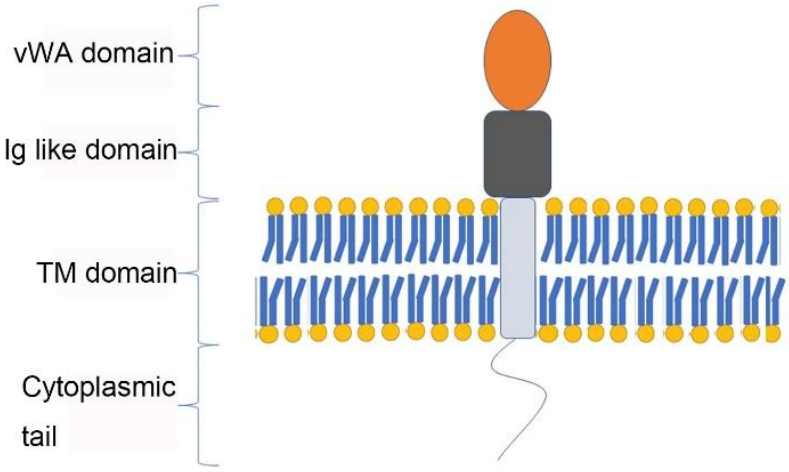

Figure 1.4 The structure of CMG2. CMG2 includes four different subdomains: vWA domin, Ig like domain, transmembrane (TM) domin and cytoplasmic tail (Deuquet et al. 2012).

1.6.2 Biological function of CMG-2

CMG2 has a function as an anthrax toxin receptor. The anthrax toxin is constructed of

three subunits: protective antigen (PA, an 83Kda protein), toxin lethal factor (LF) and oedema factor (EF). When the extracellular domain of CMG2 is bound with the PA subunit, the PA would be cleaved by furin to form a 63Kda PA residue and be anchored onto the cell membrane. The structure of cleaved PA residue is just like a pore and can bind to EF or LF subunits. During this procedure, the toxin complex is transported into the cell through the pore. When this complex arrives at the endosome, because of the acid environment, the confirmation of it will be changed, with subsequent translocation of oedema factor and LF into the cytoplasm. The EF and LF will then impair the metabolism of the cell and induce death.

Some other extracellular matrix proteins, to which anthrax toxin receptors can bind and regulate angiogenesis, are collagen I, collagen IV, fibrinogen, and fibronectin, which can facilitate angiogenesis, while thrombospondins 1 and 2 and decorin can inhibit this (Cryan and Rogers 2011b). Further, CMG-2 appears to promote both endothelial cell proliferation and tubule formation but has little influence on the migration of endothelial cells (Cryan and Rogers 2011b).

CMG2 can also promote angiogenesis induced by growth factors. Compared with TEM8, CMG2 plays an important role in mediating angiogenesis. Compared with TEM-8 Fc, CMG2 Fc significantly inhibits vessel growth induced by basic fibroblast growth factor (bFGF). Furthermore, it has been found that CMG2-/- mice exhibit a striking reduction in bFGF or VEGF induced vessel growth (Cryan et al. 2022). As with cell functions, it has been revealed that the PA subunit can bind to CMG2 and inhibit angiogenesis (Cryan et al. 2022), as the PA treatment can reduce the trans-well migration ability of HMVEC cell line (Rogers et al. 2007). Furthermore, it can also significantly inhibit the adhesion ability of the hy906 cell line (Cryan et al. 2022). Angiogenesis can be promoted by chemotaxis, and RhoA is an important molecule which can accelerate this procedure (Lawson and Ridley 2018), also CMG2 may promote angiogenesis in a similar way as RhoA (Cryan et al. 2022).

1.6.3 Diseases caused by the mutations in CMG-2.

Two typical diseases, that have significant relevance to the mutation of the CMG-2 coding gene *ANTXR2*, are juvenile hyaline fibromatosis (JHF) and infantile systemic

hyalinosis (ISH) (Dowling et al. 2003). Both systemic hyalinoses syndromes are generalized fibromatosis, characterized by accumulation of hyaline in the dermis, gingival hypertrophy, joint contractures, osteolysis, and osteoporosis (Deuquet et al. 2012). The symptoms of ISH are more severe. Fibroblasts from patients with CMG-2 mutations have altered interactions with laminin, although there is no significant difference in interactions with Collagen I or Collagen IV (Dowling et al. 2003).

1.6.4 Signal downstream of CMG2

The CMG2 signal pathways regulating cell biofunction remain unclear, although several signal pathways have been found to be related with CMG2.

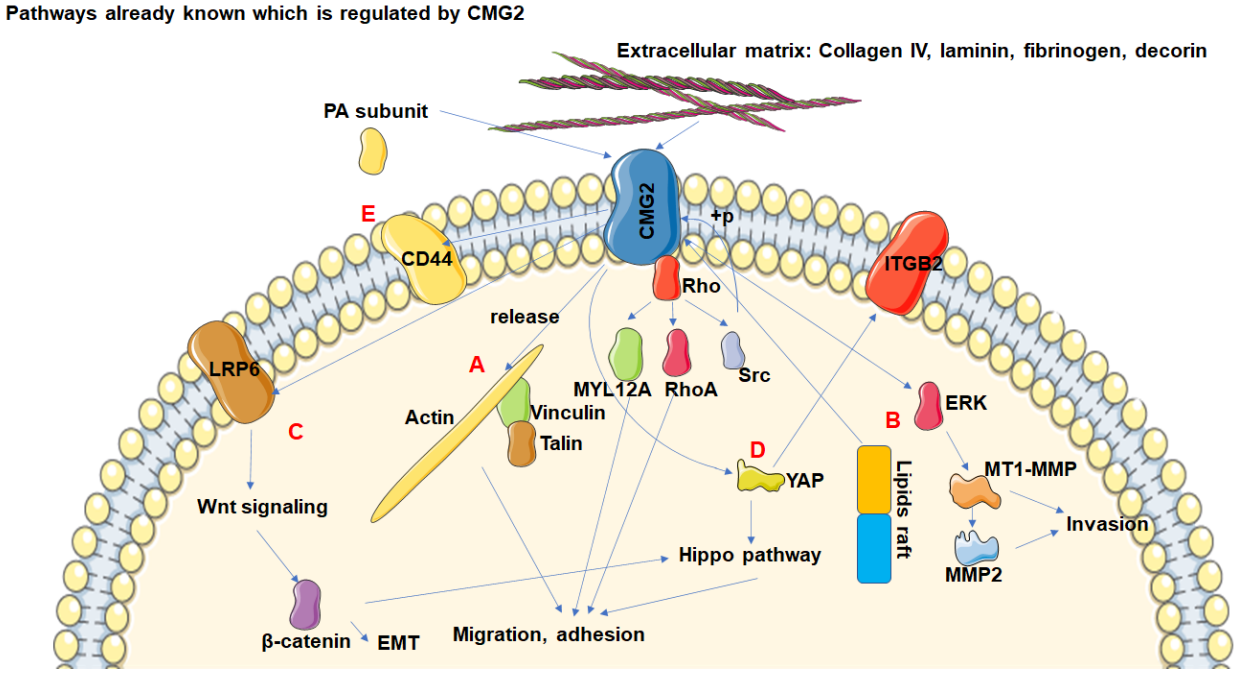

Figure 1.5 CMG2 regulated pathways and molecules. (A) Talin-to-RhoA Switch. Extracellular igands such as collagen VI can bind with the CMG2 and activate this pathway. Src is then released and an unknown protein (protein X) is phosphorylated. Following that, Talin, vinculin, and actin are released. RhoA is then able to bind with CMG2 and activate src. Src will then phosphorylate CMG2 , and promote endocytosis.(Burgi et al. 2020). (B) CMG2 enhances the activation of MT-MMP1 and MMP2 by promoting the phosphorylation of ERK. (C) CMG2 can activate the Wnt pathway by activating LRP6. (D) CMG2 can activate the Hippopathway by promoting the expression of YAP. (E) CMG2 is positively associated with CD44 expression in gastric cancer

1.6.4.1 Talin-to-RhoA Switch

Burgi et al. found that CMG2 can interact with Talin in the cytoplasm (Burgi et al 2020). Talin then binds to Vinculin and further binds to the actin cytoskeleton. When the extracellular ligand such as collagen IV, PA subunit of anthrax toxin binds to the vWA domain of CMG2, src-like-kinases will be recruited and transduce the signal (Burgi et al. 2020).

During this procedure, RhoA is be recruited first, which is a Ras related small GTPase that controls the dynamics of F-actin (Castanon et al. 2013), promoting the release of the Talin-Vinculin- Actin cytoskeleton complex from CMG2 (Burgi et al. 2020). Once the complex is released, RhoA will bind to CMG2 and recruit Src-like-kinases, which can phosphorylate the intracellular tail of CMG2. After this, the signal can be transduced into the cell. Hyaline fibromatosis syndrome (HFS) is caused by a mutation that induces malformation of Talin, which cannot bind to the intracellular tail of CMG2 properly. It can lead CMG2 to be bound with RhoA constitutively, so the CMG2 and downstream signal pathway will be activated permanently. This cell produces membrane protrusions in a deregulated pattern and cannot mediate collagen VI degradations and eventually cause HFS. (Burgi et al. 2020) (Figure 1.5A)

1.6.4.2 CMG2 and MMPs expression

CMG2 can translate the signal from the cholesterol-sphingolipids raft to ERK and then upregulate the expression of MMP1 and MMP2 (Zou et al. 2014). The cholesterol and sphingolipids are assembled to form a lipid raft in the Golgi (Brown and London 1998). Lipid rafts are implicated in the progression of cell proliferation, apoptosis, tumour migration, invasion and chemoresistance (Patra 2008). Jianwen Zou et al., (2014), found that when the amount of cholesterol is deregulated, the lipid rafts will decrease too, which can induce the upregulation of CMG2. Higher CMG2 levels will then induce the phosphorylation of extracellular signal-regulated kinase (ERK). The ERK then upregulates the expression level of MT1-MMP (MMP14) (Zou et al. 2014). MT1-MMP belongs to the MMP family and can degrade the components of the extracellular matrix. MT1-MMP can promote the activation of pro-MMP-2 (Silvius 2003). This suggests that CMG2 may play an important role in promoting tumour metastasis through the

activation of MT1-MMP and MMP2. (Figure 1.5B)

1.6.4.3 LRP6

Low-density lipoprotein (LDL) receptor related protein 6 (LRP6) is a membrane protein which can interact with CMG2, LRP6 transmits signals through Wnt signalling (Abrami et al. 2008). When the PA subunit of anthrax toxin binds to CMG2, the tyrosine residue of the receptor can be phosphorylated through Src -like kinases, Src and fyn, which is important for the uptake of anthrax toxin (Abrami et al. 2010). The anthrax toxin binding to CMG2 can also lead to phosphorylation of LRP6, which is not required for the endocytosis of the toxin, but it might accelerate this progress (Abrami et al. 2010). (Figure 1.5C)

1.6.4.4 ARAP3

Ankyrin repeat and PH domain 3 (ARAP3) is a Rho GAP protein which interacts with phosphatidylinositol-(3,4,5)-trisphosphate (Krugmann et al. 2002). It is implicated in cell attachment and cell spreading on the extracellular matrix and may be relevant for the putative roles of the anthrax receptors in angiogenesis, in the absence of anthrax toxin (I et al. 2004; Krugmann et al. 2006).

1.7 CMG2 in cancer

CMG-2 is widely expressed in normal tissues and is associated with tumour-related angiogenesis (Ye et al. 2014b). Recently, aberration of the expression level of CMG2 in both breast and prostate cancer has been reported. In breast cancer, the level of CMG2 transcripts in advanced tumours are lower compared with early-stage tumours. It has also been shown that a reduced CMG2 expression level is associated with a shorter overall survival. *In vitro* studies, in both breast and prostate cancer, demonstrated that CMG2 is implicated in cancer cell growth, adhesion, and invasion (Ye et al. 2014b; Ye et al. 2014c). Overexpression of CMG2 did not enhance the adhesion of prostate cancer cells to Matrigel, while the knockdown of CMG2 resulted in a significant decrease in matrix adherence. In addition, a significantly increased invasive capacity of the cells was seen, while an impaired invasive capacity was observed in the cells with overexpression

of CMG2 (Ye et al. 2014b). Finally, overexpression of CMG2 in PC-3 prostate cancer cells can suppress the invasion of the PC-3 cells (Ye et al. 2014b).

Glioma is the most common primary tumour of the central nervous system. It was found that CMG2 can promote the formation of laminar pseudopodia and filopodia in glioma cells. Xu et al., (2019), found that this mechanism may lie with the CMG2-induced expression of YAP, a critical factor in the Hippo signalling pathway. This pathway is important in regulating the formation of filopodia and pseudopodia in cancer cells (Xu et al. 2019)

Ji et al found a high CMG2 expression level in gastric cancer linked to a poor prognosis (Ji et al. 2018). Gastric cancer cells with a silenced CMG2 expression have a lower invasiveness and metastastatic capacity, which is associated with a decline of epithelial-mesenchymal transition (EMT). The likely explanantion for the link is that activation of CMG2 initiates the Wnt/β-catenin pathway in gastric cancer cells through the LRP6. The study also showed that CMG2 was positively correlated with cancer stem-like cells (GCSLCs) (Ji et al. 2018), a cell population known to have role in the invasion and metastasis of gastric cancer (Yang et al. 2011; Ji et al. 2018). As previously described, CMG-2 is widely expressed in normal tissues, and it is implicated in tumour-related angiogenesis (Ye et al. 2014b). Furthermore, CMG2 has been shown to mediate the binding of prostate cancer cells to the extracellular matrix, mainly via interactions with laminin and collagen IV (Bell et al. 2001). Collectively, these early studies indicate that CMG-2 is involved in the metastatic traits of cancer cells.

The soft tissue sarcomas are a heterogeneous group of tumours which arise from mesenchymal progenitor cells (Katenkamp and Kosmehl 1995). For this cancer, distant metastasis is still an urgent problem which affects the prognosis. It has been found that CMG2 can enhance the ECM remodelling pathway, which is the metastasis-related urokinase-type plasminogen activator (u-PA) system. It includes the surface-bound uPA receptor (uPAR) and the uPA inhibitor plasminogen activator inhibitor 1 (PAI-1). This pathway can induce migration, invasion and EMT (Peters et al. 2012). In soft tissue sarcoma, a quartile of patients with a lower CMG2 expression have a poor survival (Greither et al. 2017). Despite the uPA-system, CMG2 is also positively associated with CD26, which is a member of the dipeptidyl peptidase 4 family (Greither et al. 2017), it is

also involved in tissue remoulding and putatively in metastasis. Furthermore, CMG2 is inversely correlated with Leucine Rich Repeat Containing G Protein-Coupled Receptor 5 (LGR5), which is mainly engaged in wnt-signalling.

In a recent study, we found that CMG2 is inversely correlated with sex hormones in both breast and prostate cancer. An elevated expression of CMG2 was seen in both ER positive breast cancer cells and AR positive prostate cancer cells, upon deprivation of sexual hormone or silence of ER (Fang et al. 2022). A study in 2016 found that polymorphisms in the *ANTXR2* gene induce individuals to vary in susceptibility to the anthrax toxin. These include two single nucleotide polymorphisms (SNPs) in the promoter region of the gene, at the CREB-binding motif (Zhang et al. 2015). Polymorphisms have been well documented in increased cancer susceptibility, although investigations into the role of CMG2 polymorphisms in cancer is yet to be assessed (Tan I 2010). Another study by Lazennec et al suggests that activated cyclic adenosine monophosphate cAMP responsive element binding protein (CREB) is recruited to genes deemed oestrogen responsive by an ER-coactivator complex (Lazennec et al. 2001). The involvement of CREB in cancer, has also been studied, suggesting its expression is upregulated in breast cancer bone metastasis, with breast cancer cells acquiring an overexpression of CREB during their development (Son et al. 2010).

1.8 Hypothesis and aims of present study

1.8.1 Hypothesis

The elevated expression of CMG2 in pancreatic cancer is actively involved in disease progression and metastasis by coordinating adhesion, migration and invasion.

1.8.2 Objectives:

i) The expression of CMG2 in pancreatic cancer and its role in disease progression.

CMG2 expression in pancreatic cancer was determined using both real time PCR and immunohistochemical staining. Initial discovery of CMG2 in pancreatic cancer will be further validated in other publicly available pancreatic cancer datasets, derived from RNA sequencing and gene array.

ii). CMG2 mediates the cell function change of pancreatic cancer cells.

Influence of CMG2 on the adhesion, proliferation, migration and invasion of pancreatic cancer cells will be tested. The effect of CMG2 on the adhesion of pancreatic cancer cells to mesothelial cells and hyaluronic acid will also be determined. CMG2 knockdown and overexpression models will be used.

iii). CMG2 and *anoikis* resistance of pancreatic cancer cells during the process of dissemination in the peritoneal cavity.

During cancer cell dissemination, avoiding *anoikis* is vital to the disseminating cancer cells in order to survive before subsequent colonisation. *In vitro* experiments and a flow cytometric apoptosis assay will be applied, to check whether CMG2 affects cell survival and aggregation during cancer cell dissemination in the peritoneal cavity.

iv). Molecular machinery of CMG2 regulated adhesion.

Both mass spectrometry assay and antibody-based protein array will be employed to dissect the molecular mechanisms underlying CMG2 regulated cellular functions in pancreatic cancer cells

.

Chapter 2

Materials and methods

2.1 Materials, reagents and cell lines

2.1.1 Cell lines

MiaPaCa-2 (CRL-1420), PANC-1 (CRL-1469), ASPC-1 (CRL1682), MET5A and 293T cell lines were purchased from American Type Culture Collection (ATCC, Middlesex, UK). MiaPaCa-2, PANC-1 and ASPC-1 are three pancreatic cancer cell lines. MiaPaCa-2 cell line derives from a primary pancreatic cancer tumour from a white male, who was 65 years old. PANC-1 cells exhibit epithelial morphology, which derive from the pancreatic duct of a 56-year-old white male with pancreatic cancer. ASPC-1 cell line derives from ascites of a 62-year-old white female pancreatic cancer patient. MET5A (CRL9444) is a cell line derived from pleural mesothelium. The cell line HEK 293T (CRL-3216) is from embryonic kidney and was used for packaging of lentiviral particles in the present study. Both MiaPaCa-2 and PANC1 were cultured in Dulbecco's modified Eagle's medium/ nutrient F-12 ham (DMEM) (DMEM-F12; Sigma-Aldrich), which was supplemented with 10% foetal calf serum (FCS) and a 1% cocktail of antibiotics (100X)（Thermo Fisher Scientific, Waltham, MA USA), with a final concentration of 100 unit/ml penicillin, 100 µg/ml streptomycin and 250 ng/ml amphotericin B. ASPC-1 cells were cultured with RPMI 1640 Medium (RPMI) (Sigma-Aldrich), which was supplemented with 10% FCS and antibiotics. MET5A cells were cultured in M199 medium (MEM199, Sigma-Aldrich) with 10% FCS and antibiotics.

2.1.2 Primers

All the primers, which were used for conventional polymerase chain reaction (PCR), quantitative real time PCR (QPCR), CMG2 ribozyme synthesis and amplification of human CMG2 coding sequence, are listed in Tables 2.1 to 2.3.

Table 2.1 Primers for conventional PCR

Genes	Primer name	Sequence (5'-3')	Amplicon size (bps)	Reference sequence
GAPDH	F8	GGCTGCTTTTAACTCTGGTA	421	NM_001357943.2
	R8	GACTGTGGTCATGAGTCCTT		
CMG2	F8	CAAAATCAGTAAAGGCTTGG	805	NM_001145794.2
	R8	CAAAGGTTCTTCTTCCTCCT		

Table 2.2 Primers for quantitative PCR

Genes	Primer	Sequence (5'-3')	Amplicon size (bps) (bps)	Reference sequence
GAPDH	F1	CTGAGTACGTCGTGGAGTC	92	NM_001357943.2
	ZR1	ACTGAACCTGACCGTACACAGAGATGATGACCCTTTTG		
CMG2	F1	AGCCTTTGATCTCTACTTCG	87	NM_001357943.2
	ZR	ACTGAACCTGACCGTACAGCAAGTTGCTGTACGAAATTA		
EGFR	F2	TCTTCGGGGAGCAGCGAT	133	NM_201283.2
	ZR2	ACTGAACCTGACCGTACACGTGAGCTTGTTACTCGTGC		
ITGB1	F1	CGCGCGGAAAAGATGAAT	120	NM_002211.4
	ZR1	ACTGAACCTGACCGTACATCCACATGATTTGGCATTTG		
ITGB2	F1	CTCTCCCTCGGGTGC	282	XM_047440763.1
	ZR1	ACTGAACCTGACCGTACATGTGAAGTTCAGCTTCTGG		
E-cadherin	F8	CAGAAAGTTTTCCACCAAAG	106	NM_001317185.2
	ZR8	ACTGAACCTGACCGTACAAAATGTGAGCAATTCTGCTT		
Snail	F17	CACACTGGCGAGAAGC	102	NM_005985.4
	ZR17	ACTGAACCTGACCGTACACTTCTTGACATCTGAGTGGG		
Slug	F	TGGACACACATACAGTGATT	77	NM_003068.5
	ZR	ACTGAACCTGACCGTACAGATCTCTGGTTGTGGTATGA		
TAGLN	F1	GAAACCCACCCTCTCAGTCA	124	NM_001001522.2
	ZR1	ACTGAACCTGACCGTACACAAGTCATCCGGGGCATTTC		
SOD2	F1	GGAAGCCATCAAACGTGACTT	116	NM_001322819.2
	ZR1	ACTGAACCTGACCGTACACCCGTTCCTTATTGAAACCAAGC		
SQSTM	F1	GACTACGACTTGTGTAGCGTC	139	NM_001142298.2
	ZR1	ACTGAACCTGACCGTACAAGTGTCCGTGTTTCACCTTCC		
ITGA2	F1	GGGAATCAGTATTACACAACGGG	112	NM_002203.4

	ZR1	ACTGAACCTGACCGTACACCACAA CATCTATGAGGGAAGGG		
ZO2	F1	CAAAAGAGGATTTGGAATTG		
	ZR1	ACTGAACCTGACCGTACAACTGAA CCTGACCGTACAGAGCACATCAGA AATGACAA		
ITGA3	F1	TCAACCTGGATACCCGATTCC	93	XM_054315 959.1
	ZR	ACTGAACCTGACCGTACAGCTCTG TCTGCCGATGGAG		
VCAN	F1	GTAACCCATGCGCTACATAAAGT	110	NM_001164 097.2
	ZR	ACTGAACCTGACCGTACAGGCAAA GTAGGCATCGTTGAAA		
HAPLN1	F1	TCTGGTGCTGATTTCAATCTGC	85	XM_054351 656.1
	ZR	ACTGAACCTGACCGTACA TGCTTGGATGTGAATAGCTCTG		
HABP4	F1	GAAGCGGACTCCTAGAAGAGG	110	XM_054362 392.1
	ZR	ACTGAACCTGACCGTACACATAGG GTCGGTATTCCCTGTA		
SHISA2	F1	CGAGAGTCACTGGTGGGTTC	112	NM_001007 538.2
	ZR1	ACTGAACCTGACCGTACAGCCATC CAAAGGAATCGTGC		
Rab25	F1	TCGTGGGTAACAAAAGTGCC	127	NM_020387. 4
	ZR1	ACTGAACCTGACCGTACAAGCTCA ACATTGGTAGAGTCCA		

Table 2.3 Primers for CMG2 knockdown and overexpression

Gene nane	Primer	Sequence (5’-3’)	Reference sequence
CMG2	EXP F	ATGGTGGCGGAGCGGTCCCCGGCCCG CA	NM_001145 794.2
	EXP R	AGCAGTTAGCTCTTTCTCAA	
	Rib2 F	CTGCAGAATAAACACTAGCCCCAAGTCT GATGAGTCCGTGAGGA	
	Rib2 R	ACTAGTAGAGGCAAAGATATCCAGGTTTC GTCCTCACGGACT	

2.1.3 Antibodies

Antibodies for Western blot and immunohistochemical staining (IHC) are shown in Table 2.4.

Table 2.4 Antibodies which were used in this research

Protein	Product code	Species	Supplier	Molecular weight (kDa)
GAPDH	SC 32233	Mouse	Santa Cruz Biotechnology Ltd	37 kDa
ACTIN	sc 1616	Goat	Santa Cruz Biotechnology Ltd	41kDa
ANTXR2	16723-1-ap	Rabbit	Protein tech Ltd	54 kDa
EGFR	SC 71034	Mouse	Santa Cruz Biotechnology Ltd	170 kDa
ICAM-1	SC 8439	Mouse	Santa Cruz Biotechnology Ltd	85~110 kDa
CD44	AB1N135705	Mouse	Biolegend	80-95 kDa
EGFR	SC 71034	Mouse	Santa Cruz Biotechnology Ltd	170 kDa
ICAM-1	SC 8439	Mouse	Santa Cruz Biotechnology Ltd	85-110 kDa
FAK	SC 1688	Mouse	Santa Cruz Biotechnology Ltd	125 kDa
ELK-1	SC-365876	Mouse	Santa Cruz Biotechnology Ltd	62 kDa
MEK2	SC 13159	Mouse	Santa Cruz Biotechnology Ltd	47 kDa
Shc	SC 967	Mouse	Santa Cruz Biotechnology Ltd	46-66 kDa
Vinculin	SC 73614	Mouse	Santa Cruz Biotechnology Ltd	117 kDa
Secondary antibody	**Type**	**Product Code**	**Supplier**	
Mouse	IgG	A-9044	Sigma-Aldrich Ltd	
Rabbit	IgG	A-9169	Sigma-Aldrich Ltd	
Goat	IgG	A-5420	Sigma-Aldrich Ltd	
Targeting phosphorylated proteins	**Product code**	**Species**	**Supplier**	
p-Tyr	SC 508	Mouse	Santa Cruz Biotechnology Ltd	
p-Thr	SC 5267	Mouse	Santa Cruz Biotechnology Ltd	
P-Ser	SC 81517	Mouse	Santa Cruz Biotechnology Ltd	

2.1.4 Reagents and buffers

LB medium (Liquid Broth)

10g of sodium chloride, 10g of casein digest peptone, 5g yeast extract (Melford Laboratories Ltd, Suffolk, UK), were dissolved in 1L distilled water, the pH was adjusted to 7.0. Following autoclaving, it was stored at room temperature, or at 4 ℃ if an antibiotic was added, until it was used for culture of bacteria. Ampicillin was commonly used for selection, unless a different selective marker was included in a vector.

Ampicillin

Ampicillin (Melford Laboratories Ltd, Suffolk, UK), was dissolved in PBS at a final

concentration of 100mg/ml, which was then stored at -80℃ until use.

LB agar gel

Ten grams of tryptone, 5g of yeast extract, 15g of agar and 10g of NaCl were dissolved in 1L of distilled water, with a justification of pH to 7.0 followed by autoclaving. Before pouring in plates, LB agar was melted using a microwave. After mixing with prepared LB medium to cool down the LB agar, ampicillin was added to a final concentration of 100µg/ml. Fifteen millilitres of the LB agar was poured into 10cm^2 cell culture dishes (Bibby Sterilin Ltd, Staffs, UK) and used for subsequent plating of bacteria, once the gel was set.

5X TBE buffer (Tris-Boric Acid EDTA)

275g boric acid, 46.5g of Ethylenediaminetetraacetic acid (EDTA), 540g of Tris-HCl (Melford Laboratories Ltd, Suffolk, UK), were added into 10L distilled water. HCl and NaOH were applied to adjust pH to 8.3. Concentrated TBE buffer was diluted to 1 X for preparation of agarose gels and to be used for electrophoresis. This buffer was stored at room temperature.

DEPC (Diethyl pyrocarbonate) water

DEPC water was prepared to protect RNA from degradation. One millilitre DEPC was added into 1000ml distilled water, the DEPC water was incubated for 12 hours at 37℃ followed by autoclaving.

Lysis buffer

2X RIPA lysis buffer was mixed with 2X protease inhibitor cocktail, which were used for protein extraction. 2X RIPA buffer contains 20mM Tris-HCl, 2mM EDTA, 1mM EGTA, 2% NP40, 0.2% Sodium Deoxycholate, 0.2% SDS and 280mM NaCl. This was mixed with the protease inhibitor cocktail, containing phenylmethylsulfonyl fluoride (PMSF) (100µg/ml), leupeptin (10µg/ml), sodium vanadate (5mM), aprotinin (10µg/ml) and sodium fluoride (50mM). 2X RIPA lysis buffer was stored at 4℃. 2X protease inhibitor cocktail was stored at -20℃.

10X Running buffer (Tris-glycine-SDS buffer, for electrophoresis during the Western blot.)

Glycine (1.44kg) (Melford Laboratories Ltd, Suffolk, UK), Tris (303g) and SDS (100g) (Melford Laboratories Ltd, Suffolk, UK) were added into 9L distilled water, followed by adjusting pH to 8.3. This solution was then topped up to 10L with distilled water. Before this buffer was used, it was diluted 1:10 with distilled water.

10X Tris Buffered Saline (TBS)

24.228g Tris, and 80.06g NaCl (Melford Laboratories Ltd, Suffolk, UK), were dissolved in 1L distilled water. The pH value was adjusted to 7.4 before it was stored at room temperature for further experiments.

Transfer buffer (transfer protein to the membrane)

72g glycine and 15.5g Tris (Melford Laboratories Ltd, Suffolk, UK) were added to 4L distilled water. 1L methanol was then added . This solution was stored at room temperature.

Phosphate-buffered saline (PBS)

800ml distilled was added to 8g NaCl, 1.44g Na2HPO4 and 0.24g KH2PO4. The pH value was the adjusted to 7.4 and then topped up to 1L with distilled water. The solution was then sterilized and stored at room temperature.

Antibotics (ABX)

100X antibiotics (A5955, Sigma-Aldrich) were applied for cell culture, which included 1% Streptomycin, 0.66% penicillin, and 0.0025% amphotericin B in PBS. The solution was filtered with a 0.2μm filter then stored at -20℃ and was added to 500ml medium directly before use.

Ethylenediaminetetraacetic Acid (EDTA) buffer

1.4g EDTA, 1g KCl, 1g KH_2PO_4, 40g NaCl and 5.72g Na_2HPO_4 were dissolved in 5L distilled water. The pH value was adjusted to 7.4. After autoclaving, this solution was

stored at room temperature.

EDTA/trypsin enzyme solution

500mg trypsin powder was added to 20ml PBS with 0.02% EDTA and autoclaved before being stored at -20℃.

2.2 Human pancreatic cancer tissues

A cohort of pancreatic cancer tissues were obtained from Peking University Cancer Hospital as part of institional collaboration between Cardiff University and Peking University Cancer Hospital. Clinical and pathological categories and number of patients in each group are shown in Table 2.5. All protocol and procedures used were approved by the Peking University Cancer Hospital Research Ethics Committee (MTA01062008) (Dart et al. 2019).

Table 2.5 Patients information from Beijing cohort

Variable	N
Disease state	
Tumour	153
Normal	175
Gender	
Male	93
Female	60
Subtypes	
Adeno Carcinoma	135
Ductal Carcinoma	5
Others	11
Location	
Head	44
Body	6
Body tail	26
Tail	2
Other Location	3
T statging	
T1	3
T2	17
T3	89
T4	18
Lymphnode metastasis	
Lymph node (-)	60
Lymph node (+)	3
Distant metastasis	
Meta (-)	140
Meta (+)	13
TNM staging	
TNM-1A	3
TNM-1B	9
TNM-1	12
TNM-2A	32
TNM-2B	67
TNM-2	99
TNM-3	15
TNM-4	9
Patient survival	
Alive	36
Died	108

2.3 Cell culture and storage

2.3.1 Medium for cell culture

MET5A, HEK-293T, MiaPaCa-2 and PANC-1 cell lines were cultured in DMEM/Ham's F12 with L-glutamine medium (Sigma-Aldrich). ABX (introduced in 2.1.4.4) and 10% Foetal Calf serum was added. ASPC-1 cell line was cultured in RPMI 1640 medium (Sigma-Aldrich), also supplied by ABX with 10% foetal calf serum.

2.3.2 Cell maintenance

All the cell lines were maintained at conditions of 37℃, 5% CO2 and 95% humidity. All the cell culture operations were carried out in class II laminar flow cabinets. The aseptic operation standard was strictly abided by. All the pipette tips, tubes, and universal containers, which contacted the cell or cell culture medium, were aseptic. Cells were cultured in the medium till they reached around 90% confluency before use.

2.3.3 Cell passaging and dividing

Once cell confluence reached 90% or higher, cell passaging was conducted. The medium inside the flask was aspirated. Then the cells were washed with PBS to remove remaining medium. Following that, 0.01% EDTA/trypsin buffer (described in 2.1.4.4) was applied to digest cells at 37℃. This procedure took between 3 to 15 minutes depending on adhesiveness of the cells used. Two millilitres of fresh medium with 10% FCS was then added into the flask to resuspend those detached cells and neutralise trypsin. The cell suspension was then transferred into a universal container, followed by centrifugation at 1200rpm for 5 minutes. After discarding the supernatant, 10ml of medium was added into the universal container and the cell pellet was resuspended. For cell passaging, 5ml of cell culture was added into each T25 flask with a culture area of 25 cm^2.

2.3.4 Cell stocks

Short-term cell storage was maintained in a -80℃ freezer, while liquid nitrogen was used for long-term storage. Cells were detached from the flask with the EDTA/trypsin solution at 37℃ for 3-15 minutes. Cells in a T25 flask were resuspended in 1800µl

medium, 900 µl of the cell suspension was then added into 1.8ml cryotubes (Greiner BioOne, Germany), with 100 µl dimethyl sulfoxide (DMSO) then added. After the tube was labelled with the cell line name, passage and date, the cells were frozen down in the -20℃ freezer. After a minimal period of 3 hours, the frozen samples were then stored at -80℃ for temporary or short-term storage (less than 3 months). For long-term storage, the cryotubes were transferred into a liquid nitrogen tank.

2.3.5 Reviving frozen cells

Once frozen cells were removed from liquid nitrogen or the -80℃ freezer were taken out, they were immediately defrosted in a water bath at 37℃. The defrosted cells were then added into a 25ml universal container together with 5ml of fresh warm medium. After centrifugation at 1200rpm for 5 minutes, the cells were then resuspended in 5ml fresh medium and transferred into a T25 flask. Following overnight incubation, cells were routinely checked under a microscope. The medium was changed to remove unhealthy cells.

2.3.6 Cell counting

Cells were detached from the flask using trypsin and were harvested in 2ml medium. The cells were then moved into a 25ml universal container and kept on ice. For each counting, 50µl of cell suspension was mixed with the same volume of 0.4% trypan blue, in a 0.5ml Eppendorf tube. A haemocytometer was used for cell counting (Mod-Fuchs Rosenthal, Hawksley, UK). The depth of chambers were 0.2mm, with nine large square chambers. The area of each large square is $1mm^2$, so the volume was 0.2µL. The cells were added into the space between the haemocytometer plate and cover slip. Cells were counted using an inverted light microscope (Reichert, Austria). Five chambers were selected and the cell number in each one was counted. The cell density was calculated using the following equation: Cell number/ml= average cell number in each chamber $\times$ 10000 $\div$2.

2.4 Determination of mRNA

2.4.1 RNA extraction

mRNA only accounts for about 1~2% of total cellular RNA, while it plays an important role in transferring the message from nuclear to protein synthesis. Since RNA is susceptible to RNAse, during this procedure, the temperature was stricktly controlled, with DEPC water used to protect the RNA from degradation by RNAse.

RNA was extracted from cells following the TRI reagent protocol from Sigma-Aldrich.

Step 1: Prepare cell lysate.

Total RNA was extracted from 0.5 million pancreatic cancer cells from one well in the 6-well plate. The medium was aspirated and PBS was used to wash off the remaining medium. For each well, 1ml TRIzol Reagent® (Sigma-Aldrich) was added. Cells, together with the TRIzol Reagent, were harvested and transferred into a 1.5 ml Eppendorf tube followed by incubation on ice for 5 minutes for a sufficient lysis.

Step 2: Separation of RNA.

0.2ml 1-bromo-3-chloropane was added into the Eppendorf tube (0.2mL 1-bromo-3-chloropane for 1ml TRI reagent). The tube was shaked vigorously for 15 seconds and left on ice for 10-15 minutes. After centrifugation at 12000rpm, for 15 minutes at 4℃ using a refrigerated centrifuge (Boeco, Wolf Laboratories, York, UK), the homogenate was separated into three distinct phases. The protein is dissolved in the lower pink phase, the white cloudy interphase contains DNA, and the upper clear phase contains RNA.

Step 3: Isolation of RNA sample.

The upper phase solution was placed into a new, pre-labelled Eppendorf tube and was mixed with 500µl isopropanol, which can reduce the solubility of RNA and separate it out. Following incubation on ice for 10 minutes, another centrifugation (12000rpm, 10 minutes, 4℃) was carried out and the RNA formed a visible pallet. The supernatant was discarded, then 75% ethanol (Fisher Scientific, Leicestershire, UK) in DEPC water was added to wash the pellet (centrifuge at 7500rpm, 5 minutes, 4℃). The RNA pellet was then dried at 55℃ for 5 minutes (Techne Hybridiser HB-1D, Wolf Laboratories, York, UK), before it was dissolved in 20µl DEPC water.

2.4.2 RNA quantification

An Implen Nanophotometer (Munchen, Germany) was applied to measure the concentration of RNA. Each sample comprised of 3µl RNA solution with a lid factor 10 chosen. The absorbance at 260nm and 280nm was measured, an RNA sample with good purity should have a ratio of absorbance 260nm/ absorbance 280nm between 1.8 to 2.0.

2.4.3 Complementary DNA (cDNA) synthesis

After RNA quantification, 2000ng RNA samples were used for cDNA synthesis using reverse transcription (RT), following the protocol of a reverse transcription kit (Promega, Southampton, UK).

Step 1: Prepare samples for RT. For each sample, 10µl of 2× RT mixture was added into a polymerase chain reaction (PCR) tube. After calculating the volume of the RNA sample required, PCR water was added to top up the final volume to 10µL, and was mixed with the 2× RT mixture in the tube.

Step 2: Prepared samples in the PCR tubes were placed into the Simpliamo Thermocycler (Thermo Fisher Scientific). The reaction procedure was: 25℃ for 10 minutes, 42℃ for 60 minutes and 70℃ for 15 minutes.

Step 3: Once RT was completed, samples were diluted 1:4 using PCR water. RNA samples were then moved into an 0.5ml Eppendorf tube and stored at-20℃ .

2.4.4 Polymerase Chain Reaction (PCR)

PCR was performed using the GoTaq Green Master Mix (Promega). The total volume in each tube was 12µl in total, which contained 6µL master mix, 1µl forward primer (10µM), 1µL reverse primer (10µM), 1µl cDNA sample and 3µl PCR water. The negative control group, which contains 6µL master mix, 1µl forward primer (10µM), 1µl reverse primer (10µM), and 4µl PCR water, was added to exclude unspecific bands caused by contamination. Simpliamo Thermocycler (Thermo Fisher Scientific) was used for the conventional PCR.

The steps of PCR include: initial denaturing at 94 °C for 5 minutes; 30-35 cycles of denaturing at 94 °C for 20 seconds, annealing at 55 °C for 30 seconds and extension at 72 °C for 30 seconds; a final extension at 72 °C for 5 minutes. All primers are listed in Table 2.2.

During the denaturing step, the DNA double helix was separated into two strands, followed by binding of primers bound to complementary sequences of the target gene under 55℃. At the extension step, the temperature was maintained at 72 ℃, which was suitable for the DNA polymerase to work. The amount of target transcripts was doubled every cycle during the PCR.

2.4.5 Gel electrophoresis

Electrophoresis through an agarose gel of an appropriate concentration was applied to separate and visualise PCR products depending on the product size (Table 2.6).

Table 2.6 Concentration of agarose gel for PCR products of different sizes.

PCR products (bps)	Agarose gel concentration
>2000	0.8%
100~1000	1.5%
<100	2.0%

To prepare a 1.5% agarose gel, 1.5g agarose powder (Melford Chemicals, Suffolk, UK) was added into 100ml TBE buffer (1X). After the agarose was dissolved into the TBE buffer using the microwave, 5μl SYBR safe gel stain (Invitrogen, Manchester, UK) was added to the hot agarose solution. The dye added can glow under the ultraviolet (UV) light which allows the PCR products to be visualised. The stained gel was then poured into the electrophoresis tank carefully, avoiding the formation of any air bubbles. Before the gel was set, combs were inserted to generate wells. The gel was then cooled down at room temperature for 30 minutes. Once the gel was set, 1XTBE solution was poured into the tank, to just submerge the agarose gel. After the combs were removed, samples were loaded. For each well, 8μl cDNA sample was loaded, 5μl 1000bp DNA ladder was loaded into the first well (Cat No. M106R; GenScript USA Inc).

Electrophoresis was then conducted under 120 V for 20-40 minutes using a power supply (Gibco BRL, Life Technologies Inc). During this step, the cDNA sample carries the negative charge, which moves to the cathod when an electric current is applied. The PCR products move at a different speeds according to their size, which allows them to be visualised as different bands. DNA ladder was added to show the size of the bands.

2.4.6 cDNA band visualization

Following electrophoresis, the Gel was put into a Syngene U: Genius 3 closed system (Geneflow, Elmhurst, Lichfield Staffs). The bands of stained PCR products were visualised and photographed.

2.4.7 Quantitative PCR (QPCR/ Real-time PCR)

QPCR was applied to determine gene expression quantitively. FAST 2X qPCR MasterMix (Primer Design, Chandle''s Ford, UK) was applied to perform the QPCR. A QPCR reaction was prepared as shown in Table 2.7.

Table 2.7 Components in a QPCR reaction

Reagents or samples	Volume (total 10 µl)
FAST 2X qPCR MasterMix	5µl
Primer F (1:10 dilute, 10µM)	0.3µl
Primer ZR (1:100 dilute, 1 µM)	0.3µl
Universal probe (Uniprobe, 10 µM)	0.3µl
cDNA sample	2µl
PCR water	2.1µl

The study employed the Ampliflor^{tm} technology system. In this QPCR system, F and ZR primers were used. The ZR primer contains a Z sequence (ACTGAACCTGACCGTACA), a sequence complementary to the stem region of a Molecular Beacon based probe, Uniprimer which is tagged with FAM dye for detection. In each reaction, the amount of ZR primer used was only 1/10 of the forward primer and the universal probe. During initial amplification the ZR primer would be used up, the universal probe and forward primer started to work together for the following amplification. The

universal probe (Uniprimer, Millipore, Watford, UK) comprises a short DNA oligos and a fluorophore (FAM) marked on the 5' hairpin structure, the fluorescence of which is blocked by a moiety (DABSYL). The 3' end of the Uniprimer bound with the Z' sequence during the amplification. Following that, the hairpin structure at the 5' end was unfolded under the effect of DNA polymerase and the fluorescence was unblocked. The strength of the fluorescence was recorded. Once the strength of fluorescence reached a threshold, the cycle number was taken as a CT value (Figure 2.1).

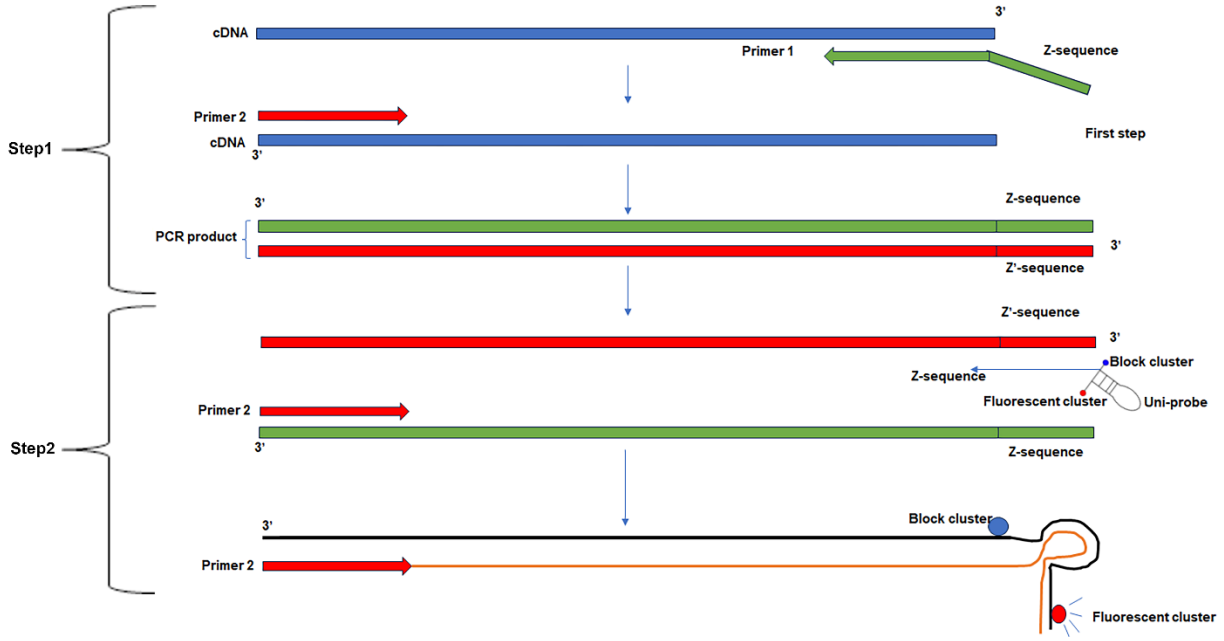

Figure 2.1 QPCR reaction procedure. Uni-probe is a primer, containing Z sequence and a pair of energy transfer molecules (Block cluster and fluorescent cluster). Uni-probe anneals to the complement to the Z sequence (Z' sequence), which is generated in the first step. Then the Uni-probe is incorporated, the hairpin is unfolded and the blockage of the fluorescent cluster is relieved due to increased distance.

QPCR reactions were prepared in a 96-well QPCR plate (Applied Biosystems™, Life Technologies Ltd, Paisley, UK), which was subsequently sealed with a MicroAmp® Optical Adhesive film (Thermo Fisher Scientific). For negative control, PCR water was added to replace the cDNA samples to exclude contamination. The plate was then centrifuged at 3000rpm for 1 minute to remove all the bubbles. Following this, the StepOne plus system (Thermo Fisher Scientific) was applied for QPCR reaction and quantification with the following thermocycling conditions:

Step 1: Initial denaturing: 95℃ for 10 minutes

Step 2: Denaturing: 95℃ for 10 seconds

Step 3 : Annealing: 55℃ for 35 seconds

Step 4: Extension: 72℃ for 10 seconds

Step 2 to step 4 were repeated for 100 cycles and the fluorescent intensity was recorded at the annealing step. A threshold was automatically generated by the software of the StepOne plus system.

The change in folds of a target gene was calculated using a $2^{-\Delta\Delta ct}$ method (Thomsen et al. 2010):

Step 1: ΔCT=CT (CMG2)-CT (GAPDH)

Step 2: ΔΔCT=ΔCT (CMG2 knockdown cell line)-ΔCT (scramble control cell line)

Step 3: Expression change was calculated as changes in folds as $2^{-\Delta\Delta ct}$.

2.5 Analysis of protein

2.5.1 Extraction of protein from samples

The cells in a T25 flask (2 million cells) were scraped off and harvested in a 25ml universal container. Following centrifugation at 1500rpm for 5 minutes, the cell pellet was washed by 4℃ PBS twice with centrifugation. The supernatant was discarded, pre-cooled 80μl cell lysis buffer (as described in 2.1.4.3) was added to lyse the cells. The cell lysate was transferred to a 1.5ml Eppendorf tube followed by a continuous rotation on a Labinco rotating wheel (Wolf Laboratories, York, UK), for 60 minutes at 4℃. In order to achieve a better lysis of the cells, cells were sonicated for 5-minutes at medium strength on an untrasound Bioruptor (Diagenode, Seraing, Belgium). During this process the Eppendorf tubes were submerged in an ice-cold water bath. The lysates were then centrifuged at 4℃, 13000 rpm for 10 minutes, proteins in the supernatant were collected in a new tube for subsequent quantification and analysis.

2.5.2 Protein quantification

A Bio-Rad protein quantification kit (Bio-Rad, Hertfordshire, UK) was used for protein quantification, with the following procedure.

Step 1: Lysis buffer was added to the first row of wells of the 96-well plate. Twenty microlitres of 100mg/ml Bovine serum albumin (BSA) was added to the first well containing 20µL lysis buffer, which gave a concentration of BSA at 50mg/ml. A series of dilutions at 1:2 was carried out to prepare BSA samples for a standard curve.

Step 2: 5µl of protein samples and BSA standards were added into each well in duplicate. Reagent A mixed with reagent S (2%) was then added at a volume of 25µl per well followed by an addition of 200µl reagent B. A blue colour was developed at room temperature for 15 minutes.

Step 3: Absorbance at 620nm was then measured with a spectrophotometer (ELx800, Bio-Tek, Wolf Laboratories, York, UK). The standard curve was plotted for the BSA standards. The equation of the trend line was employed to calculate the concentration of protein samples.

Step 4: Protein samples of 3mg/ml were then prepared using 2X Lamelli sample buffer (Sigma-Aldrich) with a denaturation at 100℃ for 10 minutes. The protein samples were stored at -20℃ until use.

2.5.3 Detection of proteins using Western blot

2.5.3.1 Gel preparation

The principle of separation of proteins, using sodium dodecyl sulfate polyacrylamide gel electrophoresis (SDS-PAGE), is that the protein samples are prepared with a lysis buffer containing protease inhibitors and detergents. Detergents can help to destroy the cell membrane and inhibitor buffer can protect the proteins from proteases and phosphatases if the phosphorylation of a protein is to be examined. Sample buffer contains an indicating dye, sodium dodecyl sulphate (SDS), and glycerol. In the sample buffer, protein molecules can be separated on SDS gel, based on their size that provide a negative electric charge. Proteins can get a same ratio for the mass-to-charge. During electrophoresis, the protein with same size can get a same electrophoretic velocity which allows a separation of proteins according to their molecular weights.

The Tris-glycine SDS-Polyacrylamide Gel Electrophoresis (SDS-PAGE) was carried out using the Omni PAGE VS10 vertical electrophoresis system (Wolf Laboratories, York, UK).

Two glass plates and two notched glass plates were cleaned and assembled into the rack. Ethanol was used to check for any leakage before casting a gel. For proteins with different predicted molecular weights, resolving gels with different concentrations were applied:

8% gel: >90KD

10% gel: 30~89KD

12% gel: 10~29KD

Two gels were prepared using one gel rack and 15ml of resolving gel was required. Resolving gel was added into the space between the two glass plates until it reached a level 1.5-2 cm below the edge of the notched glass plate. A 0.1% SDS solution was then carefully added to cover the resolving gel, to ensure the gel set with an even, smooth surface.

The resolving gel was set after incubation at room temperature for 1-3 hours. The 0.1% SDS was removed and the stacking gel was prepared and loaded (Table 2.8). A Teflon comb was inserted into the stacking gel before the gel was set. Following incubation at room temperature for one hour, the stacking gel was set. The gel cassette was then placed into an electrophoresis tank and running buffer was added. When the top edge of the gel was submerged by the running buffer, the combs were carefully removed.

During this procedure, TEMED triggers APS to release free radicals and promote the solidification of the gel. The stacking gel has a larger pore size compared with the resolving gel, which helps to concentrate the sample when the sample passes through the boundary of these two different gels. Tris can help to maintain the pH value in the gel.

Table 2.8 Components of Sodium dodecyl sulphate polyacrylamide resolving gel with different concentrations.

Gel concentration	Components	Final volume of gel (ml)		
		10ml	15ml	20ml
8%	Distilled water	4.6	6.9	9.3
	30% acrylamides mix	2.7	4.0	5.3
	1.5 M Tris (pH8.8)	2.5	3.8	5.0
	10% SDS	0.1	0.15	0.2
	10% ammonium persulfate (APS)	0.1	0.15	0.2
	TEMED	0.006	0.009	0.012
10%	Distilled water	4.0	5.9	7.9
	30% acrylamides mix	3.3	5.0	6.7
	1.5 M Tris (pH8.8)	2.5	3.8	5.0
	10% SDS	0.1	0.15	0.2
	10% ammonium persulfate (APS)	0.1	0.15	0.2
	TEMED	0.004	0.006	0.008
12%	Distilled water	3.4	4.9	6.5
	30% acrylamides mix	3.9	6.0	8.1
	1.5 M Tris (pH8.8)	2.5	3.8	5.0
	10% SDS	0.1	0.15	0.2
	10% ammonium persulfate (APS)	0.1	0.15	0.2
	TEMED	0.003	0.005	0.007

Table 2.9 Composition of 5% stacking gel for SDS-PAGE

Components	Final volume of gel (ml)		
	5ml	8ml	10ml
Distilled water	3.4	5.5	6.8
30% acrylamides mix	0.83	1.3	1.7
1.0 M Tris (pH6.8)	0.63	1.0	1.25
10% SDS	0.05	0.08	0.1
10% ammonium persulfate (APS)	0.05	0.08	0.1
TEMED	0.005	0.008	0.01

2.5.3.2 Gel electrophoresis

For each lane, 12µl of protein sample was loaded which contained 36µg of total protein, with 5µl protein molecular weight ladder (Santa Cruz Biotechnology, supplied by Insight Biotechnologies Inc, Surrey, England, UK) used for each gel. Each gel cassette contained two gels and electrophoresis was conducted for 1.5 hours with a consistent electric current of 50mA (25mA per gel).

2.5.3.3 Transfer membrane

Nitrocellulose membrane or polyvinylidene difluoride (PVDF) membrane, and filter papers were cut to a size of 7.5cm x 7.5cm. Membranes with different pore sizes were used for the electrical transferring of proteins with different molecular weight. For proteins less than 25kDa, a nitrocellulose membrane with 0.2µm pores was used, whilst a PVDF membrane with 0.45µm pores was used for the transfer of proteins greater than 25kDa. The nitrocellulose membrane has a clearer background, and the PVDF membrane has a stronger capacity for protein binding. Before the transfer, PVDF membrane was immersed in methanol for one minute and then, together with the filter paper, they were immersed in the transfer buffer for 30 minutes. Methanol activates the positive groups on the PVDF membrane, so that it can bind with the proteins that are negatively charged. Transfer buffer can also promote SDS to leave the protein during the procedure of transfer, which allows easier binding of a primary antibody to a target protein in the following probing. Nitrocellulose membrane was incubated in the transfer buffer directly for 30 minutes. When the electrophoresis was completed, SD10 Semi-Dry Maxi System blotting unit (SemiDRY, Wolf Laboratories, York, UK) was used for the following transfer. A sandwich-like assembly of the membrane, gel and filter paper were inserted into the blotting unit as shown in Figure 2.2.

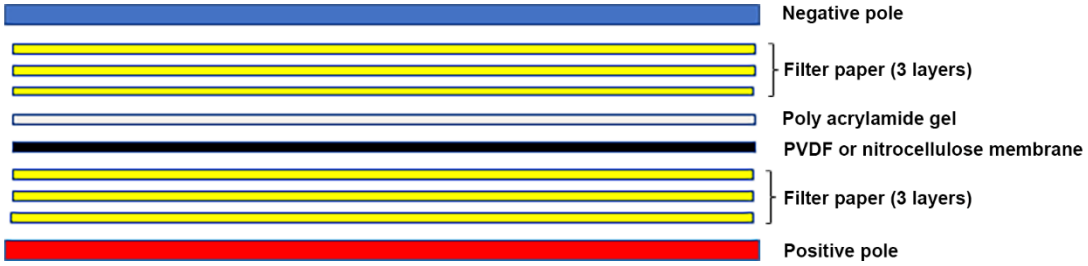

Figure 2.2 Diagram of the electrical blotting of proteins.

Protein transfer was conducted with an electric current of 450mA, 50W, 15V. The duration of the transfer was chosen according to the size of the target protein. For example, for proteins less than 30 kDa, 35 minutes was applied, whilst 45 minutes were used for proteins with a molecular weight between 30 to 90 kDa. For proteins greater than 90kDa, the transfer required approximately 1 hour.

2.5.3.4 Protein band probing

During the transfer, three different solutions were prepared for membrane blocking, washing and antibody probing:

Solution A: 10% skimmed milk in TBS, with 0.1% Tween 20.

Solution B: 3% skimmed milk in TBS, with 0.1% Tween 20.

Solution C: TBS with 0.2% Tween 20.

To block a membrane, the membrane was incubated in solution A for 1 hour at room temperature. Both PVDF and nitrocellulose membranes can bind with proteins non-specifically, including the primary antibody. Without blocking, the background signal can be extremely high at the end of the Western blot, when specific protein bands are documented. The 10% skimmed milk can block the area on the membrane without transferred proteins. The Tween 20 reduced non-specific binding of proteins in the milk to the transferred proteins on the membrane.

After blocking, the membrane was washed twice with solution B, with a continuous rotation of 10 minutes for each wash. Primary antibody was diluted in 2ml of solution B, the dilutions used are provided in Table 2.4. The membrane was then incubated with diluted primary antibody at 4℃ overnight, followed by washing three times with solution B: 15 minutes for the first wash and 5 minutes for the following washes. Secondary antibody was also diluted in solution B at 1:1000. After washing, the membrane was then incubated with the secondary antibody for 1 hour at room temperature. Once the incubation was complete, the membrane was washed with solution B, using the same procedure as washing the primary antibody, followed by two washes with solution C, 15 minutes per wash, and finally, was washed twice with TBS.

2.5.3.5 Protein band visualization

EZ-ECL kit was used to visualise the protein band (Sartorius group, Staffordshire, UK) which contains the chemiluminescent substrate. According to the kit instructions, 1ml of solution A was mixed with the same volume of solution B, and the membrane was immersed into the mixed solution. After incubation for 5 minutes, the membrane was transferred into the G:BOX (UVprochemi, UVITech Inc., Cambridge, UK) for visualising the protein bands and photos were subsequently taken.

2.5.4 Immunohistochemical staining (IHC) of CMG2 protein on pancreatic tissue microarray (TMA)

A PA2081a (Biomax, Maryland, USA) tissue microarray was used. It contained 42 cases of ductal adenocarcinoma, 3 adenosquamous carcinoma, 1 islet cell carcinoma, 6 metastatic carcinoma, 10 islet cell tumour, 2 hyperplasias, 10 inflammation, 20 adjacent normal tissue and 10 normal tissue from autopsy, duplicated cores per case. Clinical and pathological information for the samples is shown in Table 2.10 and Figure 2.3.

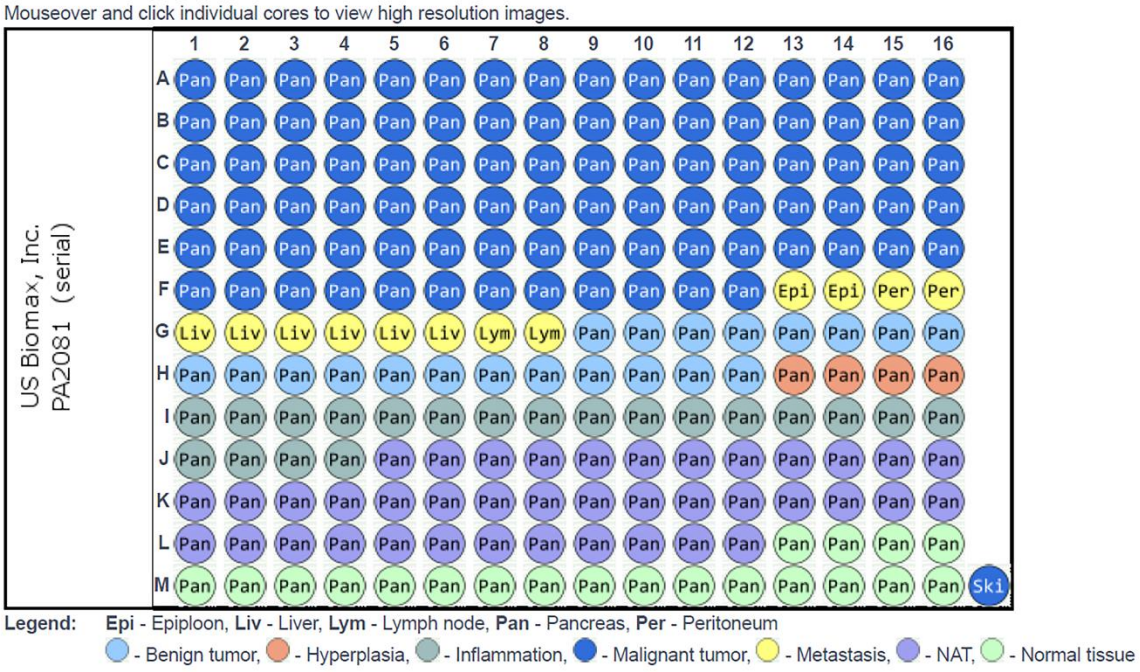

Figure 2.3 Layout of samples on tissue microarray

Table 2.10 Cases involved in PA2081a tissue microarray

Groups of patients	Number
Tissue types	
Malignant	46
Normal	10
Metastasis	6
Inflammation	10
Hyperplasia	2
Benign	10
Gender	
Female	42
Male	62
T stage	
T1	2
T2	27
T3	28
T4	2
N stage	
N0	36
N1	16
M stage	
M0	42
M1	3
Tumour subtypes	
Ductal adenocarcinoma	42
Adenosquamous carcinoma	3
Islet cell tumour	1
Non-tumour tissues	
Hyperplasias	2
Inflammation	10
Adjacent normal	20
Nomal	10

The tissue microarray slide was de-waxed and re-hydrated before retrival of antigen. The slide was immersed into different solutions in a sequential order.

100% Xylene, 5 minutes;

100% Xylene, 5 minutes;

50% xylene/ 50% Ethanol, 5 minutes;

100% Ethenol, 5 minutes;

100% Ethanol, 5 minutes;

90% Ethanol, 5minutes;

70% Ethanol, 5minutes;

50% Ethanol, 5 minutes;

Distilled water, 5 minutes;

Final wash in PBS for 5 minutes.

Antigen retrival buffer used was 10mM Sodium Citrate, pH 6.0, which is a common HIER buffer. The slide was immersed in the antigen retrival buffer and heated in the microwave for 20 minutes. During this procedure, the slide rack was taked out and shaken regullarly to remove bubbles during heating. Following this, the slide was washed and cooled with tap water and incubated in blocking buffer for 2 hours at room temperature, which comprised 10% horse serum in the washing buffer. The primary antibody used was an anti-CMG2 mouse polyclonal antibody ab70499 (Abcam, Cambridge, UK), at a dilution of 1:500. The slide was incubated in primary antibody solution overnight at 4℃, followed by two washes using the washing buffer, 10 minutes per wash. Three drops (135μL) of normal serum and 1 drop (45μL) of the Biotinylated Secondary Antibody, from the ABC Staining Kit, were added to 10ml of PBS (Vectastain Universal Elite ABC Kit, PK6200, Vector laboratories, California, USA). Four drops of prepared secondary antibody were added onto the glass plate to cover the tissue array, which was used to incubate with the slide for half an hour. The slide was then incubated in the premade ABC solution (Vectastain Universal Elite ABC Kit, PK6200, Vector laboratories, California, USA) for 30 minutes at room temperature. Once the incubation was complete, the slide was washed with washing buffer twice, 5 minutes per wash. DAB solution, containing 0.5ml aliquot DAB (D5637, Sigma-Aldrich), was mixed with 4.5ml PBS and 6μl hydrogen peroxide (H_2O_2). DAB was oxidized by H_2O_2 in the presence of peroxidase and hydrogen peroxide resulting in the deposition of a brown colour, which represented the staining of the target protein (CMG2).The slide was incubated in this solution for 7 minutes, followed by thorough washing in tap water. The nucleus was then counter stained with the haematoxylin for upto 2 minutes at room temperature, followed by washing with tap water. The slide was dehydrated afterwards as follows.

50% Ethanol, 5 minutes;

70% Ethanol, 5minutes;

90% Ethanol, 5minutes;

100% Ethanol, 5 minutes;

50% xylene/ 50% Ethanol, 5 minutes;

100% Xylene, 5 minutes;

100% Xylene, 5 minutes;

The slide was then mounted with a cover slip and the DPX mounting gel.

The immunohistochemical staining was photographed and assessed by two postdoctoral fellows (AS and SC) and subsequently verified by a pathologist (Professor Paul Griffiths). Intensity of the staining was scored as 0 for negative, 1 for a weak staining, 2 for a moderate staining and 3 for a strong staining. The IHC scores were used for following statistical analysis.

2.5.5 Proteomic analysis using mass spectrometry

2.5.5.1 Mass spectrometry

To further determine the molecules and pathways that are associated with the CMG2 expression, a proteomics analysis was conducted. Proteins smaples were prepared and sent to Bristol University for proteomic analysis, using a mass spectrometric approach. Protein samples of MiaPaCa-2^{pEF}, MiaPaCa ^{CMG2exp}, ASPC-1^{SC} and ASPC-1^{CMG2sh6} cells were prepared with the following procedure.

Step 1: Cells in flasks were washed twice with pre-cooled PBS, and were harvested with a cell scraper.

Step 2: Cells were resuspended in a universal container and centrifuged at 1800 rpm for 5 minutes, then the supernantent was discarded. The cells were then lysed in RIPA buffer (with no SDS) containing a cocktail of inhibitors for proteases and phosphatases (Cat No. ab201116 and ab201117, respectively), followed by incubation at 4℃ for 2 hours.

Step 3: The cell lysate was then placed into an Eppendorf tube and centrifuged at 13000 rpm, 4℃ for 10 minutes. The supernantent was transferred into a new tube.

Step 4: Following quantification, protein concentration of the samples was adjusted to 2mg/ml.

Step 5: Protein samples were packedged in dry ice box and sent to Bristol University for the following proteomic analysis. Protein from each sample was triplicated and each tube

contained 200µg protein (at least 100µg was required for each sample).

Mass spectrometry was conducted using TMT (TMT10plex Mass Tag Labeling Kits and Reagents, Thermo Fisher Scientific), following the protocol of TMT10plex Mass Tag Labeling Kits scientific. In brief, the proteins were first digested into polypeptides using trypsin enzyme, which was then labelled by Thermo Scientific™ TMT™ Mass Tag, which included an amine-reactive NHS-ester group, a spacer arm and a mass reporter.

To label the pipette, 100µg protein sample was added into one 0.8mg vial. For each vial, 41µl of anhydrous acetonitrile was required and added. The tubes were then vortexed for 5 minutes, allowing the reagent to be dissolved thoroughly. Next, the same volume of TMT label reagent was added into the vials, followed by incubation at room temperature for 1 hour, which was subsequently terminated by adding 8µl of 5% hydroxylamine followed by another 15-minute incubation. The samples were stored at -80℃, or analysed with a high resolution Orbitrap LC-MS/MS. The data was then analysed to identify the peptides and the reporter ion abundance was quantified.

Total protein expression levels were measured and compared between the control group and the cell lines with modified CMG2 expression. For protein phosphorylation, phospho-peptide enrichment approach was applied to detect the phosphorylation state of serine (S), threonine (T) and tyrosine (Y) residues, in different proteins. The processed data were analysed with Proteome Discoverer v2.1 software, which was carried out by a bioinformatician from Bristol University. A sequest search was run against the Uniprot Human database and against a 'Common Contaminants' database, which was included routinely. The Phospho analysis was set up as for the Total, but with phosphorylation at S, T and Y included as possible peptide modifications. For total proteome analysis, normalisation on the 'Total Peptide Amount' in each sample was included in the data analysis set up (since we started with an equal amount of each), but this was not included for the Phospho analysis as, due to the phospho-enrichment, the samples were not expected to contain the same amount of peptides. All the data was filtered using a 5%FDR cut-off.

2.5.5.2 Proteomics result analysis

Once the processed results from Bristol University were received, analysis was carried

out to find pathways and proteins associated with CMG2. KEGG dataset, containing numerous classical pathways, was applied to detect the pathways that were associated with CMG2. Protein uniprot ID was retrived using uniprot (https://www.uniprot.org/) and was further transferred into hsa ID on KEGG Mapper (https://www.genome.jp/kegg/mapper/), which can be used directly for the enrichment assay in the KEGG cohort. Another online tool, String dataset (https://string-db.org/), was used to help predict the cell-cell interaction, which further helped us to find the unknown pathways. To further detect the transcription factors involved in the pathways, which are associated with CMG2, enrichr platform was applied (https://maayanlab.cloud/Enrichr/). The design and procedure of the proteomic analysis can be seen in Chapter 6.

2.5.6 Kinexus protein array analysis

Proteins from PANC-1^{pEF} and PANC-1^{CMG2rib2} were prepared for protein array analysis. Protein samples were prepared following the procedure described in section 2.5.7 and sent for an antibody-based protein array assay (Kinexus Bioinformatics Corporation, British Columbia, Canada). The protein smaples in this experiment were adjusted to 3mg/ml, for each sample 200µg protein was prepared. KAM-880 antibody microarray kit was selected for the microarry analysis. Normalisation and initial analysis were provided by the Kinexus. Total protein levels and phosphorylated proteins were further evaluated in the present study.

2.5.7 Immunoprecipitation

Immunoprecipitation was done to check the protein phosphorylation, which includes several steps: Protein extraction, adding antibodies and A/G agarose beads to trap target proteins.

Each cell line was cultured in four 75cm^2 flasks. After the proteins were extracted and quantified (as described in 2.5.1 and 2.5.2), they were divided equally to four Eppendorf tubes. One portion was routinely adjusted to a concentration of 3mg/mL using lysis buffer and 2X sample buffer to be subsequently analysed together with the immunoprecipitation (IP) samples using Western blot. One for total protein analysis, the other three were used for an IP to pull out proteins with phosphorylated serine, tyrosine

and threonine residues, respectively. For each immunoprecipitation, 2µg antibodies were required for every 500µg total protein in a sample. After an incubation at room temperature for 2 hours, the protein A/G beads were added (50µL beads for 500µg protein), and samples were then incubated at room temperature for 1 hour. Following a centrifugation at 4℃ for 10 minutes, a pellet was formed by the beads which bound with antibodies and target proteins. The supernatant containing non-bound proteins was also collected and named as a non-IP sample to verify quanlity and efficiency of the immunoprecipitation. The beads were washed twice with lysis buffer and were finally resuspended in 1X sample buffer. In a normal cell, the phosphorylation percentage of one protein was rarely higher than 20%. The volume of 1X lysis buffer added into the beads was only 1/3rd of the total volume of non-IP samples, and the concentration of the IP samples was higher and easier to be tested. Then the total protein, non-IP samples and IP samples were boiled at 100℃, for 10 minutes. After denature, samples were stored at -20℃ for following experiment. Antibodies used to grab the phosphorylated proteins were shown in table 2.4.

2.6 CMG2 knockdown and overexpression in pancreatic cancer cell lines

2.6.1 Touch down PCR

For the CMG2 overexpression, our lab prepared the plasmids for transfection following the protocol of pEF6/V5-His TOPO® TA plasmid vector (Thermo Fisher Scientific). In brief, the coding sequence of human CMG2 was clonned in pEF6/V5-His TOPO® TA plasmid vector which was used in the present study for CMG2 overexpression in pancreatic cancer cells.

2.6.2 Plasmids amplification

To prepare a stock of plasmid, 2µl of plasmid was added to 30µl TOP10 One Shot® E. coli (Thermo Fisher Scientific). After incubation on ice for 30 minutes, heat shock was carried out at 42℃ for 30 seconds, followed by a cool down on ice for 2 minutes. Next, 200µl SOC Medium (provided) was added, before incubation at 37℃ for 1 hour, to retrieve the resistance to ampicilin. Approximately 40 µl bacteria was spreaded on an LB agar gel containing LB broth medium (L2720, Melford Laboratories, Suffolk, U.K.)

and 100μg/ml ampicillin. The remaining bacteria were added into an universal container, containing 10ml LB broth medium and 100μg/ml ampicilin, then incubated at 37℃ overnight with continuous rotation, before extraction of the plasmid.

2.6.3 Plasmid extraction

For preparation using PureYield Plasmid Maxiprep System (Promega), 8ml bacterial culture from the universal container was added into a flask containing 200ml LB medium with ampicillin (100μg/ml). When the optical density (OD) value of 100μl bacterial culture reached 0.6 at 595nm UV, plasmids were extracted. The bacteria in the universal container were mixed with same volume of 30% glycerol and was then stored at -80℃.

To pellet the bacteria, 200ml of the bacterial culture was separately centrifuged, in four 50ml centrifuge tubes, at 5000 rpm, 4℃ for 15 minutes. The bacterial pellets were resuspended in 3ml resuspension solution, then 3ml lysis solution was added. The tubes were then inverted 3 times genetly followed by incubation at room temperature for 3 minutes. To remove proteins, 5ml neutralization buffter was added into the tube, followed by inversion of the tube 6 times. The samples were then aliquoted into 2ml Eppendorf tubes and centrifuged at 12000 rpm, 4℃ for 15minutes. The solution was separated into two phases, the upper phase contained plasmids while the lower phase was formed by proteins and lipids. To isolate plasmids, PureYield Plasmid Maxiprep System (Promega) and Eluaotor™ Vacuum Elution Device (Promega) were employed. The Maxiprep kit supplies blue columns and white columns, the blue columns contain a filter which can remove the remaining protein and lipids left in the supernatant. The blue column was assembled on top of the white column which was then connected to a vacuum pump. The supernatant was then loaded and filtered through the blue column and the plasmids were then bound to the white column. Following filtration, the blue column was removed. To wash off endotoxin, 5ml of endotoxin removal wash solution containing isopropanel was added to the white column, followed by a further wash with 20ml column washing solution containing ethnol. After air drying for 10 minutes, 700μl PCR water was added into the column with an incubation of 1- 2 minutes. The plasmids were eluted into the PCR water and were then collected in a microcentrifuge tube (1.5ml) which was

connected to the Eluaotor^{TM} Vacuum Elution Device. Another 700μL PCR water was again added to elute any remaining plasmid. The concentration of plasmid collected was then measured using the Implen Nanophotometer (Munchen, Germany).

2.6.4 CMG2 knockdown with CMG2 shRNA

As an RNA interferring technique, artificial shRNA contains a tight hairpin structure and is frequently used for gene knockdown. Once the shRNA enters into a cell, it moves into the nucleus followed by transcription by polymerase, with a resultant product being similar to pri-microRNA. This product is then processed by RNA-induced silencing somplex (RISC). Upon binding to the complementary strand of mRNA, under guidance of the antisense strand, RISC cleaves the target mRNA leading to silencing of the target gene (Moore et al. 2010).

Lentiviral CMG2 shRNA6 (GCTGATTCCAAGGAGCAAGTT) was obtained from Vector builder(Illinois, USA) (Figure 2.4). Four different E.coli bacteria carrying four different plasmids, including CMG2 shRNA6, a scramble shRNA control (CCTAAGGTTAAGTCGCCTCG), psPAX2 (lentiviral packaging) and pMD2.G (envelope), respectively, were employed in the present study. To package lentiviral particles, 4μg of either CMG2 shRNA6 or scramble shRNA were mixed with 3μg psPAX2 and 1μg of pMD2.G plasmid in 1ml OPTI-MEM medium (GIBCO/BRL, Burlington, Ontario, Canada), followed by incubation at room temperature for 30 minutes. To be transfected into 293T cells, 32μl of 1.25mg/ml Poly ethylenimine (PEI) reagent was then added into the mixture. The PEI reagent is a synthetic polymer with a positive charge, while the DNA molecule is negatively charged, which can bind strongly with the positively charged polymer, forming net cationic charges. Therefore, the plasmids can enter the cells. The mixture was then added into the 293T cells, of 70%~80% confluency, drop by drop followed by incubation in 5ml OPTI-MEM medium to generate the lentiviral particles. Efficiency of the transfection was verified with an enhanced green fluorecent protein (EGFP) marker, after overnight culture. The OPTI-MEM medium was then replaced with 5ml of DMEM culture medium. The lentiviral particles in the culture medium were then collected every 24 hours for two days, followed by centrifugation to remove cellular residues. The lentiviral particles were then

stored at -80℃ until use.

To knockdown CMG2 in a target cell line, the cells were cultured in a 24-well plate to reach a confluency of about 80%. For each well, 500µl lectiviral particles were added for each transduction, together with polybrene at a final concentration of 8µg/ml to neutralize the negative charge on the cell membrane, thus facilitating entry of the lentiviral particles into the cells. The transduced cells were then cultured in DMEM and RPMI medium containing 100µg/ml G418 for selection, followed by subsequent mantainence using 50µg/ml G418.

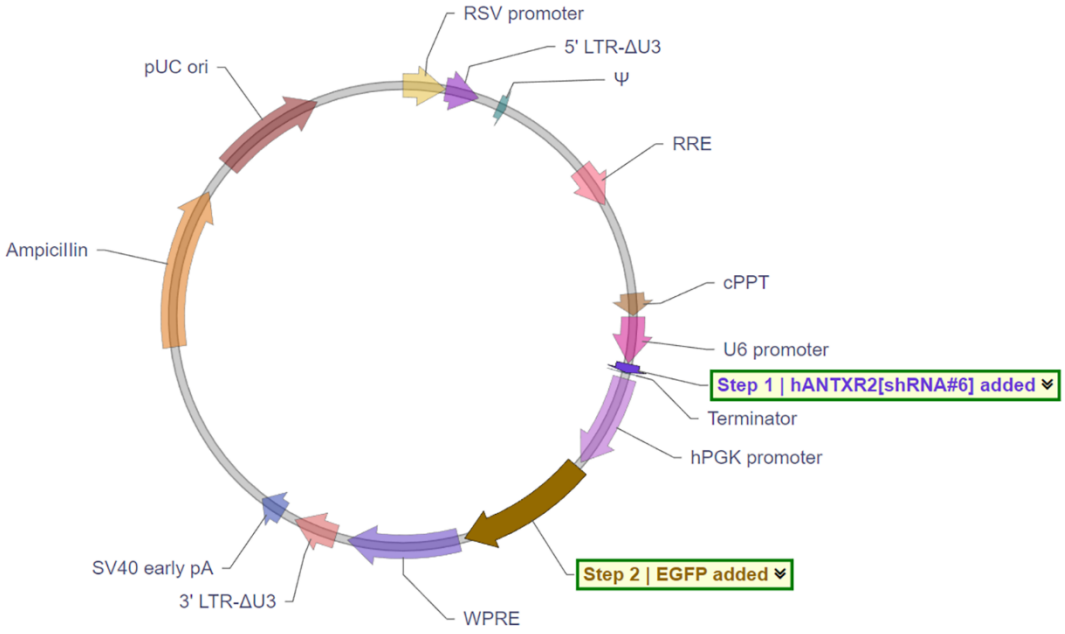

Figure 2.4 Structure and key components of the lentiviral CMG2 shRNA6 plasmid vector.

2.6.5 CMG2 knockdown with a recombinant ribozyme specifically targeting CMG2

For knockdown of CMG2, the pEF/TOPO TA plasmid vector, carrying a ribozyme targeting CMG2 and the same empty vector as a control, were emloyed as previously reported (Ye et al. 2014b). In brief, pancreatic cancer cells were seeded on a 6-well plate to reach confluency of approximately 60-80%. Before transfection, the cells were incubated with OPTI-MEM medium (GIBCO/BRL, Burlington, Ontario, Canada) for 1

hour. Meanwhile, 3μg plasmid carrying the recombinant ribozyme targeting CMG2, together with 12μl of 1.25mg/ml Poly ethylenimine (PEI) reagent and 1ml OPTI-MEM medium, were mixed in a 1.5ml Eppendorf tube followed by a 20-minute incubation at room temperature. After incubation at 37℃, for 24 hours, the medium was changed to normal DMEM culture medium. The cells were then transferred to a T25 flask for subsequent culture and selection. To select the transfected cells, 4μg/ml blasticidin was used and the selected cells were subsequently maintained in DMEM mediun with 1μg/ml blasticidin.

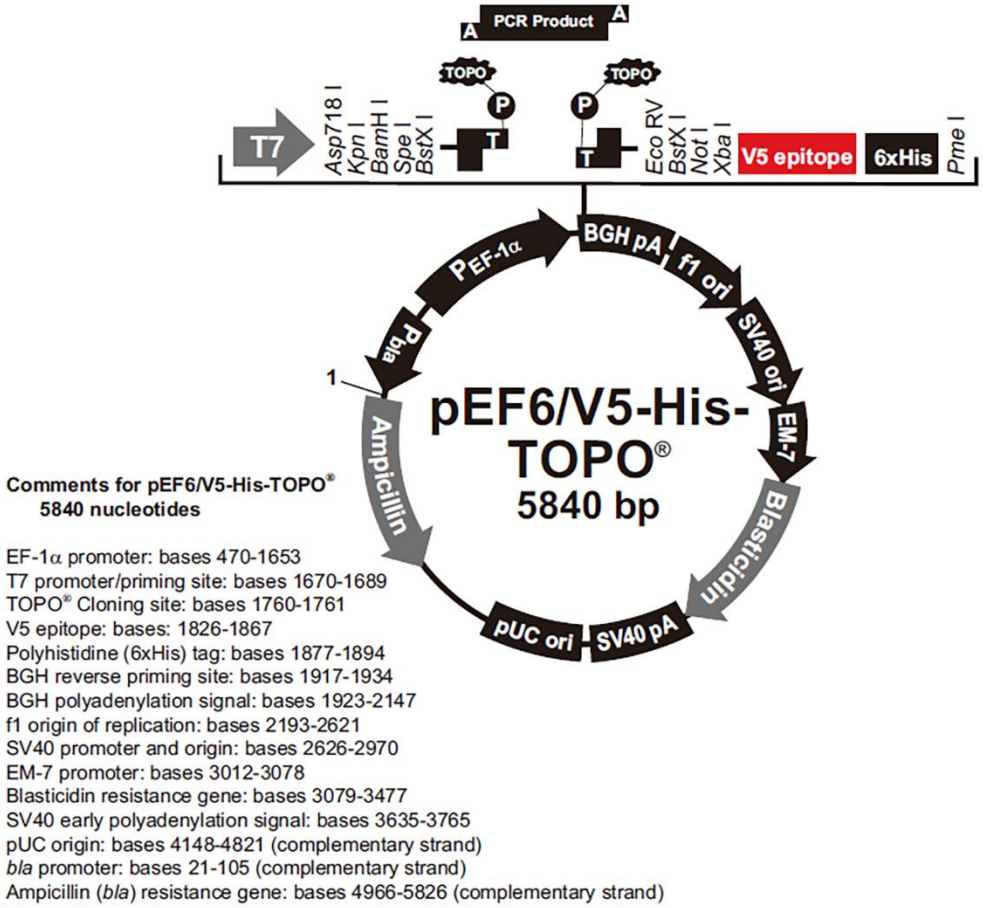

Figure 2.5 Structure of the pEF6/V5-His-TOPO TA plasmid vector (Invitrogen, Manchester, UK), used for cloning of both CMG2 coding sequence and CMG2 ribozyme.

2.6.6 CMG2 overexpression

For CMG2 overexpression, the pEF6 plasmid vector, carrying the coding squence of

human CMG2 and the empty vector were employed, which were previously developed at the host laboratory (Ye et al. 2014b). In brief, the coding sequence of human CMG2 was cloned into the pEF/V5-His-TOPO TA vector, which was verified by sequencing. The CMG2 overexpression vector and control vector were transfected into target cells, respectively. After selection with 2-5μg/ml blasticidin for a duration up to 2 weeks, the selected cells were mantained in a medium containing 0.5μg/ml blasticidin until used for the following experiments.

2.7 Cell function assays

2.7.1 *In vitro* cell proliferation assay

Cells were detached from T25 flasks using trypsin counted and seeded into three 96-well plates to be cultured over durations of 1, 3 and 5 days. The number of cells seeded differed according to the proliferating rate of the cell lines tested. For example, 2,000 MiaPaCa-2 cells were seeded in each well, whilst 3,000 PANC-1cells and 4,000 ASPC-1 cells in 200μl medium were seeded in each well. After incubation, cells in the three plates were fixed at Day 1, Day 2 and Day 5, respectively, with 100μl 4% formaldehyde per well for 15 minutes. The fixed cells were then stained with 100μl 0.5% crystal violet (w/v) at room temperature for 10 minutes. The plates were rinsed with tap water and were then air-dried. The crystal violet staining was dissolved with 10% acetic acid (200μl/well) and the absorbance was determined at 595 nm using a spectrophotometer (BIO-TEK, Elx800, UK). There were six replicates tested for each cell line per plate. Three independent experiments were performed to validate the findings. This method was modified from a protocol, which was previously reported (Liu et al. 2020).

2.7.2 Cell proliferation and viability assay

Cell Counting Kit-8 (CCK-8) was used to measure cell viability changes after CMG2 knockdown or overexpression. The main component of this kit is WST-8 (2-(2-methoxy-4-nitrophenyl)-3-(4-nitrophenyl)-5-(2,4-disulfophenyl)-2H-tetrazolium, monosodium salt), which produces a water-soluble formazan dye upon bio-reduction, in the presence of an electron carrier, 1-Methoxy PMS (1-methoxy-5-methylphenazinium methyl sulphate). CCK-8 solution was added directly to the cells, without pre-mixing with any other reagent. WST-8 is bio-reduced by cellular dehydrogenase to an orange formazan product that is soluble in tissue culture medium. The amount of formazan produced is then determined by reading the OD value. The amount of dehydrogenase is positively correlated with the number of viable cells. Cells were seeded in three 96-well plates, similar to the aforementioned proliferation assay using crystal violet. On 1st, 3rd, and 5th day, the CCK8 (cell counting kit 8) (Munich, Germany) was used to measure the cell viability by adding 10µl of CCK8 solution into each well. After incubation for 2 hours at 37 ℃ , absorbance was determined at a wavelength of 545nm, using the spectrophotometer (BIO-TEK, Elx800, UK). This procedure was following the CCK8 protocol (Munich, Germany).

2.7.3 Cell migration assay

For cell migration assays, two different methods were employed: wound healing assay and Cytodex-2 bead motility assay.

The wound healing assay was applied to determine the migration of both MiaPaCa-2 and PANC-1 cells. Cells were seeded into a 24 well plate allowing the cells to form a monolayer. The monolayer of cells was scratched using a 200µl pipette tip and photographs were taken over a 6-hour period, using an EVOS FL Auto Cell Imaging System (auto imaging system, Thermo Fisher Scientific). Migration area (also known as closure of the wound) was measured using ImageJ software (National Institutes of Health, USA).

Since the ASPC-1 cells are less adhesive and incapable of forming a monolayer, a microcarrier for cell culture, Cytodex-2 beads (collagen-coated beads, size 125-212µm, Corning cat 83 NO. 3786, USA), was employed for determining the migration of

ASPC cells. In brief, 5g of the Cytodex-2 beads were suspended in 75 ml PBS. Once the cells were harvested and counted, 1 million cells were then added to 1ml beads suspension in a universal container, in 10ml of culture medium. After overnight incubation, cells remaining suspended were washed away using PBS, cells attached to the beads were subsequently resuspended in 1ml medium and seeded 100µl per well in a 96-well plate. After a 3-hour incubation, the beads and non-migrated cells were washed off using PBS. During the incubation, cells with a higher motility migrated from the beads onto the bottom of wells. The cells attached to the bottom of the well were then fixed with 4% formaldehyde for 15 minutes and stained with 0.5% crystal violet for 10 minutes. The crystal violet staining was subsequently dissolved in 10% acetic acid, followed by determination of the absorbance at 595nm. The procedure of wound healing assay was modified from a previous report (Jiang et al. 2015).

2.7.4 Cell adhesion assay

To investigate whether CMG2 can affect cell adhesion ability, an *in vitro* adhesion assay, using an artificial basement membrane gel, was employed. A 96-well plate was precoated with Matrigel (Corning Incorporated, Flintshire, UK) by adding 100µl 50µg/ml Matrigel per well, which was prepared in serum-free medium. The Matrigel coating was air-dried at 65℃ for 2 hours followed by rehydration in 100µl of sterile water for 30 minutes. Matrigel is a gel-like substance, which is rich in laminin, collagen and many other ECM proteins, and is usually used to mimic the basement membrane during research of cancer metastasis (Kleinman and Martin 2005). To determine the adhesion, 20,000 cells in 200µl medium were seeded into each well, 6 replicates were included for each cell line or treatment. After incubation for 40 minutes at 37℃ with 5% CO_2, the non-adherent cells were removed and washed twice with PBS before the adhered cells were fixed and stained using 4% formaldehyde and 0.5% crystal violet, respectively. The plate was then rinsed with tap water before the stained cells were photographed. The absorbance was then determined by dissolving the crystal violet in 10% acetic acid at a wavelength of 595nm using the spectrophotometer (BIO-TEK, Elx800, UK). The procedure of cell-matrix assay was modified from a previous report (Jiang et al. 2015).

2.7.5 Invasion assay

A trans-well invasion assay was described by Parish et al., in 1992 (Parish et al. 1992). Briefly, trans-well inserts with 8μm pores (BD Falcon, BD Biosciences, Oxford, UK) were placed in a 24-well plate. Each insert was pre-coated with 100μl of 500μg/ml Matrigel (BD Biosciences, Berkshire, UK). After the plate was dried for 2 hours at 65℃, the gel was rehydrated in distilled water for 30 minutes. The water was then removed, before 20,000 cells in 200μl medium were added into each of the Matrigel coated inserts. The same number of cells were seeded into a spare well for each cell line tested as controls, to exclude influence from proliferation and cell death etc. After incubation for 3 days at 37℃ with 5% CO2, non-migrated cells, together with the Matrigel coat, were removed using a cotton swab. The invaded cells which had migrated to the other side of the membrane of the trans-well insert, together with the control cells, were then fixed and stained using formaldehyde and crystal violet routinely. The plate and inserts were rinsed with tap water and air dried at 55℃ for 24 hours. Cells were then visualised and photographed under a microscope. The crystal violet was re-solubilised using 600μl of 10% acetic acid. Absorbance was then determined at 595nm using the spectrophotometer (BIO-TEK, Elx800, UK). The invaded cells were also counted. Numbers and absorbance of the invaded cells were then normalised against the corresponding controls. This method was adjusted from a procedure, which has been previously reported (Jiang et al. 2015).

2.7.6 Cell aggregation and apoptosis assay

To determine whether CMG2 can affect the aggregation of pancreatic cancer cells and simultaneously occurring *anoikis,* during dissemination of the cancer cells through peritoneal cavity, *in vitro* aggregation and apoptosis assays were conducted. Pancreatic cancer cells were harvested by digestion using trypsin, followed by counting the harvested cells. To assess the aggregation, 5ml of cell suspension at a density of $1X10^5$ cell/ml were transferred into a universal container. The cells were then incubated at 37℃, 5% CO_2, with slow shaking. The number of single cells and cell clusters were counted every hour during the first 6 hours of incubation, meanwhile, 200μl cell culture was

collected at each time point and transferred to a 96-well plate followed by fixation with 75% ethanol and staining with Hoechst (final concentration: 0.1ug/100ul) (Thermo Fisher). The Hoechst is a blue fluorescent dye,which is cell membrane permeable, that can stain DNA and is capable of staining the nuclei of both living and dead cells. Cells with a condensed, lobular or breaked nucleus are identified as early or late apoptotic cells as shown in Figure 2.6). Photographs were taken with the EVOS FL Auto Cell Imaging System (Thermo Fisher Scientific) and the percentage of apoptotic cells was then calculated.

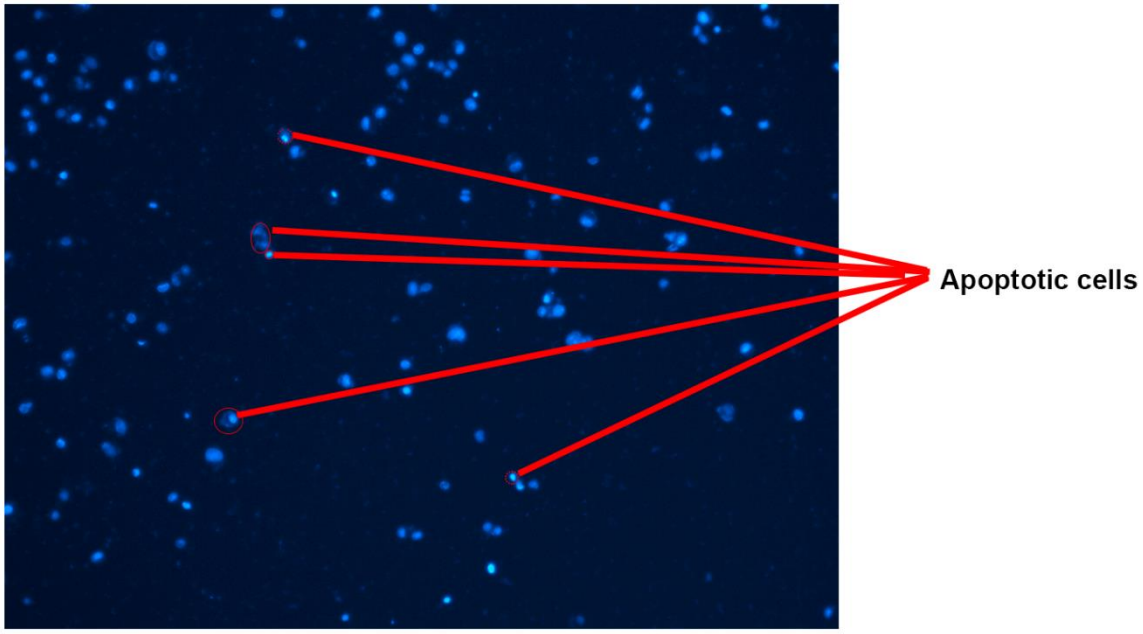

Figure 2.6 Detection of apoptotic cells using nuclear staining with Hoechst. Shown is a photo taken under fluorescent microscope (200×).

Based on the apoptosis analysis using Hoechst, a time point was identified when the biggest difference was observed for cell viability, by comparing CMG2 modified cell lines with the control. The cell viability was further determined using the CCK8 assay. In brief, 50µl CCK8 reagent were added into each sample at the beginning, the absorbance at 450nm was measured at that time point. The cell aggregation assay in this experiment was modified from a mothod which has been previously reported (Debruyne et al. 2014).

2.7.7 Flowcytometric apoptosis assay

Flowcytometry is a method that can be applied to measure cell viability and cell size. In this study, a FITC labelled Annexin-V and propidium iodide (PI) were used to determine the apoptotic cells, using an Annexin V Apoptosis Detection Kit (sc-4252-AK, Santa Cruz Biotechnology, Texas, USA).

At an early stage of cell apoptosis, the phosphatidylserine (PS) residues, located at the inner layer of biphosphlipid on the cell membrane in a healthy cell, can be translocated to the cell surface. The Annexin V dye can bind to PS but is unable to penatrate the cell membrane. However, an apoptotic cell with the translocated PS can be stained by FITC labelled Annexin V. PI is a red fluorescent dye that can bind to DNA and RNA inside a cell, but it is not permeable through the cell membrane. At the late stage of apoptosis or necrosis, the cell membrane is leaking or broken and incapable of selective permeability, so that the PI can enter cells, which can be used as a probe of late apoptotic and dead cells.

Pancreatic cancer cells were harvested, counted, and incubated in a universal container for determining *anoikis* in the suspending cells as mentioned. Apoptotic cells were then determined using a flowcytometric assay.

Step 1: The cells were collected and washed twice with ice cold PBS e and resuspended in 400µl of 1X binding buffer, with a density under $1X10^6$/ml. Each sample was tested in triplicate with 100µl of the cell suspension per test.

Step 2: The cells were then stained by adding 2µl Annexin V (0.4µg Annexin V) and 2µl PI solution to the 100µl cell suspension. For a negative control, neither Annexin V nor PI were added. For a positive control, H_2O_2 was added to induce cell apoptosis with a final concentration of 0.01%.

Step 3: Samples were pipetted gently to ensure the dyes were well mixed, followed by incubation of 15 minutes in the dark at room temperature.

Step 4: To prepare the cell suspension for detection using a flow cytometer (FACS Canto II, BD biosciences, Berkshire, UK), the cell suspension was transferred into 2ml binding buffer in a flow cytometric tube, , avoiding air bubbles. Settings for the two optical detectors, forward scatter (FSC) and side scatter (SSC), were using the non-

stained cells. Settings for both FITC and PI were subsequently adjusted with appropriate voltage, gain and speed. Suitable gates were applied to detect and record FITC and PI labelled cells.

Step 5: The recorded readings were analysed using FlowJo (https://www.flowjo.com/). All the debris and clustered cells were excluded with an appropriate gate using both FSC and SSC. The gated single cells were subsequently analysed with a 2-D plot according to the intensity of both PI (Y axis) and FITC (X axis). With corresponding thresholds, FITC positive and PI positive cells were separated from the negative cells as shown in Figure 2.7. Apoptotic population was calculated by including both early and late apoptotic cells, in comparison with the healthy population.

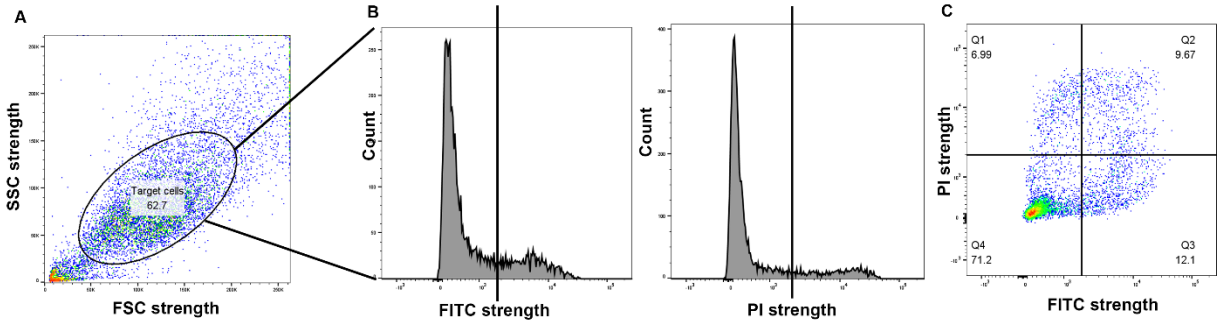

Figure 2.7 Flowcytometry analysis. Shown is an example of flowcytometry analysed based on the positive control of the PANC-1 cell line with CMG2 knockdown. (A) Based on FSC and SSC strength, cells with a suitable size were selected. (B) Histograms were produced to determine the cut off value of both FITC staining and PI staining. (C) The cut off values were applied to divide cells into four different parts. Q1 to Q4 represent nonspecific staining, late apoptotic cells/dead cells, early apoptotic cells and healthy cells, respectively.

2.8 Peritoneal metastatic models *in vitro*

2.8.1 Adhesion to mesothelial cells

To assess the influence of CMG2 on the adhesion of pancreatic cancer cells to mesothelial cells, $3X10^4$ MET5A cells were seeded into a 96 well plate. After a monolayer was formed, the pancreatic cancer cell lines, with CMG2 knockdown or overexpression, were harvested and counted. To label the pancreatic cells, 2ml of the cell suspension at a density of $5X10^5$/ml was stained with DiI (1,1'-dioctadecyl-3,3,3',3'-tetramethylindocarbocyanine perchlorate) at a concentration of 10μg/ml (Thermo Fisher

Scientific) at 37℃ for 30 minutes. After staining, the cells were centrifuged at 1600 rpm for 5 minutes and washed twice with PBS following which, 20,000 cells in 200µl medium were seeded to the mesothelial cell monolayer, followed by incubation for 40 minutes. Non-adherent cells were discarded and the plate was washed with PBS twice, adhered cells were fixed with 4% formaldehyde and were then photographed under a fluorescent microscope (EVOS FL Auto Cell Imaging System, Thermo Fisher Scientific). This assay was carried out following a protocol which has been reported previously (Yang et al. 2023).

2.8.2 Adhesion to Hyaluronic acid

As a part of the peritoneum, mesothelial cells are covered by a thin lubricating layer of hyaluronic acid (HA), which is secreted and deposited by the underlying mesothelial cells. During dissemination into the peritoneal cavity, attachment to the HA layer by the cancer cells is an indispensable step before subsequent invasion through the mesothelial cells and colonisation. Adhesion of cancer cells to HA was evaluated using HA of different molecular weights. Hyaluronic acids of different molecular weights elicit different biofunctions. In the present study, high molecular weight, low molecular weight, and ultralow molecular weight hyaluronic acid were employed to evaluate the adhesion mediated between CMG2 and HA.

High molecular weight hyaluronic acid (CLR002, Sigma-Aldrich), low molecular weight hyaluronic acid (CLR001, Sigma-Aldrich), ultralow molecular weight hyaluronic acid (CLR003, Sigma-Aldrich) and hyaluronic acid inhibitor (AS-62622, Anaspec, Fremont, US) were employed to competitively bind molecules, to evaluate the interaction between CMG2 and HA in the adhesion of pancreatic cancer cells to HA layer and mesothelial cells. MET5A cells were seeded to precoat a 96 well plate, followed by 24 hours culture until a monolayer was formed. Another 24 hours incubation of the mesothelial cells enabled a HA coating to be formed and, together with a HA coating only, was used to determine the adhesion of pancreatic cancer cells to mesothelial cells with HA coating or HA coating only, following the aforementioned procedure of adhesion of cancer cells to mesothelial cells with a DiI labelling. More

details for the specific experiments are provided in the corresponding results chapter (Chapter 5).

2.8.3 *In vitro* invasion assay through Matrigel and mesothelial cells

To mimic the structure of the peritoneum, trans-well inserts with 8μm pores were pre-coated with 50μg Matrigel, following the procedure described in the trans-well invasion assay (section 2.7.2.5). In addition to the Matrigel, 30,000 MET5A cells were seed onto the rehydrated Matrigel to form a mesothelial layer. For each insert, 20,000 cancer cells in 200μl medium were seeded. To validate the results, the same number of cells was also seeded in a spare well, as a control. One insert coated with Matrigel and MET5A cells was included as an additional control, to exclude the possibility of invasion of MET5A cells through the Matrigel. After a 3-day incubation at 37℃, 5% CO_2, the cells in the 24 well plate and inserts were fixed with 4% formalin for 10 minutes, followed by staining with crystal violet (0.5%) for 10 minutes. The plate and trans-well inserts were rinsed gently with tap water, the Matrigel, mesothelial cells and the pancreatic cancer cells, which did not remain at the inner side of the insert, were removed with a cotton swab. When the plate and inserts were air dried, photographs were taken under a microscope. Invaded cells were counted using ImageJ. The crystal violet staining was re-solubilised using 10% acetic acid, and absorbance was determined at a wavelength of 595nm. The number of invaded cells was normalised against the corresponding controls.

2.9 Transcriptomic and proteomic datasets of pancreatic cancer

2.9.1 The Cancer Genome Atlas (TCGA) (Cancer Genome Atlas Research et al. 2013).

This cohort of pancreatic cancer includes 151 PDAC samples, 9 normal pancreatic tissues, 3 non-invasive tumour samples, 8 neuroendocrine tumours, 1 acinar ductal adenocarcinoma,1 distant metastatic sample and 9 unconfirmed samples. The datasets, including both normalised RNA sequencing data and proteomic data, were downloaded from the Firebrowse website (http://firebrowse.org/) followed by curation, as described previously (Nicolle et al. 2019) before they were employed in the present study.

2.9.2 GSE71729

This dataset comprises 145 primary and 61 metastatic PDAC tumours, 17 cell lines, 46 pancreas and 88 distant site adjacent normal samples. Gene expression was determined using Agilent human whole genome 4x44K DNA microarrays (Agilent Technologies) (Moffitt et al. 2015).

2.9.3 GSE15471

This dataset contains 36 pancreatic cancer tumours and paired adjacent pancreatic tissues, with gene expression profiles determined using Affymetrix U133 Plus 2.0 whole-genome chips (Badea et al. 2008).

2.9.4 GSE19650

This includes 7 normal pancreatic tissues, 6 papillary-mucinous adenomas (IPMA), 6 intraductal papillary-mucinous carcinomas (IPMC) and 3 invasive Intraductal papillary-mucinous neoplasms (IPMN), which were quantitatively analysed using Affymetrix Human Genome U133 Plus 2.0 Array (Hiraoka et al. 2011).

2.9.5 E-MTAB-2770

This cohort includes RNA-sequencing data of 1019 human cancer cell lines. Data comes from Broad-Novartis Cancer Cell Line Encyclopedia (http://www.broadinstitute.org/ccle) (Ghandi et al. 2019).

2.10 Statistical analysis

To analyse the data, the T-test was used for comparisons between two groups, if the data were normally distributed, whilst Mann-Whitney u test was used for analysis of non-normally distributed data. For datasets containing 3 or more groups, one-way ANOVA was used for normally distributed data and the Kruskal-Wallis test was used for non-normally distributed data. Both Pearson and Spearman tests were used for analysing correlation between two genes. Kaplan-Meier survival analysis, for CMG2 in patients with pancreatic cancer, was conducted using an online survival analysis

platform (www.kmplot.com) (Nagy et al. 2021). Software used for the data processing and statistical analyses in the present study include Excel 2016 (Microsoft 365), Graphpad Prism (version 26, company Graphpad Software, California, US) and SPSS (Version 26, IBM UK Ltd., Portsmouth, UK).

Chapter 3

The expression of CMG2 in pancreatic cancer and its implication in the disease progression

3.1 Introduction

CMG2 is associated with the development of certain malignancies including breast cancer, prostate cancer, gastric cancer and glioma (Ye et al. 2014b; Xu et al. 2019). Reduced expression of CMG2 in breast cancer is associated with a poor prognosis. Overexpression of CMG2 resulted in a decreased growth of the cancer cells (Ye et al. 2014c). CMG2 plays an inhibitory role on invasiveness of prostate cancer cells (PC-3) but enhances adhesion of the cancerous cells (Ye et al. 2014b). CMG2 can promote the formation of laminar pseudopodia and filopodia in glioma cells by enhancing Hippo signalling (Xu et al. 2019). Moreover, higher CMG2 expression in gastric cancer is associated with a poor prognosis (Ji et al. 2018). CMG2 can activate the Wnt/β-catenin pathway in gastric cancer cells through an upregulation of LRP6, thus to promote the invasiveness and metastatic capacity (Ji et al. 2018), in which a positive link between CMG2 and stemness in gastric cancer may also involve (Yang et al. 2011; Ji et al. 2018). Additionally, our recent study has demonstrated that the deregulated CMG2 in endocrine related cancers including prostate cancer and breast cancer is due to a repression mediated by androgen receptor (AR) and oestrogen receptor (ER), respectively (Fang et al. 2022).

Pancreatic cancer is the 10th most common cancer in UK with a poor 5-year survival rate being less than 5% (Cancer Research UK, https://www.cancerresearchuk.org, 2023). Difficulties in the early detection and lack of effective treatment provoke more investment and effort in the research of this fatal disease. An initial evaluation of CMG2 in the disease by determining CMG2 transcripts in a cohort of pancreatic cancer showed an increased expression of CMG2 in pancreatic cancer. This provokes further research to elucidate its implication in the tumourigenesis and disease progression of pancreatic cancer. In the present study, analyses were conducted to evaluate involvement of CMG2 in tumour growth, invasion, lymph node metastasis and distant metastasis.

3.2. Materials and methods

3.2.1 Quantitative analysis of CMG2 transcript levels in pancreatic cancers

CMG2 transcripts were determined in the cohort of pancreatic cancer tissues obtained

from Peking University Cancer Hospital (section 2.2) using QPCR following a standard protocol described in section 2.4.7, which was done by Dr Ye. The pancreatic cancer cohort comprises 153 tumour and 175 normal samples. All protocol and procedures were approved by the Peking University Cancer Hospital Research Ethics Committee (MTA01062008) (Dart et al. 2019).

3.2.2 Immunohistochemical stain of CMG2 in pancreatic cancer tissue microarray

Expression of CMG2 protein in human pancreatic cancer was evaluated by conducting an immunohistochemical staining for CMG2 in a tissue microarray (TMA) (PA2081, Biomax, Maryland, USA) following a protocol described in Chapter 2 section 5. In brief, after retrivation of antigen and blocking using horse serum (1 drop in 5ml PBS), the TMA was incubated with an anti-CMG2 antibody (ab70499, 1:500, Abcam, Cambridge, UK) followed by detection using an universal biotin labelled secondary antibody (name/cat no., dilution, company and address) and Vectastain Universal Elite ABC Kit (PK6200, Vector laboratories, California, USA). A negative control was employed to exclude non-specific staining by conducting the staining without the primary antibody. The staining was evaluated and scored by three pathologists (Professor Paul Griffiths, Dr Kate Murphy and Dr Matthew Pugh).

3.2.3 Public dataset

Five public datasets were analysed: The Cancer Genome Atlas (TCGA) (http://firebrowse.org/), GSE71729 (Moffitt et al. 2015), GSE15471 (Badea et al. 2008), GSE19650 (Hiraoka et al. 2011) and Kmplot (https://kmplot.com/analysis/). More details can be found at Chapter 2.

3.2.4 Data analysis

To analyse the data, T-tests were used for comparisons between two groups if they were normally distributed, Mann-Whitney u test was used for analysis of non-normally distributed data. For datasets containing three or more groups, one-way ANOVA can be used for normally distributed data or Kruskal-Wallis test for non-normally distributed data. Spearman test were used for correlation analyses. Software used is SPSS

(Version 26, IBM UK Ltd., Portsmouth, UK). Kaplan-Meier survival analysis was conducted using the online survival analytic platform (www.KMplot.com).

3.3 Result

3.3.1 CMG2 is aberrantly expressed in pancreatic cancer cell

The quantitative analysis of CMG2 transcripts in the Beijing pancreatic cancer cohort (previously done by Dr Ye) revealed an increased expression of CMG2 in pancreatic cancers (n=153), p=0.002 compared with adjacent normal pancreatic tissues (n=174) (Table 3.1). The increased expression of CMG2 in pancreatic cancer was also observed in two publicly available datasets; GSE71729 and GSE15471 in which the expression of CMG2 in primary tumours of pancreatic cancer was compared with adjacent normal pancreatic tissues (Figure 3.1 A and B). CMG2 protein expression in pancreatic cancer was further examined in the pancreatic cancer TMA. Increased expression was seen in pancreatic cancers in comparison with normal pancreas and adjacent normal pancreatic tissues (Figure 3.1C).

Table 3.1 Transcript levels of CMG2 in pancreatic cancer

Clinical samples	N	Median (IQR)	*p*-value
Tumour	153	4 (0~568)	0.002
Normal	175	0 (0-54)	
Gender			
Male	93	3 (0~283)	0.5474
Female	60	5 (0~1093)	
Node status			
Node negative	60	21 (0~929)	0.4694
Node positive	81	2 (0-157.9)	
Differentiation			
High	7	47 (1~15659)	
Moderate high	13	2 (0~2005)	0.428 v.s. High
Moderate	56	2 (0~247)	0.765 v.s. High
Moderate low	59	3 (0~584)	0.847 v.s. High
low	10	284 (0~5209)	0.24 v.s. High
TNM staging			
1-2	111	20 (0~1109)	0.483
3-4	24	2 (0~154)	
T staging			
1-2	20	11 (0~209)	0.459
3-4	107	19 (0~1554)	
Clinical outcomes			
Dead	36	132 (0~1697)	0.093
Alive	108	2 (0~454)	
Metastasis			
No	140	6 (0~913)	0.4697
Yes	13	0 (0~107)	

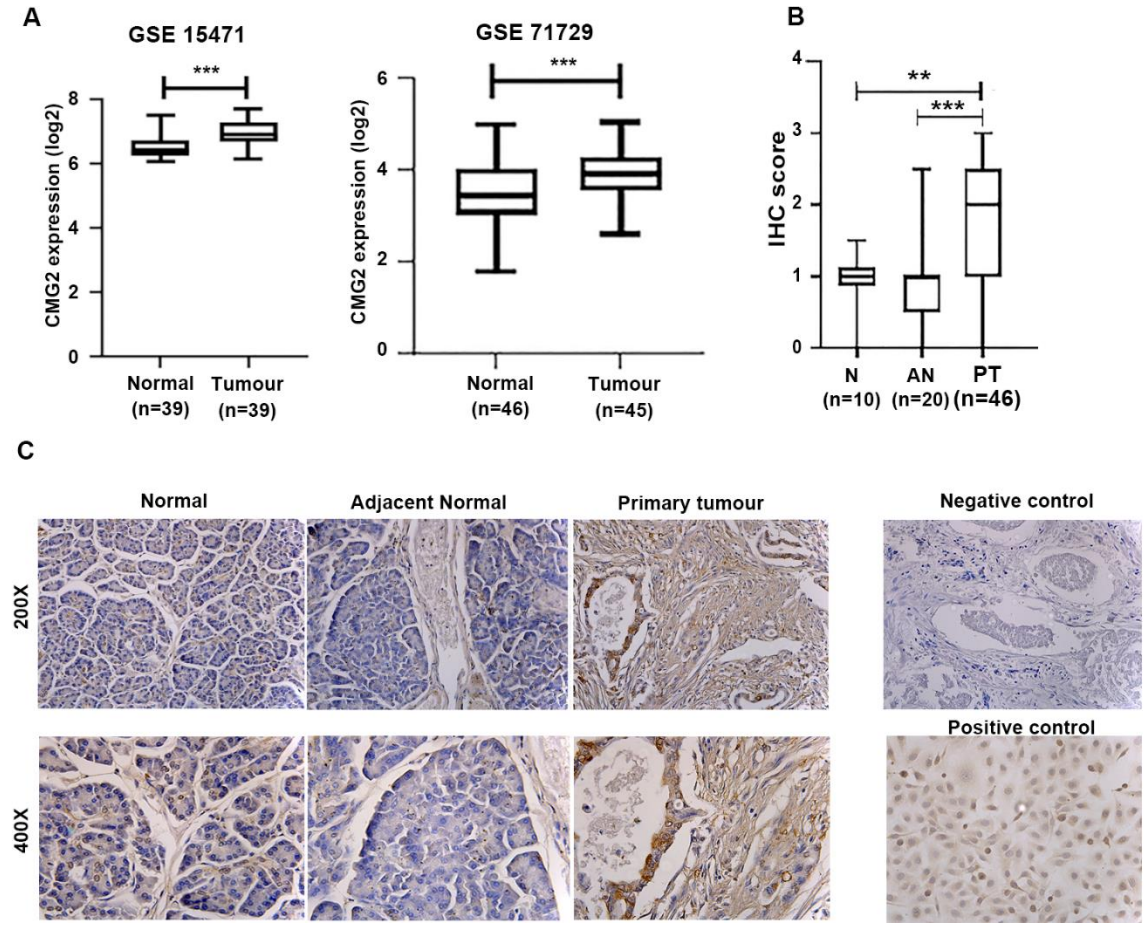

Figure 3.1 Aberrant CMG2 expression in pancreatic cancer. (A) Expression of CMG2 in pancreatic tumours was analysed in comparison with adjacent normal pancreatic tissues in two gene expression array datasets GSE71729 (Moffitt et al. 2015) and GSE15471 (Badea et al. 2008). (B) Shown are the IHC scores of normal pancreas tissues (N), adjacent normal pancreatic tissues (AN) and CMG2 staining in primary tumours (PT) on the tissue microarray (PA2081). (C) Representative images of PT, AN and N were reduced from photos taken at magnifications of 200X and 400X, respectively. Negative control was a staining performed with secondary antibody only. CMG2 overexpressing HECV cells was included as a positive control for the staining. ***p<0.001, **p<0.01, *p<0.05.

3.3.2 Expression of CMG2 in patients of different genders and ages

Expression of CMG2 in pancreatic cancers was analysed according to gender and age of patients. CMG2 expression in the primary tumours was similar in patients at age of 60 or above in comparison with those younger patients. Similar expression levels of CMG2 transcripts were seen in both female and male patients (Table 3.1). In our recent

study, it was shown that CMG2 was repressed by sex hormone in endocrine related cancer including breast cancer and prostate cancer (Fang et al. 2022). In the TCGA pancreatic cancer cohort, Spearman correlation tests showed that CMG2 expression was positively correlated with AR in male patient whilst CMG2 appeared to be inversely correlated with ER in female patients though it did not reach a statistically significant level.

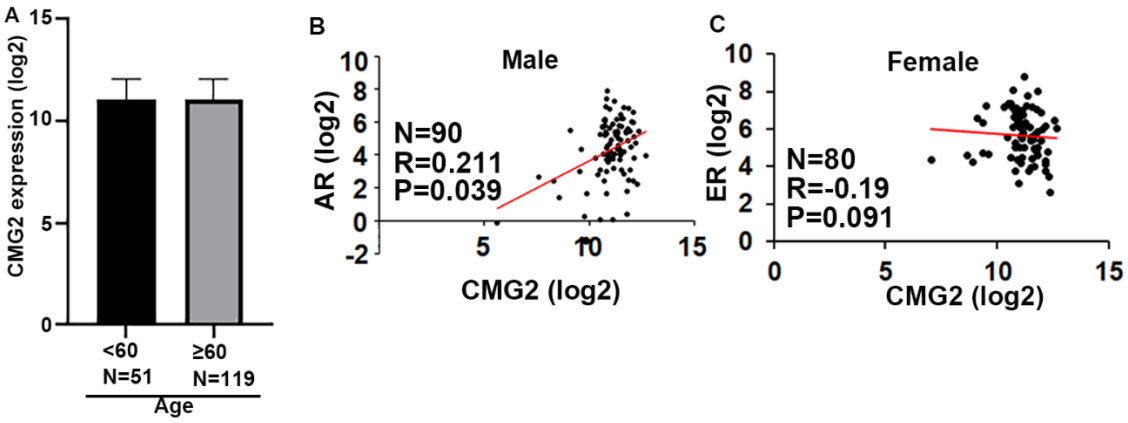

Figure 3.2 CMG2 expression in different group of pancreatic patients. Shown are in TCGA dataset, (A) CMG2 expression in patients at different ages, <60 vs ≥60. Correlations between CMG2 and AR (B) and ER (C) in the TCGA pancreatic cancer cohort was analysed using Spearman test, respectively.

3.3.3 CMG2 and lymphatic metastasis of pancreatic cancer

Regional lymphatic system is an important route for the cancer cells to spread and eventually develop regional lymph node metastases and distant metastases. Involvment of CMG2 in lymph node metastasis of pancreatic cancer was firstly assessed by analysing CMG2 expression in both TCGA PAAD cohort and the TMA which was immunochemically stained for CMG2 according to the different status of lymph node metastasis. No change of CMG2 expression was seen at both mRNA levels and protein expression in the primary tumours which presented lymphatic metastasis at the diagnosis of the disease (Figure 3.3A and B). The relationship between CMG2 and lymphangiogenesis markers was also analysed. when the TCGA and GSE71729 are combined, only the a positive correlation between CMG2 and PDPN was revealed in both TCGA and GSE71729 cohorts (Figure 3.3C).

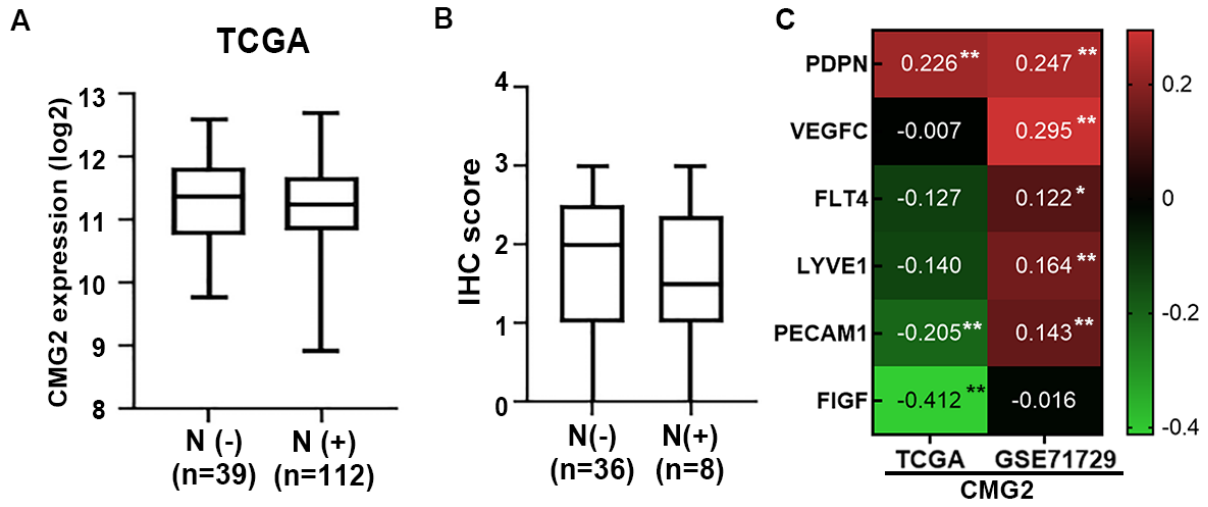

Figure 3.3 CMG2 expression and lymph node metastasis in pancreatic cancer. (A) CMG2 expression in primary tumours with/without lymph node metastasis in the TCGA cohort. (B) IHC staining of CMG2 protein in primary tumours with lymph node metastasis compared with those remained free from the lymph node metastasis (PA2081). (C) Heatmap shows correlation between CMG2 and the lymphangiogenesis markers in both TCGA and GSE71729 (Moffitt et al. 2015) datasets.

3.3.4 CMG2 and distant metastasis of pancreatic cancer

In term of the distant metastasis, a trend of increasing expression of CMG2 was seen in the primary tumours which presented distant metastases at the diagnosis of the disease although this did not reach a statistically significant level, p=0.07 when compared with its expression in primary tumours without distant metastasis (Figure 3.4A). But the TCGA cohort is insufficient for any conclusive analysis for the expression of CMG2 in tumours developed distant metastases due to smaller number of tumours that had distant metastases. However, the transcripts levels of CMG2 were significantly higher in metastatic tumours (n=61) compared with that in primary tumours (n=162) (Figure 3.4B).

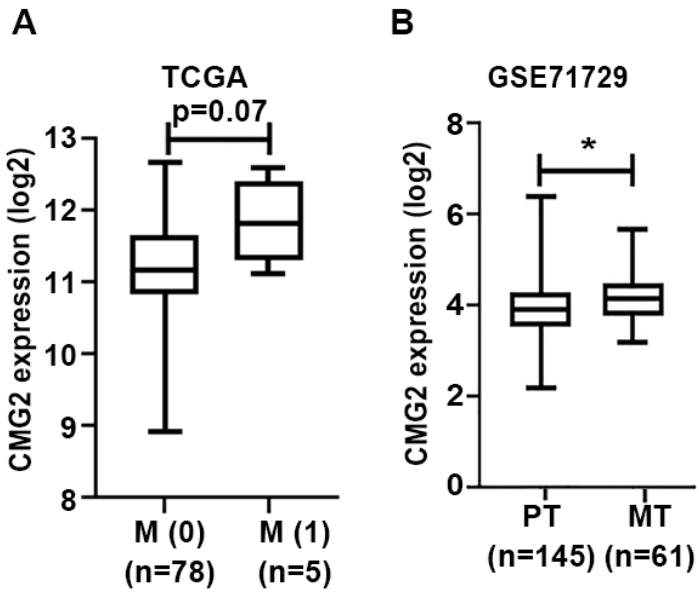

Figure 3.4 CMG2 expression and the metastasis of pancreatic cancer (A) Shown are CMG2 transcript levels in primary tumours according to status of distant metastasis, p=0.07. M (0) is primary tumour without distant metastasis. M (1) is primary tumour with distant metastasis. (B) The expression of CMG2 in primary tumours (N=162) and metastatic tumours (MT) (N=61) in the GSE71729 cohort. ***p<0.001, **p<0.01, *p<0.05.

3.3.5 Elevated expression of CMG2 in pancreatic cancer and prognosis of the disease

Association between CMG2 and pancreatic cancer prognosis was analysed using an online platform for Kaplan-Meier survival analysis (Nagy et al. 2021). A Log-rank test has been used to test the significance. Patients with high levels of CMG2 expression have a significantly shorter overall survival (OS) (P<0.001) compared with those who had a lower expression level of CMG2 (Figure 3.5A). Furthermore, patients with a higher CMG2 expression level had a shorter relapse-free survival (RFS) (Figure 3.5B).

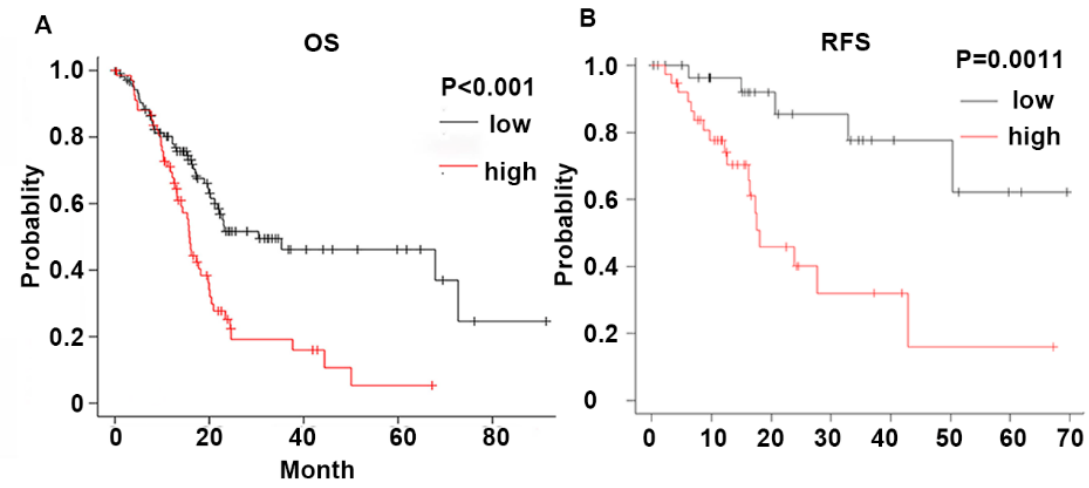

	Cut off value	Median survical (low)	Median survival (high)
OS	3184	30.43 (n=108)	15.77 (n=69)
RFS	2615	50.37 (n=93)	12.13 (n=59)

Figure 3.5 CMG2 and the prognosis of pancreatic cancer. (A) Association between CMG2 expression and patients' survival was analysed using the KMplot online platform (KMplot.com) (Nagy et al. 2021), shown are overall survival (OS, A) and relapse free survival (RFS, B).

3.3.6 CMG2 and angiogenesis in pancreatic cancer

As a gene initially identified as one of the upregulated genes in the vascular endothelial cells during *in vitro* capillary formation. The expression of CMG2 and its possible role in tumour associated angiogenesis were also evaluated. KRAS and VEGFA were positively correlated with CMG2 that were evident in both TCGA and GSE71729 cohorts of pancreatic cancer.

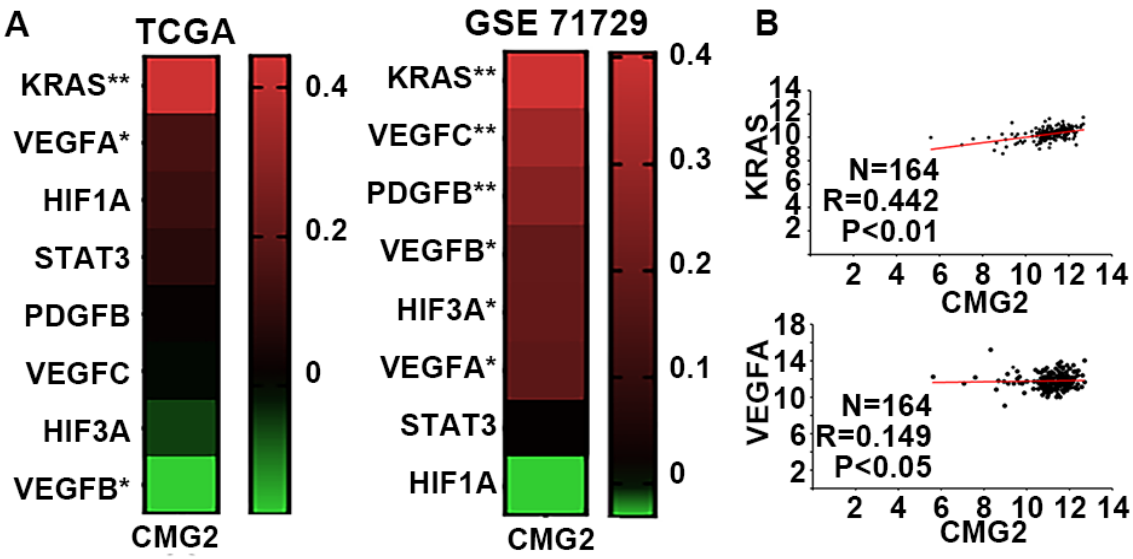

Figure 3.6 CMG2 and angiogenesis in pancreatic cancer. (A) Heatmaps present correlations between CMG2 and angiogenesis markers in the TCGA and GSE71729 pancreatic cancer cohorts, respectively. (B) Scatter plots show correlation between CMG2 and KRAS and VEGFA in the TCGA cohort, respectively.

3.3.7 Involvement of CMG2 in the development of pancreatic tumour

To assess whether CMG2 was involved in the tumorigenesis in pancreas, CMG2 mRNA expression was analysed in GSE19650 (Hiraoka et al. 2011), which includes normal Pancreatic tissues (N=7), intraductal papillary-mucinous adenomas (IPMA, N=6), intraductal papillary-mucinous carcinomas (IPMC, N=6) and invasive intraductal papillary-mucinous neoplasms (IPMN, N=3). Although there was no statistically significant difference (one-way ANOVA), an elevated expression of CMG2 was noticed in both IPMC and IPMN in comparison with IPMA and normal pancreas (Figure 3.7A). Immunochemical staining of CMG2 showed an enhanced staining in benign islet tumours compared with normal pancreases (Figure 3.7B and C). To further investigate whether CMG2 was implicated in tumorigenesis, bioinformatic analysis were also conducted. Several important and characteristic oncogenes in pancreatic cancer were analysed, including KRAS, ERBB2 (Her2), ERBB3 (Her3), FOS and MYC, in both TCGA and GSE71729 datasets, KRAS and ERBB3 are positively correlated with CMG2 (Figure 3.7D and E). Some other growth factor and their receptors alterations are also

implicated in the disease progression, including TGFA, EGFR, TGFB, FGF and FGFR (Sakorafas et al. 2000). None of them were significantly correlated with CMG2 in both TCGA and GSE71729 datasets (Figure 3.7F). In an analysis of tumour suppressors, CDKN2B was positively correlated with CMG2 whilst SMAD4 was negatively correlated with CMG2 (Figure 3.7G and H)

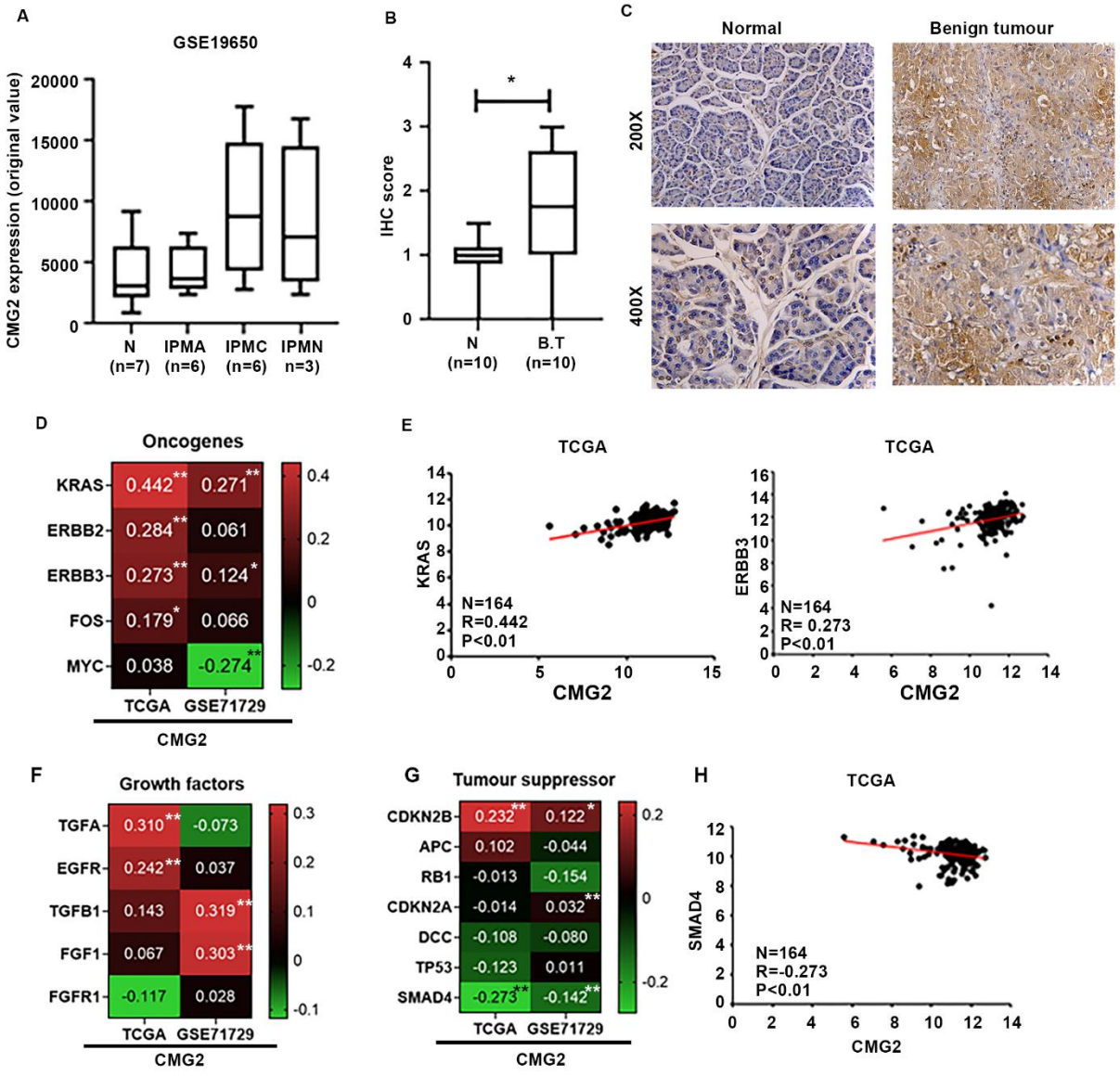

Figure 3.7 CMG2 and pancreatic tumorigenesis: (A) CMG2 (225524_at) expression in normal pancreatic tissue, intraductal papillary-mucinous adenoma (IPMA), intraductal papillary-mucinous carcinoma (IPMC) and invasive Intraductal papillary-mucinous neoplasm (IPMN) in GSE 19650 dataset. (B) The CMG2 expression in normal pancreas (N) and benign pancreatic

tumours (B.T) on the tissue microarray (PA2081). (C) Shown are representative images taken under a microscope with magnifications of 200X and 400X, respectively. (D) Heat maps show the association between CMG2 and oncogenes in pancreatic cancer in two datasets, TCGA and GSE71729. (E) Scatter plots show the expression association between CMG2 and KRAS and ERBB3 in the TCGA dataset. (F) Growth factors and some receptors expression association with CMG2 in both TCGA and GSE71729. (G) Correlation between tumour suppressors and CMG2 in both TCGA and GSE71729 datasets. (G) Correlation between SMAD4 and CMG2 in the TCGA cohort. ***p<0.001, **p<0.01, *p<0.05.

3.4 Discussion

CMG2 is ubiquitously expressed by epidermal, epithelial and endothelial cells that line as an epical layer of cells on the body surface or towards lumen of digestive tract or blood vessels (Reeves et al. 2010; Cryan and Rogers 2011a; van Rijn et al. 2020). It was initially discovered as both an angiogenesis marker and a receptor of anthrax toxin by mediating the internalization of the toxin (Sun and Jacquez 2016; Lin et al. 2019). Emerging evidence from the host lab and other labs showed that deregulated CMG2 plays a profound role in certain malignancies including breast cancer, prostate cancer, gastric cancer and glioma etc (Ye et al. 2014b; Ji et al. 2018; Tan et al. 2018; Xu et al. 2019). Preliminary study at the host lab revealed an increased expression of CMG2 in pancreatic cancer by determining CMG2 transcripts in a cohort of pancreatic cancer tissues from the Beijing Cancer Hospital. However, the exact role played by CMG2 in pancreatic cancer remains largely unknown. The present study aimed to ascertain the elevated expression of CMG2 in pancreatic cancer by assessing its expression in other pancreatic cancer cohorts and presence of CMG2 protein, its implication in the development and progression of the disease was further evaluated.

Previous studies from the host lab have showed that CMG2 is deregulated in both breast and prostate cancer. In breast cancer, reduced expression of CMG2 is associated with poor survival (Ye et al. 2014b), whilst knockdown of CMG2 resulted in a reduced cell adhesion ability and enhanced invasion (Ye et al. 2014b).The current study showed that CMG2 expression was higher in pancreatic cancers in comparison with adjacent normal pancreatic tissues in GSE71729, GSE15471 and Beijing Cohort. IHC staining of CMG2 in pancreatic cancer tissue microarray assured an increased protein

expression of CMG2 in pancreatic tumours. A recent study of CMG2 in gastric cancer revealed a higher expression of CMG2 in the tumours compared with normal tissues (Ji et al. 2018). It suggests that CMG2 plays a different role in gastrointestinal tumours, at least in pancreatic and gastric cancers compared with the endocrine-related cancers.

Further analysis showed that the elevated CMG2 expression in pancreatic cancer was associated with a poor prognosis, which is similar with the observation in gastric cancer (Ji et al. 2018). The increased expression of CMG2 in pancreatic tumours appeared to be generally present in tumours of different T stages. Similarly, there is no significant change observed for the CMG2 expression in the primary tumours regarding regional lymph node metastasis suggesting that CMG2 unlikely have a specific implication in both tumour growth/invasion and regional lymph node metastasis in pancreatic cancer. Interestingly, CMG2 expression was significantly higher in those primary tumours which developed distant metastases in comparison with the primary tumours without distant metastasis. A remarkedly higher expression of CMG2 was also evident in the metastatic tumours from pancreatic cancer compared with the primary tumours. It suggests that the upregulated CMG2 in pancreatic cancer may be involved in the dissemination of pancreatic cancer cells to a distant site. Together the recent evidence from a study of CMG2 in gastric cancer suggesting a possible role of CMG2 in the peritoneal metastasis in pancreatic cancer which will be further assessed in the present study.

Another interesting observation from the present study was that the IHC staining revealed the upregulated CMG2 presenting in both benign tumours and malignant tumours in pancreas. A further analysis of CMG2 transcripts in the GSE19650 cohort which comprises normal pancreatic tissues and precancerous lesions although the sample sizes were inadequate for a conclusion. Elevated expression was seen in IPMN and IPMC lesions compared with normal and IPMA samples. IPMA, IPMC and IPMN are premalignant lesions, the malignancy is elevated in a shift from IPMA to IPMN. The upregulated CMG2 expression in precancerous lesions and benign tumours in pancreas together with the increased expression in pancreatic cancers suggests a possible role of CMG2 in the tumourigenesis of pancreatic cancer. Therefore, the association between CMG2 and some oncogenes and tumour suppressors were analysed. Oncogene KRAS

and ERBB3 are positively correlated with CMG2, and tumour suppressor SMAD4 is inversely correlated with CMG2 in both TCGA and GSE71729 cohorts. Mutations of KRAS were evident in bout 90% pancreatic cancer (Bannoura et al. 2021), which can activate PI3K-AKT pathway, inducing the uncontrolled cell proliferation and promoting the migration. KRAS can also activate the Notch and promote cell proliferation (Namikawa et al. 2023). In addition to that, it can also enhance cell migration by activating Hedgehog pathway (Morris et al. 2010). ERBB3, also known as HER3, is associated with a poor prognosis in pancreatic cancer (Liles et al. 2010). It can also enhance resistance to EGFR and Her2 target therapies (Liles et al. 2010). SMAD4 is a tumour suppressor, loss of this gene has been found in 55% pancreatic cancer (Blackford et al. 2009), which is associated with the EMT (Ioannou et al. 2018). Additionally, a positive correlation was also observed between CMG2 and other oncogenic factors including TGFα, TGFβ1, EGFR and FGF1 in only one dataset but not commonly in both cohorts that were evaluated. The involvement of CMG2 in tumourigenesis of pancreatic cancer in conjunction with oncogenes and tumour suppressor genes warrants further investigation.

Our recent study has shown that CMG2 is inversely correlated with oestrogen receptor (ER) and androgen receptor (AR) in breast and prostate cancer, respectively (Fang et al. 2022). An elevated expression of CMG2 was seen in both ER-positive breast cancer cells and AR-positive prostate cancer cells since both ER and AR mediate a repression on the expression of CMG2 (Fang et al. 2022). In the present study of CMG2 in pancreatic cancer, similar transcript levels of CMG2 were seen in both female and male patients although a weak positive correlation between CMG2 and AR presented in those male patients (TCGA cohort). This at least partially accounts for the upregulated CMG2 expression in pancreatic cancer which is more commonly downregulated in breast cancer and prostate cancer due to the ER and AR mediated repression. However, the mechanism underlying the upregulated CMG2 in pancreatic cancer remains an interesting area for exploration.

Since CMG2 is expressed and upregulated in vascular endothelial cells during formation of new vasculature and the vital role of angiogenesis in the tumour growth and dissemination of cancer cells, correlation between CMG2 and angiogenesis

markers in the pancreatic tumours was also evaluated in both TCGA and GSE71729 cohorts. KRAS and VEGFA are positively correlated with CMG2. KRAS as a member of the Ras family, regulates various cellular events including angiogenesis (Shao et al. 2019). VEGFA is a well-known pro-angiogenic factor. It has been demonstrated that cancer associated fibroblasts secreted VEGFA promotes the angiogenesis to facilitate growth of metastatic lesions. Angiogenesis plays an important role in mediating the distant metastasis. The unmatured structure new blood vessels in tumours offers a route and higher possibility of distant dissemination through blood circulation (Li et al. 2019). In addition to the elevated expression of CMG2 in pancreatic cancer cells, involvement of CMG2 in angiogenesis warrants a separate study to shed light on the CMG2 related angiogenesis in pancreatic cancer.

Taken together, CMG2 is upregulated in pancreatic cancer. The elevated CMG2 expression is associated with distant metastasis and poor prognosis of the disease. Influence of CMG2 on the cellular functions of pancreatic cancer cells and their capability of disseminating to peritoneum will be investigated in the following chapters.

Chapter 4

Influence of CMG2 on *in vitro* cellular functions of pancreatic cancer cell lines

4.1 Introduction

In Chapter 3, CMG2 was evaluated for its implication in pancreatic cancer by determining its expression using both real time PCR and IHC. In addition to those, bioinformatical analyses were also conducted to further dissect its role in disease progression, i.e., distant metastasis and prognosis etc. The expression of CMG2 at both transcript and protein level was increased in pancreatic tumours, compared with adjacent normal pancreatic tissues. The increased expression of CMG2 in pancreatic cancer was significantly associated with poor prognosis. CMG2 is also positively associated with oncogenes, indicating it may be involved in tumourigenesis in pancreas. Furthermore, CMG2 was also highly expressed in metastatic tumours compared with primary tumours. This suggests that CMG2 more likely plays an important role in pancreatic cancer, from an early stage during tumourigenesis to the later disease progression and distant dissemination.

In contrast to the elevated expression of CMG2 in gastrointestinal cancers (Ji et al. 2018; Ziqian Fang 2021), a reduced CMG2 expression has been revealed in both breast and prostate cancers, due to repression mediated by ER and AR (Fang et al. 2022). CMG2 can inhibit the growth of breast cancer cells *in vitro* and *in vivo* (Ye et al. 2014c), but has little impact on the proliferation of an AR negative prostate cancer cell line (PC-3) (Ye et al. 2014b). However, CMG2 has an inhibitory effect on invasiveness of PC-3 cells (Ye et al. 2014b). In addition, in glioma and gastric cancer, it has been demonstrated that high expression of CMG2 is involved in disease progression (Ji et al. 2018; Xu et al. 2019). In glioma, CMG2 can promote cell adhesion and migration by upregulating YAP (Xu et al. 2019). In gastric cancer, CMG2 can promote cancer cell proliferation, invasion, EMT and stemness (Ji et al. 2018). CMG2 can promote proliferation of vascular endothelial cells (Reeves et al. 2010). Targeting CMG2 can prevent tubule formation by vascular endothelial cells *in vitro*, with a potential to inhibit tumour associated angiogenesis (Ye et al. 2014d). The diverse and contrasting effects of CMG2 on cellular functions, revealed in the previous study, suggest that the influence of CMG2 on cellular functions depends on its expression profile and functions of CMG2-releated molecules and pathways. However, influence of increased CMG2 expression in pancreatic cancer on cellular functions remains largely unknown.

In this Chapter, to examine the impact of CMG2 on cellular functions of pancreatic cancer cells, both knockdown and overexpression of CMG2 cell line models were developed in pancreatic cancer cell lines, followed by determination of various cellular functions including proliferation, adhesion, migration and invasion.

4.2 Materials and methods

4.2.1 Cell lines

MiaPaCa-2 and PANC-1 cell lines were cultured using DMEM medium, with 10% FCS and antibiotics. ASPC-1 cell line was cultured in RPMI1640, also with 10% FCS and antibiotics (Described in section 2.1.1).

4.2.2 CMG2 knockdown and overexpression

CMG2 shRNA vectors were ordered from the Vectorbuilder (Illinois, USA). PANC-1 and ASPC-1 cell lines were transduced with the CMG2 shRNA lentiviral particles and scramble shRNA control lentiviral particles. The transduced cells were selected with G418 (250-500µg/ml) for a duration up to two weeks, followed by maintenance using 50µg/ml G418. A pEF6/V5-His TOPO® TA expression plasmid vector (Thermo Fisher Scientific, Waltham, USA) was used for cloning of CMG2 coding sequence, as previously described (Ye et al. 2014b). Both CMG2 expression vectors and empty vectors were used to establish CMG2 overexpression and control cells, respectively in both MiaPaCa-2 and PANC-1 cell lines. Blasticidin (1-2.5µg/ml) was used for selection and 0.5µg/ml of blasticidin was employed for subsequent maintenance. More technical details can be found in section 2.6.5.

4.2.3 RNA extraction, reverse transcription PCR and quantitative PCR

Total RNA was isolated using TRI reagent (Sigma-Aldrich, Dorset, UK). First strand cDNA synthesis was undertaken using the iScriptTM cDNA Synthesis Kit (Bio-Rad laboratories, Hertfordshire, UK). PCR was performed using GoTaq Green MasterMix (Promega, Dorset, UK). Products were visualised using a 1% agarose gel stained with SYBR Safe (Invitrogen, Paisley, UK). QPCR for GAPDH and CMG2 was performed using FAST 2X qPCR MasterMix (Primer Design, Chandle''s Ford, UK). Primers and

detailed protocol are described in section 2.4.7

4.2.4 Protein extraction and Western blot

Western blot was used in order to check whether the CMG2 knockdown and overexpression were successful. The cells were lysed in RIPA buffer following the protocol described in section 2.5.1. During Western blotting, proteins were separated using 10％ SDS-PAGE gel (Sigma-Aldrich, Dorset, UK) followed by a detection using anti-CMG2 antibody (16723-1-ap, 1:2000 dilution) and anti-Actin antibody (SC 1616,1:4000 dilution). Protein bands were visualised using the EZ-ECL kit (Sartorius group, Staffordshire, UK). Details of secondary antibody (anti-goat antibody: A-5420, 1:4000 dilution, anti-rabbit antibody: A-9169, 1:1000)

4.2.5 *In vitro* cell growth assay

Cells were plated into a 96-well plate at 3,000 cells/well. Cell growth was assessed after 1, 3 and 5 days. After fixation with 4% formalin, the cells were stained with crystal violet. The crystal violet staining was then extracted using 10% acetic acid, and its absorbance was measured at 595 nm, using a spectrophotometer (BioTek, Elx800, UK). In addition, on 1st, 3rd, and 5th day, the CCK8 (cell counting kit 8) (Munich, Germany) was used to measure the cell viability, by adding 10μl of CCK8 solution into each well. After incubation for 2 hours at 37℃, absorbance was determined at a wavelength of 545nm.

4.2.6 *In vitro* invasion assay

This assay was carried out by following the protocol described in section 2.7.5. Trans-well inserts, with 8μm pore size, were coated with 50μg Matrigel and air-dried. Following rehydration, 20,000 cells were added to each insert. After a 72-hour incubation, the cells that had migrated through the matrix were fixed and stained with crystal violet. The absorbance of the acetic acid extract of the crystal violet staining was then determined at 595 nm.

4.2.7 *In vitro* migration assay

A scratch wound cell migration assay was performed as previously described (Liang et

al. 2007). Two hundred thousand pancreatic cancer cells were seeded into a 24-well plate and left to form a confluent monolayer overnight. Cells were wounded using a 200µl pipette tip and photographs were taken every hour, over 6 hours, using an EVOS FL Auto Cell Imaging System (Life Technologies). Migration was measured using ImageJ software (National Institutes of Health, Maryland, USA). For ASPC-1 cells, which are less adhesive, the microcarrier beads assay was used to determine the migration (Sigma-Aldrich, Dorset, UK). Firstly, 5g of the Cytodex-2 beads were suspended in 75 ml PBS, 1 million cells were then added to 1ml beads suspension in a universal container, in 10ml of culture medium. After overnight incubation, cells remaining suspended were washed away using PBS, cells attached to the beads were subsequently resuspended in 1ml medium and seeded 100µl per well in a 96-well plate. After a 3-hour incubation, the beads and non-migrated cells were washed off. Cells attached to the bottom of the well were then fixed and stained using crystal violet. The absorbance of the crystal violet extract was determined at 595 nm.

4.2.8 Cell-matrix adhesion assay

A cell-matrix adhesion assay was performed, as previously described in section 2.7.4. In brief, 20,000 cells were added to each well of a 96-well plate, which was pre-coated with Matrigel (5µg/well). Following 40 minutes incubation, non-adherent cells were removed using BSS buffer. Adherent cells were fixed and stained using crystal violet. The absorbance of the crystal violet extract was determined at 595 nm.

4.2.9 Statistics

For comparison between two groups, Mann–Whitney test was applied for non-normally distributed data, with t-test was used for normally distributed data. All the statistical analyses were performed using SPSS software (version 26, SPSS, Chicago, IL, USA). Results were considered as statistically significant when $p<0.05$.

4.3 Results

4.3.1 CMG2 knockdown and overexpression in pancreatic cancer cell lines

Conventional PCR and Western blot analysis showed that CMG2 was highly expressed

in ASPC-1 cells, while a moderate expression was seen in PANC-1 cells. A lower expression of CMG2 was shown in MiaPaCa-2 cells (Figure 4.1 A and B). To investigate the impact of CMG2 on the cellular functions of pancreatic cancer cells, lentiviral CMG2 shRNAs were employed to knockdown CMG2 expression in ASPC-1 and PANC-1 cells, while an overexpression of CMG2 in MiaPaCa-2 and PANC-1 cells was conducted using the plasmid vectors. CMG2 knockdown and overexpression were verified using PCR and Western blot (Figure 4.1 C, D and E).

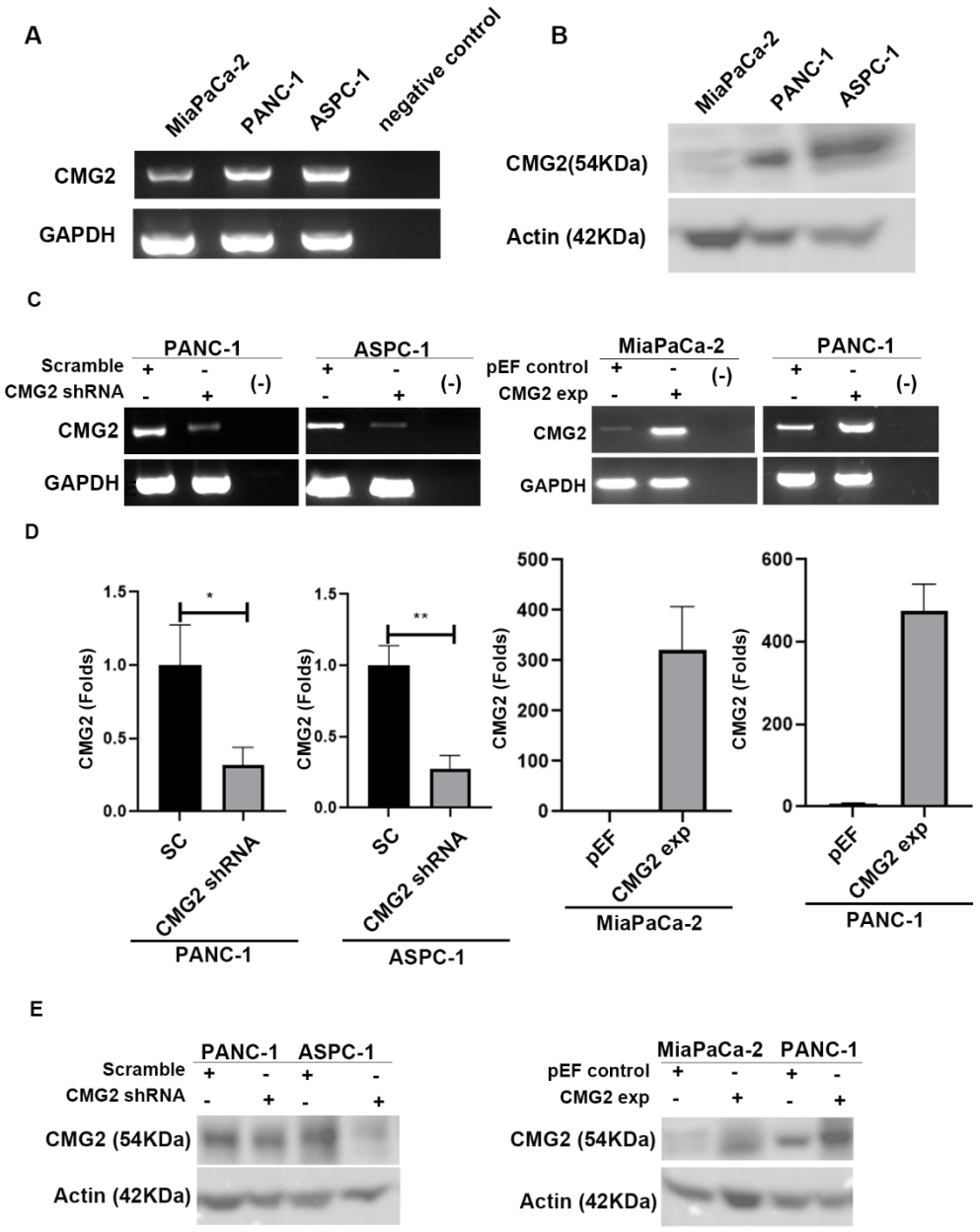

Figure 4.1 Knockdown and overexpression of CMG2 in pancreatic cancer cell lines. (A) The expression of CMG2 was determined in MiaPaCa-2, PANC-1 and ASPC-1 cell lines using conventional PCR. (B) Western blot was applied to determine the CMG2 protein expression in MiaPaCa-2, ASPC-1 and PANC-1 cell lines. The knockdown and overexpression were successfully established, which were verified using conventional PCR (C), QPCR (D) and Western blot (E). *** indicate p<0.001, ** indicate p<0.01, * indicates p<0.05.

4.3.2 CMG2 expression in pancreatic cancer cell lines regulates their adhesion

Following the verification of the CMG2 knockdown and overexpression, the influence of CMG2 on cell adhesion was determined. The effect of CMG2 knockdown or overexpression on pancreatic cancer cell adhesion was assessed by performing an *in vitro* Matrigel adhesion assay. CMG2 overexpression resulted in increased adhesion of PANC-1 cells but not the MiaPaCa-2 cells (Figure 4.2A, B). A significant decrease of cell adhesion was seen in both ASPC-1 and PANC-1 cells following the knockdown of CMG2 (Figure 4.2C, D).

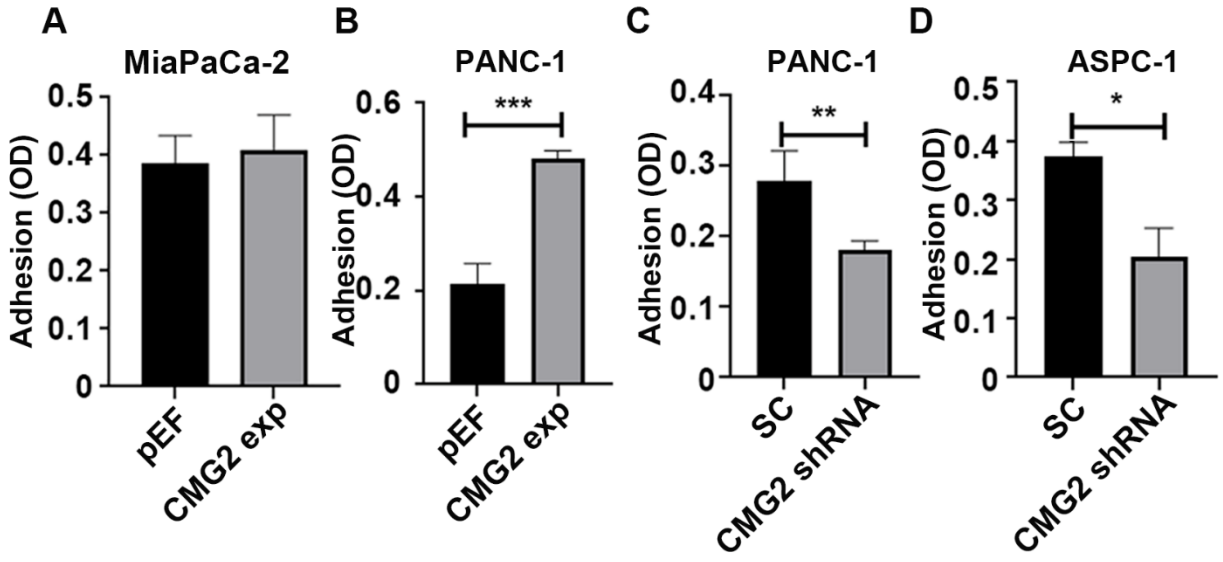

Figure 4.2 The effect of CMG2 expression on adhesion of pancreatic cancer cells. Adhesion to an artificial basement membrane (Matrigel) was determined in the CMG2 overexpressed MiaPaCa-2 (A) and PANC-1 (B) cell lines, and CMG2 knockdown cells of PANC-1 (C) and ASPC-1 (D). Six replicates were examined for each cell line in an experiment. Three independent experiments were conducted. Shown are the representative data from one experiment. *** indicate p<0.001, ** indicate p<0.01, * indicates p<0.05.

4.3.3 The influence of CMG2 expression in pancreatic cancer cell proliferation and viability

Cell proliferation was first assessed using a crystal violet staining assay. Neither knockdown nor overexpression of CMG2 exhibited an obvious effect on the *in vitro* proliferation of the three pancreatic cancer cell lines examined, although PANC-1^{CMG2exp} cells appeared to be greater, whilst PANC-1CMG2shRNA tended to be less, compared with the corresponding controls (Figure 4.3). CCK8 was employed for further verification of the viable cells. There was no significant change seen in the proliferation of both MiaPaCa-2^{CMG2exp} cells (Figure 4.4 A) and ASPC-1CMG2shRNA cells (Figure 4.4 D), compared with the corresponding control. Interestingly, a higher live population was seen in PANC-1^{CMG2exp} cells whilst a reduced population was seen in PANC-1CMG2shRNA cells (Figure 4.4 B and C).

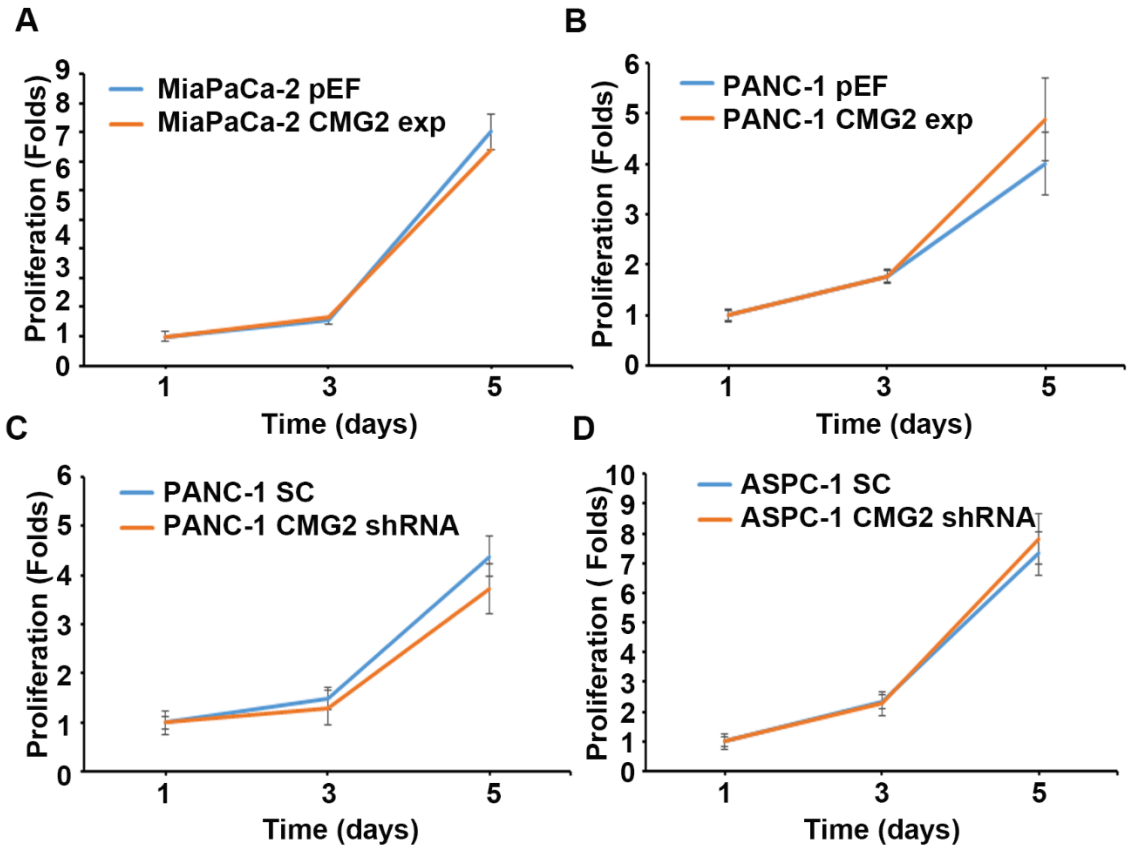

Figure 4.3 The effect of CMG2 knockdown or overexpression on the proliferation of pancreatic cancer cells. Influence of CMG2 expression on the proliferation of MiaPaCa-2 (A), PANC-1 (B and C) and ASPC-1 (D) were determined using crystal violet staining. Six replicates

were examined for each cell line in an experiment. Three independent experiments were conducted. Shown are the change in folds of absorbance against the corresponding absorbance of day one.

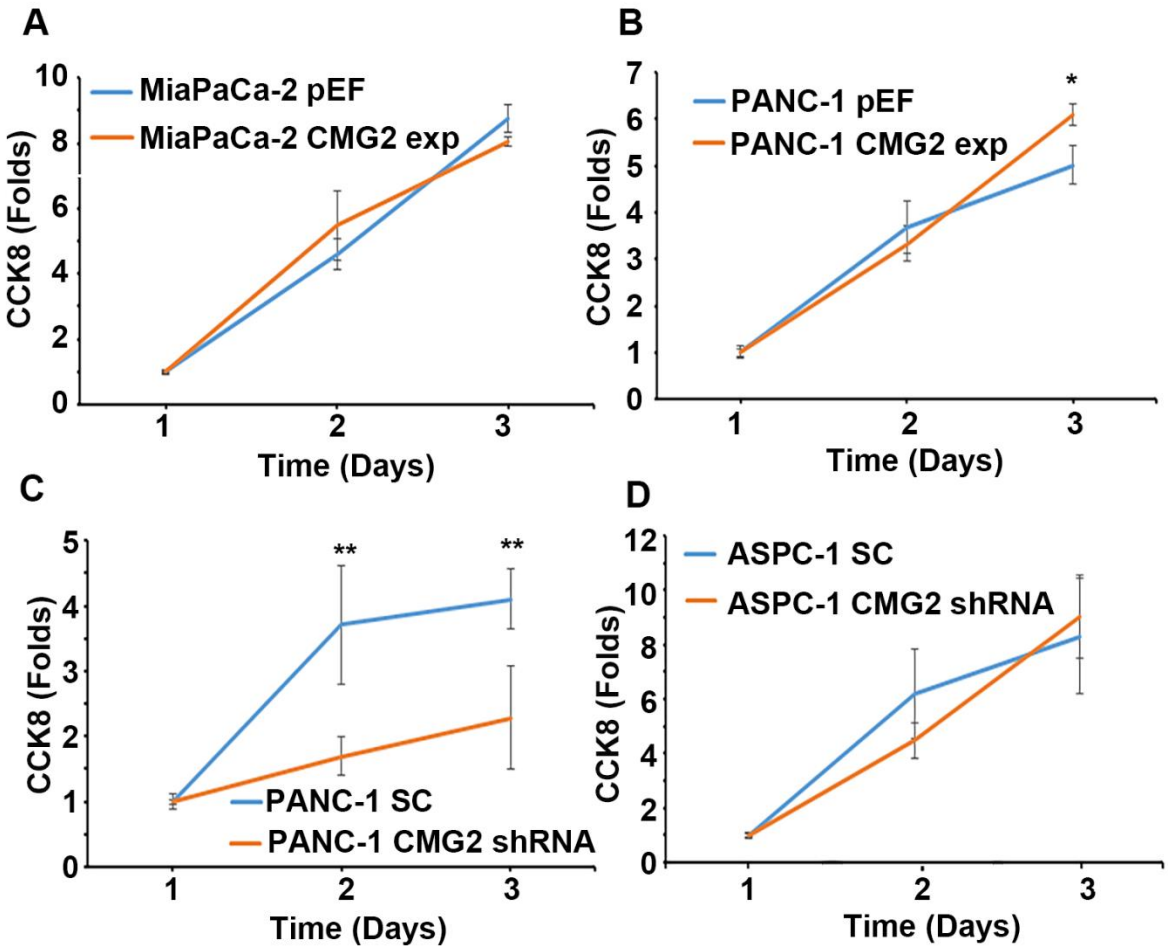

Figure 4.4 The effect of CMG2 knockdown or overexpression on the proliferation of pancreatic cancer cells was determined using CCK8. CMG2 overexpressed MiaPaCa-2^{CMG2exp} (A) and PANC-1^{CMG2exp} (B) cell lines, and CMG2 knockdown cells of PANC-1^{CMG2shRNA} (C) and ASPC-1^{CMG2shRNA} (D) were determined in comparison to the respective control. Six replicates were examined for each cell line in an experiment. Three independent experiments were done. Shown are the change in folds against the corresponding absorbance of day one. *** indicate $p<0.001$, ** indicate $p<0.01$, * indicates $p<0.05$.

4.3.4 The influence of CMG2 expression in pancreatic cancer cell migration

The influence of CMG2 on pancreatic cancer migration was determined using both wound healing assay and microcarrier assay. Little effect was observed in the MiaPaCa-2 and PANC-1 cells, following the manipulation of CMG2 expression, which was determined using the wound healing assay (Figure 4.5). In comparison with these two cell lines, ASPC-1 cells were less adhesive. A migration test using microcarrier beads was used, which presented little change in the ASPC-1 CMG2 knockdown cells (Figure 4.5D).

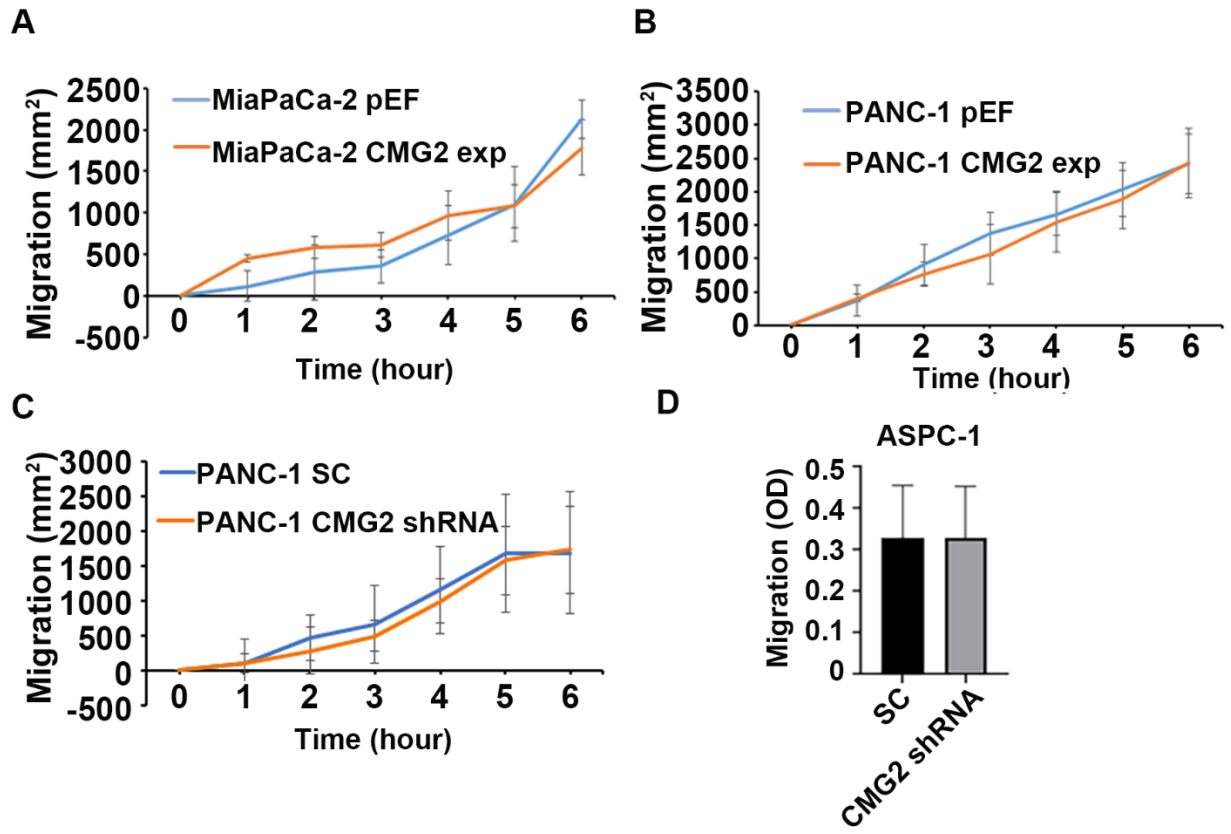

Figure 4.5 The effect of CMG2 knockdown or overexpression on cell migration ability of pancreatic cancer cell lines. Wound healing assay was employed for MiaPaCa-2 (A) and PANC-1 (B and C) cells, microcarrier was used for ASPC-1 (D) cell. Four replicates were examined for each cell line in a wound healing assay, while six replicates were examined in each microcarrier beads assay. Three independent experiments were performed. Shown are the migration area for wound healing assay and absorbance of crystal violet staining from the migrated cells in a microcarrier beads assay.

4.3.5 CMG2 and invasion of pancreatic cancer cells

During the procedure of cancer metastasis, invasion through the ECM is an important procedure. An *in vitro* trans-well invasion assay was performed, to determine whether CMG2 expression can regulate cell invasion ability. Neither knockdown nor overexpression of CMG2 exhibited a significant effect on the invasion of the three pancreatic cancer cell lines (Figure 4.6).

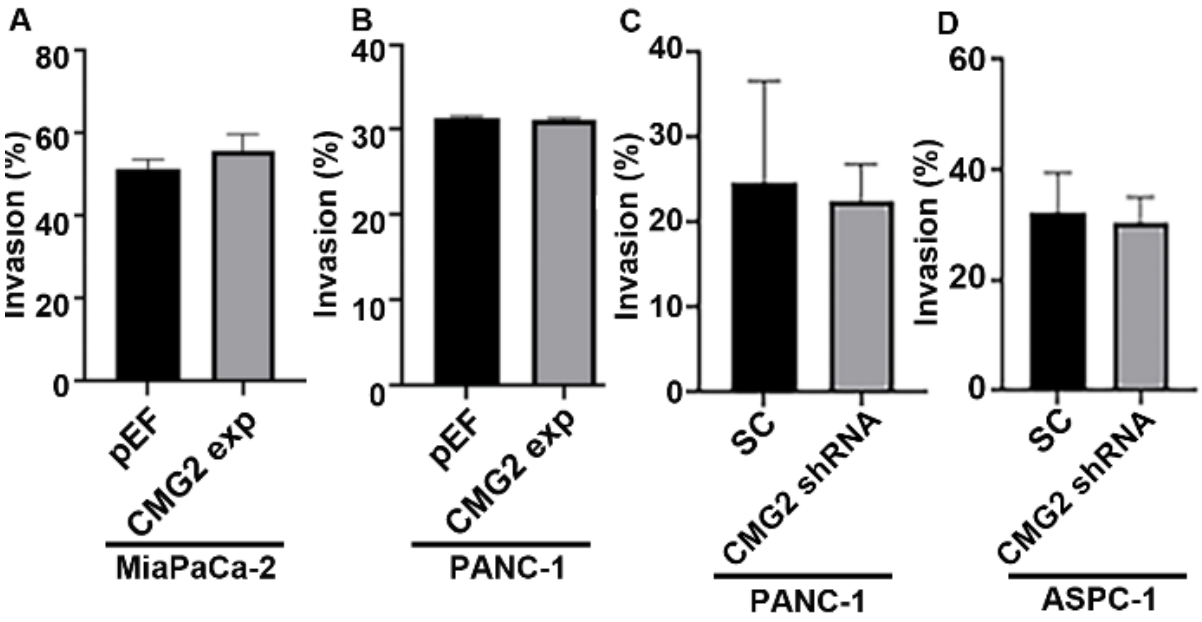

Figure 4.6 The effect of CMG2 knockdown or overexpression on the invasiveness of pancreatic cancer cells. Trans-well invasion assay was used to determine the effect of CMG2 on invasion of MiaPaCa-2 (A), PANC-1 (B and C) and ASPC-1 (D) cells. Shown are the percentage of invaded cells against controls.

4.4 Discussion

In Chapter 3, an elevated expression of CMG2 was revealed in pancreatic cancer, which was significantly associated with disease progression, especially distant migration. In this Chapter, CMG2 expression was initially assessed in three different pancreatic cancer cell lines, including MiaPaCa-2, PANC-1 and ASPC-1. CMG2 expression level was lower in MiaPaCa-2, which was suitable for a CMG2 overexpression model, while a knockdown model was chosen for ASPC-1 cells, which presented a higher expression of CMG2. Both CMG2 knockdown and overexpression were established in PANC-1 cells, which had a moderate CMG2 expression among the three cell lines examined. Influence of CMG2 on four different cell functions including proliferation, adhesion, migration and adhesion was subsequently evaluated.

Cell adhesions are vital for maintaining cellular plasticity and tissue homeostasis mediating attachment, migration and interactions with the extracellular matrix (ECM) (Wolfenson et al. 2013; Seetharaman and Etienne-Manneville 2020; Kanchanawong and Calderwood 2023). Deregulated adhesion plays an important role in local invasion and distant dissemination of cancer cells (Jiang 1996; Yilmaz and Christofori 2009). The cell CMG2 is a transmembrane protein with an extracellular vWA domain, which mediates interactions with laminin and collagens thus coordinating cell adhesion and spreading (Finnell et al. 2020). In the present study, knockdown of CMG2 resulted in a marked decrease of cell adhesion to the Matrigel, in both PANC-1 and ASPC-1 cells whilst an increased adhesion was seen in the PANC1 cells following the overexpression of CMG2. However, little change of adhesion was observed in the MiaPaCa-2^{NOGexp} cells. These findings suggest that CMG2 plays an important role in the cell-substrate adhesion of pancreatic cancer however, adhesiveness of some pancreatic cancer cells with lower expression of CMG2 appears to be less dependent on the CMG2 protein. In line with this finding, knockdown of CMG2 in a prostate cancer cell line (PC-3) also resulted in a reduction of cell adhesion (Ye et al. 2014b). In addition to its role in mediating the endocytosis of anthrax toxin, CMG2 binds with some extracellular matrix proteins, including collagen I, collagen IV, laminin, fibrinogen, and fibronectin (Cryan and Rogers 2011). These can partially explain why CMG2 can promote the cell adhesion ability. CMG2 is also involved in ECM remodelling through regulation of u-PA,

thus to enhance cell migration, invasion and EMT in Soft Tissue Sarcoma (Dass et al. 2008; Noh et al. 2013; Greither et al. 2017).

Crystal violet cell proliferation assay showed that CMG2 knockdown and overexpression did not have any significant effect on cell proliferation, in all the three pancreatic cell lines. However, CCK8 assay, which detected viable cells, revealed an increased healthy population in PANC-1^{CMG2exp} cells whilst a reduced amount of viable cells was seen in the PANC-1 cells, following the knockdown of CMG2. Crystal violet can stain both RNA and DNA in the fixed cells, with a loss of non-adherent and less adhesive cells during the fixation and staining process. The CCK8 assay is a more accurate assay to determine viable cells, including both adherent and non-adherent populations, in comparison with both the crystal violet assay and classical MTT assay. Loss of anchorage in epithelial cells can lead to a programmed cell death, as a kind of apoptosis also known as '*anoikis*' (Taddei et al. 2012). The reduced viability in PANC1 CMG2 knockdown cells can be a result of the impaired adhesion of these cells. No change of cell viability was observed in MiaPaCa-2 and ASPC-1 cells. CMG2 overexpression also exhibited little effect on adhesion of MiaPaCa-2 cells, whilst ASPC-1 cells appeared to be more robust even with a loss of adhesion, since they were initially derived from ascites. In contrast to the current findings, CMG2 has little impact on proliferation of a prostate cancer cell line (PC-3) (Ye et al. 2014b), but can inhibit proliferation of breast cancer cells (Ye et al. 2014c). Moreover, CMG2 can promote proliferation of gastric cancer cells (Ji et al. 2018). This suggests that CMG2 can maintain cell viability by a regulation of cell adhesion, which will be further examined in the present study.

Previous studies have shown that CMG2 can regulate migration and invasion. In prostate cancer, CMG2 presented an inhibitory effect on invasiveness of PC-3 cells (Ye et al. 2014b). In glioma, CMG2 enhanced the cell migration and EMT, through upregulation of YAP and Hippo pathways (Xu et al. 2019). CMG2 can also enhance the spread and migration of endothelial cells, as a chemotactic response to angiogenic factors (Cryan and Rogers 2011b). However, in the present study, no obvious effect on invasion and migration was observed in the three pancreatic cancer cell lines examined, following the knockdown and overexpression of CMG2.

Taken together, CMG2 enhanced the adhesion of a pancreatic cancer cell line to an artificial base membrane, which may affect cell viability. In Chapter 3, we found that CMG2 is significantly increased in metastatic lesions. The peritoneum is one of the most common distant metastastatic sites in pancreatic cancer (Avula et al. 2020). Survival, during the spreading in peritoneal fluid and subsequent attachement to the peritoneum, is vital for pancreatic cancer cells to disseminate in the peritoneum. Involvement of CMG2 coordinated adhesion and viability in peritoneal metastasis will be further dissected in the following Chapter, using the cell line models established in this Chapter.

Chapter 5

CMG2 mediates the interaction between pancreatic cancer cells and peritoneal mesothelial cells

5.1 Introduction

During distant metastasis, especially the peritoneum metastasis in pancreatic cancer, the ability of cancer cells to survive and subsequently attach to the peritoneum plays an important role. Once pancreatic cancer cells leave the primary lesion, they will enter the peritoneum cavity and suspend in the peritoneal fluid or die unless they adhere to the peritoneum. In Chapter 4, the results show that CMG2 can enhance the adhesion to the artificial basement membrane in pancreatic cancer cell lines. The enhanced adhesiveness may assist pancreatic cancer cells to adhere to the peritoneum and meanwhile can shorten the duration of suspending in the peritoneal cavity. Higher CMG2 expression was also positively correlated with cell viability which was another important factor that can promote distant metastasis. In this chapter, further experiments were done to check whether CMG2 expression has an impact on the capability of pancreatic cancer cells to disseminate in peritoneum using *in vitro* experimental assays. Furthermore, as the cytoskeleton can also affect the cell adhesion and subsequent spreading (Mege and Ishiyama 2017), the influence of CMG2 on the spreading of pancreatic cancer cells will also be examined. On the other hand, evasion from the *anoikis* is another important ability of cancer cells to disseminate through peritoneal cavity and blood circulation due to a loss of anchorage. There are several ways that cancer cells acquired to escape from the *anoikis*, including aggregation to form cell clusters (Han et al. 2021), and activating survival pathways, such as the EGFR pathway, MAPK pathway and PI3K-AKT pathway (Boroughs and DeBerardinis 2015; Degirmenci et al. 2020; Han et al. 2021). In addition to the evasion of *anoikis*, the mesothelial cell of the peritoneum can secrete hyaluronic acid (HA) which will form a lubricating film (Soliman et al. 2022). HA film also forms a natural barrier to block attachment of cancerous cells which has been be implicated in the peritoneal metastasis. Targeting hyaluronic acid can inhibit the peritoneal metastasis of colorectal cancer (Soliman et al. 2022). There are several HA interacting molecules, including CD44, RHAMM, LYVE and ICAM-1 which mediate the cell-HA binding (McCourt et al. 1994; Entwistle et al. 1995; Goodison et al. 1999). Therefore, hyaluronic acid plays a crucial role during the peritoneum metastasis progress.

In the present chapter, the established pancreatic cancer cell line models were employed to determine the influence of CMG2 on the aggregation/clustering and surivival/*anoikis* of the pancreatic cancer cells upon a loss of anchorage using a suspension cell culture to mimic the process of peritoneal metastasis. Adhesion of pancreatic cancer cells to mesothelial cells was employed as an *in vitro* peritoneal metastatic assay.

5.2 Materials and Methods

5.2.1 Adhesion to the mesothelial cell layer

MET5A cells were seeded in a 96-well plate with 200μl medium, after an overnight culture, a cell monolayer was formed. After a staining with 10 μg/ml DiI (Thermo Fisher Scientific, Waltham, USA), 20000 pancreatic cancer cells were seeded onto the MET5A monolayer. Following an incubation of 40 minutes, nonadherent cells were washed off using PBS. Adhered cells were then fixed and photographed using the EVOS FL Auto Cell Imaging System (auto imaging system, Thermo Fisher Scientific, Waltham, MA USA). Detailed protocol was described in section 2.8.1.

5.2.2 Hyaluronic acid and cell adhesion

MET5A cells were seeded in a 96-well plate, after the mesothelial cell monolayer was formed, pancreatic cancer cell lines with modified CMG2 were stained with 10 μg/mL DiI. To evaluate the influence of HA on adhesion of pancreatic cancer cells to the mesothelial cells, 20000 the pre-stained cancer cells were seeded into each well. During the following 40-minute incubation, the cells were treated with HA at different concentrations: 100μg/ml, 50μg/ml and 25μg/ml. High, low and ultralow molecular weight hyaluronic acid (CLR002, CLR001, CLR003, Sigma-Aldrich, Dorset, UK) was used. Meanwhile, a hyaluronic acid inhibitor (AS-62622, Anaspec, Fremont, US) of a concentration up to 2μM was also used to verify the in involvement of HA in the adhesion of cancer cells to mesothelial cells. The adhered cells were determined following the aforementioned procedure.

5.2.3 Cell aggregation assay

Pancreatic cancer cells were suspended in 5 ml medium at a density of $1X10^5$ cells/ml in a 30ml universal container followed by an incubation up to 24 hours. The number of cell clusters were counted every hour during the first 6 hours of the incubation and at the end of the 24-hour incubation following a method previously described in section in 2.7.6.

5.2.4 Hoechst staining to detect apoptosis cells

In the aforementioned aggregation test, 200µl of the suspending cancer cells were collected every hour during the first 6 hours and also at the end of the 24-hour suspending culture. After a staining with 0.1µg/100µl Hoechst (Thermo Fisher Scientific, Waltham, USA) for 20 minutes, apoptotic cells were counted under a fluorescent microscope. Cells with a condensed or lobular-shape nucleus were counted as apoptotic cells as illustrated in section 2.7.6.

5.2.5 Cell viability test by CCK8

According to the Hoechst staining results, a time point at which cell viability reaches the largest difference between the CMG2 knockdow/overexpression cells and corresponding controls was selected. At the beginning of the suspending culture, 50µl of CCK8 reagent were added into each 5ml suspending cell culture. At the selected time points, the absorbance representing viable cells was measured at 450nm. For MiaPaCa-$2^{CMG2exp}$ cells, PANC-$1^{CMG2exp}$ cells and the control cells, the duration was 4 hours. PANC-1 CMG2 knockdown cells and the controls cells were incubated for 3 hours before the absorbance was determined. Duration of the suspending culture for ASPC-1 cells was 6 hours.

5.2.6 CMG2 knockdown by ribozyme

PANC-$1^{CMG2shRNA}$ was labbled by green fluroscence, which can not be used for flowcytonetry. Ribozyme plasmid was used to knockdown CMG2 expression in PANC-1 cells, the pEF/TOPO TA plasmid vector, carrying a ribozyme targeting CMG2 and the same empty vector as a control, were emloyed as previously reported (Ye et al. 2014b). Pancreatic cancer cells were seeded on a 6-well plate to reach confluency of approximately 60-80%. 3µg plasmid carrying the recombinant ribozyme targeting CMG2,

together with 12µl of 1.25mg/ml Poly ethylenimine (PEI) reagent and 1ml OPTI-MEM medium was used for the transfection. More details can be seen in section 2.6.5.

5.2.7 Protein extraction and Western blot

Western blot was applied check whether the CMG2 knockdown in PANC-1 cells. Proteins were extracted using RIPA buffer. Proteins were separated using 10% SDS-PAGE gel (Sigma-Aldrich, Dorset, UK) and then transferred onto PVDF or nitrocellulose membrane. The membranes were probed using anti-CMG2 antibody (16723-1-ap, 1:2000) and anti-Actin antibody (SC 1616,1:4000). Protein bands were visualised by the EZ-ECL kit (company). Details of secondary antibody (anti-rabbit antibody: A-6169, 1:1000, anti-goat antibody: A-5420, 1:1000). Methods details were described in section 2.5.1

5.2.8 RNA extraction, cDNA synthesis and conventional PCR

RNA samples were extracted using TRI reagent (Sigma-Aldrich, Dorset, UK). Reverse transcription was performed to synthesis cDNA samples using the iScriptTM cDNA Synthesis Kit (Bio-Rad laboratories, Hertfordshire, UK). PCR was performed using GoTaq Green MasterMix (Promega, Dorset, UK). Products were visualised using a 1% agarose gel stained with SYBR Safe (Invitrogen, Paisley, UK). QPCR for GAPDH and CMG2 was performed using FAST 2X qPCR MasterMix (Primer Design, Chandle''s Ford, UK). Primers and detailed protocol are described in section 2.4.7

5.2.9 Flow cytometric apoptosis assay

The Annexin V Apoptosis Detection Kit (sc-4252-AK, Santa Cruz Biotechnology, Texas, USA) was applied for the apoptosis assay using a flow cytometer (FACS Canto II, BD biosciences, Berkshire, UK). FITC-labelled Annexin-V stains cells in early or late apoptosis stage. Propidium iodide (PI), a membrane impermeable red fluorescent dye, was used to stain dead or late-stage apoptotic cells with a leaking membrane. Apoptotic cells were determined using the flow cytometer at a duration of suspending culture as aforementioned in the apoptosis assays using Hoechst. In brief,

In brief, the harvested suspending cells was adjusted to a density of $1X10^6$ cells/ml, and 100µl of the adjusted cell suspension were added with 2µL FITC-Annexin V (0.4µg Annexin V), 2µl of the PI solution. For a positive control, 0.01% H_2O_2 was added to induce apoptosis. A negative control was also included in which the cells were not stained with neither Annexin V nor PI. After a staining at 37℃ for 15 minutes in an incubator, apoptotic cells were determined using FACS Canto II (BD biosciences, Berkshire, UK). Apoptotic population was analysed with FlowJo (https://www.flowjo.com/). Further details can be seen in section 2.7.7.

5.2.10 Statistical analysis

T-tests were used for a comparison between two groups if the data were normally distributed, otherwise Mann-Whitney u test was applied using SPSS (Version 26, IBM UK Ltd., Portsmouth, UK).

5.3 Results

5.3.1 Influence of CMG2 expression on adhesion of pancreatic cancer cells to the peritoneum

To determine whether CMG2 can affect the adhesion to mesothelial cells, pancreatic cancer cell lines with CMG2 overexpression and knockdown were seeded onto MET5A cell monolayer. CMG2 overexpression did not affect cell adhesion to mesothelial cells in MiaPaCa-2 cells (Figure 5.1A). CMG2 knockdown in both ASPC-1 and PANC-1 induced a reduction of adhesion to the mesothelial cells (Figure 5.1 B and C).

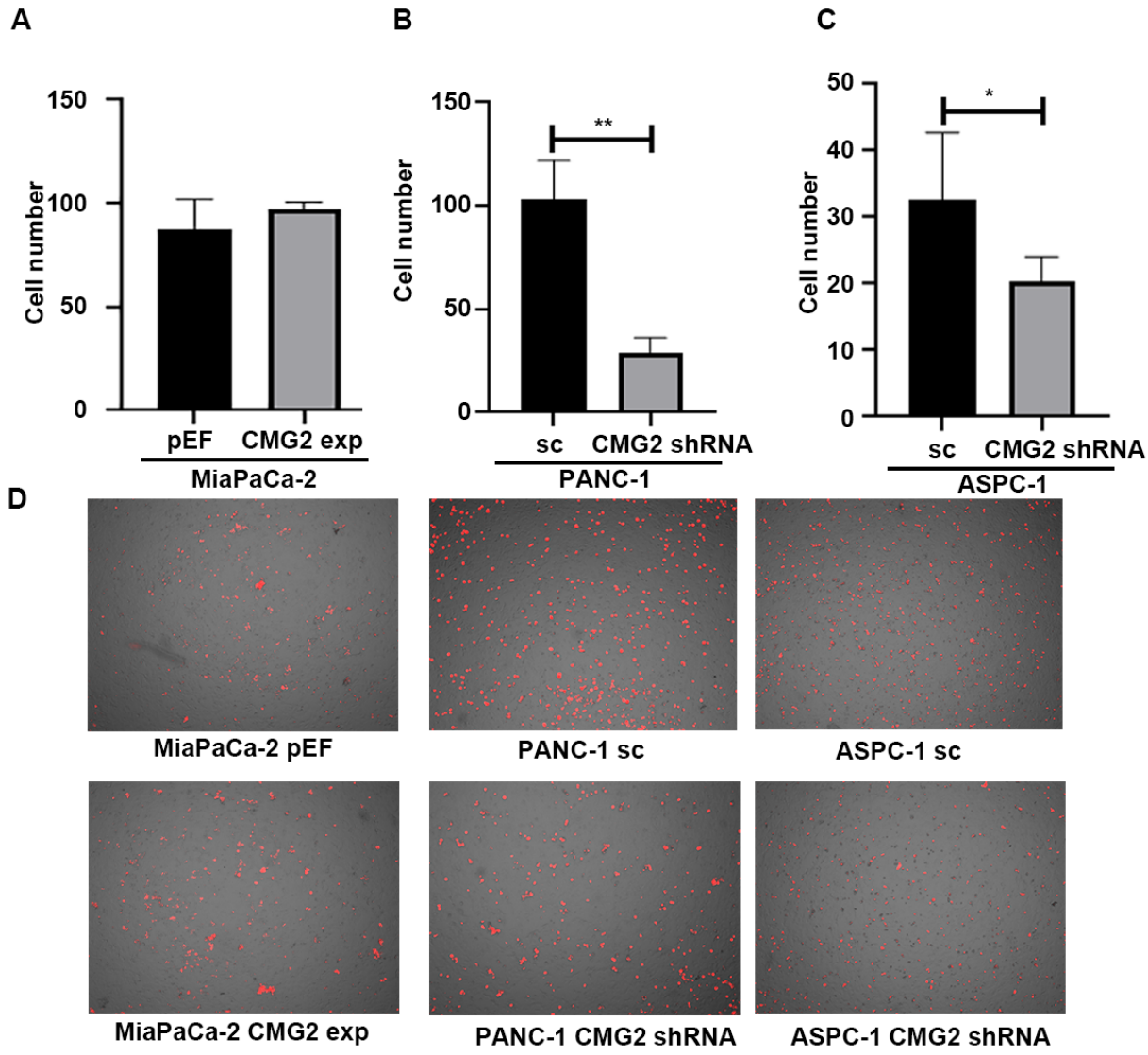

Figure 5.1 CMG2 and pancreatic cancer adhesion to mesothelial cell layer. Adhesion to mesothelial cells was determined in MiaPaCa-2^{CMG2exp} (A), PANC-1^{CMG2shRNA} (B) and ASPC-1^{shRNA} (C) against corresponding control groups, respectively. Three independent experiments were conducted. (D) Shown are representative photos. *** indicate $p<0.001$, ** indicate $p<0.01$, * indicates $p<0.05$.

5.3.2 Impact of CMG2 expression on pancreatic cancer cell spreading

Previous results showed that CMG2 promoted adhesion of pancreatic cancer cells to both Matrigel and mesothelial cells (Section 4.3.2 and 5.3.1). The effect of CMG2 on spreading of pancreatic cancer cells was also determined. After attaching to the Matrigel,

the size of pancreatic cancer cells was measured using ImageJ. CMG2 has little effect on all the three pancreatic cancer cell lines with CMG2 overexpression (Figure 5.2A) or knockdown (Figure 5.2 B and C).

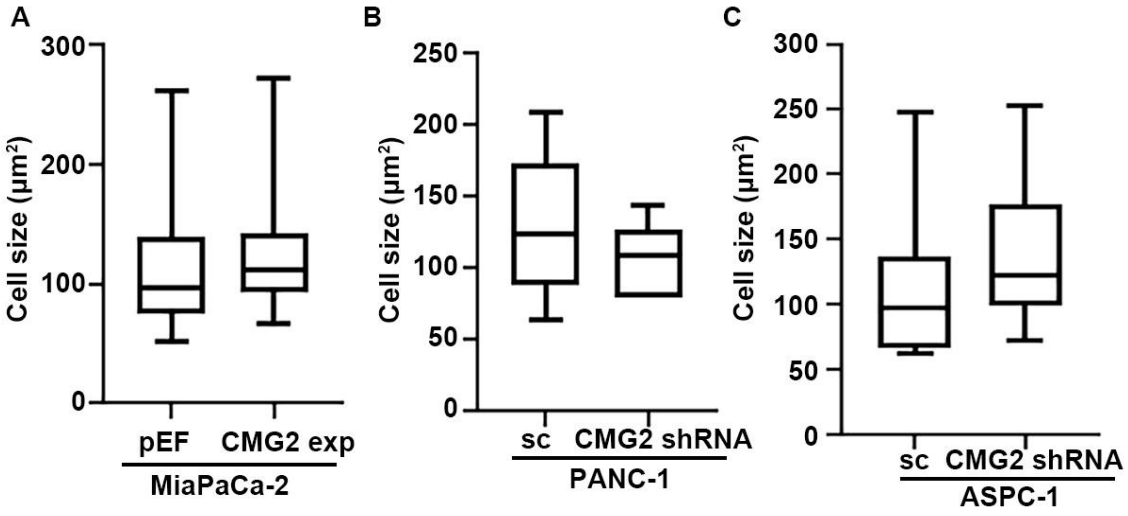

Figure 5.2 CMG2 and cell spreading. Influence of CMG2 on cell spreading were determined in pancreatic cancer cells MiaPaCa-2 (A), PANC-1 (B) and ASPC-1 (C) cells with CMG2 overexpression and knockdown, respectively. Shown are the size of cells adhered to Matrigel.

5.3.3 Involvement of CMG2-HA interaction in the attachment of pancreatic cancer cells to the mesothelial cells

HA is a component secreted by the mesothelial cell and has been implicated in the peritoneal metastasis (Soliman et al. 2022). To investigate whether CMG2-enhanced adhesion of cancer cells to mesothelial cells is mediated or partially mediated by HA, PANC-1 cells with CMG2 overexpression were treated with HA of different molecular weights and a HA inhibitor, respectively. When high molecular weight HA concentration was increased, the number of PANC-1^{CMG2exp} cells attached to MET5A cells were decreased significantly compared with the PANC-1^{pEF} cells. However, the high molecular weight HA of a concentration at 100μg/mL, was unable to eliminate the CMG2 promoted adhesion in comparison with the corresponding control although the adhesion was reduce upon the treatment (Figure 5.3A). Low molecular weight HA of concentrations up to 100μg/ml did not present an obvious inhibition of the cancer cell-mesothelial cell adhesion in both PANC-1^{CMG2exp} and the control cells. (Figure 5.3B).

Ultra-low molecular weight HA had a similar effect as high molecular weight HA, which inhibited the adhesion significantly in PANC-1^{CMG2exp} cells compared with the control cells (Figure 5.3C). The HA inhibitor reduced the adhesion of PANC-1^{CMG2exp} cells, while had little effect on PANC-1^{pEF} cells adhesion (Figure 5.3D). Except the low molecule weight HA, the high molecule weight HA, ultralow molecule weight and the HA inhibitor elicited a remarkable inhibition of the CMG2-promoted adhesion though only the ultralow molecule weight HA (100μg/ml) can diminish the CMG2 enhanced adhesion. The high molecule weight HA also exhibited an inhibition of the adhesion in both PANC-1^{CMG2exp} and the control cells.

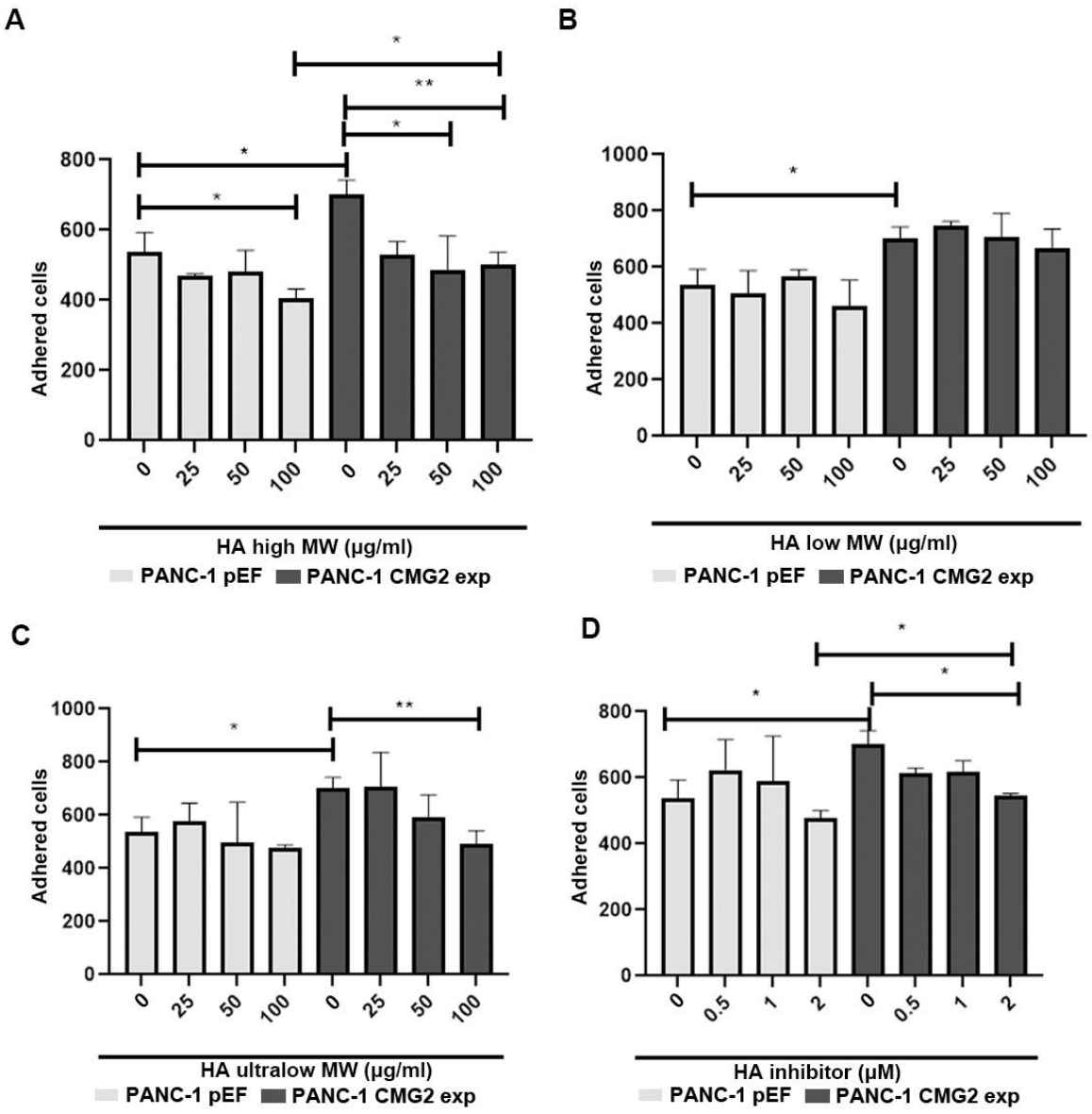

Figure 5.3 The effect of hyaluronic acid on CMG2 induced cell adhesion to mesothelial cell layer. PANC-1 cell line with CMG2 overexpression was treated with High molecular weight (A), low molecular weight (B), ultra-low molecular weight hyaluronic acid (C), and Hyaluronic acid inhibitor (D) with different concentration. Shown were the PANC-1 cell number adhered to the MET5A cell monolayer. *** indicate $p<0.001$, ** indicate $p<0.01$, * indicates $p<0.05$.

5.3.4 The influence of CMG2 on the aggregation of pancreatic cancer cells

During the spreading of cancer cells in peritoneal cavity, aggregation and clustering of cancer cells can assist them to survive and escape from the *anoikis* (Okamoto et al. 1987; Han et al. 2021). Clusters formed by the suspending pancreatic cancer cells were determined to evaluate the influence of CMG2 on the aggregation of pancreatic cancer cells upon a loss of anchorage. The number of both cells and cell-clusters formed by MiaPaCa-2^{CMG2exp} cells were markedly reduced after 1 hour suspension compared with the pEF control cells (Figure 5.4A), which remained significant difference in comparison with the control until the endpoint of the experiment (24 hours). In addition to that, CMG2 did not exhibit a similar impact on the aggregation of PANC-1 cells (Figure 5.4B and C). There was hardly a change of the aggregation observed in ASPC-1 cells even with the knockdown of CMG2 (Figure 5.4D).

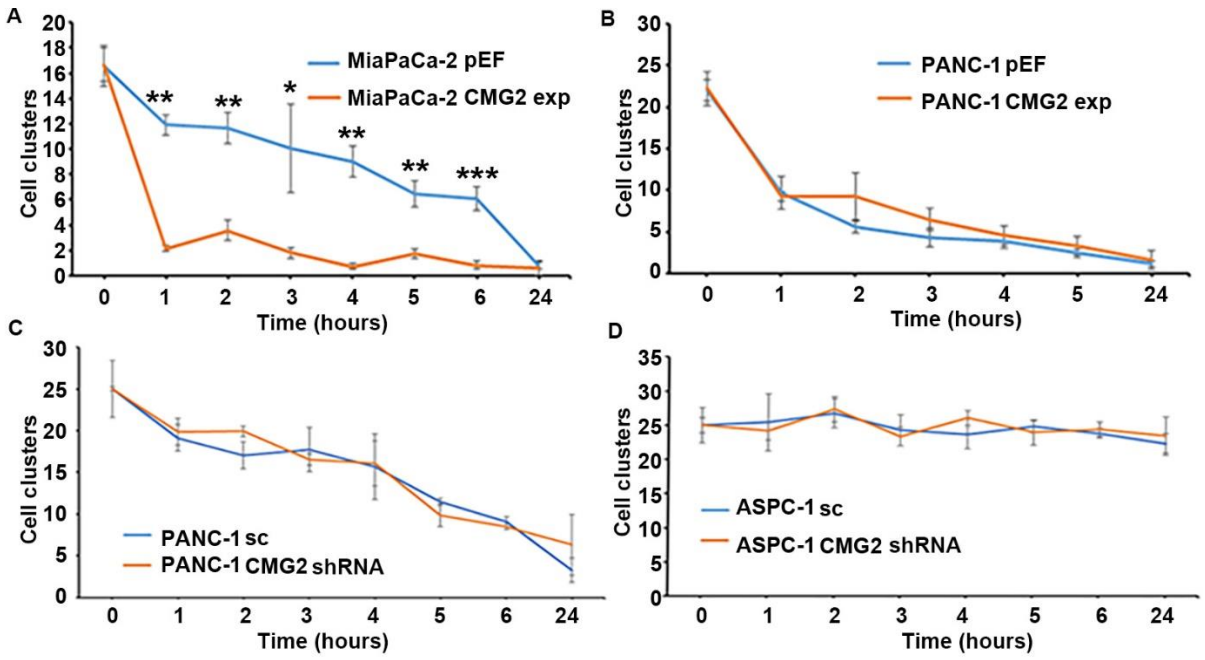

Figure 5.4 CMG2 and pancreatic cancer cell aggregation. Cell aggregation was determined in MiaPaCa-2 (A), PANC-1 (B and C) and ASPC-1 (D) cells. Shown are the numbers of clusters and cells per 0.2μl. *** indicate p<0.001, ** indicate p<0.01, * indicates p<0.05.

5.3.5 The effect of CMG2 expression on survival of pancreatic cancer cells during the dissemination

Upon the loss of anchorage, apoptotic population was significantly reduced in both MiaPaCa-2^{CMG2exp} and PANC-1^{CMG2exp} cells (Figure 5.5 A and B) over a course of suspension up to 6 hours, whilst an increase appeared in the apoptotic cells in both PANC-1 and ASPC-1 cells following the knockdown of CMG2 but to a less extend (Figure 5.5 C and D)

Furthermore, CCK8 assay was used to determine the viability of the suspending cells. In line with the influence of CMG2 on the apoptosis, an increased number of viable cells was seen in both MiaPaCa-2^{CMG2exp} and PANC-1^{CMG2exp} cells (Figure 5.5 E and F), whilst a reduced viability was evident in the CMG2 knockdown cell lines including both PANC1 and ASPC-1(Figure 5.5 G and H).

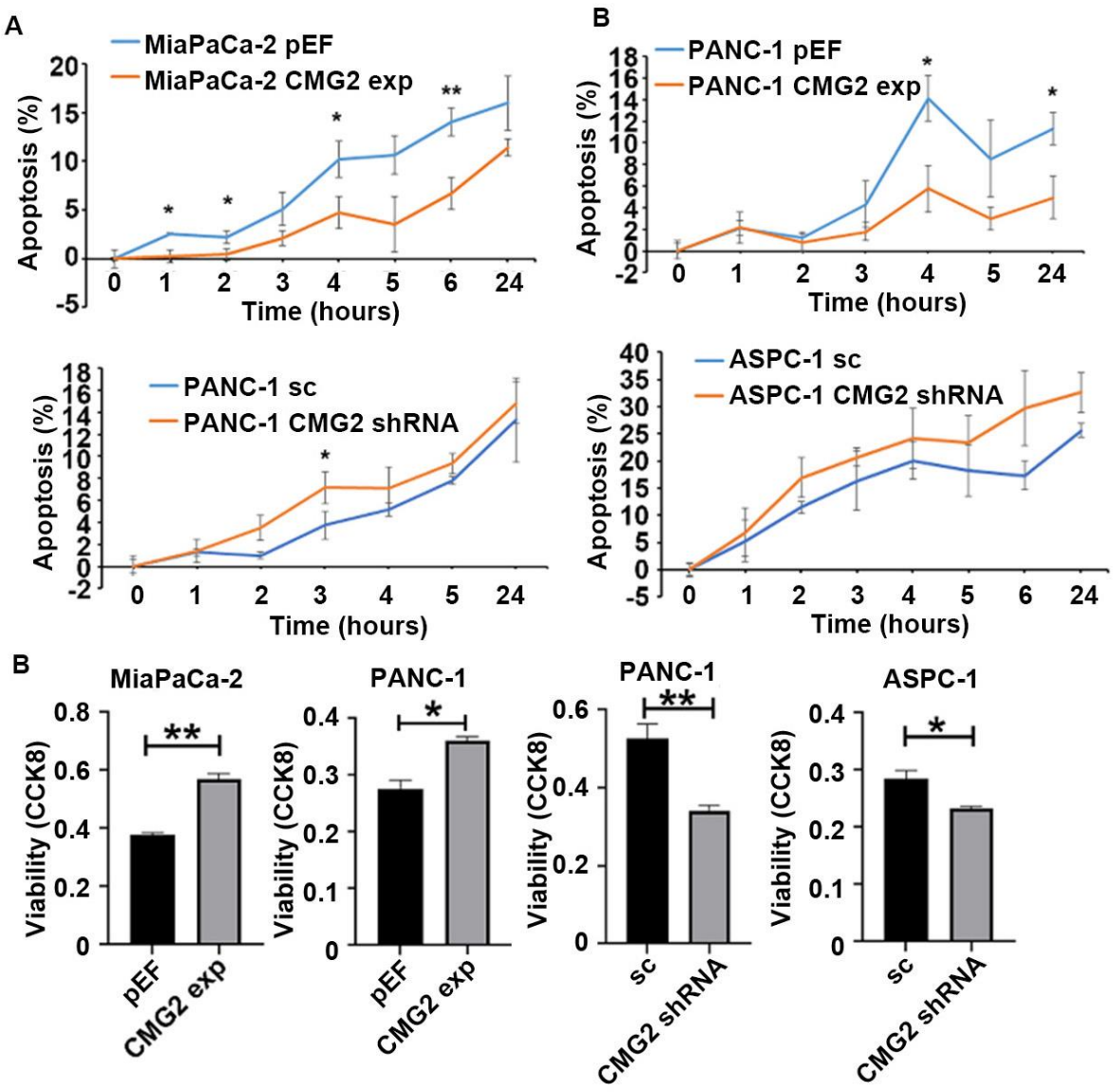

Figure 5.5 Influence of CMG2 on survival of suspending pancreatic cancer cells. Hoechst staining was used to determine the apoptotic cells in suspending MiaPaCa-2 (A), PANC-1 (B and C) and ASPC-1 (D) cells with CMG2 overexpression or knockdown. CCK8 was also used to determine cell viability in MiaPaCa-2 (E), PANC-1 (F and G) and ASPC-1 (H) cells with CMG2 overexpression or knockdown. *** indicate $p<0.001$, ** indicate $p<0.01$, * indicates $p<0.05$.

A flow cytometric apoptosis assay was employed to validate the influence CMG2 on *anoikis* in the pancreatic cancer cells. PANC-1^{CMG2sh6} cells carrying a EGFP marker were unable be used in the flow cytometric apoptosis assay which used FITC-Annexin V and PI. A plasmid vector carrying ribozymes target CMG2 was employed to

knockdown CMG2 expression in PANC-1 cells following a previously reported procedure (Ye et al. 2014c). The knockdown of CMG2 in PANC-1 cells using the ribozyme was verified (Figure 5.6A). There was a reduction in the apoptotic population in MiaPaCa-2^{CMG2exp} cells whilst increased apoptotic cells were seen in the PANC-1 cells following the knockdown of CMG2 (Figure 5.6 B, C and D).

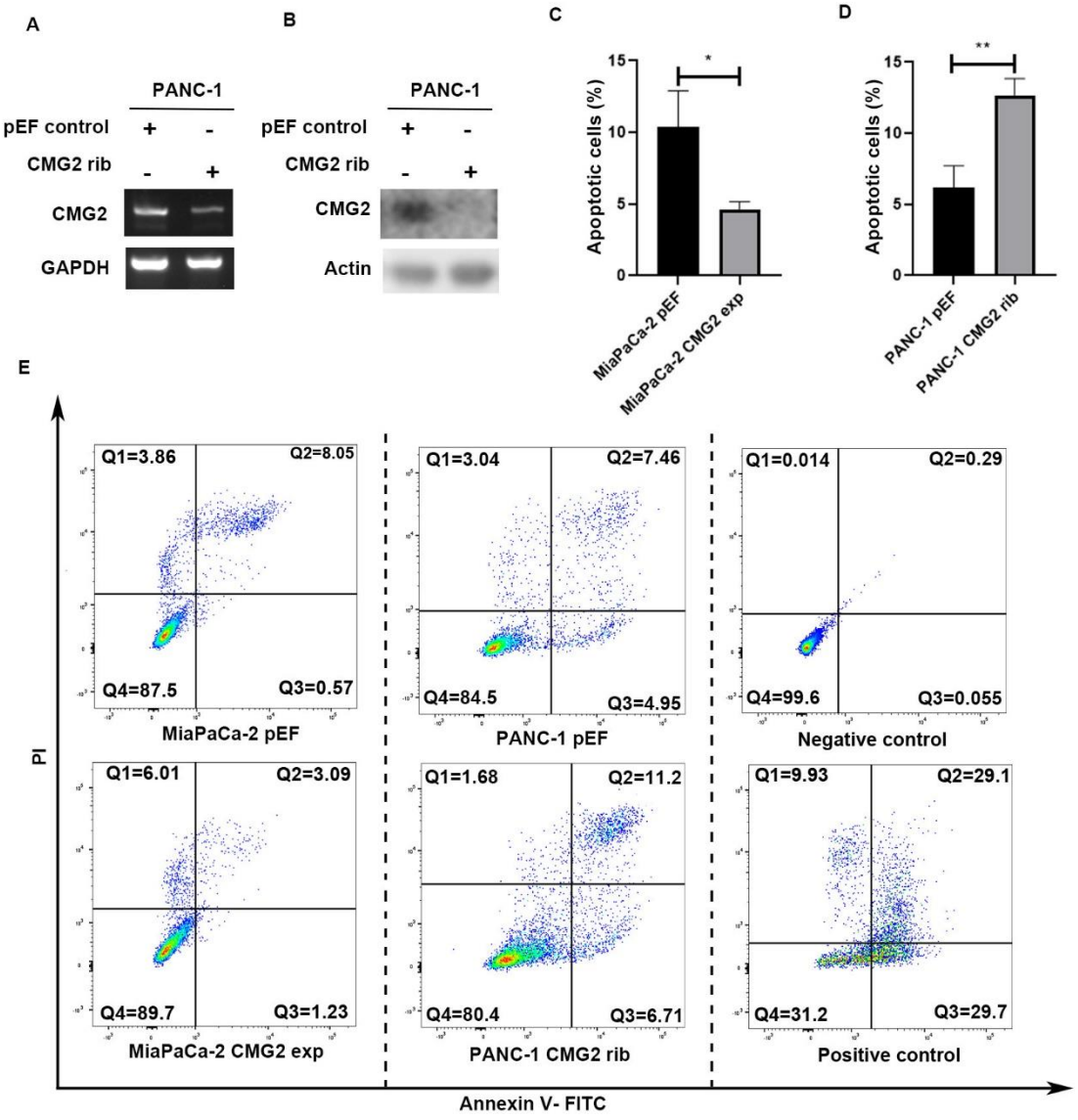

Figure 5.6 The effect of CMG2 on the *anoikis* in pancreatic cancer cells. CMG2 knockdown in PANC-1 cells using the ribozyme was verified using PCR (A) and Western blot (B). Apoptosis in the suspending MiaPaCa-2 (C) and PANC-1 (D) cells were determined using the flow

cytometric apoptosis assay. Apoptotic population included both early apoptotic (Q3) and late apoptotic (Q2) cells. Three independent experiments were conducted. (E) Shown are the representative figures from one experiment, Q1 was unspecific fluorescence, Q2 part represents late apoptosis stage, Q3 was early apoptosis, and Q4 represents healthy cells. *** indicate $p<0.001$, ** indicate $p<0.01$, * indicates $p<0.05$.

5.4 Discussion

The result shows that CMG2 was positively associated with the adhesion to mesothelial cells, suggesting higher CMG2 expression may promote peritoneum metastasis.

Mesothelial cells of the peritoneum can secrete a glycoprotein called hyaluronic acid which is implicated in cell-cell adhesion (Knudson et al. 1995; Evanko et al. 2007) and is also associated with cell proliferation and migration (Evanko et al. 2007). However, hyaluronic acid has other physiological functions, including maintaining the water balance, osmotic pressure, lubrication, and protecting wounds (Laurent and Fraser 1992; Laurent et al. 1996). During the adhesion of pancreatic cancer cells to the peritoneum, they first encounter a barrier formed by the HA.

HA of different molecular weights can elicit different effects through interactions with HA interacting molecules(Amorim et al. 2020; Schmidt et al. 2020; Park et al. 2023). In the present study, the treatment with different molecule weight HAs exhibited different levels of inhibition on the CMG2 enhanced adhesin. Further experiments showed that the adhesion of pancreatic cancer cells to the mesothelial cells was prevented by HA and HA inhibitor. It suggests that CMG2 may either enhance the adhesion via a regulation of HA interacting molecules, or itself directly interact with HA. Therefore, more likely, both mechanisms are involved in the CMG2 enhanced adhesion.

Several well-known hyaluronan interacting molecules can promote the interaction between mesothelial cells and other cells, including pancreatic cancer cells (Avula et al. 2020; Wiedmann et al. 2023). For example, CD44 also known as P-glycoprotein-1, was found to be positively correlated with CMG2 in gastric cancer (Ji et al. 2018). It is referred as the primary receptor of HA, which has eleven different variants (Joy et al. 2018). CD44 has three different states, including constitutively bound with hyaluronic acid form, unbound form and unbound but activated form. Before binding with hyaluronic acid, CD44 needs to be activated by a glycosylation or phosphorylation,

which is associated with the formation of lamellipodia and a promotion of cell migration (Naor et al. 1997). Hyaluronic acid with different molecular weights shows a different effect when it binds with the CD44. Upon a binding with CD44, high molecular weight HA can inhibit inflammation and angiogenesis (Noble 2002). In contrast, HA of a low molecular weight binds with CD44 and elicits a distinct effect, which can promote the cell proliferation, inflammation, and angiogenesis (Noble 2002; Wang et al. 2011). In addition to that, interaction between HA and CD44 induce an upregulation of the activity of EGFR kinase in head and neck squamous cell carcinoma (Bourguignon et al. 2006). Interaction between HA and CD44 can also activate the TGF-β receptor, in breast cancer, this activation is essential for cancer cell migration and invasion (Bourguignon et al. 2002).

The receptor for hyaluronan-mediated motility (RHAMM) was another HA interaction molecule, which is also named as CD168. CD168 is located on the cell membrane and in the cytoplasm. Membrane CD168 can enhance the activity of ERK and further promote the expression of PDGF and cell motility (Bourguignon et al. 2002). Intracellular CD168 plays an important role in regulating cytoskeletal proteins (Bourguignon et al. 2002). HA with a high molecular weight can interact with CD168, which is associated with cell proliferation and motility, further promoting the invasion of cancer cells (Toole 1997). In breast cancer cell lines, it has been found that the interactions among CD168, CD44 and ERK1/2 can promote cell migration. Additionally, CD168 can up-regulate the distribution of CD44 on the cell membrane, making it easier to be accessed by ERK (Joy et al. 2018).

LYVE-1 is another hyaluronic acid interacting molecule, only a few researches focus on its function in the interaction with HA, as it is usually expressed by lymphatic endothelial cells, with a structure being similar to the CD44. The interaction between HA and LYVE1 can enhance the migration of lymphocytes. In cancer, a high density of LYVE1 is associated with lymph node metastasis (Jackson et al. 2001).

Hyaluronic acid binding proteins (HABPs) are a group of proteins which can interact with hyaluronic acid and have been implicated in the inflammation and the synthesis of mitochondria protein (Ghosh et al. 2007)

In addition to these proteins, there are many other Hyaluronic acid interacting

molecules, while very little research has been done to explore their function in tumour. Hyalectans are a group of proteins which can interact with hyaluronic acid, including brevican, versican, aggrecan and neurocan. Brevican and neurocan are associated with brain development (Schaefer and Schaefer 2010). Versican was associated with inflammation (Wight 2008) and aggrecan was found in both brain and cartilage (Roughley 2006).

Despite this, the results also showed that when the cells were treated with high, low molecular weight hyaluronic acid and hyaluronic acid inhibitor, the CMG2 overexpression induced cell-adhesion was not totally inhibited, suggesting that CMG2 overexpression can promote cell-cell adhesion not only by promoting the expression of hyaluronic acid interacting molecules expression, some other cell-cell adhesion molecules may also be involved. In the following chapters, integrins, cadherins and other adhesion molecules will also be examined for their association with CMG2 in pancreatic cancer cell.

The result also showed that in MiaPaCa-2 cell line, CMG2 expression was positively associated with cell aggregation. During the dissemination in the peritoneal cavity, cancer cells encounter several stresses which will affect their viability, including shear forces, oxidative stress and immune system attacking. The cancer cells can form clusters to protect themselves from these stresses and attack (Massague and Obenauf 2016). Therefore, cell-cell interaction molecules shall be evaluated for their involvement in the CMG2 enhanced aggregation of MiaPaCa-2 cells.

Interestingly, without a change of cell aggregation, viability and apoptosis of PANC-1 and ASPC-1 cells were markedly affected by CMG2 when the cells were suspended. It indicates that higher CMG2 can enhance survival of suspending cancer cells not only by promoting cell-cell aggregation, other survival or apoptotic pathways may also be regulated by CMG2. Forming cell cluster during the cancer cell dissemination enhance the cell viability and promote distant metastasis. (Zhao et al. 2010; Fabisiewicz and Grzybowska 2017). Compared with epithelial cell, mesenchymal cell has a better ability to cope with the *anoikis* stress for their dependency on cell-matrix adhesion which was not as strong as epithelial cells (Melzer et al. 2017), suggesting that EMT may play an important role in enhanced survival of disseminating

cancer cells in peritoneal cavity.

In summary, CMG2 can enhance adhesion of pancreatic cancer cells to mesothelial cells, promote cell-cell adhesion and survival of pancreatic cancer cells upon a loss of anchorage. This leads to a further investigation in the following chapters to dissect pathways and molecules that are involved in the CMG2 induced cell-matrix adhesion, cell-cell adhesion and cell-HA interaction.

Chapter 6

Identification of CMG2-regulated proteins and pathways in pancreatic cancer cell

6.1 Introduction

Results presented in previous Chapters showed that higher CMG2 can enhance pancreatic cancer cell adhesion to Matrigel and mesothelial cells, which varied in different pancreatic cancer cell lines. In addition to the direct involvement of CMG2 in enhanced adhesion, HA interacting molecules, cell-cell adhesion molecules and other adhesion molecules may also be involved, as a result of the manipulated CMG2 expression. Furthermore, higher CMG2 can enhance cell aggregation and survival. CMG2 is a transmembrane protein which receives extracellular signals and mediates angiogenesis. CMG2 receives these signals by interacting with collagen I, collagen IV, fibrinogen, and fibronectin (Cryan and Rogers 2011b). This at least partially explains why CMG2 can promote cell adhesion. In addition to this, CMG2 can promote angiogenesis due to activation by pro-angiogenic factors such as bFGF or VEGF (Wycoff et al. 2011; Wycoff et al. 2015; Cryan et al. 2022) Growth factors and their receptors promote the development of many cancers. EGFR (epidermal growth factor receptor) is one member, being vital for enhancing migration and adhesion of pancreatic cancer cells, through activation of ELK1 (ETS Transcription Factor ELK1) (Sepulveda et al. 2005). Additionally, CMG2 can also induce the Talin-to-RhoA Switch. Upon binding with collagen IV or PA subunit of anthrax toxin, CMG2 can bind with talin and interact with vinculin, thus promoting synthesis of actin, with a further enhancement of cell adhesion (Burgi et al. 2020). LRP6 (Low-density lipoprotein receptor-related protein 6) was found to rely signalling from CMG2 to the Wnt pathway, leading to promotion of cell survival and stemness, in gastric cancer cells (Ji et al. 2018). In a prostate cancer cell line (PC-3), CMG2 enhanced adhesion but presented an inhibition of invasion (Ye et al. 2014b). In glioma, CMG2 can activate the hippo pathway by upregulating its expression level and further enhance cell adhesion and migration (Xu et al. 2019). Although it has been shown that CMG2 can enhance cell adhesion, the exact molecular machinery underlying CMG2 enhanced cell-matrix adhesion, cell-cell adhesion and cell aggregation in pancreatic cancer remains largely unknown.

In this Chapter, the molecules and pathways that were altered by CMG2 in pancreatic cancer cells were determined and analysed using mass spectrometric proteomic analysis, protein array analysis and analysis of RNA sequencing data from

the TCGA database. The analyses were aimed at identifying CMG2 regulated proteins, altered proteins with corresponding changes at mRNA level as responsive genes, activation of proteins and pathways as a strategy and a workflow as shown in Figure 6.1.

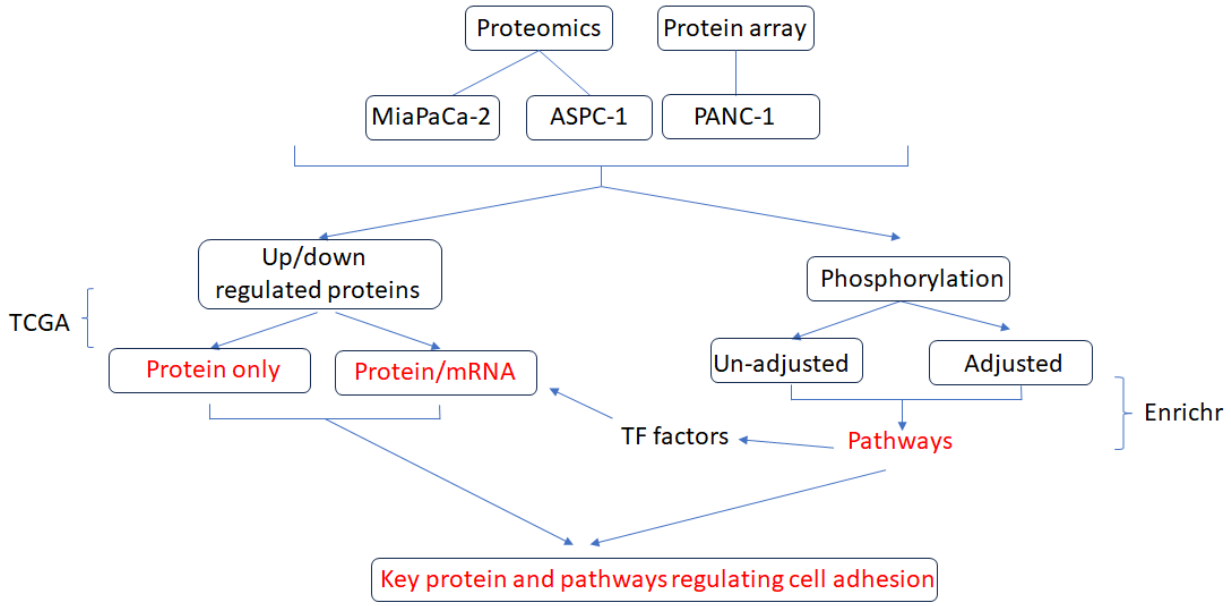

Figure 6.1: The workflow to identify candidate proteins, responsive genes and pathways underlying CMG2 regulated molecular and cellular events in pancreatic cancer.

6.2 Materials and methods

6.2.1 Cell lines

MiaPaCa-2^{pEF}, MiaPaCa-2^{CMG2exp}, PANC-1^{pEF} and PANC-1^{CMG2rib} were cultured in DMEM medium with 1µg/ml blasticidin. ASPC-1^{sc} and ASPC-1^{CMG2shRNA} were cultured in RPMI medium with 50µg/ml G418.

6.2.2 Proteomic analysis using mass spectrometry

Proteins were extracted from MiaPaCa-2^{pEF}, MiaPaCa-2^{CMG2exp}, ASPC-1^{SC} and ASPC-1^{CMG2shRNA} cell lines, using RIPA cell lysis buffer with phosphatase inhibitors (Cat No. ab201116 and ab201117, Abcam, Cambridge, UK). After quantification of the protein concentration, using a Bio-Rad protein quantification kit (Bio-Rad, Hertfordshire, UK), concentration of the protein samples was adjusted to 2mg/ml. Triplicates of each sample were prepared, which contained 200µg of total proteins. The samples were sent to Bristol

University for proteomic analysis, using mass spectrometry. The data were processed and analysed by a bioinformatician from Bristol University, using Proteome Discoverer v2.1 software as described in section 2.5.7.1.

6.2.3 Kinexus protein array analysis

RIPA buffer, without SDS, was applied to extract the protein from PANC-1^{pEF} and PANC-1^{CMG2rib} cell lines. After protein quantification, using a Bio-Rad protein quantification kit (Bio-Rad, Hertfordshire, UK), the concentration was adjusted to 3mg/ml. Subsequently, 200µg protein was used for the protein array, KAM-880 antibody microarray kit was applied (described in 2.5.8).

6.2.4 RNA sequencing and protein expression data from public datasets

The Cancer Genome Atlas (TCGA) includes 151 PDAC samples, 9 normal pancreatic tissues, 3 non-invasive tumours, 8 neuroendocrine tumours, 1 acinar ductal adenocarcinoma,1 distant metastatic sample and 9 unconfirmed samples. The data was curated according to a previous report (Nicolle et al. 2019). TCGA dataset includes both RNA sequencing dataset and the expression of a number of proteins.

6.2.5 Differential expressing gene analysis

In the TCGA cohort, the patients were divided into CMG2 high expression group and CMG2 low expression group, based on the expression level of CMG2, with a cut-off value of 11.42 which was determined by analysing the distribution of CMG2 expression. According to differential gene expression analysis, genes that were increased or decreased significantly in the CMG2 high group were employed for further analysis.

6.2.6 Analysis of CMG2-associated protein and protein phosphorylation

To identify the CMG2 coordinated genes and pathways at protein level, the change of different proteins was ranked based on the change ratio first. Different cut-off values were applied in different cell lines to sort out proteins with an obvious change. Candidate proteins were further ranked according to their abundancy. Altered proteins, with corresponding change at mRNA level, as revealed in the analysis of differentially

expressed genes in the TCGA cohort, were identified as responsive genes to the CMG2 overexpression.

6.2.7 Enrichment analysis for candidate transcription factors and pathways

The top upregulated or down regulated proteins were studied for further analysis of their intracellular location, molecular and biological functions using Enrich r (https://maayanlab.cloud/Enrichr/) (Chen et al. 2013; Kuleshov et al. 2016). The responsive genes were further analysed to identify corresponding transcription factors (TF) using Enrichr. The identified TFs, together with the shortlisted phosphorylated proteins, were subsequently employed for analysis of associated pathways, using Enrichr.

6.2.8 RNA extraction, cDNA synthesis and QPCR

Total RNA was isolated using TRI reagent (Sigma-Aldrich, Dorset, UK), followed by reverse transcription, using the iScriptTM cDNA Synthesis Kit (Bio-Rad laboratories, Hertfordshire, UK). QPCR was performed using FAST 2X qPCR MasterMix (Primer Design, Chandler's Ford, UK). Details of the primers are shown in section 2.1.2.

6.2.9 Protein extraction and Western blot

Cells were lysed in RIPA buffer following a protocol described in section 2.5.1. Proteins were separated using 10％ SDS-PAGE gel (Sigma-Aldrich, Dorset, UK) followed by a detection with primary antibodies: Anti-PTK2 (SC 1688, 1:1000 dilution), Anti-EGFR (SC71034, 1:1000 dilution), Anti-shc (SC967, 1:1000 dilution), Anti-MEK2 (SC13159, 1:1000 dilution), Anti-ELK1 (SC365876, 1:1000 dilution), Anti-VCL (SC73614, 1:1000 dilution), anti ICAM-1 (SC8439, 1:1000 dilution) and anti-GAPDH (SC32233, 1:5000 dilution). Secondary antibodies used were Anti-Mouse antibody (A-9044,1:1000 dilution)

6.2.10 Immunoprecipitation

Cells were cultured in a 75cm^2 flask. After the proteins were extracted and quantified, 2µg of primary antibody was added to 500µg protein sample. After incubation at room temperature for 2 hours, Protein G or A or G/A coupled agarose beads were added

(50μL beads for 500μg protein). After another hour incubation at room temperature, samples were centrifuged at 8000rpm at 4℃ for 10 minutes. The pellet included immunoprecipitants being referred as an IP sample, while the supernatant was referred to as a non-IP sample. The original total cell lysate was also prepared as a control. Details of the antibodies are provided in section 2.1.3.

6.2.11 Statistical analysis

T-tests were used for comparisons between two groups if they were normally distributed, Mann-Whitney u test was used for the analysis of non-normally distributed data. Spearman test were used for correlation analyses using SPSS (Version 26, IBM UK Ltd., Portsmouth, UK).

6.3 Results

6.3.1 CMG2 positively correlated proteins in pancreatic cancer cells

There were 1,953 proteins significantly upregulated in the MiaPaCa-2^{CMG2exp} cells, in comparison with the scramble control cells ($p<0.05$), of which 397 upregulated proteins presented a ratio of change above 50%. The top 30 of those upregulated proteins are shown in Supplementary Table 6.1. In consideration of the overall abundance and absolute change, the top 20 upregulated proteins are listed in Figure 6.2A. The mass spectrometric analysis of ASPC CMG2 knockdown cells showed that 1,170 proteins were markedly downregulated, of which 61 proteins were reduced with a change in fold greater than 30%, compared with the control. The top 30 of these downregulated proteins are listed in Supplementary Table 6.2. The top 20 down-regulated proteins in ASPC-1^{CMG2shRNA} cells were shortlisted according to their overall abundance and changes (Figure 6.2C).

There were 364 proteins upregulated in the MiaPaCa-2^{CMG2exp} cells that were also downregulated in ASPC-1^{CMG2shRNA} cells, which are proposed to be proteins positively correlated with CMG2, that were commonly observed in both CMG2 overexpression and knockdown cell lines ($P<0.05$). The top 30 of these proteins are shown in Supplementary Table 6.3. In those CMG2 positively correlated proteins, the

top 20 proteins that were upregulated in MiaPaCa-2^{CMG2exp} cells and also downregulated in ASPC-1^{CMG2shRNA} cells, were shortlisted according to their ranks, in their abundance and changes, for further analysis (Figure 6.2B).

In addition to the mass spectrometric analysis, the Kinexus protein array was also employed to determine protein and protein phosphorylation in PANC-1^{CMG2rib} cells, to explore activities of a panel of pathways, 233 proteins were decreased after CMG2 knockdown. The top 30 proteins, ranked by their absolute change, are shown in Supplementary Table 6.4. The top 20 downregulated proteins were shortlisted for the following analysis (Table 6.1).

The candidate proteins were categorised according to the biological functions that are commonly regulated by these proteins. In the ASPC-1 cell line, downregulated PTGIS (Prostaglandin I2 Synthase), QPRT (Quinolinate Phosphoribosyltransferase), GPX1 (Glutathione Peroxidase 1), SOD2 (Superoxide Dismutase 2), SQSTM1 (Sequestosome 1), DEPTOR (DEP Domain Containing MTOR Interacting Protein), and CTSH (Cathepsin H) can weaken cell survival, whilst downregulated PODXL (Podocalyxin Like), CTSH (Cathepsin H), SOD2, and SORL1 (Sortilin Related Receptor 1) may impair cell migration (Figure 6.3C). In the MiaPaCa-2 cell line, enhanced molecular functions can be divided into several groups, including cell-matrix adhesion enhanced by MSN (Moesin) and ICAM-1 (Intercellular Adhesion Molecule 1); cell differentiation promoted by MSN, ICAM1, CSRP1 (Cysteine And Glycine Rich Protein 1) and CAV1 (Caveolin 1) and cell-matrix adhesion mediated by MYO1B (Myosin IB) and CALD1 (Caldesmon 1) (Figure 6.3A). Biological functions that were enhanced by the positive correlated proteins, identified in both MiaPaCa-2 and ASPC-1 cell lines, included cell-cell adhesion, cell-matrix adhesion, cell proliferation and cell survival (Figure 6.3B). ACTN1 (Actinin Alpha 1), MYH9 (Myosin Heavy Chain 9) and VCL (Vinculin) can promote the cell-cell adhesion, while MYO1C (Myosin IC), TPM3 (Tropomyosin 3), ACTN1 and STMN1 (Stathmin 1) can enhance cell-matrix adhesion.

The molecular functions of these molecules were also analysed using Enrich r. In the ASPC-1 cell line, several CMG2 positively correlated proteins were identified which can enhance cell-matrix adhesion, energy metabolism and protein metabolism (Figure 6.3F). Among these molecules, FHL3 (Four and a Half LIM Domains 3) and PFN3

(Profilin 3) are implicated in actin binding and cell-matrix adhesion. In the MiaPaCa-2 cell line, cell-matrix adhesion and vasodilatation were the two main molecular functions (Figure 6.3D). CALD1, MAP1B (Microtubule Associated Protein 1B), MSN, SPTAN1 (Spectrin Alpha, Non-Erythrocytic 1), VCL and SPTBN1 (Spectrin Beta, Non-Erythrocytic 1) mediate cell-matrix adhesion. When these two cell lines were combined, it was obvious that the top positively correlated molecules are involved in cell-matrix adhesion, energy metabolism and lipid metabolism (Figure 6.3E). MYH9 (Myosin Heavy Chain 9), FLNB (Filamin B), IQGAP1 (IQ Motif Containing GTPase Activating Protein 1) and VCL are associated with cell-matrix adhesion.

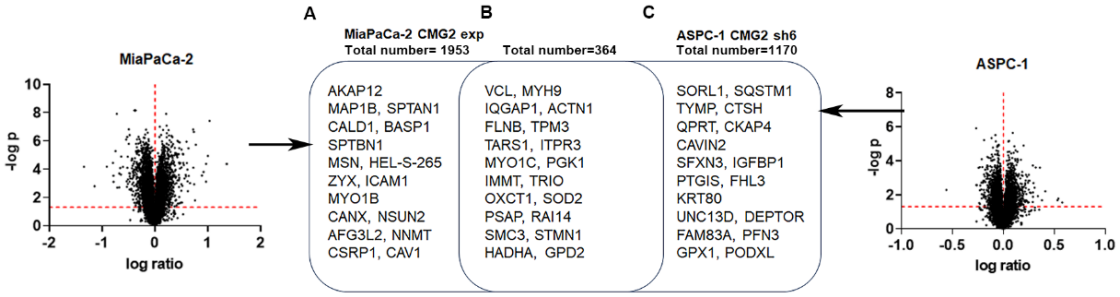

Figure 6.2 Proteins positively correlated with CMG2. Volcano plots show the total upregulated proteins in MiaPaCa-2^{CMG2exp} cells and down-regulated proteins in ASPC-1 cells ($p<0.05$). The top 20 CMG2 positively correlated proteins in (A) MiaPaCa-2, (B) both MiPaCa-2 and ASPC-1 cell lines and (C) ASPC-1 cell line were ranked by their absolute change.

Table 6.1 Down-regulated proteins in PANC-1 cell line with CMG2 knockdown (CFC%<-20, Ranked by absolute change, shown are original values in proteomics)

	PANC-1 ^{pEF}	PANC-1 $^{CMG2\ rib}$		
Target Protein Name	Mean	Mean	Absolute change	%CFC
mTOR	23390.86	14753.8	-8637.06	-37.13
Bcl-XL (BCL2L1)	20275.06	12484.27	-7790.79	-38.62
ALK	30861.99	23564.89	-7297.1	-23.89
MKK4 (MAP2K4)	24234.09	17382.7	-6851.39	-28.5
Hsc70 (HSPA8)	15576.22	9516.31	-6059.91	-39.1
STAT5B	8887.92	5147.43	-3740.49	-42.27
CDK5	11303.67	8767.57	-2536.1	-22.68
Bid (BID)	9067.77	6622.06	-2445.71	-27.2
PP1 (PPP1CC)	10935.72	8715.04	-2220.68	-20.56
PP4C (PPP4C)	9691.71	7696.73	-1994.98	-20.84
Hsp40 (DNAJB1)	7852.19	5914.06	-1938.13	-24.92
A-Raf (RAF1)	9115.26	7218.24	-1897.02	-21.06
Hsp105 (HSPH1)	4238.93	2715.42	-1523.51	-36.14
Bcl-Xs	7217.77	5792.11	-1425.66	-20.01
NFkappaB (NFKB1)	6748.55	5384.31	-1364.24	-20.47
STAT6 (STAT6)	6512.11	5191.11	-1321	-20.54
Cdc2 (CDK1)	3464.34	2483.94	-980.4	-28.53
PAK1 (PAK1)	4143.45	3201.84	-941.61	-22.97
MEKK2 (MAP3K2)	4178.46	3272.43	-906.03	-21.93
KAP (CDKN3)	3513.89	2778.6	-735.29	-21.18

Note: Shown is ranked by sum of absolute changes of the shortlisted proteins.

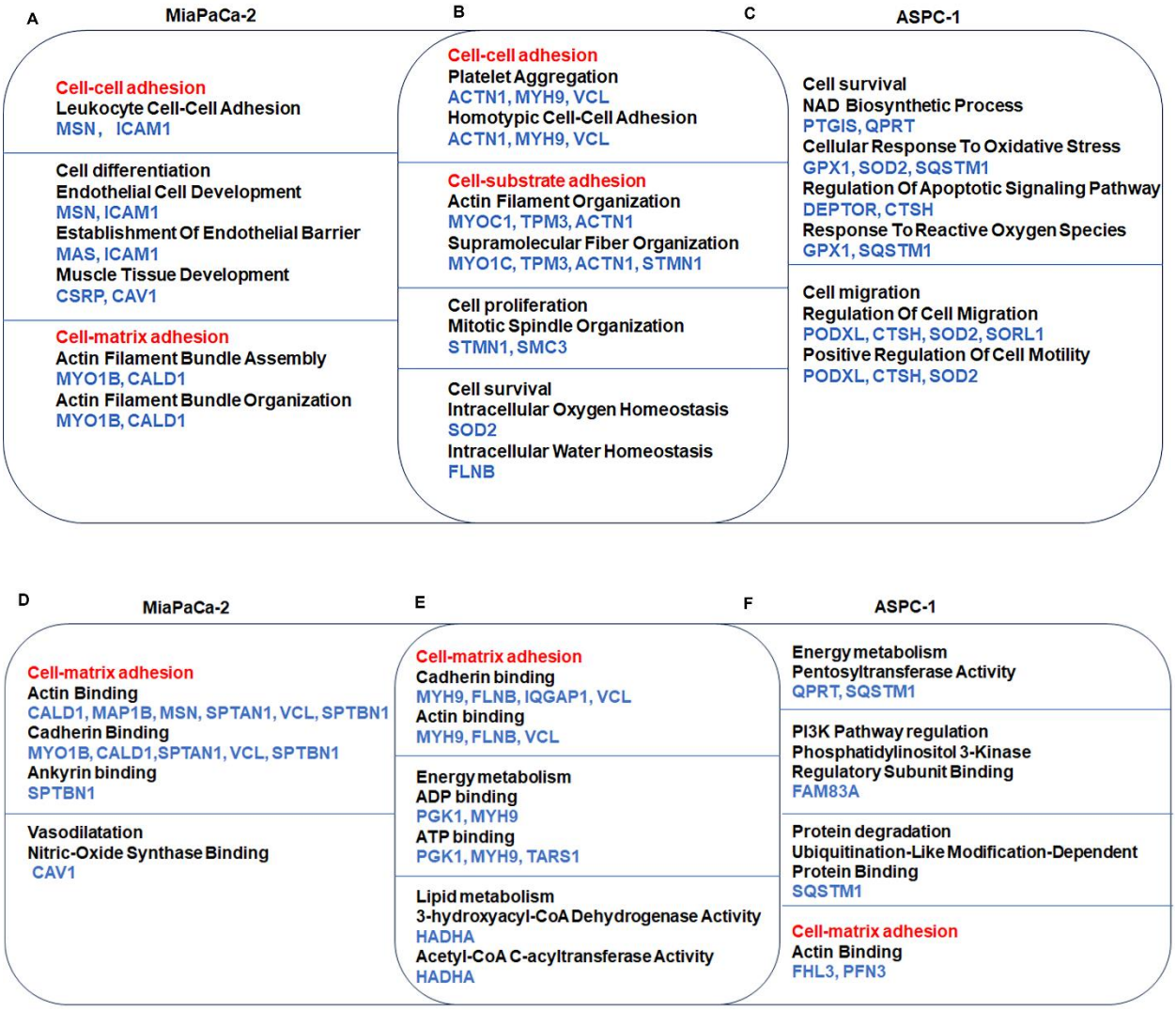

Figure 6.3 Biological functions and molecular functions of CMG2 positively correlated proteins. Shown are the biological functions, which are enhanced by CMG2 positively correlated proteins, in MiaPaCa-2 (A) cell line, in both MiaPaCa-2 and ASPC-1 cell lines (B), and ASPC-1 cell line (C). Molecular functions regulated by the CMG2 positively correlated proteins were also analysed in MiaPaCa-2 cell line (D), both MiaPaCa-2 and ASPC-1 cell lines (E), and in ASPC-1 cell line (F). Analyses of molecular functions and biological functions were conducted using Enrich r, respectively.

6.3.2 Transcriptionally up-regulated genes/proteins by CMG2 in pancreatic cancer cells

Upregulated genes, at mRNA level in pancreatic tumours with higher expression of CMG2, were analysed and shortlisted using the TCGA RNA sequencing data. The CMG2 positively correlated proteins, with a consistent change at mRNA level in the pancreatic tumours, were considered as responsive genes of CMG2 for further analysis of their molecular and biological functions. Figure 6.4 shows the responsive genes that were shortlisted, by considering CMG2 positively correlated proteins identified in the proteomic analyses. Ontology analysis was done to assess the biological and molecular functions of CMG2 responsive genes, or positively correlated genes, which presented a coherent change in both transcript and protein level. In MiaPaCa-2 cell line, CMG2 positively correlated proteins VCL, SPTAN1, CALD1, SPTBN1, ACTN1, ZYX (Zyxin) and CSBP1 (Mitogen-Activated Protein Kinase 14, MAPK14) were also positively correlated with CMG2 in transcripts level (Figure 6.4A). In the ASPC-1^{CMG2shRNA} cell line, SQSTM1, SFXN3 (Sideroflexin 3), IGFBP1 (Insulin Like Growth Factor Binding Protein 1), UNC13D (Unc-13 Homolog D), and FAM83A (Family with Sequence Similarity 83 Member A) were decreased in both transcript and protein (Figure 6.4B). A consistent change of transcripts and proteins was also seen for VCL, MYH9, IQGAP1, ACTN1, FLNB, TPM3 (Tropomyosin 3), MYO1C, PGK1 (Phosphoglycerate Kinase 1), RAI14 (Retinoic Acid Induced 14) and GPD2 (Glycerol-3-Phosphate Dehydrogenase 2), which were positively correlated to CMG2, in both MiaPaCa-2 and ASPC-1 cell lines (Figure 6.4C). In the PANC-1 cell line, six of the top 20 CMG2 positively correlated proteins were also positively associated with CMG2 at transcript levels in the tumours, including PAK1 (P21 (RAC1) Activated Kinase 1), DNAJB1 (DnaJ Heat Shock Protein Family (Hsp40) Member B1), HSPH1 (Heat Shock Protein Family H (Hsp110) Member 1), BCL2L1 (BCL2 Like 1) and STAT6 (Signal Transducer And Activator Of Transcription 6) (Figure 6.4D).

In the MiaPaCa-2 cell line, CSRP1 (cysteine and glycine rich protein 1), ACTN1 and VCL are implicated in platelet aggregation and homotypic aggregation (Figure 6.5A). CALD1, SPTAN1, VCL and SPTBN1 are involved in actin binding and cadherin binding (Figure 6.5D). These responsive genes/proteins are mainly involved in cell-cell

adhesion or cell-matrix adhesion. In the ASPC-1 cell line, SQSTM1 (Sequestosome 1) is associated with cell survival. UNC13D is associated with the immunity response (Figure 6.5C). FAM83A and IGFBP1 (Insulin Like Growth Factor Binding Protein 1) are implicated in PI3K/Akt and IGFR pathways, respectively (Figure 6.5F). ACTN1, MYH9 and VCL are possibly involved in homotypic aggregation in both ASPC-1 and MiaPaCa-2 cell lines (Figure 6.5B). In these two cell lines, some molecular biofunctions may be enhanced by CMG2, including cadherin binding, ADP binding and actin binding. Among these functions, cadherin binding and actin binding are vital for cell adhesion (Figure 6.5E).

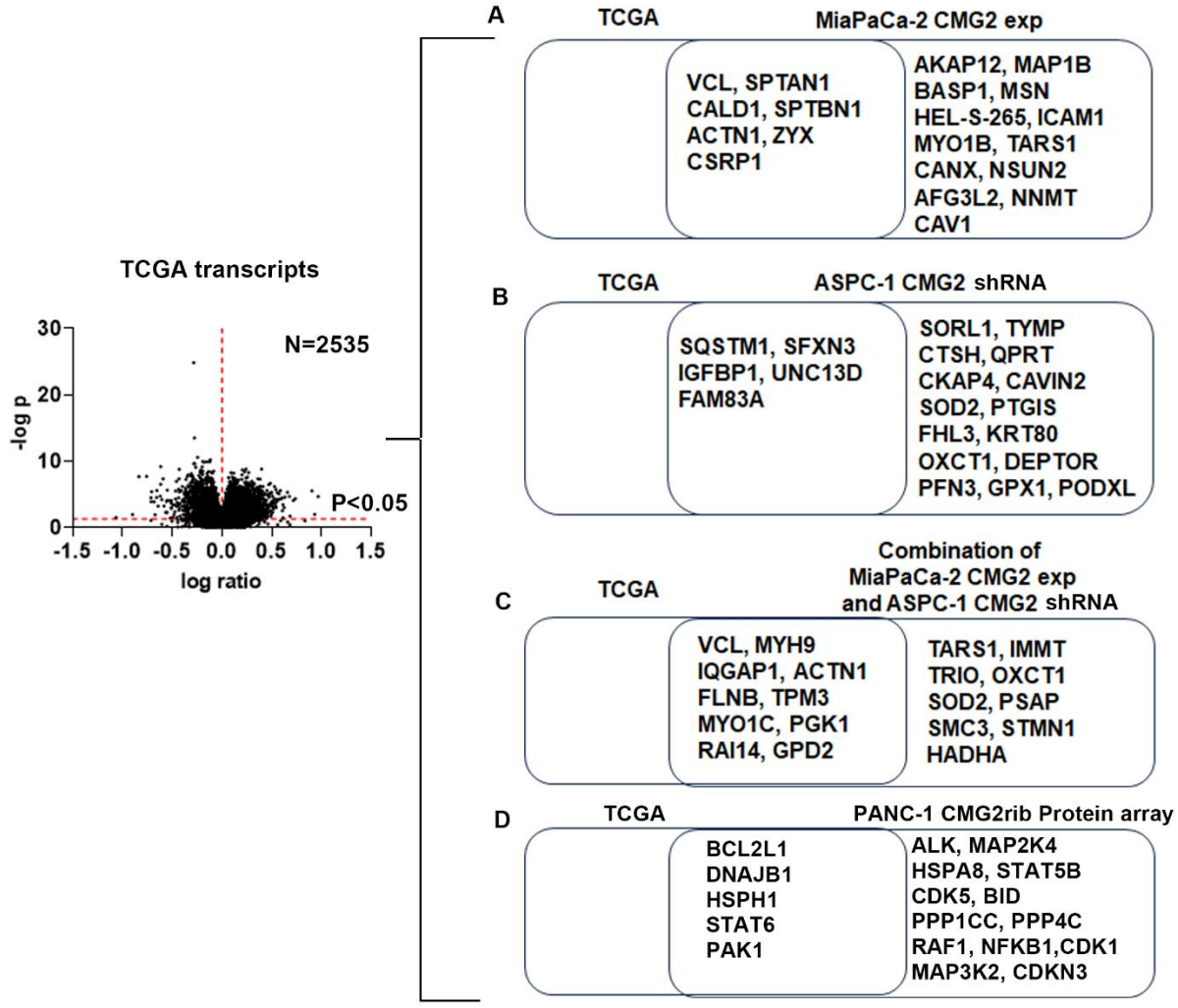

Figure 6.4 Genes positively correlated with CMG2 at both protein and transcript levels. Genes located in the overlap areas between upregulated genes (transcript) in pancreatic

tumours (TCGA RNA sequencing data) and the CMG2 positively correlated proteins in MiaPaCa-2 (A), ASPC-1 (B), both MiaPaCa-2 and ASPC-1 cell lines (C) and PANC-1 cell line (D) were considered as CMG2 responsive genes, or positively correlated genes, in pancreatic cancer cells.

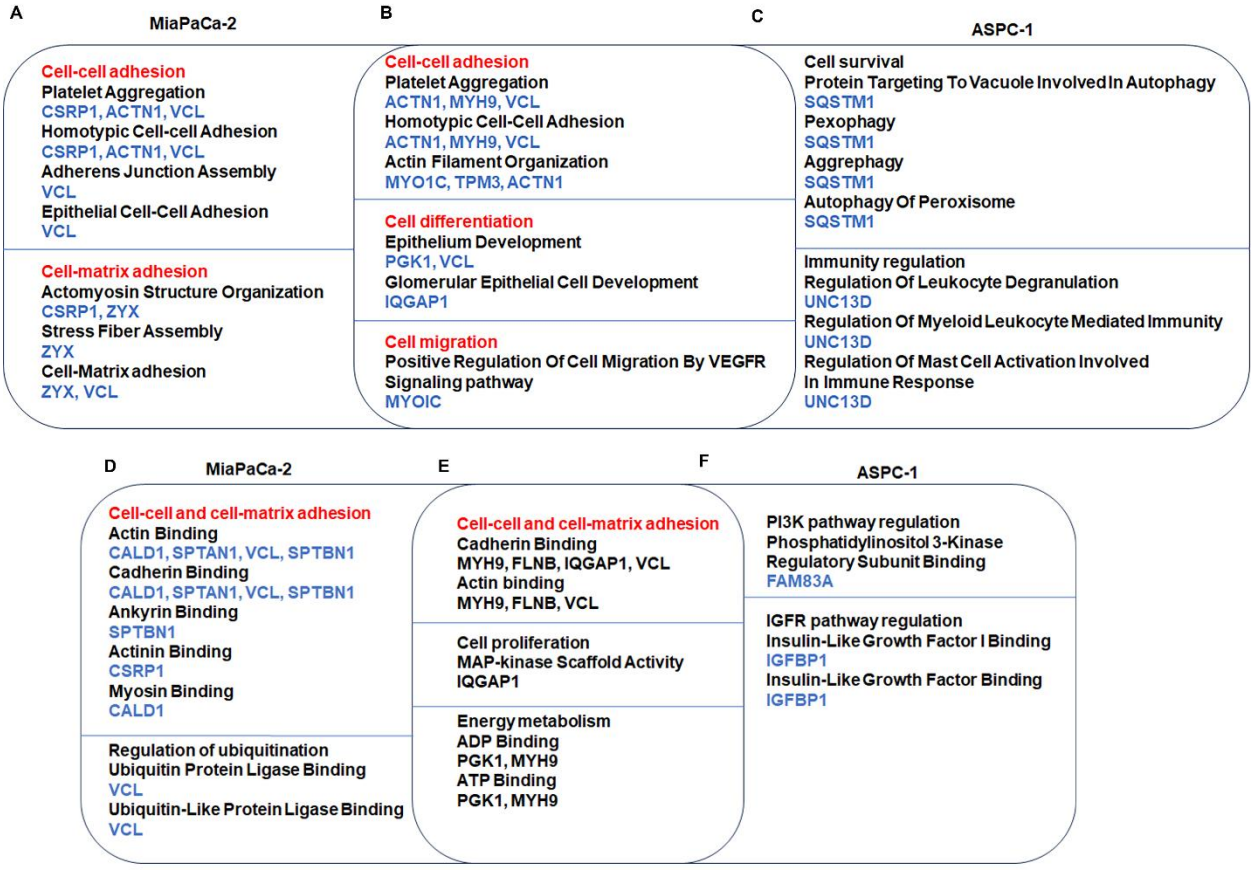

Figure 6.5 Biological and molecular functions of CMG2 positively correlated genes. Shown are the biological functions of the CMG2 positively correlated genes identified in MiaPaCa-2 cells (A), both MiaPaCa-2 and ASPC-1 cells (B) and in ASPC-1 cells (C); and molecular functions of the CMG2 responsive genes in MiaPaCa-2 cells (D), both MiaPaCa-2 and ASPC-1 cells (E), and ASPC-1 cells (F), respectively.

6.3.3 CMG2 coordinated protein phosphorylation

There were 531 proteins that had an increase of unadjusted phosphorylation in the MiaPaCa-2^{CMG2exp} cells, while in the ASPC-1^{CMG2shRNA} cells, 446 proteins presented an unadjusted decrease of phosphorylation ($P<0.05$). These phosphorylated proteins were considered to be positively correlated with CMG2 in both cell lines. After justification

against the total protein levels, 437 proteins exhibited an increase in the adjusted phosphorylation in the MiaPaCa-2^{CMG2exp} cell line, while the adjusted phosphorylation of 399 proteins were positively correlated with CMG2 in the ASPC-1^{CMG2shRNA} cells ($P<0.05$). The adjusted phosphorylation of 127 proteins was positively correlated with CMG2 in both MiaPaCa-2 and ASPC-1 cell lines ($P<0.05$). Both adjusted and unadjusted phosphorylation were further analysed. The top 20 proteins with adjusted and unadjusted phosphorylation, that were positively correlated with CMG2 in MiaPaCa-2 (Figure 6.6A), ASPC-1 (Figure 6.6C), both MiaPaCa-2 and ASPC-1 (Figure 6.6B) and PANC-1 (Figure 6.6D) were listed. Phosphorylation of 222 proteins was measured in the PANC-1^{CMG2rib} cells, 129 proteins had a decrease of phosphorylation. They were ranked by the absolute change (Supplementary table 6.5), in which the top 20 were shortlisted for following analysis (Figure 6.6D).

In the MiaPaCa-2^{CMG2exp} cell line, the top phosphorylated proteins are mainly involved in cell-cell adhesion, cell-matrix adhesion, energy metabolism, cell migration and cell proliferation (Figure 6.7A). For example, GNAS (GNAS Complex Locus), FLNA (Filamin A) and TLN1 (Talin 1) are involved in cell adhesion. Regarding molecular functions, ubiquitination regulation and cell adhesion are associated with these phosphorylated proteins (Figure 6.7D). Cadherin binding is one molecular function which can enhance cell adhesion. PKM (Pyruvate Kinase M1/2), CALD1, FLNA, TLN1 and RTN4 (Reticulon 4) are proteins associated with the cadherin binding. In ASPC-1^{CMG2shRNA} cells, EGFR, PICALM (Phosphatidylinositol Binding Clathrin Assembly Protein), and SQSTM1 are associated with cell adhesion (Figure 6.7C). LAD1 (Ladinin 1), EGFR, PICALM and PLEC (Plectin) were involved in cadherin binding (Figure 6.7F). In these phosphorylated proteins, that are positively correlated with CMG2 in both MiaPaCa-2 and ASPC-1 cell lines, cell adhesion was enhanced by the result of orchestrated biological functions, including the regulation of protein localisation to the cell cortex, translocation of proteins to the cell periphery and cell surface (Figure 6.7B). Many of these proteins are implicated in the molecular functions of cadherin binding and actin binding (Figure 6.7E).

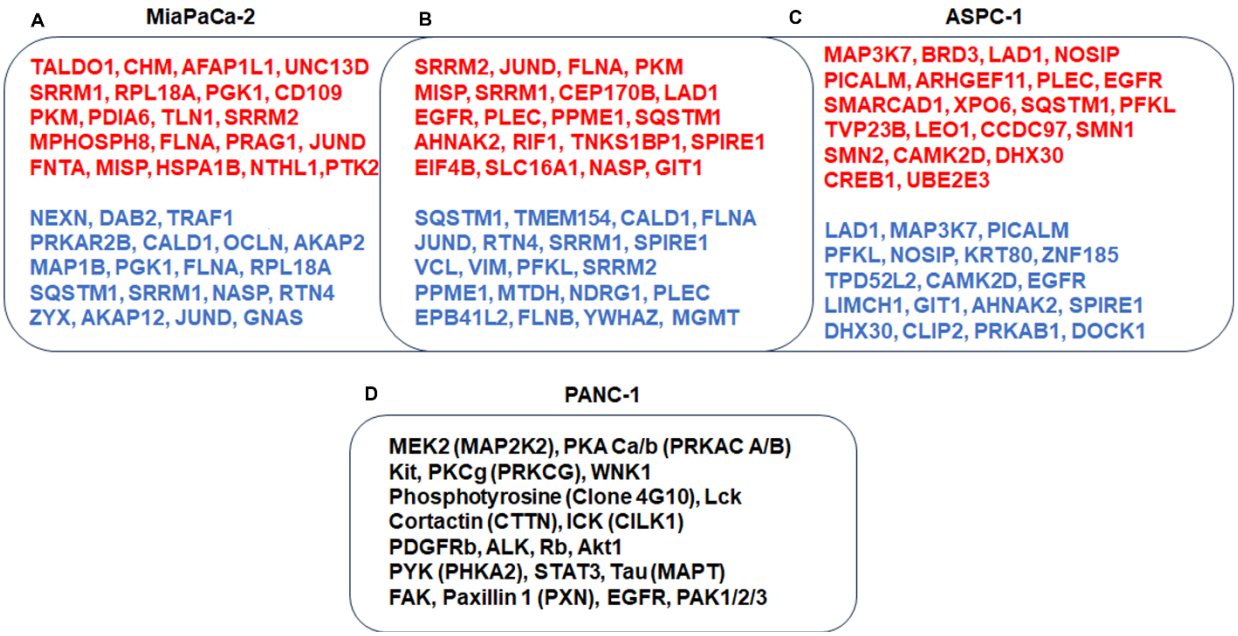

Figure 6.6 CMG2 positively correlated proteins with adjusted and un-adjusted phosphorylation. Shown are the top 20 proteins ranked by their change in folds (Log FC) with phosphorylation that was positively correlated with CMG2 in MiaPaCa-2 (A), both MiaPaCa-2 and ASPC-1 (B), ASPC-1 (C), and PANC-1 cells (D). Red: Adjusted phosphorylation. Blue: Un-adjusted phosphorylation.

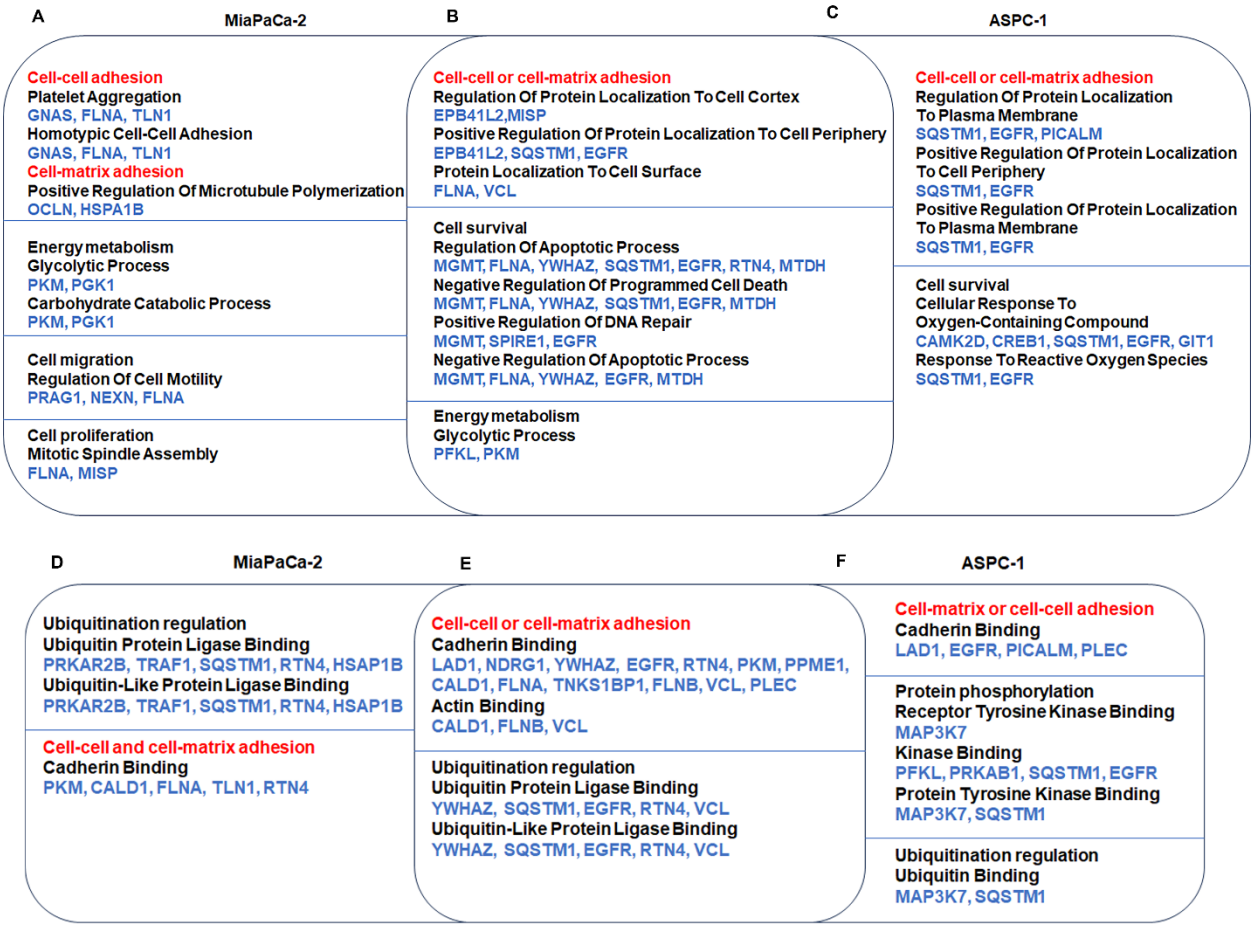

Figure 6.7 Biological and molecular functions of the top phosphorylated proteins. Shown are the biological functions that are related to the shortlisted phosphorylated proteins in MiaPaCa-2 cells (A), both MiaPaCa-2 and ASPC-1 cell lines (B), and ASPC-1 cells (C); molecular functions of these proteins in MiaPaCa-2 cells (D) both MiaPaCa-2 and ASPC-1 cells (E), and ASPC-1 cells (F).

6.3.4 Pathways regulated by CMG2 in pancreatic cancer cells

Three approaches were taken to dissect CMG2 coordinated pathways. The CMG2 responsive genes, i.e., positive correlated genes with coherent changes at both protein and mRNA levels, were firstly employed to identify the relevant transcription factors, with subsequent analysis for corresponding upstream pathways. Various transcription factors were identified by analysing the CMG2 positively correlated genes, in the pancreatic cancer cell line models (Figure 6.8). In the MiaPaCa-2 cell line, SMAD2 (SMAD Family Member 2), SMAD3, STAT1 and STAT6 are involved in the Th17 cell

differentiation pathway. STAT1 and STAT6 are located downstream of the Th1 and Th2 cell differentiation pathway. SMAD3, ACTN1, ZYX and VCL can be regulated by the focal adhesion pathway or adheres junction pathway (Figure 6.9A). Most of the pathways identified in the ASPC-1 cell line regulate cell survival, differentiation and tumorigenesis (Figure 6.9C). Pathways identified in both MiaPaCa-2 and ASPC-1 cells can enhance adhesion, proliferation and survival of cells (Figure 6.9B). Adherent junction and regulation of actin cytoskeleton were the two cell adhesion pathways regulating SMAD3, ACTN1, IQGAP1, VCL and MYH9. In the PANC-1 cell line, JAK-STAT pathway and ERBB (erythroblastic oncogene B2) signalling pathway were identified that can promote cell adhesion. The JAK-STAT pathway regulates STAT4, STAT6, and BCL2L1. JUN and PAK1 can be regulated by the ERBB signalling pathway (Figure 6.9D).

In addition to the identification of the transcription factors and associated pathways, CMG2 regulated pathways were also dissected by analysing the phosphorylated proteins identified in the cell line models (Figure 6.10). In the MiaPaCa-2 CMG2 exp cell line, ZYX, FLNA and TLN1 were hyperphosphorylated, these are associated with an activation of the focal adhesion pathway. JUND (JunD Proto-Oncogene, AP-1 Transcription Factor Subunit), FLNA and HSPA1B (Heat Shock Protein Family A (Hsp70) Member 1B) are implicated in MAPK pathway. PGK1 (Phosphoglycerate Kinase 1) and PKM (Pyruvate Kinase M1/2) are associated with a pathway that regulates energy metabolism (Figure 6.10A). In the ASPC-1 cell line, activated pathways can promote cell adhesion, energetic balance and cell differentiation (Figure 6.10C). The phosphorylated proteins DOCK1 (Dedicator Of Cytokinesis 1), EGFR and GIT1 (GIT ArfGAP 1) are involved in the regulation of actin and cell adhesion. Pathways of regulating actin, adhesion junctions and focal adhesion were activated in both ASPC-1 and MiaPaCa-2 cell lines with higher CMG2 expression (Figure 6.10B). In the PANC-1^{CMG2rib} cell line, GAP junction, focal adhesion, ERBB and MAPK pathways were repressed, which have been implicated in the regulation of cell adhesion (Figure 6.10D).

Furthermore, some proteins were only changed at protein level, without a change of transcript or phosphorylation. Pathways were also analysed for these upregulated

proteins in the pancreatic cancer cell lines with higher expression CMG2. In the MiaPaCa-2 cell line, MSN and ICAM1 can enhance trans-endothelial migration of leukocytes (Figure 6.11A). Some pathways associated with lipid metabolism were identified in both MiaPaCa-2 and ASPC-1 cell lines (Figure 6.11B and C). In the PANC-1 cell line, MAP3K2 (Mitogen-Activated Protein Kinase Kinase Kinase 2), MAP2K4, HSPA8 (Heat Shock Protein Family A (Hsp70) Member 8), RAF1 (Raf-1 Proto-Oncogene, Serine/Threonine Kinase) and NFKB1 (Nuclear factor-κB) are associated with the MAPK pathway (Figure 6.11D). Moreover, the KEGG dataset was also employed to determine the pathways that were activated in pancreatic cancer cell lines with higher CMG2 expression. Similarly, pathways that regulate leukocyte trans-endothelial migration, focal adhesion and the EGFR pathway were highlighted as pathways activated in the pancreatic cancer cell lines with higher CMG2 expression. To further examine the activation of EGFR and focal adhesion, other key proteins involved were also evaluated using the proteomic data. It was found that in addition to FAK and PAKs, the phosphorylation of SHC1, Raf1 and MEK2 was positively correlated with CMG2 in both MiaPaCa-2 and ASPC-1 cell line models. These proteins are downstream molecules of EGFR that are actively involved in cell adhesion.

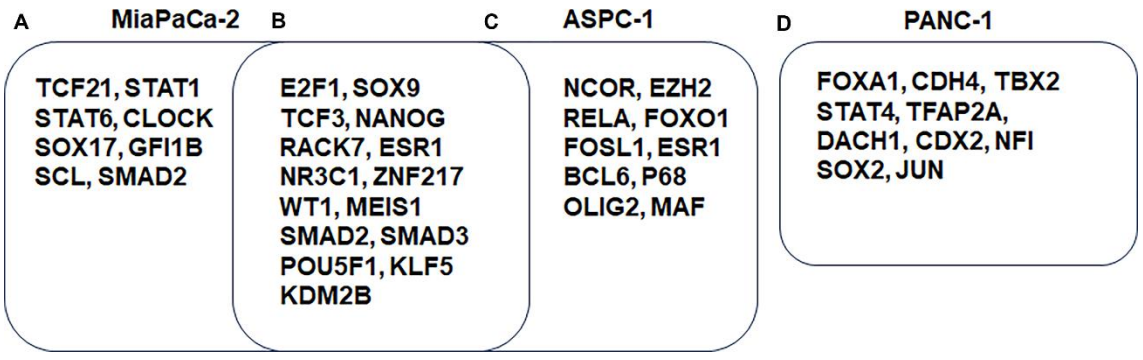

Figure 6.8 Transcription factors regulating the expression of CMG2 positively correlated genes. Shown are the transcriptions factors, which are possibly involved in the regulation of the CMG2 positively correlated genes in MiaPaCa-2 cells (A), both MiaPaCa-2 and ASPC-1 cells (B), ASPC-1 cells (C), and PANC-1 cell lines (D).

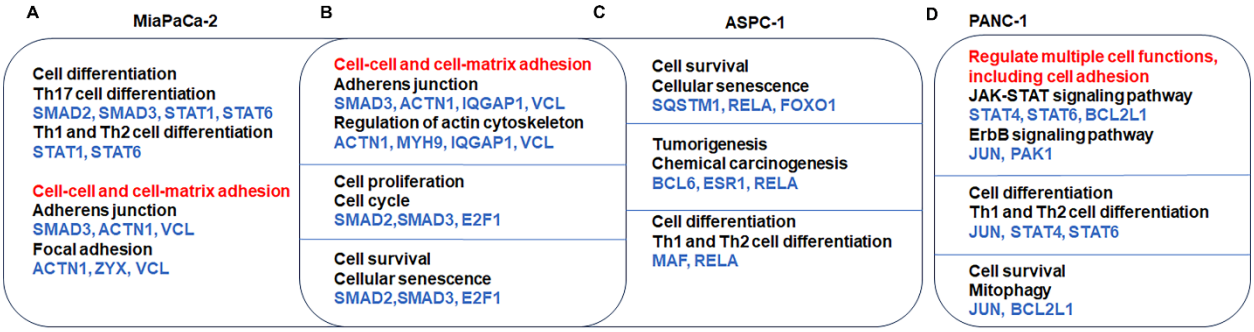

Figure 6.9 Pathways regulating CMG2 positively correlated genes. Pathways were shortlisted for their possible involvement in the regulation of the CMG2 positively correlated genes in MiaPaCa-2 (A), both MiaPaCa-2 and ASPC-1 (B), ASPC-1 (C) and PANC-1 (D) cell lines.

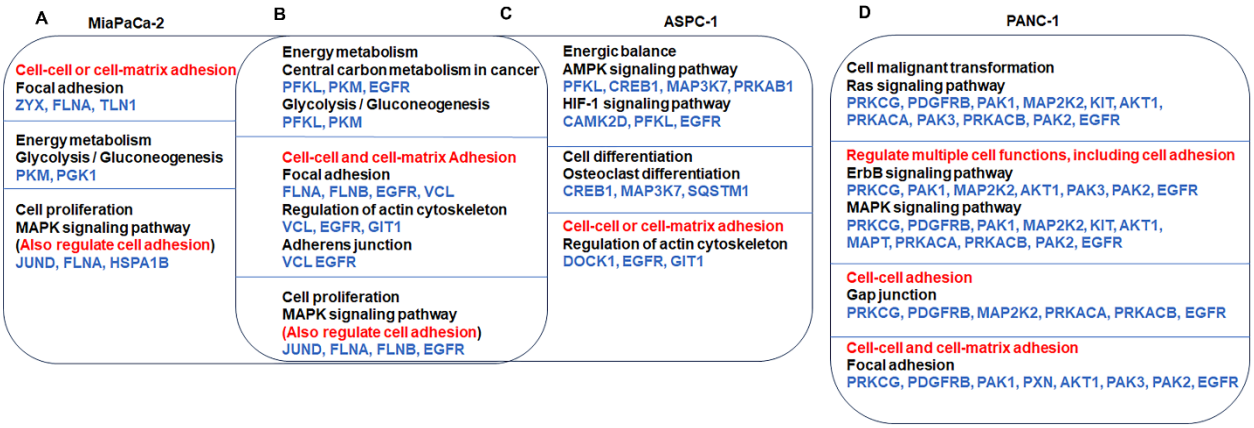

Figure 6.10 Pathways activated by CMG2. Shown are pathways that were shortlisted according to analyses of the top phosphorylated proteins in MiaPaCa-2 (A), both MiaPaCa-2 and ASPC-1 (B), ASPC-1 (C) and PANC-1 (D) cell lines.

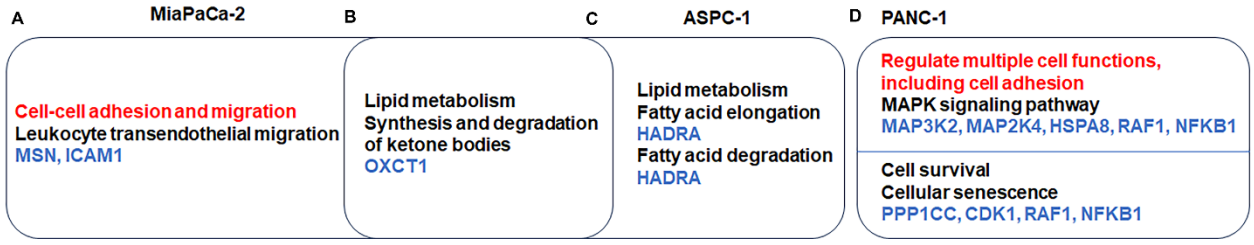

Figure 6.11 Pathways enhanced by proteins with an upregulation of protein only. Shown are pathways which might be enhanced by the upregulated proteins which presented a change

of protein only in MiaPaCa-2 (A), both MiaPaCa-2 and ASPC-1(B), ASPC-1 (C), and PANC-1 (D) cell lines.

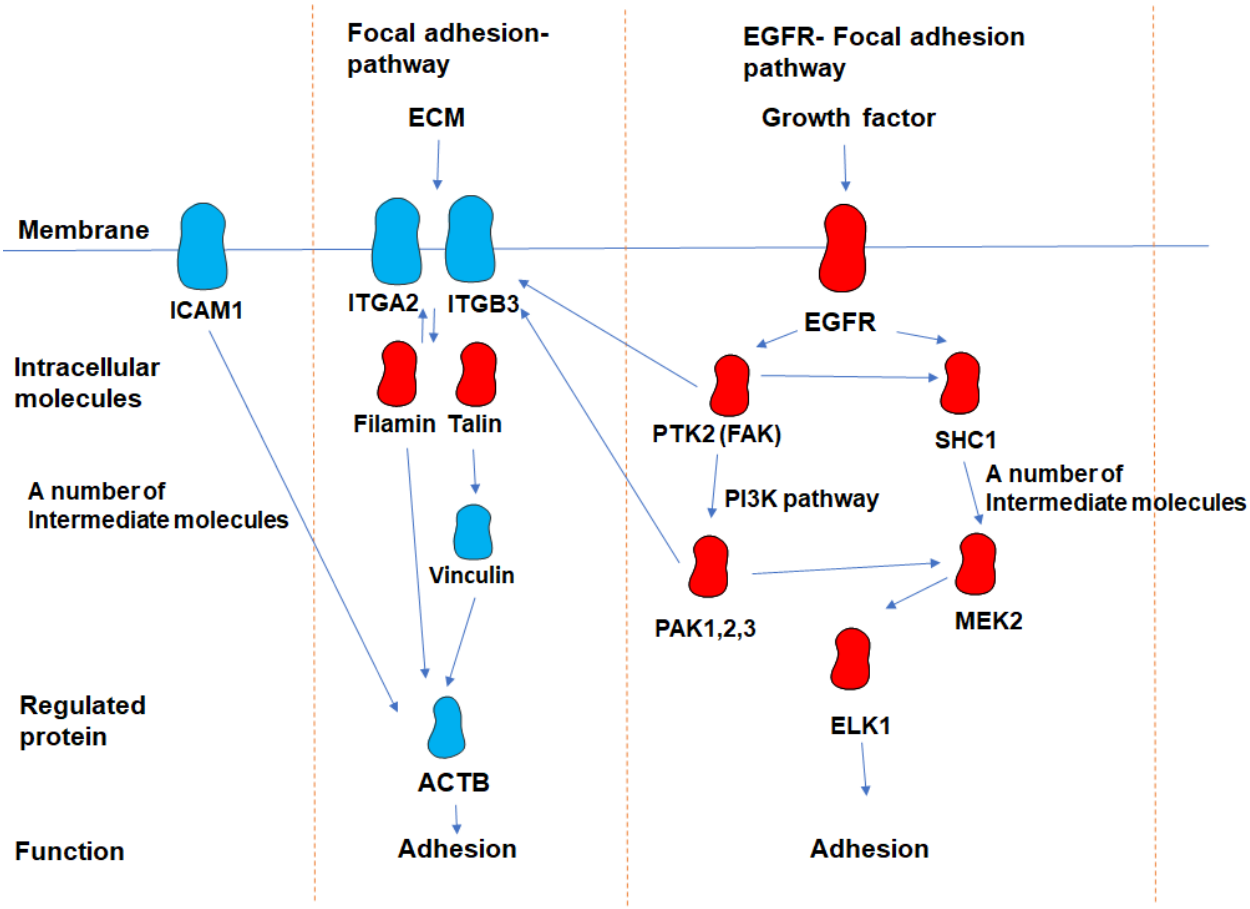

Figure 6.12 Pathways activated by CMG2 can promote cell adhesion. Focal adhesion pathway and EGFR pathway were activated in pancreatic cancer cell lines with higher CMG2 expression.

6.3.5 Pathways and proteins which were inversely correlated with CMG2

There were 2,348 proteins significantly downregulated in the MiaPaCa-2^{CMG2exp} cells in comparison with the pEF control cells ($p<0.05$), in which 112 downregulated proteins presented a ratio of change above 50%. With consideration of the overall abundance and net change, the top 20 downregulated proteins are listed in Supplementary Table 6.6. The mass spectrometric analysis of ASPC^{CMG2shRNA} cells showed that 1,040 proteins were upregulated markedly, in which 93 proteins were increased with a change

in folds greater than 40%, compared with the control group. Similarly, the top 20 upregulated proteins in ASPC-1^{CMG2shRNA} cells were shortlisted according to their overall abundancy and net change (Supplementary Table 6.7).

There were 297 proteins downregulated in the MiaPaCa-2^{CMG2exp} cells that were also upregulated in with ASPC-1^{CMG2shRNA} cells, which were identified to be proteins inversely correlated with CMG2 ($P<0.05$). In those inversely correlated proteins, the top 20 proteins that were downregulated in MiaPaCa-2^{CMG2exp} and upregulated in ASPC-1^{CMG2shRNA} cells were shortlisted according to their abundance and changes for further analysis (Supplementary Table 6.8). Their possible role in CMG2 regulated biological functions in pancreatic cancer was subsequently analysed.

In addition to the mass spectrometric analysis, the Kinuex protein array data of PANC-1^{CMG2rib} cells was also employed, to explore activities of a panel of pathways. There were 128 proteins increased following CMG2 knockdown. The top 20 of the upregulated proteins were shortlisted for further analysis (Supplementary Table 6.9).

There were 749 proteins in the MiaPaCa-2^{CMG2exp} cells that presented a decreased level of unadjusted phosphorylation, while in the ASPC-1^{CMG2shRNA} cell line, 192 proteins showed an increase of unadjusted phosphorylation ($P<0.05$). Among these phosphorylated proteins, 111 proteins were inversely correlated with CMG2 in both cell lines. Following justification of the phosphorylation against quantity of the corresponding total protein, 981 proteins had an adjusted decreased phosphorylation in the MiaPaCa-2^{CMG2exp} cell line, while 311 proteins had an increase of the adjusted phosphorylation in the ASPC-1^{CMG2shRNA} cell line ($P<0.05$). There were 167 proteins that exhibited an adjusted phosphorylation, being inversely correlated with CMG2, in both MiaPaCa-2 and ASPC-1 cell lines ($P<0.05$). The top 20 proteins with adjusted or unadjusted phosphorylation were referred as CMG2 inversely correlated phosphorylated proteins (Supplementary table 6.10). The phosphorylation of 222 proteins was determined in the PANC-1^{CMG2rib} cells using the Kinexus assay, 93 proteins showed an increase of phosphorylation, and the top 20 are shown in Supplementary Table 6.12.

Subsequent ontology analysis did not show any involvement of the shortlisted CMG2 inversely correlated proteins and phosphorylated proteins, in the regulation of cell adhesion.

6.3.6 Verification of CMG2 correlated proteins and pathways

The results indicated that the EGFR pathway and focal adhesion were activated in pancreatic cancer cell lines, with higher CMG2 expression. Western blot and QPCR were carried out for further verification of their expression and phosphorylation. PTK2, also known as FAK (Focal adhesion kinase), was increased in MiaPaCa-2^{CMG2exp} cells compared with the pEF control, while phosphorylated PTK2 was decreased in both PANC-1 and ASPC-1 cells, following the knockdown of CMG2. EGFR expression was decreased in PANC-1^{CMG2rib} and ASPC-1^{CMG2shRNA} cells. The phosphorylation state of EGFR at tyrosine residues appeared to be positively correlated with the expression of CMG2 PANC-1 and ASPC-1 cell lines. Shc, MEK2 and ELK1 are three downstream proteins of EGFR. The phosphorylation of shc was also positively correlated with CMG2 in MiaPaCa-2, PANC-1 and ASPC-1 cell lines. Similarly, phosphorylation of MEK2 was increased in MiaPaCa-2^{CMG2exp} cells and was decreased in ASPC-1^{CMG2shRNA} cells, while little change was seen in PANC-1^{CMG2rib} cells. Increased phosphorylation of ELK1 was seen in MiaPaCa-2^{CMG2exp} cells while a decreased phosphorylation was observed in ASPC-1^{CMG2shRNA} cells. Vinculin (VCL) is a protein which is involved in focal adhesion. A reduction in VCL protein was seen in both PANC1 and ASPC cells following the knockdown of CMG2, but no obvious change was presented in the MiaPaCa-2^{CMG2exp} cells (Figure 6.13A). ICAM-1 is a protein that mediates cell-cell interaction. Its expression was also determined in MiaPaCa-2 cells which showed an increase of ICAM-1 protein in MiaPaCa-2^{CMG2exp} cells (Figure 6.13B). QPCR was employed to determine the transcript level of the candidate ITGs. Both ITGA2 and ITGA3 were upregulated in MiaPaCa2^{CMG2exp} cells and downregulated in ASPC-1^{CMG2shRNA} Cells, while a reduce expression of ITGA2 but not ITGB3 was also seen in PANC1^{CMG2rib} cells (Figure 6.13C and D).

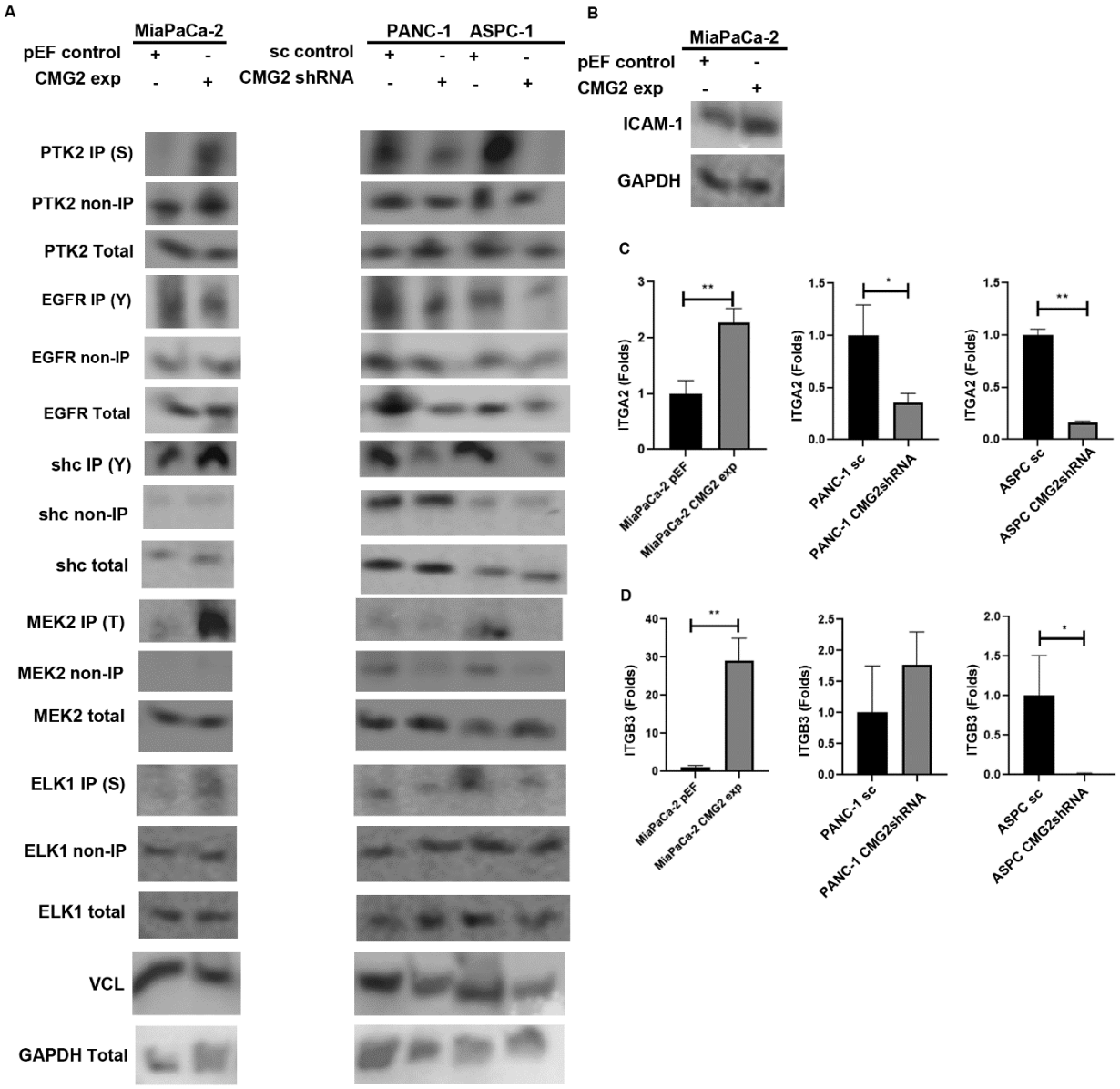

Figure 6.13 Verification of identified candidate proteins underlying CMG2 regulated cellular functions. (A) Shown are protein expression and phosphorylation in MiaPaCa-2, PANC-1 and ASPC-1 cell lines using Western blot and immunoprecipitation (IP) of proteins, with phosphorylated serine (S), phosphorylated Tyrosine (Y) and phosphorylated threonine (T). (B) Cell-cell interaction molecule ICAM was determined in MiaPaCa-2 cells using Western blot. (C) Transcripts of ITGA2 (C) and ITGB3 (D) were determined in the MiaPaCa-2, PANC-1 and ASPC-1 cell models, respectively.

6.4 Discussion

It has been demonstrated, in previous Chapters, that CMG2 can promote cell-matrix adhesion, cell-cell adhesion and cell-HA interaction, in pancreatic cancer cells. Overexpression of CMG2 promoted aggregation of MiaPaCa-2 cells, while knockdown of CMG2 impaired cell-matrix and adhesion to mesothelial cells, in both PANC-1 and ASPC-1 cells. In this Chapter, proteomic analyses revealed the top CMG2 upregulated proteins in MiaPaCa-2 cells are mainly associated with cell-matrix adhesion and cell-cell adhesion, most of the leading reduced proteins in ASPC-1 CMG2 knockdown cells are involved in cell-matrix adhesion. These altered proteins, and their biological functions, provide supportive evidence for the molecular mechanism underlying CMG2 promoted adhesion in pancreatic cancer cells, although further validation is yet to be carried out. Interestingly, an upregulation of cell-matrix adhesion associated proteins was also seen in MiaPaCa-2 CMG2 overexpression cells, though little effect was observed in their adhesion to both matrix and mesothelial cells. This might be due to the strong adhesiveness exhibited by the MiaPaCa-2 cells, which was unlikely to be further enhanced by CMG2 overexpression, in comparison with the other two pancreatic cancer cell lines. Furthermore, analyses of phosphorylated proteins and activated pathways also demonstrated a promotion of cell-cell adhesion and cell-matrix adhesion by CMG2 in the pancreatic cancer cells, in which, EGFR and focal adhesion pathways were mostly commonly seen in the pancreatic cancer cell line models examined.

EGFR (ERBB1) is a receptor tyrosine kinase (RTK), which belongs to the ERBB family (Lemmon and Schlessinger 2010). EGFR expression can induce cell transformation (Velu et al. 1987). Overexpression and hyperactivation of EGFR in malignant tumours is associated with poor survival (Nicholson et al. 2001; Kim et al. 2002; Kopp et al. 2003; Arteaga and Engelman 2014). EGFR can initiate downstream signalling to regulate various cellular functions, such as cell adhesion. EGFR activation can regulate focal adhesion (Rao et al. 2020). In proteomic analysis results, PTK2, SHC1, PAK1, PAK2, PAK3, MEK2 and ELK1 were activated in pancreatic cancer cell lines with higher CMG2 expression. All these proteins are the downstream molecules of EGFR signalling and are involved in focal adhesion.

Adhesion is essential for the interaction of cancer cells with the ECM and

invasion. Focal adhesion can mediate the interaction between the plasma membrane and the extracellular matrix (Kopp et al. 2003). PTK2 is a tyrosine kinase that is located at focal adhesions (Webb et al. 2004). FAK can interact with integrins and further regulate cell adhesion (Hynes and Lane 2005). It can be activated by different receptor tyrosine kinases, including EGFR, Met, RET and VEGFR (Sieg et al. 2000; Chen and Chen 2006; Garces et al. 2006; Plaza-Menacho et al. 2011). In the present study, PTK2 was also found to be activated by CMG2 in pancreatic cancer cells, while a reduced serine phosphorylation of FAK was seen in both PANC1 and ASPC-1, following the knockdown of CMG2. PTK2 plays an important role in tissue regeneration and wound healing (Ashton et al. 2010; Ransom et al. 2018; D'Onofrio et al. 2019). In the present study, phosphorylation of EGFR was shown to be positively correlated with CMG2 and CMG2 upregulated ITGA2 and ITGB3, in pancreatic cancer cells. This suggests that FAK, EGFR and the integrins are involved in CMG2 enhanced cell-matrix adhesion, which can be further validated using specific inhibitors targeting these molecules.

PAKs are a group of proteins which can be activated through the FAK-RAC-PAK pathway (Jia et al. 2021). As an effector of RAC, the PAK family plays an important role in promoting turnover of integrin-mediated adhesion (Rane and Minden 2014). Furthermore, PAK1/2 was found to be activated by activated EGFR and Rac1 in PDAC (Lee and Commisso 2020). In the current study, it was shown that the phosphorylation of PAK1, 2 and 3 were positively associated with the expression of CMG2, which added further evidence for the involvement of integrins in CMG2 enhanced adhesion.

SHC protein was another molecule whose phosphorylation state was positively correlated with CMG2. SHC is a protein which can be activated by EGFR (Pinkas-Kramarski et al. 1996). Activated SHC further activates the MAPK pathway (Jozefiak et al. 2021), which was found to be activated in the CMG2 high-expression pancreatic cancer cell lines in the present study. MEK2 can be activated by PAK (Sicard et al. 2011) and SHC (Xie et al. 2021), which are located downstream of the EGFR/MAPK pathways. Activated MEK2 can further activate ELK1 through ERK (Pinkas-Kramarski et al. 1996). The Western blot results showed that the phosphorylation of SHC, MEK2, and ELK1 were positively correlated with CMG2 in pancreatic cancer cells. ELK1 is a transcription factor that is vital in regulating cell proliferation, apoptosis and glucose homeostasis

(Thiel et al. 2021). A recent study also showed that ELK1 is also implicated in cell adhesion in colorectal cancer (Ma et al. 2021). The evidence further highlights the involvement of EGFR signalling in CMG2 coordinated cellular behaviours in pancreatic cancer, which provokes further investigation for their prognostic and therapeutic potential.

ITGB3 and ITGA2 are involved in focal adhesion, even though they were not ranked in the top 20 CMG2 positively correlated proteins, as seen in the proteomic analysis. The expression of both proteins and transcripts were positively correlated with CMG2 in pancreatic cancer cells. Higher Integrins can enhance cell-cell and cell-matrix adhesion (Gahmberg and Gronholm 2022). Filamin A (FLNA) can regulate cell adhesion, separation and motility (Sampson et al. 2003; Feng and Walsh 2004; Popowicz et al. 2006). Filamin promotes the vimentin-mediated integrin recycling and cell adhesion (Kim et al. 2010a; Kim et al. 2010b). On the other hand, FLNA can interact with the integrins directly, which promotes integrin clustering and cell adhesion (Ithychanda et al. 2009). FLNA contains an actin binding domain, mediating an interaction with actin, to regulate the cytoskeleton and cell adhesion (Vinogradova et al. 2002; Garcia-Alvarez et al. 2003; Debiec et al. 2014; Ye et al. 2014a). In the focal adhesion, Filamin competes with the Talin, which is an activator of integrins (Calderwood et al. 2001; Kiema et al. 2006). Talin itself does not interact with the actin but can activate vinculin (Kelley et al. 2020). Activated Talin and vinculin cooperate to recruit actin to the cell membrane, to promote cell adhesion (Kelley et al. 2020). In this study, in addition to the upregulated integrins, phosphorylation of FLNA and Talin were also upregulated by CMG2 in the pancreatic cancer cells, leading to promotion of cell adhesion.

ICAM1 (Intercellular adhesion molecule 1) was upregulated in the MiaPaCa-2^{CMG2exp} cells but only at the protein level, suggesting a profound role of ICAM-1 in CMG2 enhanced cell-cell adhesion of MiaPaCa-2 cells. ICAMs are a group of cell glycoproteins located on the cell membrane, which are associated with the immune and is usually upregulated when inflammation occurs (Hubbard and Rothlein 2000). ICAM1 is expressed in nearly all tumour microenvironments of different cancers (Benedicto et al. 2017). In lung adenocarcinoma, ICAM1 is overexpressed in adjacent epithelial cells, fibroblast and pulmonary lymphocytes (Passlick et al. 1994; Passlick et al. 1996; Jiang

et al. 1998). ICAM-1 is also increased in tumour-associated macrophages (Zhang et al. 2014; Yang et al. 2015b) and is upregulated in primary tumours with distant metastasis (Rosette et al. 2005; Sokeland and Schumacher 2019). ICAM is a protein which can mediate cell-cell adhesion, especially in leukocytes (Wee et al. 2009). ICAM can interact with the actin cytoskeleton, which can be promoted by SHC (Gardiner and D'Souza 1999). Higher ICAM-1 was also found in tumours with a more aggressive phenotype. In breast cancer ICAM-1 expression is higher in the triple-negative subtype compared with other subtypes (Guo et al. 2014). An elevated expression of ICAM-1 is also evident in non-small cell lung carcinoma (Schardt et al. 1993; Melis et al. 1996). For distant metastasis, survival of circulating tumour cells (CTCs) plays an important role for the dissemination of CTCs (Strilic and Offermanns 2017; Kim et al. 2018; Wang et al. 2018; Gkountela et al. 2019). ICAM-1 can promote aggregation and clustering of the CTCs to assist them for an evasion from apoptosis (Gkountela et al. 2019; Saini et al. 2019; Szczerba et al. 2019). However, its implication in CMG2 coordinated survival and *anoikis* in pancreatic cancer cells is yet to be elucidated. Furthermore, ICAM-1 is also implicated in the “seed and soil” progress of CTC homing to secondary organs, which can promote cancer cells adhering to endothelial cells (Ghislin et al. 2012; Zhang et al. 2014). The role of ICAM-1 in CMG2 related distant metastasis warrants an important area for further exploration.

Taking together, upregulation of the EGFR/MAPK pathway and enhanced integrin mediated focal adhesion were seen in the pancreatic cancer cells, with higher expression of CMG2. These two pathways may play a central role in the enhanced cell-cell adhesion and cell-matrix adhesion which warrants further investigation.

Chapter 7

A further analysis of molecular machinery underlying CMG2 regulated cell adhesion

7.1 Introduction

Previous Chapters have shown that CMG2 can enhance adhesion, aggregation and survival of pancreatic cancer cells, which can promote disease progression and peritoneal metastasis (Table 7.1). In Chapter 6, only the top pathways and molecules were evaluated in which a number of molecules, being pivotal for cell-cell adhesion, cell-matrix adhesion and cell-hyaluronic acid interaction, were almost excluded.

Table 7.1 Summary of cell functions affected by CMG2 expression

Clinical tumour cohort	CMG2 function
TCGA	Higher CMG2 expression is associated with distant metastasis
GSE71729	Increase in pancreatic cancer, positively associated with distant metastasis
GSE15471	Increase in pancreatic cancer
GSE19650	Elevated CMG2 is possibly associated with tumourigenesis
Beijing Cohort	Increase in pancreatic cancer
Cell lines	
MiaPaCa-2	Enhanced cell aggregation and survival during the suspending culture
PANC-1	Increased viability of the suspended cells, promoted cell-matrix adhesion, cancer cell-mesothelial cell adhesion, mediated the interaction between cell and hyaluronic acid
ASPC-1	Promoted cell-matrix adhesion, adhesin to mesothelial cells

The Integrin family includes 24 transmembrane heterodimers, which are formed by the combination of 18α and 8β subunits (Barczyk et al. 2010). The same ligand binding with different integrins can trigger different signal pathways in the cell, thus the expression of different integrins has been implicated in the response of cancer cells to the extracellular microenvironment, including dynamic remodelling of adhesions, migration, invasion and cytokinesis (De Franceschi et al. 2015).

Cadherins are a group of transmembrane proteins which mediate both the cell-matrix and cell-cell adhesion. Classical cadherins include E-cadherin, N-cadherin and P-cadherin (Colas-Algora and Millan 2019). Cadherins can interact with cadherins on adjacent cells, forming adherent junctions (AJs) (Grigorian et al. 2015). In normal tissue, cadherins are profound in maintaining cellular polarity and tissue integrity (Sousa et al. 2019). Mutation and blocking of cadherins can lead to tumourigenesis (Baranwal and Alahari 2009; Roggiani et al. 2016; Bruner and Derksen 2018; Dalle Vedove et al. 2019).

Previous results have also shown that CMG2 can promote pancreatic cancer cell aggregation and adhesion to MET5A cells. In Chapter 6, ICAM-1 was shortlisted as an adhesion molecule being involved in CMG2 enhanced cell-cell adhesion. In addition to ICAM-1, the ICAM family is also comprised of ICAM-2 (Intercellular Adhesion Molecule 2) and ICAM-3 (Intercellular Adhesion Molecule 3) (Sansom et al. 1991; Bossy et al. 1994). Tight junctions and gap junctions are classical cell-cell adhesions. Tight junctions are composed of claudins (CLDNs), and its structure can be regulated by tight junction proteins (TJPs) (Otani and Furuse 2020). Gap junctions are intercellular structures that mediate cell-cell adhesion, communication and transportation. Connexins, also called gap junction proteins, are a proteins family comprising 21 different members with a similar structure (Laird 2006; Esseltine and Laird 2016). The GAP junction between cells can enhance intracellular communication by promoting molecule exchange between two cells (Totland et al. 2020).

Furthermore, HA was implicated in peritoneal adhesion, mediated by CMG2 in PANC-1 cells. During peritoneal metastasis, the HA film, produced by the mesothelial cells. lt forms a barrier to prevent the adhesion of cancer cells to mesothelial cells (Knudson et al. 1995; Evanko et al. 2007). A number of HA interacting molecules have been implicated in progression of malignant tumours, including CD44, LYVE, VCAN (Versican), HAPLNs (Hyaluronic Acid Link Proteins) and HABPs (Hyaluronan Binding Protein) (Jackson et al. 2001; Jadin et al. 2014; Weidle et al. 2016; Watanabe 2022). HAPLN1 may promote peritoneal metastasis in pancreatic cancer (Jadin et al. 2014). In addition to cell-cell adhesion, ICAM-1 is also a HA interacting molecule (McCourt et al. 1994).

To further dissect the molecular mechanism underlying CMG2 coordinated cell-matrix, cell-cell adhesion and interaction with HA, a more comprehensive and inclusive analysis was carried out, by focusing on these adhesion molecules and HA interacting molecules.

7.2 Materials and methodology

7.2.1 Public datasets

Three public datasets were analysed: The Cancer Genome Atlas (TCGA)

(http://firebrowse.org/), GSE71729 (Moffitt et al. 2015) and E-MTAB-2770 (Ghandi et al. 2019). More details can be found in section 2.9. Correlation between CMG2 and other molecules, regulating cell-cell adhesion, cell-matrix adhesion and cell-hyaluronic adhesion, were analysed.

7.2.2 Cell adhesion proteins in pancreatic cancer cell lines

The adhesion proteins were also analysed using the proteomic data derived from the MiaPaCa-2, ASPC-1 and PANC-1 cell line models as described in section 6.2.

7.2.3 RNA extraction, reverse transcription, PCR and quantitative PCR

Transcripts of adhesion molecules were determined using both conventional PCR and QPCR, following previously described procedures (described in section 2.4). Sequences of primers used were provided in section 2.1.2.

7.2.4 Western blot

Western blot was applied to determine CD44 (AB1N135705, 1:1000 dilution) and GAPDH (SC 32233,1:4000 dilution) with a secondary antibody (anti-Mouse antibody, A9044, 1:1000 dilution) following the protocol described in section 2.5.1.

7.2.5 Statistical analysis

T-tests were used for comparisons between two groups if they were normally distributed, Mann-Whitney u test was used for the analysis of non-normally distributed data. Spearman test was used for correlation analyses using SPSS (Version 26, IBM UK Ltd.).

7.3 Results

7.3.1 Influence of CMG2 on cell-matrix adhesion molecules

In the previous Chapters, it was shown that elevated expression of CMG2 is associated with distant metastases, with CMG2 enhancing cell adhesion. In the clinical dataset TCGA, the expression of integrins and cadherins were analysed in the primary tumours, with different expression of CMG2, with a cut off value of 24, followed by verification in

the GSE71729 cohort (Cut off=4.113). Cadherins and integrins of which expression are significantly increased either TCGA or GSE71729 cohort were shown in Table 7.2. ITGA2, ITGB4, ITGA6 and ITGA3 presented an obvious increase (Ratio>1.5, absolute change>3000) in pancreatic tumours, with a higher expression of CMG2. Many cell-matrix adhesion molecules exhibited a positive correlation with CMG2, in both TCGA and GSE71729 datasets, while CDH10 (Cadherin 10) and CDH22 (Cadherin 22) were inversely correlated with CMG2 (Figure 7.1). There was no significant difference observed for the expression of ITGA2, ITGB4, ITGA6 and ITGA3 in a panel of pancreatic cancer cell lines, with regard to their expression of CMG2, according to analysis of the E-MTAB-2770 data (Figure 7.2).

The expression of these four ITGs in MiaPaCa-2, PANC-1 and ASPC-1 cell lines were also assessed in E-MTAB-2770 data. ASPC-1 cells exhibited relatively higher expression of ITGB4, while ITGA3 was relatively higher in PANC-1 cells (Supplementary Figure 7.1). Both PANC-1 and ASPC-1 cells presented a higher expression of ITGB1 compared with MiaPaCa-2 cells (Supplementary Figure 7.1). ITGA6 was detectable in the three cell lines (Supplementary Figure 7.1). ITGB2, ITGB3, CDH1 and ITGB4 were reduced significantly in ASPC-1^{CMG2shRNA} cell line, whilst increased ITGB3, ITGAV and ITGA5 were seen in MiaPaCa-2^{CMG2exp} cells (Table 7.3). In Chapter 6, the influence of CMG2 on ITGB3 and ITGA2 was already verified (Figure 6.13). ITGB3 is upregulated in MiaPaCa-2^{CMG2exp} cells and down-regulated in ASPC-1^{CMG2shRNA} cells. ITGA2 was shown to be increased in pancreatic cancer cell lines with higher CMG2 expression. CDH1 was decreased by around 10% in ASPC-1^{CMG2shRNA}, cells which appeared to be difficult to further validate.

Table 7.2 Cell-substrate adhesion molecules in pancreatic tumours with different CMG2 expression.

Gene name	CMG2 (Low) Median (IQR)	CMG2 (High) Median (IQR)	Ratio	*P*
TCGA				
ITGA2	1976.14 (1263.09~3033.81)	3987.06 (2707.75~5225.87)	2.02	0
ITGB4	8526.8 (4547.59~13452.38)	15035.17(8962.96~18449.48)	1.76	0
ITGA6	4573.31 (3414.34~6711.75)	7709.06(5977.23~9724.91)	1.69	0
ITGA3	6896.11 (3851.3~12854.07)	10960.31(8128.85~16050.95)	1.59	0
ITGB6	3401.65 (2331.42~5433.87)	5376.58(3142.25~9567.05)	1.58	0
CDH3	1828.26 (957.57~2908.2)	2579(1636.54~3726.72)	1.41	0.01
CDH1	8132.62 (6196.09~10321.08)	11179.36(8906.18~13082.82)	1.37	0
ITGB5	5820.56 (4472.3~7790.63)	7670.46(6095.84~10327.09)	1.32	0
ITGB1	18658.17(13408.61~23354.9)	21964.77(17294.61~30539.49)	1.18	0
GSE71729				
ITGB6	6.11(3.73~10.77)	10.22(5.48~15.86)	1.67	0
CDH3	86.86(46.92~149.26)	136.43(64.43~218.73)	1.57	0.01
ITGA2	7.69(4.83~12.37)	11.63(7.62~17.14)	1.51	0
ITGA3	24.13(15.13~40.62)	34.58(20.84~52.66)	1.43	0.02
ITGB5	75.95(46.94~122.17)	104.98(74.84~126.41)	1.38	0.02
ITGA6	136.19(89.39~196.58)	178.03(121.19~253)	1.31	0.03
ITGB4	75.85(43.1~124.05)	98.7(58.02~146.73)	1.3	0.17
ITGB1	105.6(60.51~152.75)	130.69(91.11~174.14)	1.24	0.03
CDH1	409.3(252.26~587.63)	379.51(220.95~576.04)	0.93	0.53

Note: Shown are original values, which are converted from log2 values in TCGA and GSE71729 cohort.

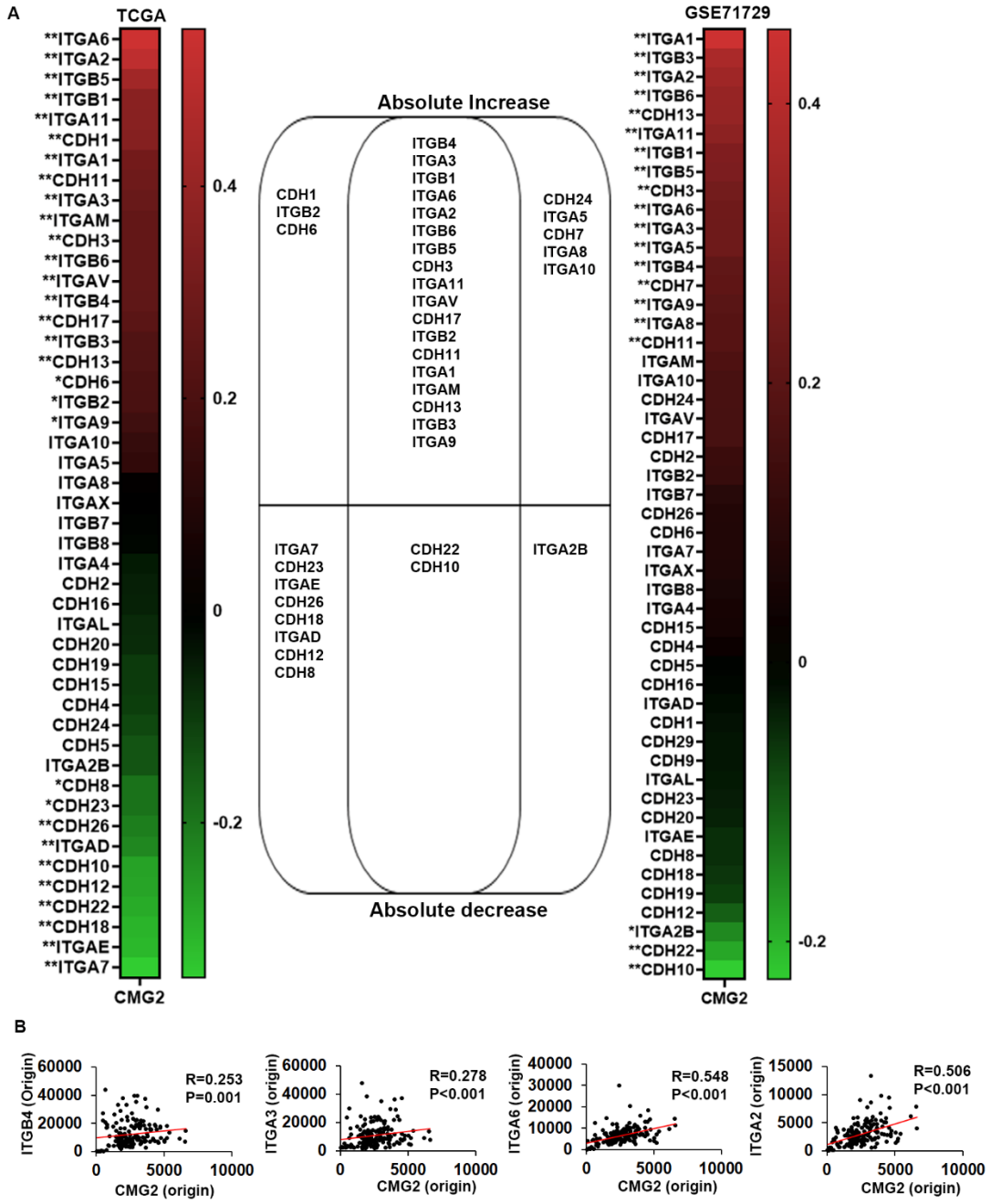

Figure 7.1 Association between cell-matrix adhesion molecules and CMG2 in pancreatic cancer. (A) Heatmap show the correlation between cell-matrix adhesion molecules and CMG2 in pancreatic cancer cohort TCGA and GSE71729. (B) Scatter plots illustrate the correlations between CMG2 and cell-matrix adhesion genes in the TCGA cohort, which presented an absolute change greater than 2000 (expression value) and a change in folds greater than 1.5. Shown are the original value converted from log2 value in TCGA cohort. ** indicates P<0.01, * indicates P<0.05.

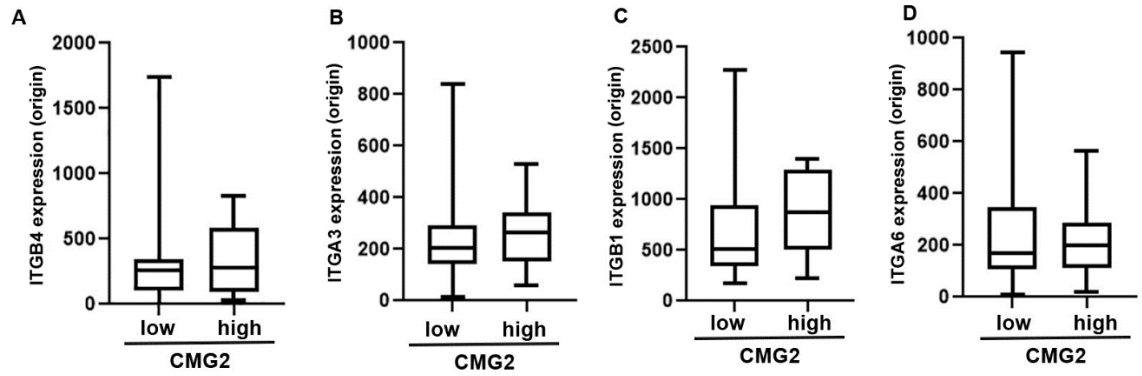

Figure 7.2 Cell-matrix adhesion genes expression in pancreatic cancer cell lines with different CMG2 expression. The expression levels of ITGB4 (A), ITGA3 (B), ITGB1 (C) and ITGA6 (D) in pancreatic cancer cell lines with CMG2 low expression and high expression (CMG2 cut off value = 24), were analysed using the E-MTAB-2770 data (Ghandi et al. 2019).

Table 7.3 Cell-substrate adhesion proteins in pancreatic cancer cell lines with manipulated CMG2 expression.

Gene name	Mean ± SD	Mean ± SD	Ratio	*P*
ASPC-1	SC	CMG2 shRNA		
ITGB2	158.27 ± 4.57	107.37 ± 8.42	0.68	0.01
ITGB3	252.7 ± 24.05	212.57 ± 7.63	0.84	0.12
CDH1	1037.17 ± 12.58	937.83 ± 29.89	0.9	0.03
ITGB4	6446.57 ± 81.9	5883.43 ± 66.01	0.91	0
MiaPaCa-2	pEF	CMG2 exp		
ITGB3	1027.43 ± 19.6	1794.57 ± 59.78	1.75	0
ITGAV	2673.1 ± 32.37	3301.03 ± 36.25	1.23	0
ITGA5	184.93 ± 2.24	273.57 ± 5.27	1.48	0

Note: Shown are the original value from proteomics.

7.3.2 Influence of CMG2 on cell-cell adhesion molecules

CMG2 not only promoted cell-adhesion but also enhanced pancreatic cancer homotypic aggregation and the adhesion to mesothelial cells. Some cell-cell adhesion molecules were found to be positively correlated with CMG2, in both TCGA and GSE71729, including CLDN18, CLDN4, GJB2, TJP2, GJB3, CLDN12, CLDN23 and GJC2 (Figure 7.3 A and B). Cell-cell adhesion molecules of which expression are significantly

increased in either TCGA or GSE71729 cohort were shown in Table7.4. CLDN18, CLDN4, GJB2 and TJP2 presented a marked increase in tumours with higher expression of CMG2 in the TCGA cohort, with a change of expression value greater than 600 (Table 7.4). Transcript levels of the four genes were not significantly associated with CMG2 in pancreatic cancer cell lines, according to analysis of the E-MTAB-2770 data (Figure 7.4).

CLDN18, GLDN4, GJB2 and TJP2 expression were evaluated individually in MiaPaCa-2, PANC-1 and ASPC-1 cell lines in the E-MTAB-2770 cohort. The expression of CLDN18 and GJB2 were barely detectable in the three cell lines (Supplementary Figure 7.2). CLDN4 was highly expressed in the ASPC-1 cells, whilst TJP2 was highly expressed in both ASPC-1 and PANC-1 cells but not MiaPaCa-2 cells (Supplementary Figure 7.2).

CLDN7 and ICAM1 protein expression were decreased in ASPC-1^{CMG2shRNA} cells, while ICAM1, TJP1 and CLDN1 were increased in MiaPaCa-2^{CMG2exp} cells CMG2 (Table 7.5).

Upregulation of ICAM-1 has already been demonstrated in MiaPaCa-2^{CMG2exp} cells, as outlined in Chapter 6 (Figure 6.12). The absolute change or change ratio of CLDN1, CLDN7 and TJP1 were too low in MiaPaCa-2 and ASPC-1 cells (Table 7.5), being hard to trigger a further evaluation. TJP2 (ZO-2) and CLDN4 were two genes that presented an increase in pancreatic tumours with higher expression of CMG2.

Table 7.4 Cell-cell adhesion molecules in pancreatic tumours with different expression of CMG2.

Gene name	CMG2 (Low) Median (IQR)	CMG2 (High) Median (IQR)	Ratio	*P*
TCGA				
CLDN18	2261.05 (233.42~9293.02)	7536.88 (1981.34~18891.8)	3.33	0
GJB2	1213.71 (704.07~2394.83)	2293.65 (1272.3~3264.35)	1.89	0.01
GJB3	670.25 (445.2~1299.81)	1170.39 (878.89~1650.75)	1.75	0
TJP3	1013.7 (524.21~1531.59)	1530.28 (798.87~2473.93)	1.51	0
CLDN4	7697.26 (4199~12901.6)	11417.8 (8407.44~17927.8)	1.48	0
TJP2	2250.58 (1706.6~2723.73)	3080.36 (2460.05~3721.76)	1.37	0
GSE71729				
GJB2	30.36 (14.25~61.24)	54.27 (22.71~103.06)	1.79	0
CLDN18	4.66 (2.69~13.69)	6.51(3.41~20.07)	1.4	0.8
CLDN4	14.86 (9.94~24.42)	20.13 (9.25~36.03)	1.35	0.01
TJP2	18.77 (15.15~24.44)	22.58 (19.22~28.08)	1.2	0.1
GJB3	8.06 (5.81~10.93)	9.28 (7.35~11.76)	1.15	0.02
TJP3	6.82 (5.17~9.33)	7.75 (5.9~11.11)	1.14	0.01

Note: Shown are original values, which are converted from log2 values in TCGA and GSE71729 cohort.

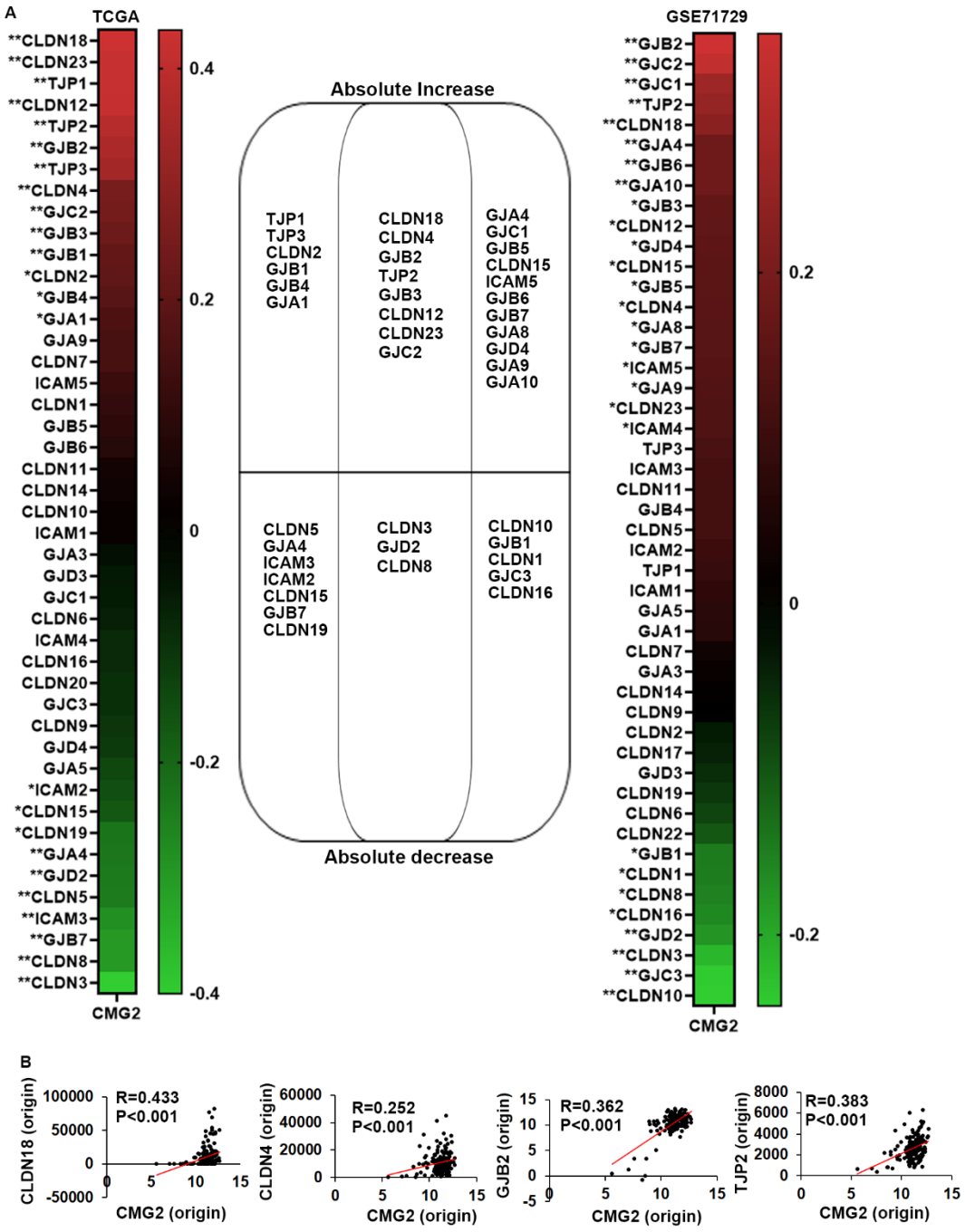

Figure 7.3 Correlation between cell-matrix adhesion molecules and CMG2 in pancreatic cancer. (A) Correlation between cell-cell adhesion molecules and CMG2 was analysed using Spearman test, in both TCGA and GSE71729 cohorts. (B) Correlation between CMG2 and cell-cell adhesion genes, that presented an increase of the expression value greater than 800 and a change ratio greater than 1.3, are shown in the scatter plots. Shown are the original value converted from log2 value in TCGA cohort. ** indicates P<0.01, * indicates P<0.05.

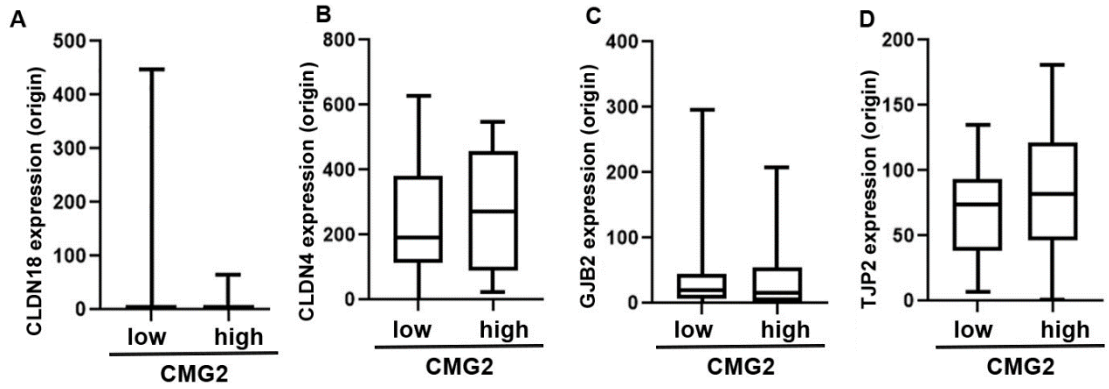

Figure 7.4 Cell-cell adhesion genes expression in pancreatic cancer cell lines with different CMG2 expression. The expression level of CLDN18 (A), CLDN4 (B), GJB2 (C) and TJP2 (D) in pancreatic cancer cell lines with CMG2 low expression and high expression (CMG2 cut off value: 24) in the E-MTAB-2770 cohort (Ghandi et al. 2019).

Table 7.5 Cell-cell adhesion proteins in pancreatic cancer cell lines with CMG2 overexpression or knockdown

Gene name	Mean ± SD	Mean ± SD	Ratio	P value
ASPC-1	SC	CMG2 shRNA		
CLDN7	108.37 ± 8.73	92.27 ± 9.53	0.85	0.16
ICAM1	226.87 ± 17.38	207.5 ± 25.1	0.91	0.41
MiaPaCa-2	pEF	CMG2 exp		
ICAM1	2467.93 ± 50.95	4825.1 ± 113.56	1.96	0
TJP2	1726.57 ± 28.66	2404.37 ± 7.85	1.39	0
TJP1	2069.27 ± 8.36	2189.5 ± 42.15	1.06	0.05
CLDN1	79.9 ± 2.15	123.9 ± 5.82	1.55	0

Note: Shown are the original value from proteomics.

7.3.3 CMG2 and HA interacting molecules

In the TCGA cohort, VCAN and CD44 transcripts were significantly higher in the tumours with higher CMG2 expression. In the GSE71729 cohort, only VCAN was positively correlated with CMG2, while CD44 presented a subtle increase in tumours with high expression of CMG2. Elevated expression of the HA interacting molecules was seen in at least one of the two cohorts assessed Table 7.6. VCAN was positively correlated with CMG2 in both pancreatic cancer cohorts (Figure 7.5 A, B). VCAN exhibited a low expression in most pancreatic cancer cell lines, with little difference seen in the cell lines with a higher expression of CMG2 (Figure 7.6). VCAN expression was relatively higher in ASPC-1 cells in comparison with MiaPaCa-2 and PANC-1 in E-MTAB-2770 cohort (Supplementary figure 7.3).

VCAN protein was reduced in the ASPC-1^{CMG2shRNA}, cells whilst little change was seen in MiaPaCa-2^{CMG2exp} cells in comparison with the corresponding controls. Both CD44 and HABP4 were upregulated in MiaPaCa-2^{CMG2exp} cells (Table 7.7).

Table 7.6 Hyaluronic acid interacting molecules in pancreatic cancer with higher CMG2 in the clinical cohort.

Gene name	CMG2 (Low) Median (IQR)	CMG2 (High) Median (IQR)	Ratio	*P*
TCGA				
VCAN	8826.04(5511.46~15375.59)	11145.1(5824.56~18480.14)	1.26	0.04
CD44	7774.38(5676.54~9497.51)	8980.1(6632.88~11449.84)	1.16	0.03
GSE71729				
VCAN	100.13(41.72~226.77)	164.73(75.35~277.05)	1.65	0.01
CD44	235.65(184.92~330.27)	254.06(187.02~323.36)	1.08	0.55

Note: Shown are original values, which are converted from log2 values in TCGA and GSE71729 cohort.

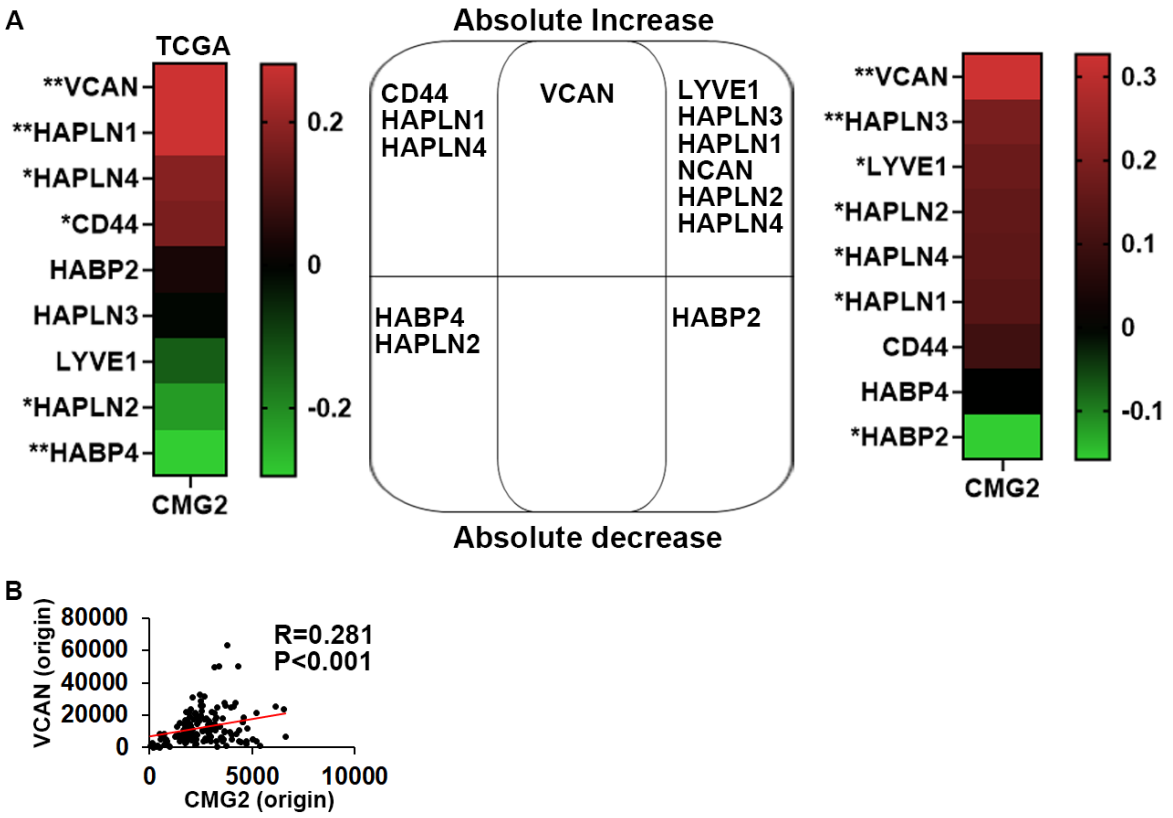

Figure 7.5 Association between HA interacting molecules and CMG2. (A) Correlation between HA interacting molecules and CMG2 in pancreatic cancer were analysed in both TCGA and GSE71729 cohorts using Spearman test. (B) Correlation between CMG2 and VCAN in pancreatic cancer was analysed in the TCGA cohort using Spearman test. Shown are the original value converted from log2 value in TCGA cohort. ** indicate p<0.01, * indicates p<0.05.

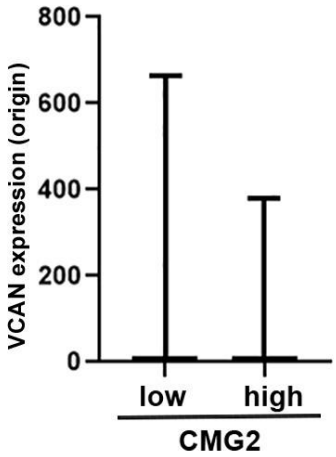

Figure 7.6 HA interacting molecules expression in pancreatic cancer cell lines with different CMG2 expression. The expression level of VCAN in pancreatic cancer cell lines with CMG2 low expression and high expression (CMG2 cut off value = 24) in the E-MTAB-2770 cohort (Ghandi et al. 2019).

Table 7.7 Hyaluronic acid interacting proteins in the pancreatic cancer cell models.

Gene name	Mean ± SD	Mean ± SD	Ratio	P value
ASPC-1	SC	CMG2 shRNA		
VCAN	2343.7 ± 9.72	2077.5 ± 78.63	0.89	0.04
MiaPaCa-2	pEF	CMG2 exp		
CD44	3181.73 ± 33.44	4276.3 ± 50.84	1.34	0
HABP4	265.43 ± 11.85	526.73 ± 49.6	1.98	0.01

Note: Shown are the original value from proteomics.

7.3.5 Verification of candidate genes enhanced by CMG2

The candidate cell-cell adhesion molecules, cell-matrix adhesion molecules and HA interacting molecules were further verified. ITGB1 was decreased in both PANC-1 and ASPC-1 cells following the knockdown of CMG2 (Figure 7.7A). ITGA3 expression was decreased in the PANC-1^{CMG2shRNA} cells, although not being statistically significant (p=0.0502), whilst little change in ITGA3 was seen in ASPC-1^{CMG2shRNA} cells (Figure 7.7B). VCAN was decreased in both PANC-1^{CMG2shRNA} and ASPC-1^{CMG2shRNA} cells (Figure 7.7C). TJP2 (ZO-2) expression appeared to show an increased trend in MiaPaCa-2^{CMG2exp} and reduced PANC-1^{CMG2shRNA} cells but did not reach a statistical significance (Figure 7.7D). CD44 expression was decreased in PANC-1CMG2shRNA cells, whilst CD44 protein was undetectable in the ASPC-1 cells, although CD44 transcripts were detected in the same cell line (Figure 7.7 E and F)

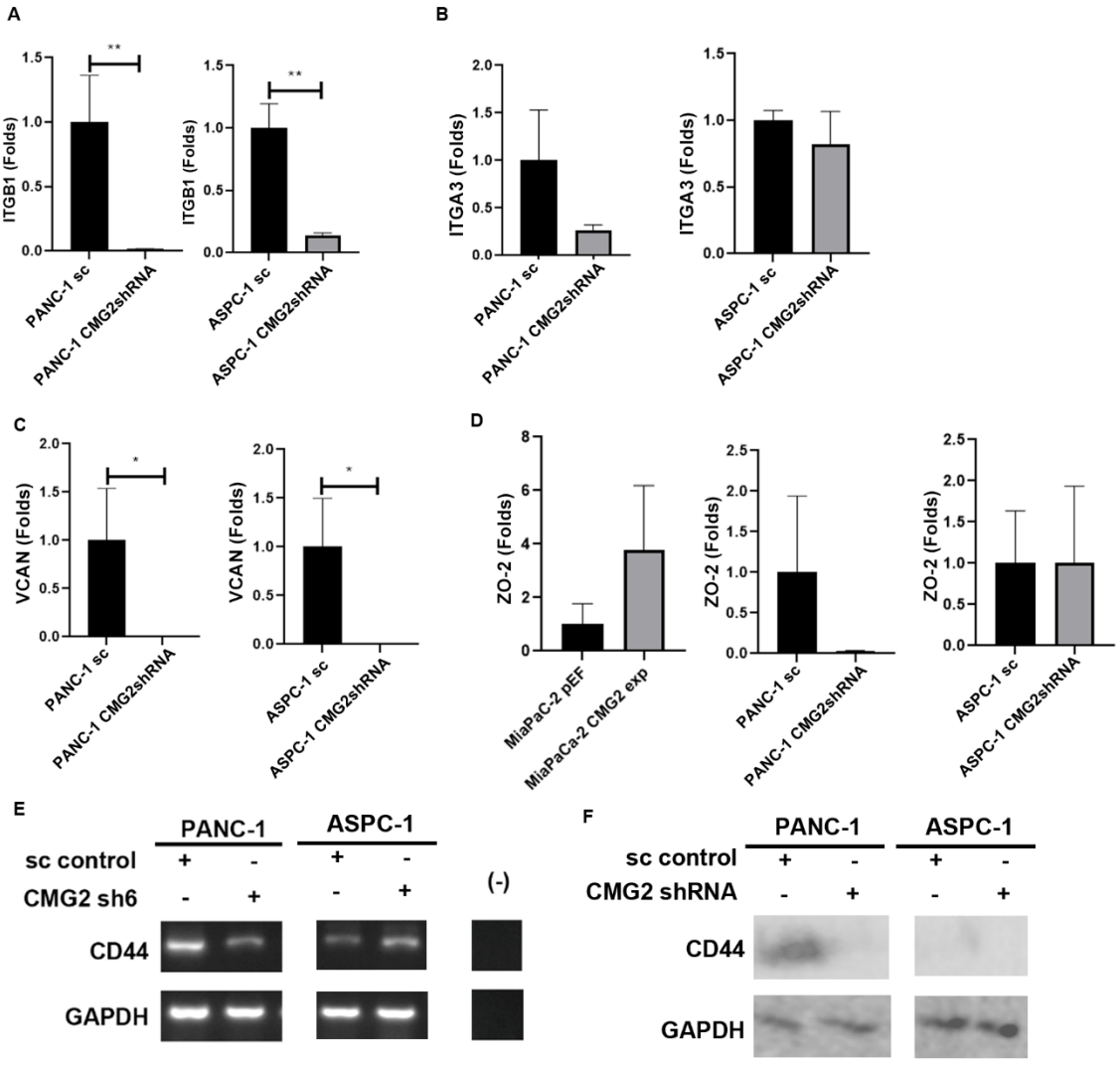

Figure 7.7 Verification of candidate proteins in the cell line models. The expression of ITGB1 (A), ITGA3 (B) and VCAN (C) in PANC-1 and ASPC-1 cell lines with CMG2 knockdown, were determined by QPCR. (D) The expression of TJP2 (ZO-2) in three pancreatic cancer cell lines with CMG2 overexpression or knockdown are shown. CD44 expression in PANC-1 and ASPC-1 cell lines with CMG2 knockdown were verified in transcripts (E) and at protein level (F). *** indicate p<0.001, ** indicate p<0.01, * indicates p<0.05.

7.4 Discussion

It has been demonstrated in the present study that CMG2 can enhance cell adhesion, in which FAK and EGFR may play an important role. In the present Chapter, further analysis was conducted to evaluate the involvement of cell-cell adhesion molecules,

cell-matrix adhesion molecules and HA interacting molecules in CMG2 regulated adhesion in pancreatic cancer cells.

Integrins are implicated in nearly every step of cancer disease progression. Integrins can upregulate the expression of MMPs and other proteases, thus facilitating local invasion of cancer cells (Ahmed et al. 2002; Gu et al. 2002; Munshi and Stack 2006; Baum et al. 2007; Yue et al. 2012; Kesanakurti et al. 2013). Invasive cancer cells penetrate the stroma and disseminate into the surrounding tissue by different integrin-mediated mechanisms. CAFs (Cancer-associated fibroblasts) can promote cancer cell invasion by integrin-dependent pathways too (Munshi and Stack 2006; Gaggioli et al. 2007). In addition, circulating cancer cells (CTCs) are an important part of blood metastasis of cancer, normal epithelial cells will undergo *anoikis* during this step, CTCs can avoid this by the pathways which are associated with altered integrins (Strilic and Offermanns 2017). Following that, cancer cells need to be seeded into the perivascular tissue to form a metastatic lesion and Integrins play an important role in this step, by interacting with the ECM (Cagnet et al. 2014). In addition to the implications in distant metastasis, integrins can also promote tumourigenesis, most of the integrins containing β1 subunits play a pivotal role during tumourigenesis in mammary glands (White et al. 2004; Cagnet et al. 2014). Furthermore, integrins can promote stemness in cancer cells (Seguin et al. 2015). They can also promote cell survival and growth by themselves or in conjunction with different growth factor receptors (Trusolino et al. 2001; Guo et al. 2006; Mai et al. 2014; Novitskaya et al. 2014; Alanko et al. 2015; Seguin et al. 2015; Hamidi et al. 2016). Integrins mediated cell-ECM interaction can induce a negative feedback loop, which will inhibit E-cadherin-mediated cell-cell interaction (Borghi et al. 2010), suggesting an inhibiting role of integrins in cell-cell adhesion (Hamidi and Ivaska 2018). In this Chapter, ITGB1 was downregulated in both PANC-1 and ASPC-1 cells, following the knockdown of CMG2. Together with the involvement of ITGA2 and ITGB3, in CMG2 regulated cell-matrix adhesion, that was revealed in Chapter 6, this suggests that these integrins play an important role in CMG2 enhanced cell-matrix adhesion in pancreatic cancer cells. This is also supported by the reduced activation of FAK observed in the pancreatic cancer cells, following the knockdown of CMG2.

Claudins are a group of proteins which form the structure of tight junctions and

play a key role in tumourigenesis (Tureci et al. 2011). Claudin is a transmembrane protein located at the apical junctions between cells, maintaining the polarity of epithelial and endothelial cells. The phosphorylation of claudin can lead to a change of cell polarity, which is associated with disease progression of malignant tumours (Nichols et al. 2004). Claudin 18 has two subtypes, claudin 18.1 and claudin 18.2. Claudin 18.1 is expressed in normal lung and lung cancer tissues, while expression of claudin 18.2 is evident in gastric cancer, pancreatic cancer and oesophageal cancer (Deissler et al. 2010). Claudin 18.2 cannot be detected in normal pancreatic tissue, while its expression is significantly increased in tumour tissue (Sahin et al. 2008; Lee et al. 2011; Li et al. 2020). In early-stage pancreatic cancer, claudin 18 is significantly upregulated in the IPMN stage, suggesting it is associated with tumourigenesis (Tanaka et al. 2011; Huang et al. 2020). Moreover, claudin expression is positively correlated with pancreatic cancer stage, lymphatic infiltration, and nerve invasion (Wang et al. 2022). Higher claudin 18.2 is associated with a poor prognosis of pancreatic cancer (Wang et al. 2023). An upregulation of Claudin 4 has been implicated in ductal pancreatic cancer, PanIN, IPMN and MCN (Romero-Calvo et al. 2019). However, it has also been shown that claudin-4 may inhibit aggressiveness and distant metastasis of pancreatic cancer (Michl et al. 2003; Kyuno et al. 2011; Luo et al. 2020). Higher claudin-4 has also been associated with a better prognosis, being similar to E-cadherin, reduced claudin-4 in epithelial cells will impair cell contact inhibition leading to promotion of cancer cell invasion (Joo et al. 2002; Torres et al. 2018). Claudin 18 can interact with EGFR to promote cell proliferation and migration. Treatment with EGF and RAS overexpression can induce the expression of claudin 18 (Dottermusch et al. 2019). In pancreatic cancer, claudin-1 is also increased and positively correlated with tumour proliferation, which is promoted by TNF-α (Kondo et al. 2008; Bhat et al. 2020). The expression of claudin-7 was reduced in pancreatic ductal adenocarcinoma while CLDN7 knockdown in the MiaPaCa-2 cell line resulted in an inhibition of cell proliferation (Okui et al. 2019; Wang et al. 2023). Claudin-12 presents an oncogenic effect in pancreatic cancer cells (Zhang et al. 2022). It can also promote cell proliferation and migration in osteosarcoma (Tian et al. 2019) and promote proliferation, migration and invasion of pancreatic cancer cells (PANC-1) (Wang et al. 2023). Claudin-23 is another potential oncogene in pancreatic

cancer, by activation of MEK (Wang et al. 2010). In the present study, CLDN1, ClDN4, CLDN7 and CLDN18 were found to be positively correlated with CMG2 in pancreatic cancer. It suggests that these TJ molecules are potentially involved in CMG2 regulated cellular functions in pancreatic cancer cells, which requires a further investigation.

In addition to the claudins, TJP1 (ZO-1) and TJP2 (ZO-2) expression were also positively correlated with CMG2 in pancreatic cancer. TJP2 (ZO2) is a scaffold protein located at the intracellular part of tight junctions, which help to stabilise the tight junction (Gumbiner et al. 1991). Both ZO-1 and ZO-2 can induce the polymerization of claudins and assembly of tight junctions (Umeda et al. 2006). ZO-2 has two different isoforms, ZO-2A and ZO-2C (Chlenski et al. 2000). Expression of ZO-2C has been observed in pancreatic ductal adenocarcinoma (Chlenski et al. 1999). Although these TJ associated proteins, ZO1 and ZO2 are positively correlated with CMG2, their implication in pancreatic cancer and their role in the CMG2 regulated cellular functions are yet to be dissected.

Cx26 (GJB2) expression was increased in those pancreatic tumours which had a higher expression of CMG2 (Figure 7.3). Cx26 has been implicated in certain cancers with an association with lymphatic vessel invasion, lymph node metastasis, lung metastasis, tumour growth, and disease recurrence (Naoi et al. 2007; Ezumi et al. 2008; Naoi et al. 2008; Inose et al. 2009). Overexpression of Cx26 can induce EMT via activation of the PI3K/AKT pathway (Yang et al. 2015a). The exact role of Cx26 in CMG2 regulated cell-cell adhesion and deregulated behaviour of pancreatic cancer cells is yet to be evaluated. In this Chapter, the association between HA interacting molecules and CMG2 was studied. VCAN was reduced in both PANC-1 and ASPC-1 with CMG2 knockdown. Decreased CD44 was observed in PANC-1 CMG2 knockdown cells but not in the ASPC-1 cells. CD44 is a cancer stem cell marker which is positively correlated with CMG2 in gastric cancer (Ji et al. 2018). The interaction between CD44 and HA can mediate the adhesion of cancer cells to mesothelial cells (Weidle et al. 2016).VCAN is upregulated in leiomyosarcoma compared with normal tissue (Keire et al. 2014), which can promote cell proliferation and migration in LMS (leiomyosarcoma) (Keire et al. 2014). Lack of VCAN in a mouse fibrosarcoma is associated with deregulation of CAFs (Fanhchaksai et al. 2016). In pancreatic cancer VCAN is also

associated with a poor prognosis (Ozdemir et al. 2014). In future study, the exact influence of CMG2 on HA interacting molecules needs to be further evaluated.

In summary, in addition to ICAM-1, FAK and EGFR identified in the previous proteomic analysis and validation, integrins (ITGB4, ITGA3, ITGA6, ITGA2), claudins (CLDN4, CLDN18), ZO2, VCAN and CD44 may also play a role in CMG2 promoted adhesion, aggregation and distant dissemination which provokes further investigation.

Chapter 8

General Discussion

CMG2 was initially discovered as a protein in tumour associated angiogenesis (Wycoff et al. 2011; Ye et al. 2014b; Wycoff et al. 2015). More evidence has shown that CMG2 can directly participate in the disease progression of certain cancers, by regulating functions of cancer cells. In breast cancer, the level of CMG2 transcripts in advanced tumours is lower compared with early-stage tumours, while reduced CMG2 expression is associated with shorter overall survival. CMG2 can inhibit the growth of breast cancer cells (Ye et al. 2014c). In contrast, CMG2 has little impact on the proliferation of an AR negative prostate cancer cell line (PC-3), instead it can inhibit the invasion of the PC-3 cells (Ye et al. 2014b). CMG2 can also enhance cell adhesion and aggregation in glioma, by activating the Hippo pathway (Xu et al. 2019). In gastric cancer, CMG2 promotes EMT, formation of cancer stem-like cells (GCSLCs) and proliferation (Ji et al. 2018). In soft tissue sarcomas, CMG2 can promote EMT and distant metastasis by activating u-PA (Peters et al. 2012). The present study aimed to dissect the role of CMG2 in pancreatic cancer and disease specific peritoneal metastasis.

8.1 Elevated expression of CMG2 in pancreatic cancer

CMG2 expression was increased significantly in pancreatic cancers compared with adjacent normal tissues, in the Beijing cohort. This is supported by findings in the analysis of other pancreatic cancer cohorts and IHC staining of CMG2 in pancreatic cancer. Increased CMG2 expression was associated with poor survival in pancreatic cancer. CMG2 expression was increased in distant metastases from pancreatic cancer, in comparison with its expression in the primary tumours. In pancreatic cancer, distant metastasis usually results in a poor prognosis. Even a micro-metastasis can also cause a dismal outcome and these patients cannot benefit from t local treatments (Makary et al. 1998). CMG2 expression was also increased in early-stage pancreatic tumours and was positively correlated with several oncogenes. In pancreatic cancer, higher expression of CMG2 was associated with disease progression and poor prognosis. In contrast, in prostate cancer and breast cancer, CMG2 is reduced and the reduced expression is associated with a poor prognosis (Ye et al. 2014b; Ye et al. 2014c). In line with our finding in pancreatic cancer, CMG2 promote cell invasion, proliferation and metastasis in gastric cancer (Ji et al. 2018), suggesting CMG2 plays a different role in

gastrointestinal cancers in comparison with endocrine-related cancers.

8.2 CMG2 promotes adhesion of pancreatic cancer cells

Although both overexpression and knockdown of CMG2 had little effect on the invasion and migration of pancreatic cancer cells, CMG2 knockdown markedly impaired the adhesion of both PANC-1 and ASPC-1 cells. In line with this finding, overexpression of CMG2 enhanced adhesion in PANC-1 cells. This suggests that CMG2 plays a vital role in the adhesiveness of pancreatic cancer cells. Enhanced cell-matrix adhesion was not observed in MiaPaCa-2 cells with CMG2 overexpression, suggesting MiaPaCa-2 cells are specific compared with another two cell lines. On the other hand, MiaPaCa-2 cells are already more adhesive, even with a lower expression of CMG2, suggesting other adhesion molecules are sufficient to support their adhesion.

Further analysis of proteins and protein phosphorylation revealed that a number of integrins, including ITGA2, ITGB1 and ITGB3, were upregulated by CMG2 in pancreatic cancer cells, in which an increased phosphorylation of PTK2/FAK was also observed. PTK2 is a pivotal kinase in the focal adhesion complex and plays a profound role in the regulation of cell adhesion, migration and invasion (Zhao and Guan 2011; Tapial Martinez et al. 2020). This suggests that, in addition to CMG2 mediated adhesion to matrix, CMG2 can also enhance cell adhesion by upregulating integrins and integrin-mediated focal adhesion. Activation of Shc, MEK2 and ELK1 was reduced in the pancreatic cancer cells, following knockdown of CMG2. These proteins are key downstream molecules in the EGFR pathways. EGFR can initiate downstream signalling to regulate various cellular functions, such as cell adhesion. EGFR activation can also activate focal adhesion (Rao et al. 2020). However, the involvement of EGFR, PTK2 and integrins in CMG2 coordinated cell adhesion is yet to be fully examined.

8.3 CMG2 enhances adhesion of pancreatic cancer cells to peritoneum

The peritoneum is the second most common metastatic site of pancreatic cancer (Yachida and Iacobuzio-Donahue 2009). During peritoneal metastasis, adhesion of disseminating cancer cells to the peritoneum is a crucial step before they can invade through the peritoneum. Reduced adhesion to mesothelial cells was found in PANC-1

and ASPC-1 cells, with CMG2 knockdown, suggesting CMG2 plays an important role in the adhesion of pancreatic cancer cells to the peritoneum. In line with this finding, a recent study of CMG2 in gastric cancer also showed that CMG2 can promote peritoneal metastasis, by upregulating CD44. This suggests that CMG2 enhanced adhesion plays an important role in the dissemination of cancer cells, which contributes to the contrasting role played by CMG2 in gastrointestinal cancers.

There exists a HA film covering the peritoneum which forms a native barrier, to prevent adhesion of disseminating cancer cells. HA interacting molecules, expressed by cancer cells, are actively involved in peritoneal metastasis (Soliman et al. 2022). In the present study, it was shown that CMG2 enhanced adhesion of pancreatic cancer cells to mesothelial cells can be inhibited by treatment with soluble HA. Moreover, CD44 as a HA-interacting molecule, is expressed by both cancer and mesothelial cells. The interaction between CD44 and HA can mediate the adhesion of cancer cells to mesothelial cells (Weidle et al. 2016). CD44 expression was found to be reduced in PANC-1 cells with knockdown of CMG2. Some other molecules can also promote cancer-mesothelial cell adhesion such as IL-1, β/ β1 integrin interaction, ICAM-1 (Ziprin et al. 2004; Watanabe et al. 2012), VCAN (Watanabe 2022) and MSLN-MUC6 interaction (Kaneko et al. 2009). Among these proteins, ICAM-1 and VCAN expression was found to be enhanced by CMG2 in pancreatic cancer cells. This suggests that CMG2 can promote adhesion of pancreatic cancer cells to mesothelial cells by upregulation of HA interacting molecules. The therapeutic potential of targeting CMG2, HA and HA interacting molecules for peritoneal metastasis in pancreatic cancer warrants further exploration.

8.4 CMG2 promotes cell aggregation and viability during dissemination

Viability of epithelial cells is maintained by attachment to the ECM. Loss of anchorage can induce apoptosis in the epithelial cells, which is called *anoikis* (Frisch and Francis 1994; Douma et al. 2004). As epithelial cell-derived malignant cells, when they disseminate in the peritoneal cavity, they encounter several stresses which will affect their viability, including shear forces, oxidative stress and immune system attacking. *Anoikis* is one of those challenges encountered by the disseminating cancer cells. The

disseminating cancer cells can form clusters to protect themselves from *anoikis* (Massague and Obenauf 2016). In a suspended cell culture assay, CMG2 promoted cell aggregation significantly in MiaPaCa-2 cells. Cell viability and apoptosis of the suspended cells were also determined. CMG2 can promote survival and reduce apoptosis in the suspended pancreatic cancer cells. Furthermore, the proteomic analysis also revealed an increased expression of ICAM-1 in MiaPaCa-2 CMG2 overexpression cells. In addition to interacting with HA, ICAM-1 is also an important adhesion protein mediating cell-cell adhesion (Taftaf et al. 2021). ICAM-1 can promote the formation of CTC (circulating cancer cell) clusters in lung cancer, by promoting cell aggregation (Taftaf et al. 2021). ICAM-1 expression is usually increased in more aggressive cancers, including triple-negative subtype breast cancer (Guo et al. 2014) and non-small cell lung carcinoma (Schardt et al. 1993; Melis et al. 1996). Moreover, the expression of CLDN18 and CLDN4 were positively associated with CMG2 in pancreatic tumours. TJP2 was found to be increased in PANC-1 and MiaPaCa-2 cells, which had overexpression of CMG2. This suggests that CMG2 can facilitate aggregation/clustering and increase viability of the suspended pancreatic cancer cells, to enhance their survival during dissemination. The involvement of ICAM-1 and TJ molecules in CMG2 enhanced cell aggregation and survival is yet to be fully examined.

8.5 Pathways and molecules regulated by CMG2 in pancreatic cancer cells

CMG2 can promote the phosphorylation of EGFR, MEK2, Shc and ELK1, suggesting the EGFR pathway can be activated by CMG2. Activated EGFR can bind with other ERBB family proteins and further activate downstream signalling, including the RAS–RAF–MEK–ERK–MAPK pathway and PI3K–AKT–mTOR pathways (Ciardiello and Tortora 2008; Rao et al. 2020; Nanba et al. 2021). EGFR can promote cell proliferation, survival, angiogenesis and metastasis in various cancers (Ciardiello and Tortora 2008). To date, several drugs targeting EGFR and its downstream signalling have been applied to treat cancer, including erlotinib, cetuximab, panitumumab and gefitinib (Ciardiello and Tortora 2008). However, involvement of EGFR in CMG2 coordinated biological activities in pancreatic cancer cells and corresponding therapeutic opportunities are yet to dissected and evaluated.

Focal adhesion complexes play an important role in promoting cell-matrix adhesion and the connection between the ECM and the cytoskeleton, which further promotes cell survival, differentiation, proliferation, and migration (Legate and Fassler 2009; Legate et al. 2009; Lim et al. 2018). In addition, cell-ECM adhesion mediated by focal adhesion is associated with higher drug and radiation therapy resistance (Damiano et al. 2001; Cordes and Meineke 2003; Park et al. 2006; Nam et al. 2010; Eke et al. 2012). PTK2 (FAK) is a pivotal molecule in focal adhesion and its downstream signalling. PTK2 can be activated by EGFR (Shen and Guo 2020). CMG2 promoted phosphorylation of PTK2 in the three pancreatic cancer cells that were examined in the present study. PTK2 interacts with integrins and further promotes cell adhesion (Hynes and Lane 2005). The interaction between integrins and PTK2 can also promote the phosphorylation of PTK2 (Mitra and Schlaepfer 2006). ITGB3 and ITGA2 are the two integrins which are involved in focal adhesion and their expression was enhanced by CMG2 in pancreatic cancer cells. Integrins enhance some cell functions, including survival and migration (Brakebusch and Fassler 2005; Hehlgans et al. 2007; Ross et al. 2013; Lim et al. 2018). Interestingly, the activated focal adhesion pathway can also inhibit the efficiency of an EGFR-targeting drug, Cetuximab (Eke et al. 2013a; Eke et al. 2013b). This may partially explain why EGFR inhibitor does not work well in pancreatic cancer. CMG2 is increased in pancreatic cancer and its expression not only activates EGFR but also activate the focal adhesion pathway. Taken together, both EGFR and focal adhesion are two important players to be further investigated for their role in CMG2 regulated cellular functions of pancreatic cancer cells, which can also shed light on their therapeutic potential.

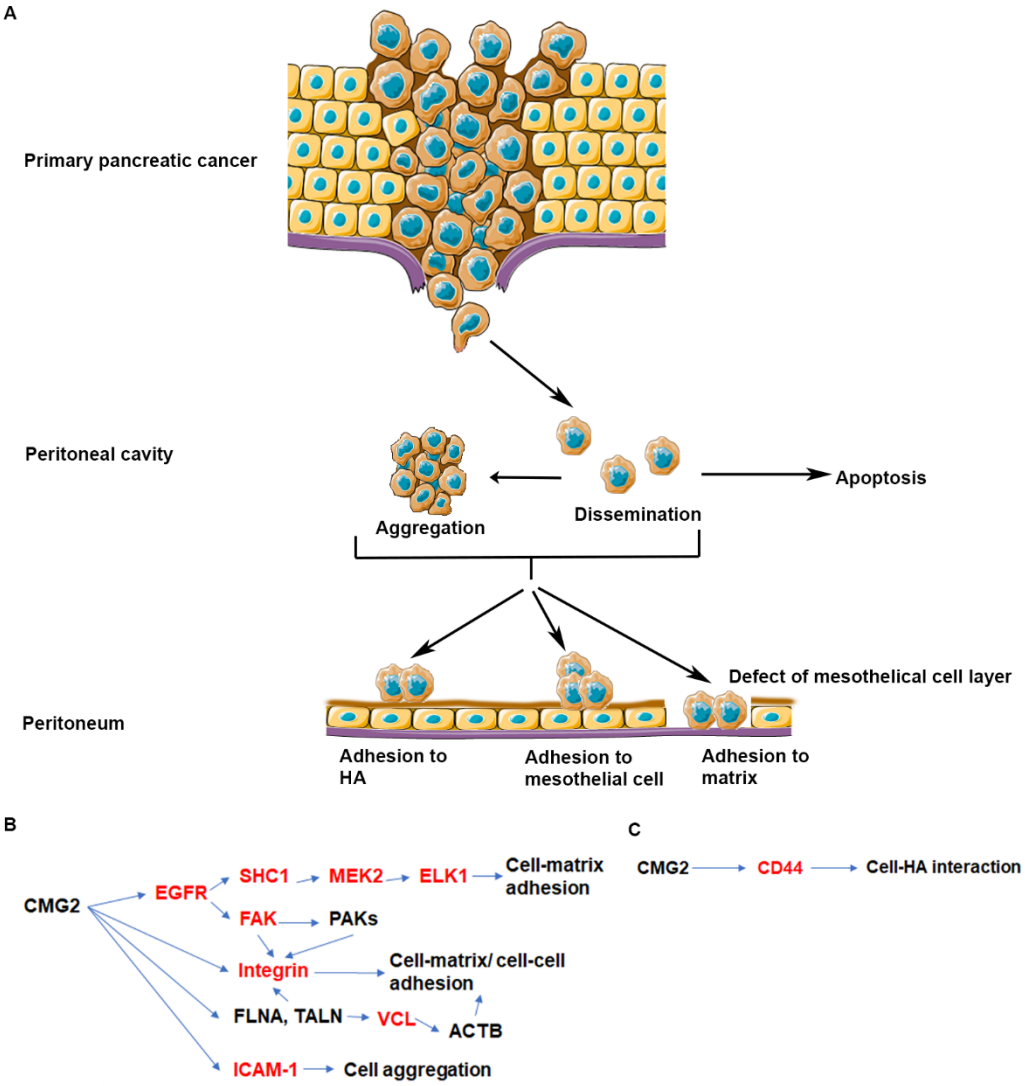

Figure 8.1 Cell functions and pathways regulated by CMG2 in pancreatic cancer cell lines. (A) CMG2 is associated with pancreatic cancer peritoneal metastasis, which can promote cell aggregation, adhesion and inhibit cell apoptosis. (B) EGFR pathway, integrins, ICAM-1 and focal adhesion can be upregulated by CMG2 to promote the cell adhesion. (C) CMG2 can upregulate CD44 to promote cell-HA interaction.

8.6 Conclusion and perspectives

In summary, CMG2 is upregulated in pancreatic cancer. Higher expression of CMG2 is associated with distant metastasis and shorter survival. CMG2 promotes cell-matrix-adhesion, cell-cell adhesion, cell-hyaluronic acid adhesion and cell viability during dissemination, in which CMG2 orchestrated EGFR signalling, focal adhesion, integrins,

TJ proteins and HA interacting molecules are involved (Figure 8.1A and B). This suggests that CMG2 plays an important role in pancreatic cancer development and metastasis. Its potential and application for early detection and target therapy of pancreatic cancer provokes more intensive research. Since an increased expression of CMG2 has also been seen in benign tumours and precancerous lesions in the pancreas, its potential in early detection of the disease should be evaluated.

Bibliography

National Comprehensive Cancer Network. Available from: URL: https://www. nccn.org/professionals/physician_gls/pdf/pancreatic.pdf,

2023a. Available at: https://www.genecards.org/cgi-bin/carddisp.pl?gene=ANTXR2#expression [Accessed.

2023b. *Integrins and Cell Adhesion Molecules*. Available at: https://www.bio-rad-antibodies.com/integrins-and-cell-adhesion-molecules.html [Accessed.

Abrami, L., Kunz, B., Deuquet, J., Bafico, A., Davidson, G. and van der Goot, F. G. 2008. Functional interactions between anthrax toxin receptors and the WNT signalling protein LRP6. *Cell Microbiol* 10(12), pp. 2509-2519. doi: 10.1111/j.1462-5822.2008.01226.x

Abrami, L., Kunz, B. and van der Goot, F. G. 2010. Anthrax toxin triggers the activation of src-like kinases to mediate its own uptake. *Proc Natl Acad Sci U S A* 107(4), pp. 1420-1424. doi: 10.1073/pnas.0910782107

Acehan, D., Jiang, X., Morgan, D. G., Heuser, J. E., Wang, X. and Akey, C. W. 2002. Three-dimensional structure of the apoptosome: implications for assembly, procaspase-9 binding, and activation. *Mol Cell* 9(2), pp. 423-432. doi: 10.1016/s1097-2765(02)00442-2

Acharyya, S. et al. 2012. A CXCL1 paracrine network links cancer chemoresistance and metastasis. *Cell* 150(1), pp. 165-178. doi: 10.1016/j.cell.2012.04.042

Adorno, M. et al. 2009. A Mutant-p53/Smad complex opposes p63 to empower TGFbeta-induced metastasis. *Cell* 137(1), pp. 87-98. doi: 10.1016/j.cell.2009.01.039

Agarwal, B., Abu-Hamda, E., Molke, K. L., Correa, A. M. and Ho, L. 2004. Endoscopic ultrasound-guided fine needle aspiration and multidetector spiral CT in the diagnosis of pancreatic cancer. *Am J Gastroenterol* 99(5), pp. 844-850. doi: 10.1111/j.1572-0241.2004.04177.x

Aguirre, A. J. et al. 2003. Activated Kras and Ink4a/Arf deficiency cooperate to produce metastatic pancreatic ductal adenocarcinoma. *Genes Dev* 17(24), pp. 3112-3126. doi: 10.1101/gad.1158703

Aguirre, A. R. and Abensur, H. 2014. [Physiology of fluid and solute transport across the peritoneal membrane]. *J Bras Nefrol* 36(1), pp. 74-79. doi: 10.5935/0101-2800.20140013

Ahmed, N. et al. 2002. Overexpression of alpha(v)beta6 integrin in serous epithelial ovarian cancer regulates extracellular matrix degradation via the plasminogen activation cascade. *Carcinogenesis* 23(2), pp. 237-244. doi: 10.1093/carcin/23.2.237

Al-Hawary, M. M. et al. 2014. Pancreatic ductal adenocarcinoma radiology reporting template: consensus statement of the Society of Abdominal Radiology and the American Pancreatic Association. *Radiology* 270(1), pp. 248-260. doi: 10.1148/radiol.13131184

Alanko, J. et al. 2015. Integrin endosomal signalling suppresses anoikis. *Nat Cell Biol* 17(11), pp. 1412-1421. doi: 10.1038/ncb3250

Almeida, E. A. et al. 2000. Matrix survival signaling: from fibronectin via focal adhesion kinase to c-Jun NH(2)-terminal kinase. *J Cell Biol* 149(3), pp. 741-754. doi: 10.1083/jcb.149.3.741

Altomare, D. A. and Testa, J. R. 2005. Perturbations of the AKT signaling pathway in human cancer. *Oncogene* 24(50), pp. 7455-7464. doi: 10.1038/sj.onc.1209085

Ammann, R. W., Akovbiantz, A., Largiader, F. and Schueler, G. 1984. Course and outcome of chronic pancreatitis. Longitudinal study of a mixed medical-surgical series of 245 patients. *Gastroenterology* 86(5 Pt 1), pp. 820-828.

Amorim, S., Soares da Costa, D., Pashkuleva, I., Reis, C. A., Reis, R. L. and Pires, R. A. 2020. Hyaluronic Acid of Low Molecular Weight Triggers the Invasive "Hummingbird" Phenotype on Gastric Cancer Cells. *Adv Biosyst* 4(11), p. e2000122. doi: 10.1002/adbi.202000122

Andersson, A. M., Moran, N., Gaardsvoll, H., Linnemann, D., Bjerkvig, R., Laerum, O. D. and Bock, E. 1991. Characterization of NCAM expression and function in BT4C and BT4Cn glioma cells. *Int J Cancer* 47(1), pp. 124-129. doi: 10.1002/ijc.2910470122

Arteaga, C. L. and Engelman, J. A. 2014. ERBB receptors: from oncogene discovery to basic science to mechanism-based cancer therapeutics. *Cancer Cell* 25(3), pp. 282-303. doi: 10.1016/j.ccr.2014.02.025

Ashton, G. H. et al. 2010. Focal adhesion kinase is required for intestinal regeneration and tumorigenesis downstream of Wnt/c-Myc signaling. *Dev Cell* 19(2), pp. 259-269. doi: 10.1016/j.devcel.2010.07.015

Attieh, Y. and Vignjevic, D. M. 2016. The hallmarks of CAFs in cancer invasion. *Eur J Cell Biol* 95(11), pp. 493-502. doi: 10.1016/j.ejcb.2016.07.004

Avila, J. L. and Kissil, J. L. 2013. Notch signaling in pancreatic cancer: oncogene or tumor suppressor? *Trends Mol Med* 19(5), pp. 320-327. doi: 10.1016/j.molmed.2013.03.003

Avizienyte, E. and Frame, M. C. 2005. Src and FAK signalling controls adhesion fate and the epithelial-to-mesenchymal transition. *Curr Opin Cell Biol* 17(5), pp. 542-547. doi: 10.1016/j.ceb.2005.08.007

Avula, L. R., Hagerty, B. and Alewine, C. 2020. Molecular mediators of peritoneal metastasis in pancreatic cancer. *Cancer Metastasis Rev* 39(4), pp. 1223-1243. doi: 10.1007/s10555-020-09924-4

Baba, K. et al. 2017. Hypoxia-induced ANGPTL4 sustains tumour growth and anoikis resistance through different mechanisms in scirrhous gastric cancer cell lines. *Sci Rep* 7(1), p. 11127. doi: 10.1038/s41598-017-11769-x

Baccarini, M. 2005. Second nature: biological functions of the Raf-1 "kinase". *FEBS Lett* 579(15), pp. 3271-3277. doi: 10.1016/j.febslet.2005.03.024

Badea, L., Herlea, V., Dima, S. O., Dumitrascu, T. and Popescu, I. 2008. Combined gene expression analysis of whole-tissue and microdissected pancreatic ductal adenocarcinoma identifies genes specifically overexpressed in tumor epithelia. *Hepatogastroenterology* 55(88), pp. 2016-2027.

Bai, F. H. et al. 2012. Screening and identification of peritoneal metastasis-related genes of gastric adenocarcinoma using a cDNA microarray. *Genet Mol Res* 11(2), pp. 1682-1689. doi: 10.4238/2012.June.25.1

Bailey, P. et al. 2016. Genomic analyses identify molecular subtypes of pancreatic cancer. *Nature* 531(7592), pp. 47-52. doi: 10.1038/nature16965

Bannoura, S. F. et al. 2021. Targeting KRAS in pancreatic cancer: new drugs on the horizon. *Cancer Metastasis Rev* 40(3), pp. 819-835. doi: 10.1007/s10555-021-09990-2

Bao, B. et al. 2011. Notch-1 induces epithelial-mesenchymal transition consistent with cancer stem cell phenotype in pancreatic cancer cells. *Cancer Lett* 307(1), pp. 26-36. doi: 10.1016/j.canlet.2011.03.012

Baranwal, S. and Alahari, S. K. 2009. Molecular mechanisms controlling E-cadherin expression in breast cancer. *Biochem Biophys Res Commun* 384(1), pp. 6-11. doi: 10.1016/j.bbrc.2009.04.051

Barbolina, M. V. 2018. Molecular Mechanisms Regulating Organ-Specific Metastases in Epithelial Ovarian Carcinoma. *Cancers (Basel)* 10(11), doi: 10.3390/cancers10110444

Barczyk, M., Carracedo, S. and Gullberg, D. 2010. Integrins. *Cell Tissue Res* 339(1), pp. 269-280. doi: 10.1007/s00441-009-0834-6

Barrow-McGee, R. et al. 2016. Corrigendum: Beta 1-integrin-c-Met cooperation reveals an inside-in survival signalling on autophagy-related endomembranes. *Nat Commun* 7, p. 12392. doi: 10.1038/ncomms12392

Bartolazzi, A., Peach, R., Aruffo, A. and Stamenkovic, I. 1994. Interaction between CD44 and hyaluronate is directly implicated in the regulation of tumor development. *J Exp Med* 180(1), pp. 53-66. doi: 10.1084/jem.180.1.53

Bartsch, D. K. et al. 2002. CDKN2A germline mutations in familial pancreatic cancer. *Ann Surg* 236(6), pp. 730-737. doi: 10.1097/00000658-200212000-00005

Baum, O. et al. 2007. Increased invasive potential and up-regulation of MMP-2 in MDA-MB-231 breast cancer cells expressing the beta3 integrin subunit. *Int J Oncol* 30(2), pp. 325-332.

Bauman, M. D. et al. 2018. Laparoscopic distal pancreatectomy for pancreatic cancer is safe and effective. *Surg Endosc* 32(1), pp. 53-61. doi: 10.1007/s00464-017-5633-7

Behrenbruch, C., Hollande, F., Thomson, B., Michael, M., Warrier, S. K., Lynch, C. and Heriot, A. 2017. Treatment of peritoneal carcinomatosis with hyperthermic intraperitoneal chemotherapy in colorectal cancer. *ANZ J Surg* 87(9), pp. 665-670. doi: 10.1111/ans.14077

Bell, S. E., Mavila, A., Salazar, R., Bayless, K. J., Kanagala, S., Maxwell, S. A. and Davis, G. E.

2001. Differential gene expression during capillary morphogenesis in 3D collagen matrices: regulated expression of genes involved in basement membrane matrix assembly, cell cycle progression, cellular differentiation and G-protein signaling. *J Cell Sci* 114(Pt 15), pp. 2755-2773.

Belzacq, A. S., Vieira, H. L., Kroemer, G. and Brenner, C. 2002. The adenine nucleotide translocator in apoptosis. *Biochimie* 84(2-3), pp. 167-176. doi: 10.1016/s0300-9084(02)01366-4

Benedicto, A., Romayor, I. and Arteta, B. 2017. Role of liver ICAM-1 in metastasis. *Oncol Lett* 14(4), pp. 3883-3892. doi: 10.3892/ol.2017.6700

Bertelli, E., Di Gregorio, F., Bertelli, L. and Mosca, S. 1995. The arterial blood supply of the pancreas: a review. I. The superior pancreaticoduodenal and the anterior superior pancreaticoduodenal arteries. An anatomical and radiological study. *Surg Radiol Anat* 17(2), pp. 97-106, 101-103. doi: 10.1007/BF01627566

Bertelli, E., Di Gregorio, F., Mosca, S. and Bastianini, A. 1998. The arterial blood supply of the pancreas: a review. V. The dorsal pancreatic artery. An anatomic review and a radiologic study. *Surg Radiol Anat* 20(6), pp. 445-452. doi: 10.1007/BF01653138

Berx, G. and van Roy, F. 2009. Involvement of members of the cadherin superfamily in cancer. *Cold Spring Harb Perspect Biol* 1(6), p. a003129. doi: 10.1101/cshperspect.a003129

Bevilacqua, M. P., Pober, J. S., Mendrick, D. L., Cotran, R. S. and Gimbrone, M. A., Jr. 1987. Identification of an inducible endothelial-leukocyte adhesion molecule. *Proc Natl Acad Sci U S A* 84(24), pp. 9238-9242. doi: 10.1073/pnas.84.24.9238

Bhat, A. A. et al. 2020. Claudin-1, A Double-Edged Sword in Cancer. *Int J Mol Sci* 21(2), doi: 10.3390/ijms21020569

Birch, M., Mitchell, S. and Hart, I. R. 1991. Isolation and characterization of human melanoma cell variants expressing high and low levels of CD44. *Cancer Res* 51(24), pp. 6660-6667.

Blackford, A. et al. 2009. SMAD4 gene mutations are associated with poor prognosis in pancreatic cancer. *Clin Cancer Res* 15(14), pp. 4674-4679. doi: 10.1158/1078-0432.CCR-09-0227

Blanco, M. J., Moreno-Bueno, G., Sarrio, D., Locascio, A., Cano, A., Palacios, J. and Nieto, M. A. 2002. Correlation of Snail expression with histological grade and lymph node status in breast carcinomas. *Oncogene* 21(20), pp. 3241-3246. doi: 10.1038/sj.onc.1205416

Bonni, A., Brunet, A., West, A. E., Datta, S. R., Takasu, M. A. and Greenberg, M. E. 1999. Cell survival promoted by the Ras-MAPK signaling pathway by transcription-dependent and -independent mechanisms. *Science* 286(5443), pp. 1358-1362. doi: 10.1126/science.286.5443.1358

Borghi, N., Lowndes, M., Maruthamuthu, V., Gardel, M. L. and Nelson, W. J. 2010. Regulation of cell motile behavior by crosstalk between cadherin- and integrin-mediated adhesions. *Proc Natl Acad Sci U S A* 107(30), pp. 13324-13329. doi: 10.1073/pnas.1002662107

Boroughs, L. K. and DeBerardinis, R. J. 2015. Metabolic pathways promoting cancer cell survival and growth. *Nat Cell Biol* 17(4), pp. 351-359. doi: 10.1038/ncb3124

Bossen, C. et al. 2006. Interactions of tumor necrosis factor (TNF) and TNF receptor family members in the mouse and human. *J Biol Chem* 281(20), pp. 13964-13971. doi: 10.1074/jbc.M601553200

Bossy, D., Mattei, M. G. and Simmons, D. L. 1994. The human intercellular adhesion molecule 3 (ICAM3) gene is located in the 19p13.2-p13.3 region, close to the ICAM1 gene. *Genomics* 23(3), pp. 712-713. doi: 10.1006/geno.1994.1565

Bottcher, R. T., Lange, A. and Fassler, R. 2009. How ILK and kindlins cooperate to orchestrate integrin signaling. *Curr Opin Cell Biol* 21(5), pp. 670-675. doi: 10.1016/j.ceb.2009.05.008

Bouchard, V. et al. 2007. Fak/Src signaling in human intestinal epithelial cell survival and anoikis: differentiation state-specific uncoupling with the PI3-K/Akt-1 and MEK/Erk pathways. *J Cell Physiol* 212(3), pp. 717-728. doi: 10.1002/jcp.21096

Boudreau, N., Sympson, C. J., Werb, Z. and Bissell, M. J. 1995. Suppression of ICE and apoptosis in mammary epithelial cells by extracellular matrix. *Science* 267(5199), pp. 891-893. doi: 10.1126/science.7531366

Bouillet, P. and Strasser, A. 2002. BH3-only proteins - evolutionarily conserved proapoptotic Bcl-2 family members essential for initiating programmed cell death. *J Cell Sci* 115(Pt 8), pp. 1567-1574. doi: 10.1242/jcs.115.8.1567

Bourguignon, L. Y., Gilad, E., Brightman, A., Diedrich, F. and Singleton, P. 2006. Hyaluronan-CD44 interaction with leukemia-associated RhoGEF and epidermal growth factor receptor promotes Rho/Ras co-activation, phospholipase C epsilon-Ca2+ signaling, and cytoskeleton modification in head and neck squamous cell carcinoma cells. *J Biol Chem* 281(20), pp. 14026-14040. doi: 10.1074/jbc.M507734200

Bourguignon, L. Y., Singleton, P. A., Zhu, H. and Zhou, B. 2002. Hyaluronan promotes signaling interaction between CD44 and the transforming growth factor beta receptor I in metastatic breast tumor cells. *J Biol Chem* 277(42), pp. 39703-39712. doi: 10.1074/jbc.M204320200

Bourguignon, L. Y., Zhu, H., Chu, A., Iida, N., Zhang, L. and Hung, M. C. 1997. Interaction between the adhesion receptor, CD44, and the oncogene product, p185HER2, promotes human ovarian tumor cell activation. *J Biol Chem* 272(44), pp. 27913-27918. doi: 10.1074/jbc.272.44.27913

Bournet, B., Selves, J., Grand, D., Danjoux, M., Hanoun, N., Cordelier, P. and Buscail, L. 2015. Endoscopic ultrasound-guided fine-needle aspiration biopsy coupled with a KRAS mutation assay using allelic discrimination improves the diagnosis of pancreatic cancer. *J Clin Gastroenterol* 49(1), pp. 50-56. doi: 10.1097/MCG.0000000000000053

Brabletz, T., Jung, A., Spaderna, S., Hlubek, F. and Kirchner, T. 2005. Opinion: migrating cancer stem cells - an integrated concept of malignant tumour progression. *Nat Rev Cancer* 5(9), pp. 744-749. doi: 10.1038/nrc1694

Brakebusch, C. and Fassler, R. 2005. beta 1 integrin function in vivo: adhesion, migration and more. *Cancer Metastasis Rev* 24(3), pp. 403-411. doi: 10.1007/s10555-005-5132-5

Brenner, D. and Mak, T. W. 2009. Mitochondrial cell death effectors. *Curr Opin Cell Biol* 21(6), pp. 871-877. doi: 10.1016/j.ceb.2009.09.004

Brodsky, A. S. et al. 2014. Expression profiling of primary and metastatic ovarian tumors reveals differences indicative of aggressive disease. *PLoS One* 9(4), p. e94476. doi: 10.1371/journal.pone.0094476

Brookes, S. et al. 2002. INK4a-deficient human diploid fibroblasts are resistant to RAS-induced senescence. *EMBO J* 21(12), pp. 2936-2945. doi: 10.1093/emboj/cdf289

Brown, D. A. and London, E. 1998. Functions of lipid rafts in biological membranes. *Annu Rev Cell Dev Biol* 14, pp. 111-136. doi: 10.1146/annurev.cellbio.14.1.111

Bruner, H. C. and Derksen, P. W. B. 2018. Loss of E-Cadherin-Dependent Cell-Cell Adhesion and the Development and Progression of Cancer. *Cold Spring Harb Perspect Biol* 10(3), doi: 10.1101/cshperspect.a029330

Buchs, N. C. et al. 2007. Vascular invasion in pancreatic cancer: evaluation of endoscopic ultrasonography, computed tomography, ultrasonography, and angiography. *Swiss Med Wkly* 137(19-20), pp. 286-291. doi: 2007/19/smw-11701

Bukowski, R. M., Balcerzak, S. P., O'Bryan, R. M., Bonnet, J. D. and Chen, T. T. 1983. Randomized trial of 5-fluorouracil and mitomycin C with or without streptozotocin for advanced pancreatic cancer. A Southwest Oncology Group study. *Cancer* 52(9), pp. 1577-1582. doi: 10.1002/1097-0142(19831101)52:9<1577::aid-cncr2820520906>3.0.co;2-8

Burgi, J. et al. 2020. Ligand Binding to the Collagen VI Receptor Triggers a Talin-to-RhoA Switch that Regulates Receptor Endocytosis. *Dev Cell* 53(4), pp. 418-430 e414. doi: 10.1016/j.devcel.2020.04.015

Burkhart, D. L. and Sage, J. 2008. Cellular mechanisms of tumour suppression by the retinoblastoma gene. *Nat Rev Cancer* 8(9), pp. 671-682. doi: 10.1038/nrc2399

Burleson, K. M., Casey, R. C., Skubitz, K. M., Pambuccian, S. E., Oegema, T. R., Jr. and Skubitz, A. P. 2004. Ovarian carcinoma ascites spheroids adhere to extracellular matrix components and mesothelial cell monolayers. *Gynecol Oncol* 93(1), pp. 170-181. doi: 10.1016/j.ygyno.2003.12.034

Burris, H. A., 3rd et al. 1997. Improvements in survival and clinical benefit with gemcitabine as first-line therapy for patients with advanced pancreas cancer: a randomized trial. *J Clin Oncol* 15(6), pp. 2403-2413. doi: 10.1200/JCO.1997.15.6.2403

Cagnet, S., Faraldo, M. M., Kreft, M., Sonnenberg, A., Raymond, K. and Glukhova, M. A. 2014. Signaling events mediated by alpha3beta1 integrin are essential for mammary tumorigenesis. *Oncogene* 33(34), pp. 4286-4295. doi: 10.1038/onc.2013.391

Cairns, R. A., Harris, I. S. and Mak, T. W. 2011. Regulation of cancer cell metabolism. *Nat Rev Cancer* 11(2), pp. 85-95. doi: 10.1038/nrc2981

Calcagnile, O. and Gisselsson, D. 2007. Telomere dysfunction and telomerase activation in cancer--a pathological paradox? *Cytogenet Genome Res* 118(2-4), pp. 270-276. doi:

10.1159/000108310

Calderwood, D. A., Huttenlocher, A., Kiosses, W. B., Rose, D. M., Woodside, D. G., Schwartz, M. A. and Ginsberg, M. H. 2001. Increased filamin binding to beta-integrin cytoplasmic domains inhibits cell migration. *Nat Cell Biol* 3(12), pp. 1060-1068. doi: 10.1038/ncb1201-1060

Callery, M. P., Chang, K. J., Fishman, E. K., Talamonti, M. S., William Traverso, L. and Linehan, D. C. 2009. Pretreatment assessment of resectable and borderline resectable pancreatic cancer: expert consensus statement. *Ann Surg Oncol* 16(7), pp. 1727-1733. doi: 10.1245/s10434-009-0408-6

Campbell, S. L., Khosravi-Far, R., Rossman, K. L., Clark, G. J. and Der, C. J. 1998. Increasing complexity of Ras signaling. *Oncogene* 17(11 Reviews), pp. 1395-1413. doi: 10.1038/sj.onc.1202174

Cancer Genome Atlas Research, N. et al. 2013. The Cancer Genome Atlas Pan-Cancer analysis project. *Nat Genet* 45(10), pp. 1113-1120. doi: 10.1038/ng.2764

cancerresearchuk.org, w. https://www.cancerresearchuk.org/health-professional/cancer-statistics-for-the-uk (available on 2021).

Cao, Y. et al. 2013. Neuropilin-2 promotes extravasation and metastasis by interacting with endothelial alpha5 integrin. *Cancer Res* 73(14), pp. 4579-4590. doi: 10.1158/0008-5472.CAN-13-0529

Carmichael, J., Fink, U., Russell, R. C., Spittle, M. F., Harris, A. L., Spiessi, G. and Blatter, J. 1996. Phase II study of gemcitabine in patients with advanced pancreatic cancer. *Br J Cancer* 73(1), pp. 101-105. doi: 10.1038/bjc.1996.18

Carmignani, C. P., Sugarbaker, T. A., Bromley, C. M. and Sugarbaker, P. H. 2003. Intraperitoneal cancer dissemination: mechanisms of the patterns of spread. *Cancer Metastasis Rev* 22(4), pp. 465-472. doi: 10.1023/a:1023791229361

Carpino, G. et al. 2021. Thrombospondin 1 and 2 along with PEDF inhibit angiogenesis and promote lymphangiogenesis in intrahepatic cholangiocarcinoma. *J Hepatol* 75(6), pp. 1377-1386. doi: 10.1016/j.jhep.2021.07.016

Carter, S. K. and Comis, R. L. 1975. The integration of chemotherapy into a combined modality approach for cancer treatment. VI. Pancreatic adenocarcinoma. *Cancer Treat Rev* 2(3), pp. 193-214. doi: 10.1016/s0305-7372(75)80003-x

Casper, E. S. et al. 1994. Phase II trial of gemcitabine (2,2'-difluorodeoxycytidine) in patients with adenocarcinoma of the pancreas. *Invest New Drugs* 12(1), pp. 29-34. doi: 10.1007/BF00873232

Castanon, I., Abrami, L., Holtzer, L., Heisenberg, C. P., van der Goot, F. G. and Gonzalez-Gaitan, M. 2013. Anthrax toxin receptor 2a controls mitotic spindle positioning. *Nat Cell Biol* 15(1), pp. 28-39. doi: 10.1038/ncb2632

Cavallaro, U. and Christofori, G. 2004. Cell adhesion and signalling by cadherins and Ig-CAMs in cancer. *Nat Rev Cancer* 4(2), pp. 118-132. doi: 10.1038/nrc1276

Chan, B. M., Matsuura, N., Takada, Y., Zetter, B. R. and Hemler, M. E. 1991. In vitro and in vivo consequences of VLA-2 expression on rhabdomyosarcoma cells. *Science* 251(5001), pp. 1600-1602. doi: 10.1126/science.2011740

Chan, C. E. and Odde, D. J. 2008. Traction dynamics of filopodia on compliant substrates. *Science* 322(5908), pp. 1687-1691. doi: 10.1126/science.1163595

Chandler, N. M., Canete, J. J. and Callery, M. P. 2004. Increased expression of NF-kappa B subunits in human pancreatic cancer cells. *J Surg Res* 118(1), pp. 9-14. doi: 10.1016/S0022-4804(03)00354-8

Charafe-Jauffret, E. et al. 2009. Breast cancer cell lines contain functional cancer stem cells with metastatic capacity and a distinct molecular signature. *Cancer Res* 69(4), pp. 1302-1313. doi: 10.1158/0008-5472.CAN-08-2741

Chen, C., Pore, N., Behrooz, A., Ismail-Beigi, F. and Maity, A. 2001. Regulation of glut1 mRNA by hypoxia-inducible factor-1. Interaction between H-ras and hypoxia. *J Biol Chem* 276(12), pp. 9519-9525. doi: 10.1074/jbc.M010144200

Chen, E. Y. et al. 2013. Enrichr: interactive and collaborative HTML5 gene list enrichment analysis tool. *BMC Bioinformatics* 14, p. 128. doi: 10.1186/1471-2105-14-128

Chen, M. B., Lamar, J. M., Li, R., Hynes, R. O. and Kamm, R. D. 2016a. Elucidation of the Roles of Tumor Integrin beta1 in the Extravasation Stage of the Metastasis Cascade. *Cancer Res* 76(9), pp. 2513-2524. doi: 10.1158/0008-5472.CAN-15-1325

Chen, S. Y. and Chen, H. C. 2006. Direct interaction of focal adhesion kinase (FAK) with Met is required for FAK to promote hepatocyte growth factor-induced cell invasion. *Mol Cell Biol* 26(13), pp. 5155-5167. doi: 10.1128/MCB.02186-05

Chen, X., Liu, F., Xue, Q., Weng, X. and Xu, F. 2021. Metastatic pancreatic cancer: Mechanisms and detection (Review). *Oncol Rep* 46(5), doi: 10.3892/or.2021.8182

Chen, X., Su, Z., Wang, S. and Xu, H. 2016b. Clinical and prognostic significance of Arl4c expression in colorectal cancer. *Cancer Biomark* 16(2), pp. 253-257. doi: 10.3233/CBM-150562

Cheng, J. Q., Jiang, X., Fraser, M., Li, M., Dan, H. C., Sun, M. and Tsang, B. K. 2002. Role of X-linked inhibitor of apoptosis protein in chemoresistance in ovarian cancer: possible involvement of the phosphoinositide-3 kinase/Akt pathway. *Drug Resist Updat* 5(3-4), pp. 131-146. doi: 10.1016/s1368-7646(02)00003-1

Cheng, S. H., Cheng, Y. J., Jin, Z. Y. and Xue, H. D. 2019. Unresectable pancreatic ductal adenocarcinoma: Role of CT quantitative imaging biomarkers for predicting outcomes of patients treated with chemotherapy. *Eur J Radiol* 113, pp. 188-197. doi: 10.1016/j.ejrad.2019.02.009

Chin, L. et al. 1999. p53 deficiency rescues the adverse effects of telomere loss and cooperates with telomere dysfunction to accelerate carcinogenesis. *Cell* 97(4), pp. 527-538. doi: 10.1016/s0092-8674(00)80762-x

Chlenski, A. et al. 1999. zo-2 gene alternative promoters in normal and neoplastic human pancreatic duct cells. *Int J Cancer* 83(3), pp. 349-358. doi: 10.1002/(sici)1097-0215(19991029)83:3<349::aid-ijc10>3.0.co;2-c

Chlenski, A., Ketels, K. V., Korovaitseva, G. I., Talamonti, M. S., Oyasu, R. and Scarpelli, D. G. 2000. Organization and expression of the human zo-2 gene (tjp-2) in normal and neoplastic tissues. *Biochim Biophys Acta* 1493(3), pp. 319-324. doi: 10.1016/s0167-4781(00)00185-8

Choudhury, A. et al. 2004. MUC4 mucin expression in human pancreatic tumours is affected by organ environment: the possible role of TGFbeta2. *Br J Cancer* 90(3), pp. 657-664. doi: 10.1038/sj.bjc.6601604

Chow, W. H., Gridley, G., Nyren, O., Linet, M. S., Ekbom, A., Fraumeni, J. F., Jr. and Adami, H. O. 1995. Risk of pancreatic cancer following diabetes mellitus: a nationwide cohort study in Sweden. *J Natl Cancer Inst* 87(12), pp. 930-931. doi: 10.1093/jnci/87.12.930

Chu, K. et al. 2008. Cadherin-11 promotes the metastasis of prostate cancer cells to bone. *Mol Cancer Res* 6(8), pp. 1259-1267. doi: 10.1158/1541-7786.MCR-08-0077

Chu, L. C., Goggins, M. G. and Fishman, E. K. 2017. Diagnosis and Detection of Pancreatic Cancer. *Cancer J* 23(6), pp. 333-342. doi: 10.1097/PPO.0000000000000290

Ciardiello, F. and Tortora, G. 2008. EGFR antagonists in cancer treatment. *N Engl J Med* 358(11), pp. 1160-1174. doi: 10.1056/NEJMra0707704

Coghlin, C. and Murray, G. I. 2010. Current and emerging concepts in tumour metastasis. *J Pathol* 222(1), pp. 1-15. doi: 10.1002/path.2727

Colas-Algora, N. and Millan, J. 2019. How many cadherins do human endothelial cells express? *Cell Mol Life Sci* 76(7), pp. 1299-1317. doi: 10.1007/s00018-018-2991-9

Colognato, H., Baron, W., Avellana-Adalid, V., Relvas, J. B., Baron-Van Evercooren, A., Georges-Labouesse, E. and ffrench-Constant, C. 2002. CNS integrins switch growth factor signalling to promote target-dependent survival. *Nat Cell Biol* 4(11), pp. 833-841. doi: 10.1038/ncb865

Connolly, D. T. et al. 1989. Tumor vascular permeability factor stimulates endothelial cell growth and angiogenesis. *J Clin Invest* 84(5), pp. 1470-1478. doi: 10.1172/JCI114322

Cordes, N. and Meineke, V. 2003. Cell adhesion-mediated radioresistance (CAM-RR). Extracellular matrix-dependent improvement of cell survival in human tumor and normal cells in vitro. *Strahlenther Onkol* 179(5), pp. 337-344. doi: 10.1007/s00066-003-1074-4

Corps, A. N., Sowter, H. M. and Smith, S. K. 1997. Hepatocyte growth factor stimulates motility, chemotaxis and mitogenesis in ovarian carcinoma cells expressing high levels of c-met. *Int J Cancer* 73(1), pp. 151-155. doi: 10.1002/(sici)1097-0215(19970926)73:1<151::aid-ijc23>3.0.co;2-i

Coughlin, S. S., Calle, E. E., Patel, A. V. and Thun, M. J. 2000. Predictors of pancreatic cancer mortality among a large cohort of United States adults. *Cancer Causes Control* 11(10), pp. 915-923. doi: 10.1023/a:1026580131793

Coveler, A. L. et al. 2021. Pancreas Cancer-Associated Pain Management. *Oncologist* 26(6), pp. e971-e982. doi: 10.1002/onco.13796

Cryan, L. M. and Rogers, M. S. 2011a. Targeting the anthrax receptors, TEM-8 and CMG-2, for anti-angiogenic therapy. *Front Biosci (Landmark Ed)* 16(4), pp. 1574-1588. doi: 10.2741/3806

Cryan, L. M. and Rogers, M. S. 2011b. Targeting the anthrax receptors, TEM-8 and CMG-2, for anti-angiogenic therapy. *Front Biosci (Landmark Ed)* 16, pp. 1574-1588. doi: 10.2741/3806

Cryan, L. M. et al. 2022. Capillary morphogenesis gene 2 (CMG2) mediates growth factor-induced angiogenesis by regulating endothelial cell chemotaxis. *Angiogenesis* 25(3), pp. 397-410. doi: 10.1007/s10456-022-09833-w

Cuervo, A. M. 2004. Autophagy: many paths to the same end. *Mol Cell Biochem* 263(1-2), pp. 55-72.

Curiel, T. J. et al. 2004. Dendritic cell subsets differentially regulate angiogenesis in human ovarian cancer. *Cancer Res* 64(16), pp. 5535-5538. doi: 10.1158/0008-5472.CAN-04-1272

Curto, M., Cole, B. K., Lallemand, D., Liu, C. H. and McClatchey, A. I. 2007. Contact-dependent inhibition of EGFR signaling by Nf2/Merlin. *J Cell Biol* 177(5), pp. 893-903. doi: 10.1083/jcb.200703010

D'Onofrio, P. M., Shabanzadeh, A. P., Choi, B. K., Bahr, M. and Koeberle, P. D. 2019. MMP Inhibition Preserves Integrin Ligation and FAK Activation to Induce Survival and Regeneration in RGCs Following Optic Nerve Damage. *Invest Ophthalmol Vis Sci* 60(2), pp. 634-649. doi: 10.1167/iovs.18-25257

Dai, J., Ai, K., Du, Y. and Chen, G. 2011. Sonic hedgehog expression correlates with distant metastasis in pancreatic adenocarcinoma. *Pancreas* 40(2), pp. 233-236. doi: 10.1097/MPA.0b013e3181f7e09f

Dalle Vedove, A. et al. 2019. Structure-Based Virtual Screening Allows the Identification of Efficient Modulators of E-Cadherin-Mediated Cell-Cell Adhesion. *Int J Mol Sci* 20(14), doi: 10.3390/ijms20143404

Damiano, J. S., Hazlehurst, L. A. and Dalton, W. S. 2001. Cell adhesion-mediated drug resistance (CAM-DR) protects the K562 chronic myelogenous leukemia cell line from apoptosis induced by BCR/ABL inhibition, cytotoxic drugs, and gamma-irradiation. *Leukemia* 15(8), pp. 1232-1239. doi: 10.1038/sj.leu.2402179

Dart, D. A., Arisan, D. E., Owen, S., Hao, C., Jiang, W. G. and Uysal-Onganer, P. 2019. Wnt-11 Expression Promotes Invasiveness and Correlates with Survival in Human Pancreatic Ductal Adeno Carcinoma. *Genes (Basel)* 10(11), doi: 10.3390/genes10110921

Dass, K., Ahmad, A., Azmi, A. S., Sarkar, S. H. and Sarkar, F. H. 2008. Evolving role of uPA/uPAR system in human cancers. *Cancer Treat Rev* 34(2), pp. 122-136. doi: 10.1016/j.ctrv.2007.10.005

Datta, S. R., Dudek, H., Tao, X., Masters, S., Fu, H., Gotoh, Y. and Greenberg, M. E. 1997. Akt

phosphorylation of BAD couples survival signals to the cell-intrinsic death machinery. *Cell* 91(2), pp. 231-241. doi: 10.1016/s0092-8674(00)80405-5

Datta, S. R., Katsov, A., Hu, L., Petros, A., Fesik, S. W., Yaffe, M. B. and Greenberg, M. E. 2000. 14-3-3 proteins and survival kinases cooperate to inactivate BAD by BH3 domain phosphorylation. *Mol Cell* 6(1), pp. 41-51.

Davies, M. A. et al. 1999. Regulation of Akt/PKB activity, cellular growth, and apoptosis in prostate carcinoma cells by MMAC/PTEN. *Cancer Res* 59(11), pp. 2551-2556.

De Craene, B. and Berx, G. 2013. Regulatory networks defining EMT during cancer initiation and progression. *Nat Rev Cancer* 13(2), pp. 97-110. doi: 10.1038/nrc3447

De Franceschi, N., Hamidi, H., Alanko, J., Sahgal, P. and Ivaska, J. 2015. Integrin traffic - the update. *J Cell Sci* 128(5), pp. 839-852. doi: 10.1242/jcs.161653

de Heer, E. C., Jalving, M. and Harris, A. L. 2020. HIFs, angiogenesis, and metabolism: elusive enemies in breast cancer. *J Clin Invest* 130(10), pp. 5074-5087. doi: 10.1172/JCI137552

Debiec, K. T., Gronenborn, A. M. and Chong, L. T. 2014. Evaluating the strength of salt bridges: a comparison of current biomolecular force fields. *J Phys Chem B* 118(24), pp. 6561-6569. doi: 10.1021/jp500958r

Debruyne, D., Boterberg, T. and Bracke, M. E. 2014. Cell aggregation assays. *Methods Mol Biol* 1070, pp. 77-92. doi: 10.1007/978-1-4614-8244-4_6

Degirmenci, U., Wang, M. and Hu, J. 2020. Targeting Aberrant RAS/RAF/MEK/ERK Signaling for Cancer Therapy. *Cells* 9(1), doi: 10.3390/cells9010198

Degterev, A. et al. 2005. Chemical inhibitor of nonapoptotic cell death with therapeutic potential for ischemic brain injury. *Nat Chem Biol* 1(2), pp. 112-119. doi: 10.1038/nchembio711

Deissler, H. L., Deissler, H. and Lang, G. E. 2010. Inhibition of protein kinase C is not sufficient to prevent or reverse effects of VEGF165 on claudin-1 and permeability in microvascular retinal endothelial cells. *Invest Ophthalmol Vis Sci* 51(1), pp. 535-542. doi: 10.1167/iovs.09-3917

Desgrosellier, J. S. et al. 2009. An integrin alpha(v)beta(3)-c-Src oncogenic unit promotes anchorage-independence and tumor progression. *Nat Med* 15(10), pp. 1163-1169. doi: 10.1038/nm.2009

Deshpande, A., Sicinski, P. and Hinds, P. W. 2005. Cyclins and cdks in development and cancer: a perspective. *Oncogene* 24(17), pp. 2909-2915. doi: 10.1038/sj.onc.1208618

Desiderio, J. et al. 2017. The 30-year experience-A meta-analysis of randomised and high-quality non-randomised studies of hyperthermic intraperitoneal chemotherapy in the treatment of gastric cancer. *Eur J Cancer* 79, pp. 1-14. doi: 10.1016/j.ejca.2017.03.030

Deuquet, J., Lausch, E., Superti-Furga, A. and van der Goot, F. G. 2012. The dark sides of capillary morphogenesis gene 2. *EMBO J* 31(1), pp. 3-13. doi: 10.1038/emboj.2011.442

Dice, J. F. 2007. Chaperone-mediated autophagy. *Autophagy* 3(4), pp. 295-299. doi:

10.4161/auto.4144

Dickson, D. W. 2004. Apoptotic mechanisms in Alzheimer neurofibrillary degeneration: cause or effect? *J Clin Invest* 114(1), pp. 23-27. doi: 10.1172/JCI22317

Dobbie, J. W. and Anderson, J. D. 1996. Ultrastructure, distribution, and density of lamellar bodies in human peritoneum. *Perit Dial Int* 16(5), pp. 488-496.

Dong, Q. G. et al. 2002. The function of multiple IkappaB : NF-kappaB complexes in the resistance of cancer cells to Taxol-induced apoptosis. *Oncogene* 21(42), pp. 6510-6519. doi: 10.1038/sj.onc.1205848

Dottermusch, M., Kruger, S., Behrens, H. M., Halske, C. and Rocken, C. 2019. Expression of the potential therapeutic target claudin-18.2 is frequently decreased in gastric cancer: results from a large Caucasian cohort study. *Virchows Arch* 475(5), pp. 563-571. doi: 10.1007/s00428-019-02624-7

Douma, S., Van Laar, T., Zevenhoven, J., Meuwissen, R., Van Garderen, E. and Peeper, D. S. 2004. Suppression of anoikis and induction of metastasis by the neurotrophic receptor TrkB. *Nature* 430(7003), pp. 1034-1039. doi: 10.1038/nature02765

Dowling, O. et al. 2003. Mutations in capillary morphogenesis gene-2 result in the allelic disorders juvenile hyaline fibromatosis and infantile systemic hyalinosis. *Am J Hum Genet* 73(4), pp. 957-966. doi: 10.1086/378781

Driessens, M. H., Stroeken, P. J., Rodriguez Erena, N. F., van der Valk, M. A., van Rijthoven, E. A. and Roos, E. 1995. Targeted disruption of CD44 in MDAY-D2 lymphosarcoma cells has no effect on subcutaneous growth or metastatic capacity. *J Cell Biol* 131(6 Pt 2), pp. 1849-1855. doi: 10.1083/jcb.131.6.1849

Dyson, H. J. and Wright, P. E. 2005. Intrinsically unstructured proteins and their functions. *Nat Rev Mol Cell Biol* 6(3), pp. 197-208. doi: 10.1038/nrm1589

Eberl, M. et al. 2012. Hedgehog-EGFR cooperation response genes determine the oncogenic phenotype of basal cell carcinoma and tumour-initiating pancreatic cancer cells. *EMBO Mol Med* 4(3), pp. 218-233. doi: 10.1002/emmm.201100201

Eke, I. et al. 2012. beta(1)Integrin/FAK/cortactin signaling is essential for human head and neck cancer resistance to radiotherapy. *J Clin Invest* 122(4), pp. 1529-1540. doi: 10.1172/JCI61350

Eke, I., Schneider, L., Forster, C., Zips, D., Kunz-Schughart, L. A. and Cordes, N. 2013a. EGFR/JIP-4/JNK2 signaling attenuates cetuximab-mediated radiosensitization of squamous cell carcinoma cells. *Cancer Res* 73(1), pp. 297-306. doi: 10.1158/0008-5472.CAN-12-2021

Eke, I., Storch, K., Krause, M. and Cordes, N. 2013b. Cetuximab attenuates its cytotoxic and radiosensitizing potential by inducing fibronectin biosynthesis. *Cancer Res* 73(19), pp. 5869-5879. doi: 10.1158/0008-5472.CAN-13-0344

Ekert, P. G. and Vaux, D. L. 2005. The mitochondrial death squad: hardened killers or innocent bystanders? *Curr Opin Cell Biol* 17(6), pp. 626-630. doi: 10.1016/j.ceb.2005.09.001

Elmore, S. 2007. Apoptosis: a review of programmed cell death. *Toxicol Pathol* 35(4), pp. 495-516. doi: 10.1080/01926230701320337

Entwistle, J. et al. 1995. Characterization of the murine gene encoding the hyaluronan receptor RHAMM. *Gene* 163(2), pp. 233-238. doi: 10.1016/0378-1119(95)00398-p

Esseltine, J. L. and Laird, D. W. 2016. Next-Generation Connexin and Pannexin Cell Biology. *Trends Cell Biol* 26(12), pp. 944-955. doi: 10.1016/j.tcb.2016.06.003

Evanko, S. P., Tammi, M. I., Tammi, R. H. and Wight, T. N. 2007. Hyaluronan-dependent pericellular matrix. *Adv Drug Deliv Rev* 59(13), pp. 1351-1365. doi: 10.1016/j.addr.2007.08.008

Ezumi, K. et al. 2008. Aberrant expression of connexin 26 is associated with lung metastasis of colorectal cancer. *Clin Cancer Res* 14(3), pp. 677-684. doi: 10.1158/1078-0432.CCR-07-1184

Faassen, A. E., Schrager, J. A., Klein, D. J., Oegema, T. R., Couchman, J. R. and McCarthy, J. B. 1992. A cell surface chondroitin sulfate proteoglycan, immunologically related to CD44, is involved in type I collagen-mediated melanoma cell motility and invasion. *J Cell Biol* 116(2), pp. 521-531. doi: 10.1083/jcb.116.2.521

Fabisiewicz, A. and Grzybowska, E. 2017. CTC clusters in cancer progression and metastasis. *Med Oncol* 34(1), p. 12. doi: 10.1007/s12032-016-0875-0

Fang, Y., Yao, Q., Chen, Z., Xiang, J., William, F. E., Gibbs, R. A. and Chen, C. 2013. Genetic and molecular alterations in pancreatic cancer: implications for personalized medicine. *Med Sci Monit* 19, pp. 916-926. doi: 10.12659/MSM.889636

Fang, Z. et al. 2022. Sex Hormone-regulated CMG2 Is Involved in Breast and Prostate Cancer Progression. *Cancer Genomics Proteomics* 19(6), pp. 703-710. doi: 10.21873/cgp.20353

Fanhchaksai, K. et al. 2016. Host stromal versican is essential for cancer-associated fibroblast function to inhibit cancer growth. *Int J Cancer* 138(3), pp. 630-641. doi: 10.1002/ijc.29804

Fattahi, R., Balci, N. C., Perman, W. H., Hsueh, E. C., Alkaade, S., Havlioglu, N. and Burton, F. R. 2009. Pancreatic diffusion-weighted imaging (DWI): comparison between mass-forming focal pancreatitis (FP), pancreatic cancer (PC), and normal pancreas. *J Magn Reson Imaging* 29(2), pp. 350-356. doi: 10.1002/jmri.21651

Fearon, K. C., Glass, D. J. and Guttridge, D. C. 2012. Cancer cachexia: mediators, signaling, and metabolic pathways. *Cell Metab* 16(2), pp. 153-166. doi: 10.1016/j.cmet.2012.06.011

Feng, Y. and Walsh, C. A. 2004. The many faces of filamin: a versatile molecular scaffold for cell motility and signalling. *Nat Cell Biol* 6(11), pp. 1034-1038. doi: 10.1038/ncb1104-1034

Feng, Z., Hu, W., de Stanchina, E., Teresky, A. K., Jin, S., Lowe, S. and Levine, A. J. 2007. The regulation of AMPK beta1, TSC2, and PTEN expression by p53: stress, cell and tissue specificity, and the role of these gene products in modulating the IGF-1-AKT-mTOR pathways. *Cancer Res* 67(7), pp. 3043-3053. doi: 10.1158/0008-5472.CAN-06-4149

Ferrara, N. 2009. Vascular endothelial growth factor. *Arterioscler Thromb Vasc Biol* 29(6), pp. 789-791. doi: 10.1161/ATVBAHA.108.179663

Fink, S. L. and Cookson, B. T. 2005. Apoptosis, pyroptosis, and necrosis: mechanistic description of dead and dying eukaryotic cells. *Infect Immun* 73(4), pp. 1907-1916. doi: 10.1128/IAI.73.4.1907-1916.2005

Finnell, J. G. et al. 2020. A Canstatin-Derived Peptide Provides Insight into the Role of Capillary Morphogenesis Gene 2 in Angiogenic Regulation and Matrix Uptake. *ACS Chem Biol* 15(2), pp. 587-596. doi: 10.1021/acschembio.0c00064

Forough, R., Weylie, B., Patel, C., Ambrus, S., Singh, U. S. and Zhu, J. 2005. Role of AKT/PKB signaling in fibroblast growth factor-1 (FGF-1)-induced angiogenesis in the chicken chorioallantoic membrane (CAM). *J Cell Biochem* 94(1), pp. 109-116. doi: 10.1002/jcb.20274

Frisch, S. M. and Francis, H. 1994. Disruption of epithelial cell-matrix interactions induces apoptosis. *J Cell Biol* 124(4), pp. 619-626. doi: 10.1083/jcb.124.4.619

Frisch, S. M., Vuori, K., Kelaita, D. and Sicks, S. 1996a. A role for Jun-N-terminal kinase in anoikis; suppression by bcl-2 and crmA. *J Cell Biol* 135(5), pp. 1377-1382. doi: 10.1083/jcb.135.5.1377

Frisch, S. M., Vuori, K., Ruoslahti, E. and Chan-Hui, P. Y. 1996b. Control of adhesion-dependent cell survival by focal adhesion kinase. *J Cell Biol* 134(3), pp. 793-799. doi: 10.1083/jcb.134.3.793

Fu, S. et al. 2010. The structure of tumor endothelial marker 8 (TEM8) extracellular domain and implications for its receptor function for recognizing anthrax toxin. *PLoS One* 5(6), p. e11203. doi: 10.1371/journal.pone.0011203

Fukata, M. and Kaibuchi, K. 2001. Rho-family GTPases in cadherin-mediated cell-cell adhesion. *Nat Rev Mol Cell Biol* 2(12), pp. 887-897. doi: 10.1038/35103068

Furuyama, H., Arii, S., Mori, A. and Imamura, M. 2000. Role of E-cadherin in peritoneal dissemination of the pancreatic cancer cell line, panc-1, through regulation of cell to cell contact. *Cancer Lett* 157(2), pp. 201-209. doi: 10.1016/s0304-3835(00)00488-2

Gaggioli, C., Hooper, S., Hidalgo-Carcedo, C., Grosse, R., Marshall, J. F., Harrington, K. and Sahai, E. 2007. Fibroblast-led collective invasion of carcinoma cells with differing roles for RhoGTPases in leading and following cells. *Nat Cell Biol* 9(12), pp. 1392-1400. doi: 10.1038/ncb1658

Gahmberg, C. G. and Gronholm, M. 2022. How integrin phosphorylations regulate cell adhesion and signaling. *Trends Biochem Sci* 47(3), pp. 265-278. doi: 10.1016/j.tibs.2021.11.003

Gapstur, S. M., Gann, P. H., Lowe, W., Liu, K., Colangelo, L. and Dyer, A. 2000. Abnormal glucose metabolism and pancreatic cancer mortality. *JAMA* 283(19), pp. 2552-2558. doi: 10.1001/jama.283.19.2552

Garces, C. A., Kurenova, E. V., Golubovskaya, V. M. and Cance, W. G. 2006. Vascular endothelial growth factor receptor-3 and focal adhesion kinase bind and suppress apoptosis in breast cancer cells. *Cancer Res* 66(3), pp. 1446-1454. doi: 10.1158/0008-5472.CAN-05-1661

Garcia-Alvarez, B. et al. 2003. Structural determinants of integrin recognition by talin. *Mol Cell* 11(1), pp. 49-58. doi: 10.1016/s1097-2765(02)00823-7

Gardel, M. L., Sabass, B., Ji, L., Danuser, G., Schwarz, U. S. and Waterman, C. M. 2008. Traction stress in focal adhesions correlates biphasically with actin retrograde flow speed. *J Cell Biol* 183(6), pp. 999-1005. doi: 10.1083/jcb.200810060

Gardiner, E. E. and D'Souza, S. E. 1999. Sequences within fibrinogen and intercellular adhesion molecule-1 (ICAM-1) modulate signals required for mitogenesis. *J Biol Chem* 274(17), pp. 11930-11936. doi: 10.1074/jbc.274.17.11930

Gavalas, N. G. et al. 2013. Angiogenesis-related pathways in the pathogenesis of ovarian cancer. *Int J Mol Sci* 14(8), pp. 15885-15909. doi: 10.3390/ijms140815885

Gazvani, R. and Templeton, A. 2002. Peritoneal environment, cytokines and angiogenesis in the pathophysiology of endometriosis. *Reproduction* 123(2), pp. 217-226. doi: 10.1530/rep.0.1230217

Gelb, M. H., Tamanoi, F., Yokoyama, K., Ghomashchi, F., Esson, K. and Gould, M. N. 1995. The inhibition of protein prenyltransferases by oxygenated metabolites of limonene and perillyl alcohol. *Cancer Lett* 91(2), pp. 169-175. doi: 10.1016/0304-3835(95)03747-k

Georgiadou, M. and Ivaska, J. 2017. Tensins: Bridging AMP-Activated Protein Kinase with Integrin Activation. *Trends Cell Biol* 27(10), pp. 703-711. doi: 10.1016/j.tcb.2017.06.004

Georgiadou, M. et al. 2017. AMPK negatively regulates tensin-dependent integrin activity. *J Cell Biol* 216(4), pp. 1107-1121. doi: 10.1083/jcb.201609066

Ghandi, M. et al. 2019. Next-generation characterization of the Cancer Cell Line Encyclopedia. *Nature* 569(7757), pp. 503-508. doi: 10.1038/s41586-019-1186-3

Ghebranious, N. and Donehower, L. A. 1998. Mouse models in tumor suppression. *Oncogene* 17(25), pp. 3385-3400. doi: 10.1038/sj.onc.1202573

Ghislin, S., Obino, D., Middendorp, S., Boggetto, N., Alcaide-Loridan, C. and Deshayes, F. 2012. LFA-1 and ICAM-1 expression induced during melanoma-endothelial cell co-culture favors the transendothelial migration of melanoma cell lines in vitro. *BMC Cancer* 12, p. 455. doi: 10.1186/1471-2407-12-455

Ghosh, I., Chattopadhaya, R., Kumar, V., Chakravarty, B. N. and Datta, K. 2007. Hyaluronan binding protein-1: a modulator of sperm-oocyte interaction. *Soc Reprod Fertil Suppl* 63, pp. 539-543.

Giancotti, F. G. 2000. Complexity and specificity of integrin signalling. *Nat Cell Biol* 2(1), pp. E13-14. doi: 10.1038/71397

Giancotti, F. G. and Ruoslahti, E. 1999. Integrin signaling. *Science* 285(5430), pp. 1028-1032. doi: 10.1126/science.285.5430.1028

Giardiello, F. M. et al. 2000. Very high risk of cancer in familial Peutz-Jeghers syndrome. *Gastroenterology* 119(6), pp. 1447-1453. doi: 10.1053/gast.2000.20228

Giesel, F. L. et al. 2021. FAPI-74 PET/CT Using Either (18)F-AlF or Cold-Kit (68)Ga Labeling: Biodistribution, Radiation Dosimetry, and Tumor Delineation in Lung Cancer Patients. *J Nucl Med* 62(2), pp. 201-207. doi: 10.2967/jnumed.120.245084

Gilley, J., Coffer, P. J. and Ham, J. 2003. FOXO transcription factors directly activate bim gene expression and promote apoptosis in sympathetic neurons. *J Cell Biol* 162(4), pp. 613-622. doi: 10.1083/jcb.200303026

Gimond, C. et al. 1999. Induction of cell scattering by expression of beta1 integrins in beta1-deficient epithelial cells requires activation of members of the rho family of GTPases and downregulation of cadherin and catenin function. *J Cell Biol* 147(6), pp. 1325-1340. doi: 10.1083/jcb.147.6.1325

Gkountela, S. et al. 2019. Circulating Tumor Cell Clustering Shapes DNA Methylation to Enable Metastasis Seeding. *Cell* 176(1-2), pp. 98-112 e114. doi: 10.1016/j.cell.2018.11.046

Gnoni, A. et al. 2013. Carcinogenesis of pancreatic adenocarcinoma: precursor lesions. *Int J Mol Sci* 14(10), pp. 19731-19762. doi: 10.3390/ijms141019731

Go, M. Y., Kim, S., Partridge, A. W., Melnyk, R. A., Rath, A., Deber, C. M. and Mogridge, J. 2006. Self-association of the transmembrane domain of an anthrax toxin receptor. *J Mol Biol* 360(1), pp. 145-156. doi: 10.1016/j.jmb.2006.04.072

Gocheva, V. et al. 2010. IL-4 induces cathepsin protease activity in tumor-associated macrophages to promote cancer growth and invasion. *Genes Dev* 24(3), pp. 241-255. doi: 10.1101/gad.1874010

Goggins, M., Hruban, R. H. and Kern, S. E. 2000. BRCA2 is inactivated late in the development of pancreatic intraepithelial neoplasia: evidence and implications. *Am J Pathol* 156(5), pp. 1767-1771. doi: 10.1016/S0002-9440(10)65047-X

Gold, E. B. and Goldin, S. B. 1998. Epidemiology of and risk factors for pancreatic cancer. *Surg Oncol Clin N Am* 7(1), pp. 67-91.

Goldstein, A. M. et al. 1995. Increased risk of pancreatic cancer in melanoma-prone kindreds with p16INK4 mutations. *N Engl J Med* 333(15), pp. 970-974. doi: 10.1056/NEJM199510123331504

Goodison, S., Urquidi, V. and Tarin, D. 1999. CD44 cell adhesion molecules. *Mol Pathol* 52(4), pp. 189-196. doi: 10.1136/mp.52.4.189

Goral, V. 2015. Pancreatic Cancer: Pathogenesis and Diagnosis. *Asian Pac J Cancer Prev* 16(14), pp. 5619-5624. doi: 10.7314/apjcp.2015.16.14.5619

Gorry, M. C. et al. 1997. Mutations in the cationic trypsinogen gene are associated with recurrent acute and chronic pancreatitis. *Gastroenterology* 113(4), pp. 1063-1068. doi: 10.1053/gast.1997.v113.pm9322498

Greither, T. et al. 2017. CMG2 Expression Is an Independent Prognostic Factor for Soft Tissue Sarcoma Patients. *Int J Mol Sci* 18(12), doi: 10.3390/ijms18122648

Grigorian, I. Y., Linkova, N. S., Polyakova, V. O., Paltseva, E. M. and Kozlov, K. L. 2015. [Signal molecules of endometrium: gerontological and general pathhological aspects]. *Adv Gerontol* 28(3), pp. 453-461.

Grzesiak, J. J. et al. 2011. Knockdown of the beta(1) integrin subunit reduces primary tumor growth and inhibits pancreatic cancer metastasis. *Int J Cancer* 129(12), pp. 2905-2915. doi: 10.1002/ijc.25942

Gu, D. et al. 2018. Simultaneous Inhibition of MEK and Hh Signaling Reduces Pancreatic Cancer Metastasis. *Cancers (Basel)* 10(11), doi: 10.3390/cancers10110403

Gu, X., Niu, J., Dorahy, D. J., Scott, R. and Agrez, M. V. 2002. Integrin alpha(v)beta6-associated ERK2 mediates MMP-9 secretion in colon cancer cells. *Br J Cancer* 87(3), pp. 348-351. doi: 10.1038/sj.bjc.6600480

Gumbiner, B., Lowenkopf, T. and Apatira, D. 1991. Identification of a 160-kDa polypeptide that binds to the tight junction protein ZO-1. *Proc Natl Acad Sci U S A* 88(8), pp. 3460-3464. doi: 10.1073/pnas.88.8.3460

Guo, P. et al. 2014. ICAM-1 as a molecular target for triple negative breast cancer. *Proc Natl Acad Sci U S A* 111(41), pp. 14710-14715. doi: 10.1073/pnas.1408556111

Guo, W., Pylayeva, Y., Pepe, A., Yoshioka, T., Muller, W. J., Inghirami, G. and Giancotti, F. G. 2006. Beta 4 integrin amplifies ErbB2 signaling to promote mammary tumorigenesis. *Cell* 126(3), pp. 489-502. doi: 10.1016/j.cell.2006.05.047

Hahn, W. C., Counter, C. M., Lundberg, A. S., Beijersbergen, R. L., Brooks, M. W. and Weinberg, R. A. 1999. Creation of human tumour cells with defined genetic elements. *Nature* 400(6743), pp. 464-468. doi: 10.1038/22780

Hamidi, H. and Ivaska, J. 2018. Every step of the way: integrins in cancer progression and metastasis. *Nat Rev Cancer* 18(9), pp. 533-548. doi: 10.1038/s41568-018-0038-z

Hamidi, H., Pietila, M. and Ivaska, J. 2016. The complexity of integrins in cancer and new scopes for therapeutic targeting. *Br J Cancer* 115(9), pp. 1017-1023. doi: 10.1038/bjc.2016.312

Han, H. J. et al. 2021. Fibronectin regulates anoikis resistance via cell aggregate formation. *Cancer Lett* 508, pp. 59-72. doi: 10.1016/j.canlet.2021.03.011

Hanahan, D. and Weinberg, R. A. 2011. Hallmarks of cancer: the next generation. *Cell* 144(5), pp. 646-674. doi: 10.1016/j.cell.2011.02.013

Hanlon, L. et al. 2010. Notch1 functions as a tumor suppressor in a model of K-ras-induced pancreatic ductal adenocarcinoma. *Cancer Res* 70(11), pp. 4280-4286. doi: 10.1158/0008-5472.CAN-09-4645

Hehlgans, S., Haase, M. and Cordes, N. 2007. Signalling via integrins: implications for cell survival and anticancer strategies. *Biochim Biophys Acta* 1775(1), pp. 163-180. doi: 10.1016/j.bbcan.2006.09.001

Heldin, P. and Pertoft, H. 1993. Synthesis and assembly of the hyaluronan-containing coats around normal human mesothelial cells. *Exp Cell Res* 208(2), pp. 422-429. doi: 10.1006/excr.1993.1264

Hermann, P. C. et al. 2007. Distinct populations of cancer stem cells determine tumor growth and metastatic activity in human pancreatic cancer. *Cell Stem Cell* 1(3), pp. 313-323. doi: 10.1016/j.stem.2007.06.002

Hersh, D., Monack, D. M., Smith, M. R., Ghori, N., Falkow, S. and Zychlinsky, A. 1999. The Salmonella invasin SipB induces macrophage apoptosis by binding to caspase-1. *Proc Natl Acad Sci U S A* 96(5), pp. 2396-2401. doi: 10.1073/pnas.96.5.2396

Hezel, A. F., Kimmelman, A. C., Stanger, B. Z., Bardeesy, N. and Depinho, R. A. 2006. Genetics and biology of pancreatic ductal adenocarcinoma. *Genes Dev* 20(10), pp. 1218-1249. doi: 10.1101/gad.1415606

Hingorani, S. R. et al. 2005. Trp53R172H and KrasG12D cooperate to promote chromosomal instability and widely metastatic pancreatic ductal adenocarcinoma in mice. *Cancer Cell* 7(5), pp. 469-483. doi: 10.1016/j.ccr.2005.04.023

Hippo, Y. et al. 2001. Differential gene expression profiles of scirrhous gastric cancer cells with high metastatic potential to peritoneum or lymph nodes. *Cancer Res* 61(3), pp. 889-895.

Hirano, T. et al. 2002. Dominant negative MEKK1 inhibits survival of pancreatic cancer cells. *Oncogene* 21(38), pp. 5923-5928. doi: 10.1038/sj.onc.1205643

Hiraoka, N., Yamazaki-Itoh, R., Ino, Y., Mizuguchi, Y., Yamada, T., Hirohashi, S. and Kanai, Y. 2011. CXCL17 and ICAM2 are associated with a potential anti-tumor immune response in early intraepithelial stages of human pancreatic carcinogenesis. *Gastroenterology* 140(1), pp. 310-321. doi: 10.1053/j.gastro.2010.10.009

Hishinuma, S., Ogata, Y., Tomikawa, M., Ozawa, I., Hirabayashi, K. and Igarashi, S. 2006. Patterns of recurrence after curative resection of pancreatic cancer, based on autopsy findings. *J Gastrointest Surg* 10(4), pp. 511-518. doi: 10.1016/j.gassur.2005.09.016

Hofmann, M., Rudy, W., Zoller, M., Tolg, C., Ponta, H., Herrlich, P. and Gunthert, U. 1991. CD44 splice variants confer metastatic behavior in rats: homologous sequences are expressed in human tumor cell lines. *Cancer Res* 51(19), pp. 5292-5297.

Holmgren, L., O'Reilly, M. S. and Folkman, J. 1995. Dormancy of micrometastases: balanced proliferation and apoptosis in the presence of angiogenesis suppression. *Nat Med* 1(2), pp. 149-153. doi: 10.1038/nm0295-149

Hoskovec, D., Krska, Z., Dytrych, P. and Vocka, M. 2019. Peritoneal Carcinomatosis of Gastric Origin - Treatment Possibilities. *Klin Onkol* 32(5), pp. 345-348. doi: 10.14735/amko2019345

Hosotani, R. et al. 2002. Expression of integrin alphaVbeta3 in pancreatic carcinoma: relation to MMP-2 activation and lymph node metastasis. *Pancreas* 25(2), pp. e30-35. doi: 10.1097/00006676-200208000-00021

Howe, G. R. and Burch, J. D. 1996. Nutrition and pancreatic cancer. *Cancer Causes Control*

7(1), pp. 69-82. doi: 10.1007/BF00115639

Hu, Q. et al. 2018. Identification of ARL4C as a Peritoneal Dissemination-Associated Gene and Its Clinical Significance in Gastric Cancer. *Ann Surg Oncol* 25(3), pp. 745-753. doi: 10.1245/s10434-017-6292-6

Huang, B. et al. 2020. Molecular characterization of organoids derived from pancreatic intraductal papillary mucinous neoplasms. *J Pathol* 252(3), pp. 252-262. doi: 10.1002/path.5515

Hubbard, A. K. and Rothlein, R. 2000. Intercellular adhesion molecule-1 (ICAM-1) expression and cell signaling cascades. *Free Radic Biol Med* 28(9), pp. 1379-1386. doi: 10.1016/s0891-5849(00)00223-9

Huck, L., Pontier, S. M., Zuo, D. M. and Muller, W. J. 2010. beta1-integrin is dispensable for the induction of ErbB2 mammary tumors but plays a critical role in the metastatic phase of tumor progression. *Proc Natl Acad Sci U S A* 107(35), pp. 15559-15564. doi: 10.1073/pnas.1003034107

Hugen, N., van de Velde, C. J. H., de Wilt, J. H. W. and Nagtegaal, I. D. 2014. Metastatic pattern in colorectal cancer is strongly influenced by histological subtype. *Ann Oncol* 25(3), pp. 651-657. doi: 10.1093/annonc/mdt591

Hugo, H., Ackland, M. L., Blick, T., Lawrence, M. G., Clements, J. A., Williams, E. D. and Thompson, E. W. 2007. Epithelial--mesenchymal and mesenchymal--epithelial transitions in carcinoma progression. *J Cell Physiol* 213(2), pp. 374-383. doi: 10.1002/jcp.21223

Hungerford, J. E., Compton, M. T., Matter, M. L., Hoffstrom, B. G. and Otey, C. A. 1996. Inhibition of pp125FAK in cultured fibroblasts results in apoptosis. *J Cell Biol* 135(5), pp. 1383-1390. doi: 10.1083/jcb.135.5.1383

Hussain, F., Wang, J., Ahmed, R., Guest, S. K., Lam, E. W., Stamp, G. and El-Bahrawy, M. 2010. The expression of IL-8 and IL-8 receptors in pancreatic adenocarcinomas and pancreatic neuroendocrine tumours. *Cytokine* 49(2), pp. 134-140. doi: 10.1016/j.cyto.2009.11.010

Hynes, N. E. and Lane, H. A. 2005. ERBB receptors and cancer: the complexity of targeted inhibitors. *Nat Rev Cancer* 5(5), pp. 341-354. doi: 10.1038/nrc1609

Hynes, R. O. 1987. Integrins: a family of cell surface receptors. *Cell* 48(4), pp. 549-554. doi: 10.1016/0092-8674(87)90233-9

I, S. T. et al. 2004. ARAP3 is transiently tyrosine phosphorylated in cells attaching to fibronectin and inhibits cell spreading in a RhoGAP-dependent manner. *J Cell Sci* 117(Pt 25), pp. 6071-6084. doi: 10.1242/jcs.01526

Ichikawa, T., Haradome, H., Hachiya, J., Nitatori, T., Ohtomo, K., Kinoshita, T. and Araki, T. 1997. Pancreatic ductal adenocarcinoma: preoperative assessment with helical CT versus dynamic MR imaging. *Radiology* 202(3), pp. 655-662. doi: 10.1148/radiology.202.3.9051012

Idogawa, M., Adachi, M., Minami, T., Yasui, H. and Imai, K. 2003. Overexpression of BAD preferentially augments anoikis. *Int J Cancer* 107(2), pp. 215-223. doi: 10.1002/ijc.11399

Iida-Norita, R., Kawamura, M., Suzuki, Y., Hamada, S., Masamune, A., Furukawa, T. and Sato, Y. 2019. Vasohibin-2 plays an essential role in metastasis of pancreatic ductal adenocarcinoma. *Cancer Sci* 110(7), pp. 2296-2308. doi: 10.1111/cas.14041

Ilic, M. and Ilic, I. 2016. Epidemiology of pancreatic cancer. *World J Gastroenterol* 22(44), pp. 9694-9705. doi: 10.3748/wjg.v22.i44.9694

Inose, T. et al. 2009. Correlation between connexin 26 expression and poor prognosis of esophageal squamous cell carcinoma. *Ann Surg Oncol* 16(6), pp. 1704-1710. doi: 10.1245/s10434-009-0443-3

Ioannou, M., Kouvaras, E., Papamichali, R., Samara, M., Chiotoglou, I. and Koukoulis, G. 2018. Smad4 and epithelial-mesenchymal transition proteins in colorectal carcinoma: an immunohistochemical study. *J Mol Histol* 49(3), pp. 235-244. doi: 10.1007/s10735-018-9763-6

Ishigami, H. et al. 2018. Phase III Trial Comparing Intraperitoneal and Intravenous Paclitaxel Plus S-1 Versus Cisplatin Plus S-1 in Patients With Gastric Cancer With Peritoneal Metastasis: PHOENIX-GC Trial. *J Clin Oncol* 36(19), pp. 1922-1929. doi: 10.1200/JCO.2018.77.8613

Ishizawa, K. et al. 2010. Tumor-initiating cells are rare in many human tumors. *Cell Stem Cell* 7(3), pp. 279-282. doi: 10.1016/j.stem.2010.08.009

Ithychanda, S. S. et al. 2009. Identification and characterization of multiple similar ligand-binding repeats in filamin: implication on filamin-mediated receptor clustering and cross-talk. *J Biol Chem* 284(50), pp. 35113-35121. doi: 10.1074/jbc.M109.060954

Ito, K., Takemura, N., Inagaki, F., Mihara, F., Kurokawa, T. and Kokudo, N. 2019. Arterial blood supply to the pancreas from accessary middle colic artery. *Pancreatology* 19(5), pp. 781-785. doi: 10.1016/j.pan.2019.05.458

Ito, T., Yorioka, N., Yamamoto, M., Kataoka, K. and Yamakido, M. 2000. Effect of glucose on intercellular junctions of cultured human peritoneal mesothelial cells. *J Am Soc Nephrol* 11(11), pp. 1969-1979.

Jackson, D. G., Prevo, R., Clasper, S. and Banerji, S. 2001. LYVE-1, the lymphatic system and tumor lymphangiogenesis. *Trends Immunol* 22(6), pp. 317-321. doi: 10.1016/s1471-4906(01)01936-6

Jacobs, K., Feys, L., Vanhoecke, B., Van Marck, V. and Bracke, M. 2011. P-cadherin expression reduces melanoma growth, invasion, and responsiveness to growth factors in nude mice. *Eur J Cancer Prev* 20(3), pp. 207-216. doi: 10.1097/CEJ.0b013e3283429e8b

Jacquemet, G., Green, D. M., Bridgewater, R. E., von Kriegsheim, A., Humphries, M. J., Norman, J. C. and Caswell, P. T. 2013. RCP-driven alpha5beta1 recycling suppresses Rac and promotes RhoA activity via the RacGAP1-IQGAP1 complex. *J Cell Biol* 202(6), pp. 917-935. doi: 10.1083/jcb.201302041

Jacquemet, G., Paatero, I., Carisey, A. F., Padzik, A., Orange, J. S., Hamidi, H. and Ivaska, J. 2017. FiloQuant reveals increased filopodia density during breast cancer progression. *J Cell Biol* 216(10), pp. 3387-3403. doi: 10.1083/jcb.201704045

Jadin, L. et al. 2014. Characterization of a novel recombinant hyaluronan binding protein for tissue hyaluronan detection. *J Histochem Cytochem* 62(9), pp. 672-683. doi: 10.1369/0022155414540176

Jaeger, A. et al. 2023. Activated granulocytes and inflammatory cytokine signaling drive T-cell lymphoma progression and disease symptoms. *Blood* 141(23), pp. 2824-2840. doi: 10.1182/blood.2022015653

Jalkanen, S. and Jalkanen, M. 1992. Lymphocyte CD44 binds the COOH-terminal heparin-binding domain of fibronectin. *J Cell Biol* 116(3), pp. 817-825. doi: 10.1083/jcb.116.3.817

Jan, Y. et al. 2004. A mitochondrial protein, Bit1, mediates apoptosis regulated by integrins and Groucho/TLE corepressors. *Cell* 116(5), pp. 751-762. doi: 10.1016/s0092-8674(04)00204-1

Jayne, D. 2007. Molecular biology of peritoneal carcinomatosis. *Cancer Treat Res* 134, pp. 21-33. doi: 10.1007/978-0-387-48993-3_2

Jayne, D. G. 2003. The molecular biology of peritoneal carcinomatosis from gastrointestinal cancer. *Ann Acad Med Singap* 32(2), pp. 219-225.

Jayne, D. G., O'Leary, R., Gill, A., Hick, A. and Guillou, P. J. 1999. A three-dimensional in-vitro model for the study of peritoneal tumour metastasis. *Clin Exp Metastasis* 17(6), pp. 515-523. doi: 10.1023/a:1006606006878

Jenning, S., Pham, T., Ireland, S. K., Ruoslahti, E. and Biliran, H. 2013. Bit1 in anoikis resistance and tumor metastasis. *Cancer Lett* 333(2), pp. 147-151. doi: 10.1016/j.canlet.2013.01.043

Jeon, S. M., Chandel, N. S. and Hay, N. 2012. AMPK regulates NADPH homeostasis to promote tumour cell survival during energy stress. *Nature* 485(7400), pp. 661-665. doi: 10.1038/nature11066

Ji, C. et al. 2018. Capillary morphogenesis gene 2 maintains gastric cancer stem-like cell phenotype by activating a Wnt/beta-catenin pathway. *Oncogene* 37(29), pp. 3953-3966. doi: 10.1038/s41388-018-0226-z

Ji, S. Q., Cao, J., Zhang, Q. Y., Li, Y. Y., Yan, Y. Q. and Yu, F. X. 2013. Adipose tissue-derived stem cells promote pancreatic cancer cell proliferation and invasion. *Braz J Med Biol Res* 46(9), pp. 758-764. doi: 10.1590/1414-431X20132907

Jia, B., Yu, S., Yu, D., Liu, N., Zhang, S. and Wu, A. 2021. Mycotoxin deoxynivalenol affects myoblast differentiation via downregulating cytoskeleton and ECM-integrin-FAK-RAC-PAK signaling pathway. *Ecotoxicol Environ Saf* 226, p. 112850. doi: 10.1016/j.ecoenv.2021.112850

Jiang, W. G. 1996. E-cadherin and its associated protein catenins, cancer invasion and metastasis. *Br J Surg* 83(4), pp. 437-446. doi: 10.1002/bjs.1800830404

Jiang, W. G. et al. 2015. YangZheng XiaoJi exerts anti-tumour growth effects by antagonising the effects of HGF and its receptor, cMET, in human lung cancer cells. *J Transl Med* 13, p. 280. doi: 10.1186/s12967-015-0639-1

Jiang, Z., Woda, B. A., Savas, L. and Fraire, A. E. 1998. Expression of ICAM-1, VCAM-1, and LFA-1 in adenocarcinoma of the lung with observations on the expression of these adhesion molecules in non-neoplastic lung tissue. *Mod Pathol* 11(12), pp. 1189-1192.

Jonjic, N. et al. 1992. Expression of adhesion molecules and chemotactic cytokines in cultured human mesothelial cells. *J Exp Med* 176(4), pp. 1165-1174. doi: 10.1084/jem.176.4.1165

Joo, Y. E., Rew, J. S., Park, C. S. and Kim, S. J. 2002. Expression of E-cadherin, alpha- and beta-catenins in patients with pancreatic adenocarcinoma. *Pancreatology* 2(2), pp. 129-137. doi: 10.1159/000055903

Joy, R. A., Vikkath, N. and Ariyannur, P. S. 2018. Metabolism and mechanisms of action of hyaluronan in human biology. *Drug Metab Pers Ther* 33(1), pp. 15-32. doi: 10.1515/dmpt-2017-0031

Joyce, J. A. and Pollard, J. W. 2009. Microenvironmental regulation of metastasis. *Nat Rev Cancer* 9(4), pp. 239-252. doi: 10.1038/nrc2618

Jozefiak, A., Larska, M., Pomorska-Mol, M. and Ruszkowski, J. J. 2021. The IGF-1 Signaling Pathway in Viral Infections. *Viruses* 13(8), doi: 10.3390/v13081488

Kabashima, A. et al. 2009. Side population of pancreatic cancer cells predominates in TGF-beta-mediated epithelial to mesenchymal transition and invasion. *Int J Cancer* 124(12), pp. 2771-2779. doi: 10.1002/ijc.24349

Kamyabi, N., Bernard, V. and Maitra, A. 2019. Liquid biopsies in pancreatic cancer. *Expert Rev Anticancer Ther* 19(10), pp. 869-878. doi: 10.1080/14737140.2019.1670063

Kanchanawong, P. and Calderwood, D. A. 2023. Organization, dynamics and mechanoregulation of integrin-mediated cell-ECM adhesions. *Nat Rev Mol Cell Biol* 24(2), pp. 142-161. doi: 10.1038/s41580-022-00531-5

Kaneko, O., Gong, L., Zhang, J., Hansen, J. K., Hassan, R., Lee, B. and Ho, M. 2009. A binding domain on mesothelin for CA125/MUC16. *J Biol Chem* 284(6), pp. 3739-3749. doi: 10.1074/jbc.M806776200

Karasawa, K. et al. 2017. Multi-atlas pancreas segmentation: Atlas selection based on vessel structure. *Med Image Anal* 39, pp. 18-28. doi: 10.1016/j.media.2017.03.006

Karnoub, A. E. et al. 2007. Mesenchymal stem cells within tumour stroma promote breast cancer metastasis. *Nature* 449(7162), pp. 557-563. doi: 10.1038/nature06188

Katenkamp, D. and Kosmehl, H. 1995. Heterogeneity in malignant soft tissue tumors. *Curr Top Pathol* 89, pp. 123-151. doi: 10.1007/978-3-642-77289-4_7

Kaur, H., Phillips-Mason, P. J., Burden-Gulley, S. M., Kerstetter-Fogle, A. E., Basilion, J. P., Sloan, A. E. and Brady-Kalnay, S. M. 2012. Cadherin-11, a marker of the mesenchymal phenotype, regulates glioblastoma cell migration and survival in vivo. *Mol Cancer Res* 10(3), pp. 293-304. doi: 10.1158/1541-7786.MCR-11-0457

Kazerounian, S., Yee, K. O. and Lawler, J. 2008. Thrombospondins in cancer. *Cell Mol Life Sci*

65(5), pp. 700-712. doi: 10.1007/s00018-007-7486-z

Keire, P. A. et al. 2014. A role for versican in the development of leiomyosarcoma. *J Biol Chem* 289(49), pp. 34089-34103. doi: 10.1074/jbc.M114.607168

Kelley, C. F., Litschel, T., Schumacher, S., Dedden, D., Schwille, P. and Mizuno, N. 2020. Phosphoinositides regulate force-independent interactions between talin, vinculin, and actin. *Elife* 9, doi: 10.7554/eLife.56110

Kelsen, D. 1994. The use of chemotherapy in the treatment of advanced gastric and pancreas cancer. *Semin Oncol* 21(4 Suppl 7), pp. 58-66.

Kenny, H. A. et al. 2014. Mesothelial cells promote early ovarian cancer metastasis through fibronectin secretion. *J Clin Invest* 124(10), pp. 4614-4628. doi: 10.1172/JCI74778

Kenny, H. A., Kaur, S., Coussens, L. M. and Lengyel, E. 2008. The initial steps of ovarian cancer cell metastasis are mediated by MMP-2 cleavage of vitronectin and fibronectin. *J Clin Invest* 118(4), pp. 1367-1379. doi: 10.1172/JCI33775

Kent, O. A. et al. 2010. Repression of the miR-143/145 cluster by oncogenic Ras initiates a tumor-promoting feed-forward pathway. *Genes Dev* 24(24), pp. 2754-2759. doi: 10.1101/gad.1950610

Kesanakurti, D., Chetty, C., Dinh, D. H., Gujrati, M. and Rao, J. S. 2013. Role of MMP-2 in the regulation of IL-6/Stat3 survival signaling via interaction with alpha5beta1 integrin in glioma. *Oncogene* 32(3), pp. 327-340. doi: 10.1038/onc.2012.52

Kessenbrock, K., Plaks, V. and Werb, Z. 2010. Matrix metalloproteinases: regulators of the tumor microenvironment. *Cell* 141(1), pp. 52-67. doi: 10.1016/j.cell.2010.03.015

Khanna, R., Krediet, R.T. 2009. the peritoneal microcirculation inperitoneal dialysis. *Nolph and Gokal's Textbook of Peritoneal Dialysis, 3rded. Springer.*
Chapter 4

Khorana, A. A. et al. 2019. Potentially Curable Pancreatic Adenocarcinoma: ASCO Clinical Practice Guideline Update. *J Clin Oncol* 37(23), pp. 2082-2088. doi: 10.1200/JCO.19.00946

Khwaja, A., Rodriguez-Viciana, P., Wennstrom, S., Warne, P. H. and Downward, J. 1997. Matrix adhesion and Ras transformation both activate a phosphoinositide 3-OH kinase and protein kinase B/Akt cellular survival pathway. *EMBO J* 16(10), pp. 2783-2793. doi: 10.1093/emboj/16.10.2783

Kiema, T. et al. 2006. The molecular basis of filamin binding to integrins and competition with talin. *Mol Cell* 21(3), pp. 337-347. doi: 10.1016/j.molcel.2006.01.011

Kim, H., Nakamura, F., Lee, W., Hong, C., Perez-Sala, D. and McCulloch, C. A. 2010a. Regulation of cell adhesion to collagen via beta1 integrins is dependent on interactions of filamin A with vimentin and protein kinase C epsilon. *Exp Cell Res* 316(11), pp. 1829-1844. doi: 10.1016/j.yexcr.2010.02.007

Kim, H., Nakamura, F., Lee, W., Shifrin, Y., Arora, P. and McCulloch, C. A. 2010b. Filamin A is

required for vimentin-mediated cell adhesion and spreading. *Am J Physiol Cell Physiol* 298(2), pp. C221-236. doi: 10.1152/ajpcell.00323.2009

Kim, J. H., Lee, S. Y., Oh, S. Y., Han, S. I., Park, H. G., Yoo, M. A. and Kang, H. S. 2004. Methyl jasmonate induces apoptosis through induction of Bax/Bcl-XS and activation of caspase-3 via ROS production in A549 cells. *Oncol Rep* 12(6), pp. 1233-1238.

Kim, Y. R., Yoo, J. K., Jeong, C. W. and Choi, J. W. 2018. Selective killing of circulating tumor cells prevents metastasis and extends survival. *J Hematol Oncol* 11(1), p. 114. doi: 10.1186/s13045-018-0658-5

Kim, Y. T., Park, S. W. and Kim, J. W. 2002. Correlation between expression of EGFR and the prognosis of patients with cervical carcinoma. *Gynecol Oncol* 87(1), pp. 84-89. doi: 10.1006/gyno.2002.6803

Kincade, P. W., Zheng, Z., Katoh, S. and Hanson, L. 1997. The importance of cellular environment to function of the CD44 matrix receptor. *Curr Opin Cell Biol* 9(5), pp. 635-642. doi: 10.1016/s0955-0674(97)80116-0

Kirkegard, J., Mortensen, F. V. and Cronin-Fenton, D. 2017. Chronic Pancreatitis and Pancreatic Cancer Risk: A Systematic Review and Meta-analysis. *Am J Gastroenterol* 112(9), pp. 1366-1372. doi: 10.1038/ajg.2017.218

Kishore, U. et al. 2005. Surfactant proteins SP-A and SP-D in human health and disease. *Arch Immunol Ther Exp (Warsz)* 53(5), pp. 399-417.

Klapman, J. B., Logrono, R., Dye, C. E. and Waxman, I. 2003. Clinical impact of on-site cytopathology interpretation on endoscopic ultrasound-guided fine needle aspiration. *Am J Gastroenterol* 98(6), pp. 1289-1294. doi: 10.1111/j.1572-0241.2003.07472.x

Klein, A. P., Hruban, R. H., Brune, K. A., Petersen, G. M. and Goggins, M. 2001. Familial pancreatic cancer. *Cancer J* 7(4), pp. 266-273.

Klein, C. L., Bittinger, F., Skarke, C. C., Wagner, M., Kohler, H., Walgenbach, S. and Kirkpatrick, C. J. 1995. Effects of cytokines on the expression of cell adhesion molecules by cultured human omental mesothelial cells. *Pathobiology* 63(4), pp. 204-212. doi: 10.1159/000163953

Kleinman, H. K. and Martin, G. R. 2005. Matrigel: basement membrane matrix with biological activity. *Semin Cancer Biol* 15(5), pp. 378-386. doi: 10.1016/j.semcancer.2005.05.004

Klimstra, D. S. and Longnecker, D. S. 1994. K-ras mutations in pancreatic ductal proliferative lesions. *Am J Pathol* 145(6), pp. 1547-1550.

Klymkowsky, M. W. and Savagner, P. 2009. Epithelial-mesenchymal transition: a cancer researcher's conceptual friend and foe. *Am J Pathol* 174(5), pp. 1588-1593. doi: 10.2353/ajpath.2009.080545

Knowles, L. M., Gurski, L. A., Engel, C., Gnarra, J. R., Maranchie, J. K. and Pilch, J. 2013. Integrin alphavbeta3 and fibronectin upregulate Slug in cancer cells to promote clot invasion and metastasis. *Cancer Res* 73(20), pp. 6175-6184. doi: 10.1158/0008-5472.CAN-13-0602

Knudson, C. B., Munaim, S. I. and Toole, B. P. 1995. Ectodermal stimulation of the production of hyaluronan-dependent pericellular matrix by embryonic limb mesodermal cells. *Dev Dyn* 204(2), pp. 186-191. doi: 10.1002/aja.1002040209

Kobayashi, H., Enomoto, A., Woods, S. L., Burt, A. D., Takahashi, M. and Worthley, D. L. 2019. Cancer-associated fibroblasts in gastrointestinal cancer. *Nat Rev Gastroenterol Hepatol* 16(5), pp. 282-295. doi: 10.1038/s41575-019-0115-0

Kohda, D., Morton, C. J., Parkar, A. A., Hatanaka, H., Inagaki, F. M., Campbell, I. D. and Day, A. J. 1996. Solution structure of the link module: a hyaluronan-binding domain involved in extracellular matrix stability and cell migration. *Cell* 86(5), pp. 767-775. doi: 10.1016/s0092-8674(00)80151-8

Kojima, N. and Hakomori, S. 1991. Cell adhesion, spreading, and motility of GM3-expressing cells based on glycolipid-glycolipid interaction. *J Biol Chem* 266(26), pp. 17552-17558.

Kondo, J., Sato, F., Kusumi, T., Liu, Y., Motonari, O., Sato, T. and Kijima, H. 2008. Claudin-1 expression is induced by tumor necrosis factor-alpha in human pancreatic cancer cells. *Int J Mol Med* 22(5), pp. 645-649.

Kopp, R. et al. 2003. Clinical implications of the EGF receptor/ligand system for tumor progression and survival in gastrointestinal carcinomas: evidence for new therapeutic options. *Recent Results Cancer Res* 162, pp. 115-132. doi: 10.1007/978-3-642-59349-9_10

Kourtidis, A., Lu, R., Pence, L. J. and Anastasiadis, P. Z. 2017. A central role for cadherin signaling in cancer. *Exp Cell Res* 358(1), pp. 78-85. doi: 10.1016/j.yexcr.2017.04.006

Krugmann, S. et al. 2002. Identification of ARAP3, a novel PI3K effector regulating both Arf and Rho GTPases, by selective capture on phosphoinositide affinity matrices. *Mol Cell* 9(1), pp. 95-108. doi: 10.1016/s1097-2765(02)00434-3

Krugmann, S., Stephens, L. and Hawkins, P. T. 2006. Purification of ARAP3 and characterization of GAP activities. *Methods Enzymol* 406, pp. 91-103. doi: 10.1016/S0076-6879(06)06008-3

Kuleshov, M. V. et al. 2016. Enrichr: a comprehensive gene set enrichment analysis web server 2016 update. *Nucleic Acids Res* 44(W1), pp. W90-97. doi: 10.1093/nar/gkw377

Kunovsky, L., Tesarikova, P., Kala, Z., Kroupa, R., Kysela, P., Dolina, J. and Trna, J. 2018. The Use of Biomarkers in Early Diagnostics of Pancreatic Cancer. *Can J Gastroenterol Hepatol* 2018, p. 5389820. doi: 10.1155/2018/5389820

Kurahara, H., Takao, S., Maemura, K., Shinchi, H., Natsugoe, S. and Aikou, T. 2004. Impact of vascular endothelial growth factor-C and -D expression in human pancreatic cancer: its relationship to lymph node metastasis. *Clin Cancer Res* 10(24), pp. 8413-8420. doi: 10.1158/1078-0432.CCR-04-0379

Kuwana, T., Bouchier-Hayes, L., Chipuk, J. E., Bonzon, C., Sullivan, B. A., Green, D. R. and Newmeyer, D. D. 2005. BH3 domains of BH3-only proteins differentially regulate Bax-mediated mitochondrial membrane permeabilization both directly and indirectly. *Mol Cell* 17(4), pp. 525-535. doi: 10.1016/j.molcel.2005.02.003

Kyuno, D. et al. 2011. Protein kinase Calpha inhibitor enhances the sensitivity of human pancreatic cancer HPAC cells to Clostridium perfringens enterotoxin via claudin-4. *Cell Tissue Res* 346(3), pp. 369-381. doi: 10.1007/s00441-011-1287-2

Laird, D. W. 2006. Life cycle of connexins in health and disease. *Biochem J* 394(Pt 3), pp. 527-543. doi: 10.1042/BJ20051922

Laklai, H. et al. 2016. Genotype tunes pancreatic ductal adenocarcinoma tissue tension to induce matricellular fibrosis and tumor progression. *Nat Med* 22(5), pp. 497-505. doi: 10.1038/nm.4082

Lambert, A. W., Pattabiraman, D. R. and Weinberg, R. A. 2017. Emerging Biological Principles of Metastasis. *Cell* 168(4), pp. 670-691. doi: 10.1016/j.cell.2016.11.037

Lamouille, S., Xu, J. and Derynck, R. 2014. Molecular mechanisms of epithelial-mesenchymal transition. *Nat Rev Mol Cell Biol* 15(3), pp. 178-196. doi: 10.1038/nrm3758

Lancaster, J. M. et al. 2006. Identification of genes associated with ovarian cancer metastasis using microarray expression analysis. *Int J Gynecol Cancer* 16(5), pp. 1733-1745. doi: 10.1111/j.1525-1438.2006.00660.x

Lardy, S. et al. 2017. Telomere erosion varies with sex and age at immune challenge but not with maternal antibodies in pigeons. *J Exp Zool A Ecol Integr Physiol* 327(9), pp. 562-569. doi: 10.1002/jez.2142

Laurent, T. C. and Fraser, J. R. 1992. Hyaluronan. *FASEB J* 6(7), pp. 2397-2404.

Laurent, T. C., Laurent, U. B. and Fraser, J. R. 1996. The structure and function of hyaluronan: An overview. *Immunol Cell Biol* 74(2), pp. A1-7. doi: 10.1038/icb.1996.32

Lawson, C. D. and Ridley, A. J. 2018. Rho GTPase signaling complexes in cell migration and invasion. *J Cell Biol* 217(2), pp. 447-457. doi: 10.1083/jcb.201612069

Lazennec, G., Thomas, J. A. and Katzenellenbogen, B. S. 2001. Involvement of cyclic AMP response element binding protein (CREB) and estrogen receptor phosphorylation in the synergistic activation of the estrogen receptor by estradiol and protein kinase activators. *J Steroid Biochem Mol Biol* 77(4-5), pp. 193-203. doi: 10.1016/s0960-0760(01)00060-7

Lee, J. H., Kim, K. S., Kim, T. J., Hong, S. P., Song, S. Y., Chung, J. B. and Park, S. W. 2011. Immunohistochemical analysis of claudin expression in pancreatic cystic tumors. *Oncol Rep* 25(4), pp. 971-978. doi: 10.3892/or.2011.1132

Lee, S. W. and Commisso, C. 2020. Rac1 and EGFR cooperate to activate Pak in response to nutrient stress. *Biochem Biophys Res Commun* 533(3), pp. 437-441. doi: 10.1016/j.bbrc.2020.09.043

Lee, Y. J. and Streuli, C. H. 1999. Extracellular matrix selectively modulates the response of mammary epithelial cells to different soluble signaling ligands. *J Biol Chem* 274(32), pp. 22401-22408. doi: 10.1074/jbc.274.32.22401

Legate, K. R. and Fassler, R. 2009. Mechanisms that regulate adaptor binding to beta-integrin cytoplasmic tails. *J Cell Sci* 122(Pt 2), pp. 187-198. doi: 10.1242/jcs.041624

Legate, K. R., Wickstrom, S. A. and Fassler, R. 2009. Genetic and cell biological analysis of integrin outside-in signaling. *Genes Dev* 23(4), pp. 397-418. doi: 10.1101/gad.1758709

Lemmon, M. A. and Schlessinger, J. 2010. Cell signaling by receptor tyrosine kinases. *Cell* 141(7), pp. 1117-1134. doi: 10.1016/j.cell.2010.06.011

Lemoine, L., Sugarbaker, P. and Van der Speeten, K. 2016. Pathophysiology of colorectal peritoneal carcinomatosis: Role of the peritoneum. *World J Gastroenterol* 22(34), pp. 7692-7707. doi: 10.3748/wjg.v22.i34.7692

Lesley, J., English, N., Perschl, A., Gregoroff, J. and Hyman, R. 1995. Variant cell lines selected for alterations in the function of the hyaluronan receptor CD44 show differences in glycosylation. *J Exp Med* 182(2), pp. 431-437. doi: 10.1084/jem.182.2.431

Lesley, J., Hyman, R. and Kincade, P. W. 1993. CD44 and its interaction with extracellular matrix. *Adv Immunol* 54, pp. 271-335. doi: 10.1016/s0065-2776(08)60537-4

Lewis, M. P., Reber, H. A. and Ashley, S. W. 1998. Pancreatic blood flow and its role in the pathophysiology of pancreatitis. *J Surg Res* 75(1), pp. 81-89. doi: 10.1006/jsre.1998.5268

Ley, R., Balmanno, K., Hadfield, K., Weston, C. and Cook, S. J. 2003. Activation of the ERK1/2 signaling pathway promotes phosphorylation and proteasome-dependent degradation of the BH3-only protein, Bim. *J Biol Chem* 278(21), pp. 18811-18816. doi: 10.1074/jbc.M301010200

Ley, R., Ewings, K. E., Hadfield, K. and Cook, S. J. 2005. Regulatory phosphorylation of Bim: sorting out the ERK from the JNK. *Cell Death Differ* 12(8), pp. 1008-1014. doi: 10.1038/sj.cdd.4401688

Li, C. et al. 2007. Identification of pancreatic cancer stem cells. *Cancer Res* 67(3), pp. 1030-1037. doi: 10.1158/0008-5472.CAN-06-2030

Li, J., Sasaki, H., Sheng, Y. L., Schneiderman, D., Xiao, C. W., Kotsuji, F. and Tsang, B. K. 2000. Apoptosis and chemoresistance in human ovarian cancer: is Xiap a determinant? *Biol Signals Recept* 9(2), pp. 122-130. doi: 10.1159/000014631

Li, S. et al. 2019. Angiogenesis in pancreatic cancer: current research status and clinical implications. *Angiogenesis* 22(1), pp. 15-36. doi: 10.1007/s10456-018-9645-2

Li, S. G., Ye, Z. Y., Zhao, Z. S., Tao, H. Q., Wang, Y. Y. and Niu, C. Y. 2008. Correlation of integrin beta3 mRNA and vascular endothelial growth factor protein expression profiles with the clinicopathological features and prognosis of gastric carcinoma. *World J Gastroenterol* 14(3), pp. 421-427. doi: 10.3748/wjg.14.421

Li, W. T., Jeng, Y. M. and Yang, C. Y. 2020. Claudin-18 as a Marker for Identifying the Stomach and Pancreatobiliary Tract as the Primary Sites of Metastatic Adenocarcinoma. *Am J Surg Pathol* 44(12), pp. 1643-1648. doi: 10.1097/PAS.0000000000001583

Li, W. W., Li, J. and Bao, J. K. 2012a. Microautophagy: lesser-known self-eating. *Cell Mol Life*

Sci 69(7), pp. 1125-1136. doi: 10.1007/s00018-011-0865-5

Li, X. et al. 2012b. SDF-1/CXCR4 signaling induces pancreatic cancer cell invasion and epithelial-mesenchymal transition in vitro through non-canonical activation of Hedgehog pathway. *Cancer Lett* 322(2), pp. 169-176. doi: 10.1016/j.canlet.2012.02.035

Liang, C.-C., Park, A. Y. and Guan, J.-L. 2007. In vitro scratch assay: a convenient and inexpensive method for analysis of cell migration in vitro. *Nat. Protocols* 2(2), pp. 329-333.

Ligorio, M. et al. 2019. Stromal Microenvironment Shapes the Intratumoral Architecture of Pancreatic Cancer. *Cell* 178(1), pp. 160-175 e127. doi: 10.1016/j.cell.2019.05.012

Liles, J. S. et al. 2010. ErbB3 expression promotes tumorigenesis in pancreatic adenocarcinoma. *Cancer Biol Ther* 10(6), pp. 555-563. doi: 10.4161/cbt.10.6.12532

Lim, K. H. et al. 2005. Activation of RalA is critical for Ras-induced tumorigenesis of human cells. *Cancer Cell* 7(6), pp. 533-545. doi: 10.1016/j.ccr.2005.04.030

Lim, M., Xia, Y., Bettegowda, C. and Weller, M. 2018. Current state of immunotherapy for glioblastoma. *Nat Rev Clin Oncol* 15(7), pp. 422-442. doi: 10.1038/s41571-018-0003-5

Lim, S. M. et al. 2016. Targeted sequencing identifies genetic alterations that confer primary resistance to EGFR tyrosine kinase inhibitor (Korean Lung Cancer Consortium). *Oncotarget* 7(24), pp. 36311-36320. doi: 10.18632/oncotarget.8904

Lin, S. C. et al. 2019. Targeting Anthrax Toxin Receptor 2 Ameliorates Endometriosis Progression. *Theranostics* 9(3), pp. 620-632. doi: 10.7150/thno.30655

Lin, Y. et al. 2002. A prospective cohort study of cigarette smoking and pancreatic cancer in Japan. *Cancer Causes Control* 13(3), pp. 249-254. doi: 10.1023/a:1015052710213

Liu, J. et al. 2020. Increased expression of Psoriasin is correlated with poor prognosis of bladder transitional cell carcinoma by promoting invasion and proliferation. *Oncol Rep* 43(2), pp. 562-570. doi: 10.3892/or.2019.7445

Long, J. et al. 2012. Development of a unique mouse model for pancreatic cancer lymphatic metastasis. *Int J Oncol* 41(5), pp. 1662-1668. doi: 10.3892/ijo.2012.1613

Lu, Z. et al. 2000. Phospholipase D and RalA cooperate with the epidermal growth factor receptor to transform 3Y1 rat fibroblasts. *Mol Cell Biol* 20(2), pp. 462-467. doi: 10.1128/MCB.20.2.462-467.2000

Luo, J., Wang, H., Chen, H., Gan, G. and Zheng, Y. 2020. CLDN4 silencing promotes proliferation and reduces chemotherapy sensitivity of gastric cancer cells through activation of the PI3K/Akt signalling pathway. *Exp Physiol* 105(6), pp. 979-988. doi: 10.1113/EP088112

Lv, Z. D. et al. 2010. Induction of gastric cancer cell adhesion through transforming growth factor-beta1-mediated peritoneal fibrosis. *J Exp Clin Cancer Res* 29, p. 139. doi: 10.1186/1756-9966-29-139

Lynch, H. T. et al. 2002. Phenotypic variation in eight extended CDKN2A germline mutation

familial atypical multiple mole melanoma-pancreatic carcinoma-prone families: the familial atypical mole melanoma-pancreatic carcinoma syndrome. *Cancer* 94(1), pp. 84-96. doi: 10.1002/cncr.10159

Ma, J. et al. 2021. c-KIT-ERK1/2 signaling activated ELK1 and upregulated carcinoembryonic antigen expression to promote colorectal cancer progression. *Cancer Sci* 112(2), pp. 655-667. doi: 10.1111/cas.14750

Mac Gabhann, F. and Popel, A. S. 2008. Systems biology of vascular endothelial growth factors. *Microcirculation* 15(8), pp. 715-738. doi: 10.1080/10739680802095964

Maeda, S. et al. 2008. CD133 expression is correlated with lymph node metastasis and vascular endothelial growth factor-C expression in pancreatic cancer. *Br J Cancer* 98(8), pp. 1389-1397. doi: 10.1038/sj.bjc.6604307

Mai, A., Muharram, G., Barrow-McGee, R., Baghirov, H., Rantala, J., Kermorgant, S. and Ivaska, J. 2014. Distinct c-Met activation mechanisms induce cell rounding or invasion through pathways involving integrins, RhoA and HIP1. *J Cell Sci* 127(Pt 9), pp. 1938-1952. doi: 10.1242/jcs.140657

Maisey, N. et al. 2002. Multicenter randomized phase III trial comparing protracted venous infusion (PVI) fluorouracil (5-FU) with PVI 5-FU plus mitomycin in inoperable pancreatic cancer. *J Clin Oncol* 20(14), pp. 3130-3136. doi: 10.1200/JCO.2002.09.029

Majno, G. and Joris, I. 1995. Apoptosis, oncosis, and necrosis. An overview of cell death. *Am J Pathol* 146(1), pp. 3-15.

Makary, M. A., Warshaw, A. L., Centeno, B. A., Willet, C. G., Rattner, D. W. and Fernandez-del Castillo, C. 1998. Implications of peritoneal cytology for pancreatic cancer management. *Arch Surg* 133(4), pp. 361-365. doi: 10.1001/archsurg.133.4.361

Malek, J. A. et al. 2012. Gene expression analysis of matched ovarian primary tumors and peritoneal metastasis. *J Transl Med* 10, p. 121. doi: 10.1186/1479-5876-10-121

Malik, G., Knowles, L. M., Dhir, R., Xu, S., Yang, S., Ruoslahti, E. and Pilch, J. 2010. Plasma fibronectin promotes lung metastasis by contributions to fibrin clots and tumor cell invasion. *Cancer Res* 70(11), pp. 4327-4334. doi: 10.1158/0008-5472.CAN-09-3312

Malumbres, M. and Barbacid, M. 2003. RAS oncogenes: the first 30 years. *Nat Rev Cancer* 3(6), pp. 459-465. doi: 10.1038/nrc1097

Mandriota, S. J. et al. 2001. Vascular endothelial growth factor-C-mediated lymphangiogenesis promotes tumour metastasis. *EMBO J* 20(4), pp. 672-682. doi: 10.1093/emboj/20.4.672

Marani, M., Hancock, D., Lopes, R., Tenev, T., Downward, J. and Lemoine, N. R. 2004. Role of Bim in the survival pathway induced by Raf in epithelial cells. *Oncogene* 23(14), pp. 2431-2441. doi: 10.1038/sj.onc.1207364

Marcato, P. et al. 2011. Aldehyde dehydrogenase activity of breast cancer stem cells is primarily due to isoform ALDH1A3 and its expression is predictive of metastasis. *Stem Cells* 29(1), pp. 32-45. doi: 10.1002/stem.563

Martinvalet, D., Zhu, P. and Lieberman, J. 2005. Granzyme A induces caspase-independent mitochondrial damage, a required first step for apoptosis. *Immunity* 22(3), pp. 355-370. doi: 10.1016/j.immuni.2005.02.004

Masamune, A., Kikuta, K., Watanabe, T., Satoh, K., Hirota, M. and Shimosegawa, T. 2008. Hypoxia stimulates pancreatic stellate cells to induce fibrosis and angiogenesis in pancreatic cancer. *Am J Physiol Gastrointest Liver Physiol* 295(4), pp. G709-717. doi: 10.1152/ajpgi.90356.2008

Massague, J. and Obenauf, A. C. 2016. Metastatic colonization by circulating tumour cells. *Nature* 529(7586), pp. 298-306. doi: 10.1038/nature17038

Matoba, S. et al. 2006. p53 regulates mitochondrial respiration. *Science* 312(5780), pp. 1650-1653. doi: 10.1126/science.1126863

Matsumoto, G., Omi, Y., Lee, U., Kubota, E. and Tabata, Y. 2011. NK4 gene therapy combined with cisplatin inhibits tumour growth and metastasis of squamous cell carcinoma. *Anticancer Res* 31(1), pp. 105-111.

Matsumoto, S., Fujii, S., Sato, A., Ibuka, S., Kagawa, Y., Ishii, M. and Kikuchi, A. 2014. A combination of Wnt and growth factor signaling induces Arl4c expression to form epithelial tubular structures. *EMBO J* 33(7), pp. 702-718. doi: 10.1002/embj.201386942

Matter, M. L., Zhang, Z., Nordstedt, C. and Ruoslahti, E. 1998. The alpha5beta1 integrin mediates elimination of amyloid-beta peptide and protects against apoptosis. *J Cell Biol* 141(4), pp. 1019-1030. doi: 10.1083/jcb.141.4.1019

McCourt, P. A., Ek, B., Forsberg, N. and Gustafson, S. 1994. Intercellular adhesion molecule-1 is a cell surface receptor for hyaluronan. *J Biol Chem* 269(48), pp. 30081-30084.

McGuigan, A., Kelly, P., Turkington, R. C., Jones, C., Coleman, H. G. and McCain, R. S. 2018. Pancreatic cancer: A review of clinical diagnosis, epidemiology, treatment and outcomes. *World J Gastroenterol* 24(43), pp. 4846-4861. doi: 10.3748/wjg.v24.i43.4846

Mege, R. M. and Ishiyama, N. 2017. Integration of Cadherin Adhesion and Cytoskeleton at Adherens Junctions. *Cold Spring Harb Perspect Biol* 9(5), doi: 10.1101/cshperspect.a028738

Melincovici, C. S. et al. 2018. Vascular endothelial growth factor (VEGF) - key factor in normal and pathological angiogenesis. *Rom J Morphol Embryol* 59(2), pp. 455-467.

Melis, M., Spatafora, M., Melodia, A., Pace, E., Gjomarkaj, M., Merendino, A. M. and Bonsignore, G. 1996. ICAM-1 expression by lung cancer cell lines: effects of upregulation by cytokines on the interaction with LAK cells. *Eur Respir J* 9(9), pp. 1831-1838. doi: 10.1183/09031936.96.09091831

Melzer, C., von der Ohe, J. and Hass, R. 2017. Breast Carcinoma: From Initial Tumor Cell Detachment to Settlement at Secondary Sites. *Biomed Res Int* 2017, p. 8534371. doi: 10.1155/2017/8534371

Mentzer, S. J., Gromkowski, S. H., Krensky, A. M., Burakoff, S. J. and Martz, E. 1985. LFA-1

membrane molecule in the regulation of homotypic adhesions of human B lymphocytes. *J Immunol* 135(1), pp. 9-11.

Miao, Z. F., Wang, Z. N., Zhao, T. T., Xu, Y. Y., Gao, J., Miao, F. and Xu, H. M. 2014. Peritoneal milky spots serve as a hypoxic niche and favor gastric cancer stem/progenitor cell peritoneal dissemination through hypoxia-inducible factor 1alpha. *Stem Cells* 32(12), pp. 3062-3074. doi: 10.1002/stem.1816

Micalizzi, D. S., Farabaugh, S. M. and Ford, H. L. 2010. Epithelial-mesenchymal transition in cancer: parallels between normal development and tumor progression. *J Mammary Gland Biol Neoplasia* 15(2), pp. 117-134. doi: 10.1007/s10911-010-9178-9

Michailova, K. N. and Usunoff, K. G. 2006. Serosal membranes (pleura, pericardium, peritoneum). Normal structure, development and experimental pathology. *Adv Anat Embryol Cell Biol* 183, pp. i-vii, 1-144, back cover.

Michaud, D. S., Giovannucci, E., Willett, W. C., Colditz, G. A., Stampfer, M. J. and Fuchs, C. S. 2001. Physical activity, obesity, height, and the risk of pancreatic cancer. *JAMA* 286(8), pp. 921-929. doi: 10.1001/jama.286.8.921

Michl, P. et al. 2003. Claudin-4 expression decreases invasiveness and metastatic potential of pancreatic cancer. *Cancer Res* 63(19), pp. 6265-6271.

Mikula-Pietrasik, J., Uruski, P., Tykarski, A. and Ksiazek, K. 2018. The peritoneal "soil" for a cancerous "seed": a comprehensive review of the pathogenesis of intraperitoneal cancer metastases. *Cell Mol Life Sci* 75(3), pp. 509-525. doi: 10.1007/s00018-017-2663-1

Mimeault, M. and Batra, S. K. 2008. Recent progress on normal and malignant pancreatic stem/progenitor cell research: therapeutic implications for the treatment of type 1 or 2 diabetes mellitus and aggressive pancreatic cancer. *Gut* 57(10), pp. 1456-1468. doi: 10.1136/gut.2008.150052

Mitchison, T. and Kirschner, M. 1988. Cytoskeletal dynamics and nerve growth. *Neuron* 1(9), pp. 761-772. doi: 10.1016/0896-6273(88)90124-9

Mitra, A. K., Chiang, C. Y., Tiwari, P., Tomar, S., Watters, K. M., Peter, M. E. and Lengyel, E. 2015. Microenvironment-induced downregulation of miR-193b drives ovarian cancer metastasis. *Oncogene* 34(48), pp. 5923-5932. doi: 10.1038/onc.2015.43

Mitra, S. K. and Schlaepfer, D. D. 2006. Integrin-regulated FAK-Src signaling in normal and cancer cells. *Curr Opin Cell Biol* 18(5), pp. 516-523. doi: 10.1016/j.ceb.2006.08.011

Mizushima, N., Levine, B., Cuervo, A. M. and Klionsky, D. J. 2008. Autophagy fights disease through cellular self-digestion. *Nature* 451(7182), pp. 1069-1075. doi: 10.1038/nature06639

Moffitt, R. A. et al. 2015. Virtual microdissection identifies distinct tumor- and stroma-specific subtypes of pancreatic ductal adenocarcinoma. *Nat Genet* 47(10), pp. 1168-1178. doi: 10.1038/ng.3398

Montgomery, A. M., Reisfeld, R. A. and Cheresh, D. A. 1994. Integrin alpha v beta 3 rescues melanoma cells from apoptosis in three-dimensional dermal collagen. *Proc Natl Acad Sci U S A*

91(19), pp. 8856-8860. doi: 10.1073/pnas.91.19.8856

Moore, C. B., Guthrie, E. H., Huang, M. T. and Taxman, D. J. 2010. Short hairpin RNA (shRNA): design, delivery, and assessment of gene knockdown. *Methods Mol Biol* 629, pp. 141-158. doi: 10.1007/978-1-60761-657-3_10

Morris, J. P. t., Wang, S. C. and Hebrok, M. 2010. KRAS, Hedgehog, Wnt and the twisted developmental biology of pancreatic ductal adenocarcinoma. *Nat Rev Cancer* 10(10), pp. 683-695. doi: 10.1038/nrc2899

Morton, J. P. et al. 2010. Mutant p53 drives metastasis and overcomes growth arrest/senescence in pancreatic cancer. *Proc Natl Acad Sci U S A* 107(1), pp. 246-251. doi: 10.1073/pnas.0908428107

Mostafa, M. E., Erbarut-Seven, I., Pehlivanoglu, B. and Adsay, V. 2017. Pathologic classification of "pancreatic cancers": current concepts and challenges. *Chin Clin Oncol* 6(6), p. 59. doi: 10.21037/cco.2017.12.01

Muller, P. A. et al. 2009. Mutant p53 drives invasion by promoting integrin recycling. *Cell* 139(7), pp. 1327-1341. doi: 10.1016/j.cell.2009.11.026

Munshi, H. G. and Stack, M. S. 2006. Reciprocal interactions between adhesion receptor signaling and MMP regulation. *Cancer Metastasis Rev* 25(1), pp. 45-56. doi: 10.1007/s10555-006-7888-7

Murphy, K. M. et al. 2002. Evaluation of candidate genes MAP2K4, MADH4, ACVR1B, and BRCA2 in familial pancreatic cancer: deleterious BRCA2 mutations in 17%. *Cancer Res* 62(13), pp. 3789-3793.

Mutsaers, S. E. 2004. The mesothelial cell. *Int J Biochem Cell Biol* 36(1), pp. 9-16. doi: 10.1016/s1357-2725(03)00242-5

Nagy, A., Munkacsy, G. and Gyorffy, B. 2021. Pancancer survival analysis of cancer hallmark genes. *Sci Rep* 11(1), p. 6047. doi: 10.1038/s41598-021-84787-5

Nam, J. M., Onodera, Y., Bissell, M. J. and Park, C. C. 2010. Breast cancer cells in three-dimensional culture display an enhanced radioresponse after coordinate targeting of integrin alpha5beta1 and fibronectin. *Cancer Res* 70(13), pp. 5238-5248. doi: 10.1158/0008-5472.CAN-09-2319

Namikawa, M. et al. 2023. Simultaneous activation of Kras-Akt and Notch pathways induces extrahepatic biliary cancer via the mTORC1 pathway. *J Pathol* 260(4), pp. 478-492. doi: 10.1002/path.6139

Nanba, D. et al. 2021. EGFR-mediated epidermal stem cell motility drives skin regeneration through COL17A1 proteolysis. *J Cell Biol* 220(11), doi: 10.1083/jcb.202012073

Naoi, Y. et al. 2008. Connexin26 expression is associated with aggressive phenotype in human papillary and follicular thyroid cancers. *Cancer Lett* 262(2), pp. 248-256. doi: 10.1016/j.canlet.2007.12.008

Naoi, Y., Miyoshi, Y., Taguchi, T., Kim, S. J., Arai, T., Tamaki, Y. and Noguchi, S. 2007. Connexin26 expression is associated with lymphatic vessel invasion and poor prognosis in human breast cancer. *Breast Cancer Res Treat* 106(1), pp. 11-17. doi: 10.1007/s10549-006-9465-8

Naor, D., Sionov, R. V. and Ish-Shalom, D. 1997. CD44: structure, function, and association with the malignant process. *Adv Cancer Res* 71, pp. 241-319. doi: 10.1016/s0065-230x(08)60101-3

Napoleon, B. et al. 2015. A novel approach to the diagnosis of pancreatic serous cystadenoma: needle-based confocal laser endomicroscopy. *Endoscopy* 47(1), pp. 26-32. doi: 10.1055/s-0034-1390693

Ng, S. S. W., Tsao, M. S., Chow, S. and Hedley, D. W. 2000. Inhibition of phosphatidylinositide 3-kinase enhances gemcitabine-induced apoptosis in human pancreatic cancer cells. *Cancer Res* 60(19), pp. 5451-5455.

Nichols, L. S., Ashfaq, R. and Iacobuzio-Donahue, C. A. 2004. Claudin 4 protein expression in primary and metastatic pancreatic cancer: support for use as a therapeutic target. *Am J Clin Pathol* 121(2), pp. 226-230. doi: 10.1309/K144-PHVD-DUPD-D401

Nicholson, R. I., Gee, J. M. and Harper, M. E. 2001. EGFR and cancer prognosis. *Eur J Cancer* 37 Suppl 4, pp. S9-15. doi: 10.1016/s0959-8049(01)00231-3

Nieman, K. M. et al. 2011. Adipocytes promote ovarian cancer metastasis and provide energy for rapid tumor growth. *Nat Med* 17(11), pp. 1498-1503. doi: 10.1038/nm.2492

Nishikawa, H., Goto, M., Fukunishi, S., Asai, A., Nishiguchi, S. and Higuchi, K. 2021. Cancer Cachexia: Its Mechanism and Clinical Significance. *Int J Mol Sci* 22(16), doi: 10.3390/ijms22168491

Nishimori, H. et al. 2002. A novel nude mouse model of liver metastasis and peritoneal dissemination from the same human pancreatic cancer line. *Pancreas* 24(3), pp. 242-250. doi: 10.1097/00006676-200204000-00006

Noble, P. W. 2002. Hyaluronan and its catabolic products in tissue injury and repair. *Matrix Biol* 21(1), pp. 25-29. doi: 10.1016/s0945-053x(01)00184-6

Noh, H., Hong, S. and Huang, S. 2013. Role of urokinase receptor in tumor progression and development. *Theranostics* 3(7), pp. 487-495. doi: 10.7150/thno.4218

Novitskaya, V. et al. 2014. Integrin alpha3beta1-CD151 complex regulates dimerization of ErbB2 via RhoA. *Oncogene* 33(21), pp. 2779-2789. doi: 10.1038/onc.2013.231

O'Brien, V., Frisch, S. M. and Juliano, R. L. 1996. Expression of the integrin alpha 5 subunit in HT29 colon carcinoma cells suppresses apoptosis triggered by serum deprivation. *Exp Cell Res* 224(1), pp. 208-213. doi: 10.1006/excr.1996.0130

O'Connor, K. and Chen, M. 2013. Dynamic functions of RhoA in tumor cell migration and invasion. *Small GTPases* 4(3), pp. 141-147. doi: 10.4161/sgtp.25131

Obradovic, M. M., Stojimirovic, B. B., Trpinac, D. P., Milutinovic, D. D., Obradovic, D. I. and

Nesic, V. B. 2001. [Ultrastructure of peritoneal mesothelial cells]. *Srp Arh Celok Lek* 129(7-8), pp. 175-179.

Ohmoto, A., Yachida, S. and Morizane, C. 2019. Genomic Features and Clinical Management of Patients with Hereditary Pancreatic Cancer Syndromes and Familial Pancreatic Cancer. *Int J Mol Sci* 20(3), doi: 10.3390/ijms20030561

Okamoto, H. et al. 1987. [Open heart surgery in patients associated with severe chronic renal disease]. *Kyobu Geka* 40(9), pp. 715-720.

Okui, N. et al. 2019. Claudin 7 as a possible novel molecular target for the treatment of pancreatic cancer. *Pancreatology* 19(1), pp. 88-96. doi: 10.1016/j.pan.2018.10.009

Olive, K. P. et al. 2009. Inhibition of Hedgehog signaling enhances delivery of chemotherapy in a mouse model of pancreatic cancer. *Science* 324(5933), pp. 1457-1461. doi: 10.1126/science.1171362

Oliveira, S. R., Amaral, J. D. and Rodrigues, C. M. P. 2018. Mechanism and disease implications of necroptosis and neuronal inflammation. *Cell Death Dis* 9(9), p. 903. doi: 10.1038/s41419-018-0872-7

Oppenheim, R. W., Flavell, R. A., Vinsant, S., Prevette, D., Kuan, C. Y. and Rakic, P. 2001. Programmed cell death of developing mammalian neurons after genetic deletion of caspases. *J Neurosci* 21(13), pp. 4752-4760.

Oppenheimer, S. B. 1975. Functional involvement of specific carbohydrate in teratoma cell adhesion factor. *Exp Cell Res* 92(1), pp. 122-126. doi: 10.1016/0014-4827(75)90644-8

Oral, E., Olive, D. L. and Arici, A. 1996. The peritoneal environment in endometriosis. *Hum Reprod Update* 2(5), pp. 385-398. doi: 10.1093/humupd/2.5.385

Orford, K., Orford, C. C. and Byers, S. W. 1999. Exogenous expression of beta-catenin regulates contact inhibition, anchorage-independent growth, anoikis, and radiation-induced cell cycle arrest. *J Cell Biol* 146(4), pp. 855-868. doi: 10.1083/jcb.146.4.855

Orimo, A. and Weinberg, R. A. 2006. Stromal fibroblasts in cancer: a novel tumor-promoting cell type. *Cell Cycle* 5(15), pp. 1597-1601. doi: 10.4161/cc.5.15.3112

Orlowski, R. Z. and Baldwin, A. S., Jr. 2002. NF-kappaB as a therapeutic target in cancer. *Trends Mol Med* 8(8), pp. 385-389. doi: 10.1016/s1471-4914(02)02375-4

Osborn, L., Hession, C., Tizard, R., Vassallo, C., Luhowskyj, S., Chi-Rosso, G. and Lobb, R. 1989. Direct expression cloning of vascular cell adhesion molecule 1, a cytokine-induced endothelial protein that binds to lymphocytes. *Cell* 59(6), pp. 1203-1211. doi: 10.1016/0092-8674(89)90775-7

Otani, T. and Furuse, M. 2020. Tight Junction Structure and Function Revisited. *Trends Cell Biol* 30(10), pp. 805-817. doi: 10.1016/j.tcb.2020.08.004

Ozdemir, B. C. et al. 2014. Depletion of carcinoma-associated fibroblasts and fibrosis induces immunosuppression and accelerates pancreas cancer with reduced survival. *Cancer Cell* 25(6),

pp. 719-734. doi: 10.1016/j.ccr.2014.04.005

Ozdemir, B. C. et al. 2015. Depletion of Carcinoma-Associated Fibroblasts and Fibrosis Induces Immunosuppression and Accelerates Pancreas Cancer with Reduced Survival. *Cancer Cell* 28(6), pp. 831-833. doi: 10.1016/j.ccell.2015.11.002

Padmanaban, V., Krol, I., Suhail, Y., Szczerba, B. M., Aceto, N., Bader, J. S. and Ewald, A. J. 2019. E-cadherin is required for metastasis in multiple models of breast cancer. *Nature* 573(7774), pp. 439-444. doi: 10.1038/s41586-019-1526-3

Pang, R. et al. 2010. A subpopulation of CD26+ cancer stem cells with metastatic capacity in human colorectal cancer. *Cell Stem Cell* 6(6), pp. 603-615. doi: 10.1016/j.stem.2010.04.001

Parish, C. R., Jakobsen, K. B. and Coombe, D. R. 1992. A basement-membrane permeability assay which correlates with the metastatic potential of tumour cells. *Int J Cancer* 52(3), pp. 378-383. doi: 10.1002/ijc.2910520309

Park, C. C., Zhang, H., Pallavicini, M., Gray, J. W., Baehner, F., Park, C. J. and Bissell, M. J. 2006. Beta1 integrin inhibitory antibody induces apoptosis of breast cancer cells, inhibits growth, and distinguishes malignant from normal phenotype in three dimensional cultures and in vivo. *Cancer Res* 66(3), pp. 1526-1535. doi: 10.1158/0008-5472.CAN-05-3071

Park, H. Y., Kweon, D. K. and Kim, J. K. 2023. Molecular weight-dependent hyaluronic acid permeability and tight junction modulation in human buccal TR146 cell monolayers. *Int J Biol Macromol* 227, pp. 182-192. doi: 10.1016/j.ijbiomac.2022.12.106

Parsons, J. T. 2003. Focal adhesion kinase: the first ten years. *J Cell Sci* 116(Pt 8), pp. 1409-1416. doi: 10.1242/jcs.00373

Parsons, S. J. and Parsons, J. T. 2004. Src family kinases, key regulators of signal transduction. *Oncogene* 23(48), pp. 7906-7909. doi: 10.1038/sj.onc.1208160

Passlick, B. et al. 1994. Expression of major histocompatibility class I and class II antigens and intercellular adhesion molecule-1 on operable non-small cell lung carcinomas: frequency and prognostic significance. *Eur J Cancer* 30A(3), pp. 376-381. doi: 10.1016/0959-8049(94)90259-3

Passlick, B. et al. 1996. Expression of MHC molecules and ICAM-1 on non-small cell lung carcinomas: association with early lymphatic spread of tumour cells. *Eur J Cancer* 32A(1), pp. 141-145. doi: 10.1016/0959-8049(95)00551-x

Patra, S. K. 2008. Dissecting lipid raft facilitated cell signaling pathways in cancer. *Biochim Biophys Acta* 1785(2), pp. 182-206. doi: 10.1016/j.bbcan.2007.11.002

Paul, N. R., Jacquemet, G. and Caswell, P. T. 2015. Endocytic Trafficking of Integrins in Cell Migration. *Curr Biol* 25(22), pp. R1092-1105. doi: 10.1016/j.cub.2015.09.049

Peters, D. E. et al. 2012. Capillary morphogenesis protein-2 is required for mouse parturition by maintaining uterine collagen homeostasis. *Biochem Biophys Res Commun* 422(3), pp. 393-397. doi: 10.1016/j.bbrc.2012.04.160

Petruzzelli, M. and Wagner, E. F. 2016. Mechanisms of metabolic dysfunction in cancer-

associated cachexia. *Genes Dev* 30(5), pp. 489-501. doi: 10.1101/gad.276733.115

Pinkas-Kramarski, R. et al. 1996. Diversification of Neu differentiation factor and epidermal growth factor signaling by combinatorial receptor interactions. *EMBO J* 15(10), pp. 2452-2467.

Pittet, M. J., Michielin, O. and Migliorini, D. 2022. Clinical relevance of tumour-associated macrophages. *Nat Rev Clin Oncol* 19(6), pp. 402-421. doi: 10.1038/s41571-022-00620-6

Plaza-Menacho, I. et al. 2011. Focal adhesion kinase (FAK) binds RET kinase via its FERM domain, priming a direct and reciprocal RET-FAK transactivation mechanism. *J Biol Chem* 286(19), pp. 17292-17302. doi: 10.1074/jbc.M110.168500

Pober, J. S. et al. 1987. Activation of cultured human endothelial cells by recombinant lymphotoxin: comparison with tumor necrosis factor and interleukin 1 species. *J Immunol* 138(10), pp. 3319-3324.

Pomerantz, J. et al. 1998. The Ink4a tumor suppressor gene product, p19Arf, interacts with MDM2 and neutralizes MDM2's inhibition of p53. *Cell* 92(6), pp. 713-723. doi: 10.1016/s0092-8674(00)81400-2

Popowicz, G. M., Schleicher, M., Noegel, A. A. and Holak, T. A. 2006. Filamins: promiscuous organizers of the cytoskeleton. *Trends Biochem Sci* 31(7), pp. 411-419. doi: 10.1016/j.tibs.2006.05.006

Prabhu, A., Mishra, D., Brandl, A. and Yonemura, Y. 2022. Gastric Cancer With Peritoneal Metastasis-A Comprehensive Review of Current Intraperitoneal Treatment Modalities. *Front Oncol* 12, p. 864647. doi: 10.3389/fonc.2022.864647

Prevo, R., Banerji, S., Ferguson, D. J., Clasper, S. and Jackson, D. G. 2001. Mouse LYVE-1 is an endocytic receptor for hyaluronan in lymphatic endothelium. *J Biol Chem* 276(22), pp. 19420-19430. doi: 10.1074/jbc.M011004200

Provenzano, P. P., Cuevas, C., Chang, A. E., Goel, V. K., Von Hoff, D. D. and Hingorani, S. R. 2012. Enzymatic targeting of the stroma ablates physical barriers to treatment of pancreatic ductal adenocarcinoma. *Cancer Cell* 21(3), pp. 418-429. doi: 10.1016/j.ccr.2012.01.007

Provenzano, P. P., Eliceiri, K. W., Campbell, J. M., Inman, D. R., White, J. G. and Keely, P. J. 2006. Collagen reorganization at the tumor-stromal interface facilitates local invasion. *BMC Med* 4(1), p. 38. doi: 10.1186/1741-7015-4-38

Pullan, S. et al. 1996. Requirement of basement membrane for the suppression of programmed cell death in mammary epithelium. *J Cell Sci* 109 (Pt 3), pp. 631-642. doi: 10.1242/jcs.109.3.631

Puthalakath, H. et al. 2001. Bmf: a proapoptotic BH3-only protein regulated by interaction with the myosin V actin motor complex, activated by anoikis. *Science* 293(5536), pp. 1829-1832. doi: 10.1126/science.1062257

Qaseem, A. S., Sonar, S., Mahajan, L., Madan, T., Sorensen, G. L., Shamji, M. H. and Kishore, U. 2013. Linking surfactant protein SP-D and IL-13: implications in asthma and allergy. *Mol Immunol* 54(1), pp. 98-107. doi: 10.1016/j.molimm.2012.10.039

Qian, B. Z. and Pollard, J. W. 2010. Macrophage diversity enhances tumor progression and metastasis. *Cell* 141(1), pp. 39-51. doi: 10.1016/j.cell.2010.03.014

Rahier, J., Wallon, J. and Henquin, J. C. 1981. Cell populations in the endocrine pancreas of human neonates and infants. *Diabetologia* 20(5), pp. 540-546. doi: 10.1007/BF00252762

Rane, C. K. and Minden, A. 2014. P21 activated kinases: structure, regulation, and functions. *Small GTPases* 5, doi: 10.4161/sgtp.28003

Ransom, R. C. et al. 2018. Mechanoresponsive stem cells acquire neural crest fate in jaw regeneration. *Nature* 563(7732), pp. 514-521. doi: 10.1038/s41586-018-0650-9

Rao, T. C., Ma, V. P., Blanchard, A., Urner, T. M., Grandhi, S., Salaita, K. and Mattheyses, A. L. 2020. EGFR activation attenuates the mechanical threshold for integrin tension and focal adhesion formation. *J Cell Sci* 133(13), doi: 10.1242/jcs.238840

Raynaud, C. M. et al. 2010. DNA damage repair and telomere length in normal breast, preneoplastic lesions, and invasive cancer. *Am J Clin Oncol* 33(4), pp. 341-345. doi: 10.1097/COC.0b013e3181b0c4c2

Raz, A. and Lotan, R. 1981. Lectin-like activities associated with human and murine neoplastic cells. *Cancer Res* 41(9 Pt 1), pp. 3642-3647.

Reeves, C. V., Dufraine, J., Young, J. A. and Kitajewski, J. 2010. Anthrax toxin receptor 2 is expressed in murine and tumor vasculature and functions in endothelial proliferation and morphogenesis. *Oncogene* 29(6), pp. 789-801. doi: 10.1038/onc.2009.383

Ribeiro, A. S. et al. 2010. Extracellular cleavage and shedding of P-cadherin: a mechanism underlying the invasive behaviour of breast cancer cells. *Oncogene* 29(3), pp. 392-402. doi: 10.1038/onc.2009.338

Rodriguez-Viciana, P., Warne, P. H., Vanhaesebroeck, B., Waterfield, M. D. and Downward, J. 1996. Activation of phosphoinositide 3-kinase by interaction with Ras and by point mutation. *EMBO J* 15(10), pp. 2442-2451.

Rogers, C. D., Saxena, A. and Bronner, M. E. 2013. Sip1 mediates an E-cadherin-to-N-cadherin switch during cranial neural crest EMT. *J Cell Biol* 203(5), pp. 835-847. doi: 10.1083/jcb.201305050

Rogers, M. S., Christensen, K. A., Birsner, A. E., Short, S. M., Wigelsworth, D. J., Collier, R. J. and D'Amato, R. J. 2007. Mutant anthrax toxin B moiety (protective antigen) inhibits angiogenesis and tumor growth. *Cancer Res* 67(20), pp. 9980-9985. doi: 10.1158/0008-5472.CAN-07-0829

Roggiani, F., Mezzanzanica, D., Rea, K. and Tomassetti, A. 2016. Guidance of Signaling Activations by Cadherins and Integrins in Epithelial Ovarian Cancer Cells. *Int J Mol Sci* 17(9), doi: 10.3390/ijms17091387

Romero-Calvo, I. et al. 2019. Human Organoids Share Structural and Genetic Features with Primary Pancreatic Adenocarcinoma Tumors. *Mol Cancer Res* 17(1), pp. 70-83. doi:

10.1158/1541-7786.MCR-18-0531

Rosen, J. M. and Jordan, C. T. 2009. The increasing complexity of the cancer stem cell paradigm. *Science* 324(5935), pp. 1670-1673. doi: 10.1126/science.1171837

Rosette, C., Roth, R. B., Oeth, P., Braun, A., Kammerer, S., Ekblom, J. and Denissenko, M. F. 2005. Role of ICAM1 in invasion of human breast cancer cells. *Carcinogenesis* 26(5), pp. 943-950. doi: 10.1093/carcin/bgi070

Ross, T. D., Coon, B. G., Yun, S., Baeyens, N., Tanaka, K., Ouyang, M. and Schwartz, M. A. 2013. Integrins in mechanotransduction. *Curr Opin Cell Biol* 25(5), pp. 613-618. doi: 10.1016/j.ceb.2013.05.006

Roughley, P. J. 2006. The structure and function of cartilage proteoglycans. *Eur Cell Mater* 12, pp. 92-101. doi: 10.22203/ecm.v012a11

Royal, R. E. et al. 2010. Phase 2 trial of single agent Ipilimumab (anti-CTLA-4) for locally advanced or metastatic pancreatic adenocarcinoma. *J Immunother* 33(8), pp. 828-833. doi: 10.1097/CJI.0b013e3181eec14c

Royer, C. et al. 2000. Effects of gestational hypoxia on mRNA levels of Glut3 and Glut4 transporters, hypoxia inducible factor-1 and thyroid hormone receptors in developing rat brain. *Brain Res* 856(1-2), pp. 119-128. doi: 10.1016/s0006-8993(99)02365-3

Rozenblum, E. et al. 1997. Tumor-suppressive pathways in pancreatic carcinoma. *Cancer Res* 57(9), pp. 1731-1734.

Rynne-Vidal, A., Jimenez-Heffernan, J. A., Fernandez-Chacon, C., Lopez-Cabrera, M. and Sandoval, P. 2015. The Mesothelial Origin of Carcinoma Associated-Fibroblasts in Peritoneal Metastasis. *Cancers (Basel)* 7(4), pp. 1994-2011. doi: 10.3390/cancers7040872

Sahin, U. et al. 2008. Claudin-18 splice variant 2 is a pan-cancer target suitable for therapeutic antibody development. *Clin Cancer Res* 14(23), pp. 7624-7634. doi: 10.1158/1078-0432.CCR-08-1547

Saini, M., Szczerba, B. M. and Aceto, N. 2019. Circulating Tumor Cell-Neutrophil Tango along the Metastatic Process. *Cancer Res* 79(24), pp. 6067-6073. doi: 10.1158/0008-5472.CAN-19-1972

Saito, K., Iwama, N. and Takahashi, T. 1978. Morphometrical analysis on topographical difference in size distribution, number and volume of islets in the human pancreas. *Tohoku J Exp Med* 124(2), pp. 177-186. doi: 10.1620/tjem.124.177

Sakakura, C. et al. 2002. Differential gene expression profiles of gastric cancer cells established from primary tumour and malignant ascites. *Br J Cancer* 87(10), pp. 1153-1161. doi: 10.1038/sj.bjc.6600580

Sako, A. et al. 2003. Vascular endothelial growth factor synthesis by human omental mesothelial cells is augmented by fibroblast growth factor-2: possible role of mesothelial cell on the development of peritoneal metastasis. *J Surg Res* 115(1), pp. 113-120. doi: 10.1016/s0022-4804(03)00307-x

Sakorafas, G. H., Tsiotou, A. G. and Tsiotos, G. G. 2000. Molecular biology of pancreatic cancer; oncogenes, tumour suppressor genes, growth factors, and their receptors from a clinical perspective. *Cancer Treat Rev* 26(1), pp. 29-52. doi: 10.1053/ctrv.1999.0144

Sampson, L. J., Leyland, M. L. and Dart, C. 2003. Direct interaction between the actin-binding protein filamin-A and the inwardly rectifying potassium channel, Kir2.1. *J Biol Chem* 278(43), pp. 41988-41997. doi: 10.1074/jbc.M307479200

Samraj, A. K., Keil, E., Ueffing, N., Schulze-Osthoff, K. and Schmitz, I. 2006. Loss of caspase-9 provides genetic evidence for the type I/II concept of CD95-mediated apoptosis. *J Biol Chem* 281(40), pp. 29652-29659. doi: 10.1074/jbc.M603487200

Sanchez-Heras, E., Howell, F. V., Williams, G. and Doherty, P. 2006. The fibroblast growth factor receptor acid box is essential for interactions with N-cadherin and all of the major isoforms of neural cell adhesion molecule. *J Biol Chem* 281(46), pp. 35208-35216. doi: 10.1074/jbc.M608655200

Sandoval, P. et al. 2013. Carcinoma-associated fibroblasts derive from mesothelial cells via mesothelial-to-mesenchymal transition in peritoneal metastasis. *J Pathol* 231(4), pp. 517-531. doi: 10.1002/path.4281

Sansom, D., Borrow, J., Solomon, E. and Trowsdale, J. 1991. The human ICAM2 gene maps to 17q23-25. *Genomics* 11(2), pp. 462-464. doi: 10.1016/0888-7543(91)90157-a

Sato, M. et al. 2020. BACH1 Promotes Pancreatic Cancer Metastasis by Repressing Epithelial Genes and Enhancing Epithelial-Mesenchymal Transition. *Cancer Res* 80(6), pp. 1279-1292. doi: 10.1158/0008-5472.CAN-18-4099

Sawada, K. et al. 2008. Loss of E-cadherin promotes ovarian cancer metastasis via alpha 5-integrin, which is a therapeutic target. *Cancer Res* 68(7), pp. 2329-2339. doi: 10.1158/0008-5472.CAN-07-5167

Schaefer, L. and Schaefer, R. M. 2010. Proteoglycans: from structural compounds to signaling molecules. *Cell Tissue Res* 339(1), pp. 237-246. doi: 10.1007/s00441-009-0821-y

Schafer, Z. T. et al. 2009. Antioxidant and oncogene rescue of metabolic defects caused by loss of matrix attachment. *Nature* 461(7260), pp. 109-113. doi: 10.1038/nature08268

Schaller, M. D. 2001. Biochemical signals and biological responses elicited by the focal adhesion kinase. *Biochim Biophys Acta* 1540(1), pp. 1-21. doi: 10.1016/s0167-4889(01)00123-9

Schardt, C., Heymanns, J., Schardt, C., Rotsch, M. and Havemann, K. 1993. Differential expression of the intercellular adhesion molecule-1 (ICAM-1) in lung cancer cell lines of various histological types. *Eur J Cancer* 29A(16), pp. 2250-2255. doi: 10.1016/0959-8049(93)90217-4

Schlaepfer, D. D., Hauck, C. R. and Sieg, D. J. 1999. Signaling through focal adhesion kinase. *Prog Biophys Mol Biol* 71(3-4), pp. 435-478. doi: 10.1016/s0079-6107(98)00052-2

Schmalhofer, O., Brabletz, S. and Brabletz, T. 2009. E-cadherin, beta-catenin, and ZEB1 in malignant progression of cancer. *Cancer Metastasis Rev* 28(1-2), pp. 151-166. doi:

10.1007/s10555-008-9179-y

Schmidt, J., Pilbauerova, N., Soukup, T., Suchankova-Kleplova, T. and Suchanek, J. 2020. Low Molecular Weight Hyaluronic Acid Effect on Dental Pulp Stem Cells In Vitro. *Biomolecules* 11(1), doi: 10.3390/biom11010022

Scobie, H. M., Rainey, G. J., Bradley, K. A. and Young, J. A. 2003. Human capillary morphogenesis protein 2 functions as an anthrax toxin receptor. *Proc Natl Acad Sci U S A* 100(9), pp. 5170-5174. doi: 10.1073/pnas.0431098100

Seetharaman, S. and Etienne-Manneville, S. 2020. Cytoskeletal Crosstalk in Cell Migration. *Trends Cell Biol* 30(9), pp. 720-735. doi: 10.1016/j.tcb.2020.06.004

Sefrioui, D. et al. 2017. Diagnostic value of CA19.9, circulating tumour DNA and circulating tumour cells in patients with solid pancreatic tumours. *Br J Cancer* 117(7), pp. 1017-1025. doi: 10.1038/bjc.2017.250

Seguin, L., Desgrosellier, J. S., Weis, S. M. and Cheresh, D. A. 2015. Integrins and cancer: regulators of cancer stemness, metastasis, and drug resistance. *Trends Cell Biol* 25(4), pp. 234-240. doi: 10.1016/j.tcb.2014.12.006

Semenza, G. L., Jiang, B. H., Leung, S. W., Passantino, R., Concordet, J. P., Maire, P. and Giallongo, A. 1996. Hypoxia response elements in the aldolase A, enolase 1, and lactate dehydrogenase A gene promoters contain essential binding sites for hypoxia-inducible factor 1. *J Biol Chem* 271(51), pp. 32529-32537. doi: 10.1074/jbc.271.51.32529

Sepulveda, J. L., Gkretsi, V. and Wu, C. 2005. Assembly and signaling of adhesion complexes. *Curr Top Dev Biol* 68, pp. 183-225. doi: 10.1016/S0070-2153(05)68007-6

Serrano, M., Lin, A. W., McCurrach, M. E., Beach, D. and Lowe, S. W. 1997. Oncogenic ras provokes premature cell senescence associated with accumulation of p53 and p16INK4a. *Cell* 88(5), pp. 593-602. doi: 10.1016/s0092-8674(00)81902-9

Shah, S. A., Potter, M. W., Hedeshian, M. H., Kim, R. D., Chari, R. S. and Callery, M. P. 2001. PI-3' kinase and NF-kappaB cross-signaling in human pancreatic cancer cells. *J Gastrointest Surg* 5(6), pp. 603-612; discussion 612-603. doi: 10.1016/s1091-255x(01)80102-5

Shao, Y. T., Ma, L., Zhang, T. H., Xu, T. R., Ye, Y. C. and Liu, Y. 2019. The Application of the RNA Interference Technologies for KRAS: Current Status, Future Perspective and Associated Challenges. *Curr Top Med Chem* 19(23), pp. 2143-2157. doi: 10.2174/1568026619666190828162217

Shen, T. and Guo, Q. 2020. EGFR signaling pathway occupies an important position in cancer-related downstream signaling pathways of Pyk2. *Cell Biol Int* 44(1), pp. 2-13. doi: 10.1002/cbin.11209

Sherr, C. J. and DePinho, R. A. 2000. Cellular senescence: mitotic clock or culture shock? *Cell* 102(4), pp. 407-410. doi: 10.1016/s0092-8674(00)00046-5

Shibue, T. et al. 2003. Integral role of Noxa in p53-mediated apoptotic response. *Genes Dev* 17(18), pp. 2233-2238. doi: 10.1101/gad.1103603

Shimamura, A., Ballif, B. A., Richards, S. A. and Blenis, J. 2000. Rsk1 mediates a MEK-MAP kinase cell survival signal. *Curr Biol* 10(3), pp. 127-135. doi: 10.1016/s0960-9822(00)00310-9

Shin, D. W. and Kim, J. 2020. The American Joint Committee on Cancer 8th edition staging system for the pancreatic ductal adenocarcinoma: is it better than the 7th edition? *Hepatobiliary Surg Nutr* 9(1), pp. 98-100. doi: 10.21037/hbsn.2019.08.06

Shintani, T. and Klionsky, D. J. 2004. Autophagy in health and disease: a double-edged sword. *Science* 306(5698), pp. 990-995. doi: 10.1126/science.1099993

Sica, A. et al. 1990. Monocyte chemotactic and activating factor gene expression induced in endothelial cells by IL-1 and tumor necrosis factor. *J Immunol* 144(8), pp. 3034-3038.

Sicard, A. et al. 2011. Activation of a PAK-MEK signalling pathway in malaria parasite-infected erythrocytes. *Cell Microbiol* 13(6), pp. 836-845. doi: 10.1111/j.1462-5822.2011.01582.x

Sieg, D. J., Hauck, C. R., Ilic, D., Klingbeil, C. K., Schaefer, E., Damsky, C. H. and Schlaepfer, D. D. 2000. FAK integrates growth-factor and integrin signals to promote cell migration. *Nat Cell Biol* 2(5), pp. 249-256. doi: 10.1038/35010517

Siegel, R. L., Miller, K. D. and Jemal, A. 2020. Cancer statistics, 2020. *CA Cancer J Clin* 70(1), pp. 7-30. doi: 10.3322/caac.21590

Silvius, J. R. 2003. Role of cholesterol in lipid raft formation: lessons from lipid model systems. *Biochim Biophys Acta* 1610(2), pp. 174-183. doi: 10.1016/s0005-2736(03)00016-6

Simpson, C. D., Anyiwe, K. and Schimmer, A. D. 2008. Anoikis resistance and tumor metastasis. *Cancer Lett* 272(2), pp. 177-185. doi: 10.1016/j.canlet.2008.05.029

Singh, S., Srivastava, S. K., Bhardwaj, A., Owen, L. B. and Singh, A. P. 2010. CXCL12-CXCR4 signalling axis confers gemcitabine resistance to pancreatic cancer cells: a novel target for therapy. *Br J Cancer* 103(11), pp. 1671-1679. doi: 10.1038/sj.bjc.6605968

Slack-Davis, J. K., Atkins, K. A., Harrer, C., Hershey, E. D. and Conaway, M. 2009. Vascular cell adhesion molecule-1 is a regulator of ovarian cancer peritoneal metastasis. *Cancer Res* 69(4), pp. 1469-1476. doi: 10.1158/0008-5472.CAN-08-2678

Sokeland, G. and Schumacher, U. 2019. The functional role of integrins during intra- and extravasation within the metastatic cascade. *Mol Cancer* 18(1), p. 12. doi: 10.1186/s12943-018-0937-3

Soliman, F., Ye, L., Jiang, W. and Hargest, R. 2022. Targeting Hyaluronic Acid and Peritoneal Dissemination in Colorectal Cancer. *Clin Colorectal Cancer* 21(2), pp. e126-e134. doi: 10.1016/j.clcc.2021.11.008

Solomon, S., Das, S., Brand, R. and Whitcomb, D. C. 2012. Inherited pancreatic cancer syndromes. *Cancer J* 18(6), pp. 485-491. doi: 10.1097/PPO.0b013e318278c4a6

Son, J., Lee, J. H., Kim, H. N., Ha, H. and Lee, Z. H. 2010. cAMP-response-element-binding protein positively regulates breast cancer metastasis and subsequent bone destruction.

Biochem Biophys Res Commun 398(2), pp. 309-314. doi: 10.1016/j.bbrc.2010.06.087

Sorg, H., Tilkorn, D. J., Hager, S., Hauser, J. and Mirastschijski, U. 2017. Skin Wound Healing: An Update on the Current Knowledge and Concepts. *Eur Surg Res* 58(1-2), pp. 81-94. doi: 10.1159/000454919

Soura, E., Eliades, P. J., Shannon, K., Stratigos, A. J. and Tsao, H. 2016. Hereditary melanoma: Update on syndromes and management: Genetics of familial atypical multiple mole melanoma syndrome. *J Am Acad Dermatol* 74(3), pp. 395-407; quiz 408-310. doi: 10.1016/j.jaad.2015.08.038

Sousa, B., Pereira, J. and Paredes, J. 2019. The Crosstalk Between Cell Adhesion and Cancer Metabolism. *Int J Mol Sci* 20(8), doi: 10.3390/ijms20081933

Spencer, S. L., Gaudet, S., Albeck, J. G., Burke, J. M. and Sorger, P. K. 2009. Non-genetic origins of cell-to-cell variability in TRAIL-induced apoptosis. *Nature* 459(7245), pp. 428-432. doi: 10.1038/nature08012

Srivastava, S. K., Bhardwaj, A., Singh, S., Arora, S., Wang, B., Grizzle, W. E. and Singh, A. P. 2011. MicroRNA-150 directly targets MUC4 and suppresses growth and malignant behavior of pancreatic cancer cells. *Carcinogenesis* 32(12), pp. 1832-1839. doi: 10.1093/carcin/bgr223

Stacker, S. A. et al. 1999. Biosynthesis of vascular endothelial growth factor-D involves proteolytic processing which generates non-covalent homodimers. *J Biol Chem* 274(45), pp. 32127-32136. doi: 10.1074/jbc.274.45.32127

Stambolic, V. et al. 2001. Regulation of PTEN transcription by p53. *Mol Cell* 8(2), pp. 317-325. doi: 10.1016/s1097-2765(01)00323-9

Strilic, B. and Offermanns, S. 2017. Intravascular Survival and Extravasation of Tumor Cells. *Cancer Cell* 32(3), pp. 282-293. doi: 10.1016/j.ccell.2017.07.001

Su, G. H. et al. 1999. Germline and somatic mutations of the STK11/LKB1 Peutz-Jeghers gene in pancreatic and biliary cancers. *Am J Pathol* 154(6), pp. 1835-1840. doi: 10.1016/S0002-9440(10)65440-5

Su, G. H. and Kern, S. E. 2000. Molecular genetics of ductal pancreatic neoplasia. *Curr Opin Gastroenterol* 16(5), pp. 419-425. doi: 10.1097/00001574-200009000-00005

Sudarsanam, S. and Johnson, D. E. 2010. Functional consequences of mTOR inhibition. *Curr Opin Drug Discov Devel* 13(1), pp. 31-40.

Sugarbaker, P. H. 1996. Observations concerning cancer spread within the peritoneal cavity and concepts supporting an ordered pathophysiology. *Cancer Treat Res* 82, pp. 79-100. doi: 10.1007/978-1-4613-1247-5_6

Sun, J. and Jacquez, P. 2016. Roles of Anthrax Toxin Receptor 2 in Anthrax Toxin Membrane Insertion and Pore Formation. *Toxins (Basel)* 8(2), p. 34. doi: 10.3390/toxins8020034

Sunagawa, Y. et al. 2020. Novel Prognostic Implications of DUPAN-2 in the Era of Initial Systemic Therapy for Pancreatic Cancer. *Ann Surg Oncol* 27(6), pp. 2081-2089. doi:

10.1245/s10434-019-07981-w

Sung, H., Ferlay, J., Siegel, R. L., Laversanne, M., Soerjomataram, I., Jemal, A. and Bray, F. 2021. Global Cancer Statistics 2020: GLOBOCAN Estimates of Incidence and Mortality Worldwide for 36 Cancers in 185 Countries. *CA Cancer J Clin* 71(3), pp. 209-249. doi: 10.3322/caac.21660

Sureban, S. M. et al. 2011. DCAMKL-1 regulates epithelial-mesenchymal transition in human pancreatic cells through a miR-200a-dependent mechanism. *Cancer Res* 71(6), pp. 2328-2338. doi: 10.1158/0008-5472.CAN-10-2738

Suwa, H. et al. 1998. Overexpression of the rhoC gene correlates with progression of ductal adenocarcinoma of the pancreas. *Br J Cancer* 77(1), pp. 147-152. doi: 10.1038/bjc.1998.23

Suyama, K., Shapiro, I., Guttman, M. and Hazan, R. B. 2002. A signaling pathway leading to metastasis is controlled by N-cadherin and the FGF receptor. *Cancer Cell* 2(4), pp. 301-314. doi: 10.1016/s1535-6108(02)00150-2

Sy, M. S., Guo, Y. J. and Stamenkovic, I. 1991. Distinct effects of two CD44 isoforms on tumor growth in vivo. *J Exp Med* 174(4), pp. 859-866. doi: 10.1084/jem.174.4.859

Sy, M. S., Guo, Y. J. and Stamenkovic, I. 1992. Inhibition of tumor growth in vivo with a soluble CD44-immunoglobulin fusion protein. *J Exp Med* 176(2), pp. 623-627. doi: 10.1084/jem.176.2.623

Syngal, S., Brand, R. E., Church, J. M., Giardiello, F. M., Hampel, H. L., Burt, R. W. and American College of, G. 2015. ACG clinical guideline: Genetic testing and management of hereditary gastrointestinal cancer syndromes. *Am J Gastroenterol* 110(2), pp. 223-262; quiz 263. doi: 10.1038/ajg.2014.435

Szczerba, B. M. et al. 2019. Neutrophils escort circulating tumour cells to enable cell cycle progression. *Nature* 566(7745), pp. 553-557. doi: 10.1038/s41586-019-0915-y

Taddei, M. L., Giannoni, E., Fiaschi, T. and Chiarugi, P. 2012. Anoikis: an emerging hallmark in health and diseases. *J Pathol* 226(2), pp. 380-393. doi: 10.1002/path.3000

Taftaf, R. et al. 2021. ICAM1 initiates CTC cluster formation and trans-endothelial migration in lung metastasis of breast cancer. *Nat Commun* 12(1), p. 4867. doi: 10.1038/s41467-021-25189-z

Takatsuki, H., Komatsu, S., Sano, R., Takada, Y. and Tsuji, T. 2004. Adhesion of gastric carcinoma cells to peritoneum mediated by alpha3beta1 integrin (VLA-3). *Cancer Res* 64(17), pp. 6065-6070. doi: 10.1158/0008-5472.CAN-04-0321

Takeichi, M., Nakagawa, S., Aono, S., Usui, T. and Uemura, T. 2000. Patterning of cell assemblies regulated by adhesion receptors of the cadherin superfamily. *Philos Trans R Soc Lond B Biol Sci* 355(1399), pp. 885-890. doi: 10.1098/rstb.2000.0624

Takeyama, Y. et al. 2010. Knockdown of ZEB1, a master epithelial-to-mesenchymal transition (EMT) gene, suppresses anchorage-independent cell growth of lung cancer cells. *Cancer Lett* 296(2), pp. 216-224. doi: 10.1016/j.canlet.2010.04.008

Takiguchi, S., Inoue, K., Matsusue, K., Furukawa, M., Teramoto, N. and Iguchi, H. 2017. Crizotinib, a MET inhibitor, prevents peritoneal dissemination in pancreatic cancer. *Int J Oncol* 51(1), pp. 184-192. doi: 10.3892/ijo.2017.3992

Tan I, N. J., Tan P. 2010. Role of Polymorphisms in Cancer Susceptibility. *Encyclopedia of Life Sciences*,

Tan, J. et al. 2018. Capillary morphogenesis protein 2 is a novel prognostic biomarker and plays oncogenic roles in glioma. *J Pathol* 245(2), pp. 160-171. doi: 10.1002/path.5062

Tanaka, M. et al. 2011. Claudin-18 is an early-stage marker of pancreatic carcinogenesis. *J Histochem Cytochem* 59(10), pp. 942-952. doi: 10.1369/0022155411420569

Tang, R. F., Itakura, J., Aikawa, T., Matsuda, K., Fujii, H., Korc, M. and Matsumoto, Y. 2001. Overexpression of lymphangiogenic growth factor VEGF-C in human pancreatic cancer. *Pancreas* 22(3), pp. 285-292. doi: 10.1097/00006676-200104000-00010

Tapial Martinez, P., Lopez Navajas, P. and Lietha, D. 2020. FAK Structure and Regulation by Membrane Interactions and Force in Focal Adhesions. *Biomolecules* 10(2), doi: 10.3390/biom10020179

Taraboletti, G. and Margosio, B. 2001. Antiangiogenic and antivascular therapy for cancer. *Curr Opin Pharmacol* 1(4), pp. 378-384. doi: 10.1016/s1471-4892(01)00065-0

Tavano, F. et al. 2012. Changes in miR-143 and miR-21 expression and clinicopathological correlations in pancreatic cancers. *Pancreas* 41(8), pp. 1280-1284. doi: 10.1097/MPA.0b013e31824c11f4

Thiel, G., Backes, T. M., Guethlein, L. A. and Rossler, O. G. 2021. Critical Protein-Protein Interactions Determine the Biological Activity of Elk-1, a Master Regulator of Stimulus-Induced Gene Transcription. *Molecules* 26(20), doi: 10.3390/molecules26206125

Thiery, J. P., Acloque, H., Huang, R. Y. and Nieto, M. A. 2009. Epithelial-mesenchymal transitions in development and disease. *Cell* 139(5), pp. 871-890. doi: 10.1016/j.cell.2009.11.007

Thomas, R. M., Kim, J., Revelo-Penafiel, M. P., Angel, R., Dawson, D. W. and Lowy, A. M. 2008. The chemokine receptor CXCR4 is expressed in pancreatic intraepithelial neoplasia. *Gut* 57(11), pp. 1555-1560. doi: 10.1136/gut.2007.143941

Thomassen, I., Lemmens, V. E., Nienhuijs, S. W., Luyer, M. D., Klaver, Y. L. and de Hingh, I. H. 2013. Incidence, prognosis, and possible treatment strategies of peritoneal carcinomatosis of pancreatic origin: a population-based study. *Pancreas* 42(1), pp. 72-75. doi: 10.1097/MPA.0b013e31825abf8c

Thomsen, R., Solvsten, C. A., Linnet, T. E., Blechingberg, J. and Nielsen, A. L. 2010. Analysis of qPCR data by converting exponentially related Ct values into linearly related X0 values. *J Bioinform Comput Biol* 8(5), pp. 885-900. doi: 10.1142/s0219720010004963

Tian, X., He, Y., Han, Z., Su, H. and Chu, C. 2019. The Cytoplasmic Expression Of CLDN12

Predicts An Unfavorable Prognosis And Promotes Proliferation And Migration Of Osteosarcoma. *Cancer Manag Res* 11, pp. 9339-9351. doi: 10.2147/CMAR.S229441

Tisdale, M. J. 2003. Pathogenesis of cancer cachexia. *J Support Oncol* 1(3), pp. 159-168.

Tomita, K., van Bokhoven, A., van Leenders, G. J., Ruijter, E. T., Jansen, C. F., Bussemakers, M. J. and Schalken, J. A. 2000. Cadherin switching in human prostate cancer progression. *Cancer Res* 60(13), pp. 3650-3654.

Toole, B. P. 1997. Hyaluronan in morphogenesis. *J Intern Med* 242(1), pp. 35-40. doi: 10.1046/j.1365-2796.1997.00171.x

Torphy, R. J., Fujiwara, Y. and Schulick, R. D. 2020. Pancreatic cancer treatment: better, but a long way to go. *Surg Today* 50(10), pp. 1117-1125. doi: 10.1007/s00595-020-02028-0

Torphy, R. J., Zhu, Y. and Schulick, R. D. 2018. Immunotherapy for pancreatic cancer: Barriers and breakthroughs. *Ann Gastroenterol Surg* 2(4), pp. 274-281. doi: 10.1002/ags3.12176

Torres, J. B. et al. 2018. Imaging of Claudin-4 in Pancreatic Ductal Adenocarcinoma Using a Radiolabelled Anti-Claudin-4 Monoclonal Antibody. *Mol Imaging Biol* 20(2), pp. 292-299. doi: 10.1007/s11307-017-1112-8

Totland, M. Z., Rasmussen, N. L., Knudsen, L. M. and Leithe, E. 2020. Regulation of gap junction intercellular communication by connexin ubiquitination: physiological and pathophysiological implications. *Cell Mol Life Sci* 77(4), pp. 573-591. doi: 10.1007/s00018-019-03285-0

Treadwell, J. R., Zafar, H. M., Mitchell, M. D., Tipton, K., Teitelbaum, U. and Jue, J. 2016. Imaging Tests for the Diagnosis and Staging of Pancreatic Adenocarcinoma: A Meta-Analysis. *Pancreas* 45(6), pp. 789-795. doi: 10.1097/MPA.0000000000000524

Trusolino, L., Bertotti, A. and Comoglio, P. M. 2001. A signaling adapter function for alpha6beta4 integrin in the control of HGF-dependent invasive growth. *Cell* 107(5), pp. 643-654. doi: 10.1016/s0092-8674(01)00567-0

Tureci, O. et al. 2011. Claudin-18 gene structure, regulation, and expression is evolutionary conserved in mammals. *Gene* 481(2), pp. 83-92. doi: 10.1016/j.gene.2011.04.007

Turner, H. E., Harris, A. L., Melmed, S. and Wass, J. A. 2003. Angiogenesis in endocrine tumors. *Endocr Rev* 24(5), pp. 600-632. doi: 10.1210/er.2002-0008

Ue, T., Yokozaki, H., Kitadai, Y., Yamamoto, S., Yasui, W., Ishikawa, T. and Tahara, E. 1998. Co-expression of osteopontin and CD44v9 in gastric cancer. *Int J Cancer* 79(2), pp. 127-132. doi: 10.1002/(sici)1097-0215(19980417)79:2<127::aid-ijc5>3.0.co;2-v

Umeda, K. et al. 2006. ZO-1 and ZO-2 independently determine where claudins are polymerized in tight-junction strand formation. *Cell* 126(4), pp. 741-754. doi: 10.1016/j.cell.2006.06.043

Urano, T., Emkey, R. and Feig, L. A. 1996. Ral-GTPases mediate a distinct downstream signaling pathway from Ras that facilitates cellular transformation. *EMBO J* 15(4), pp. 810-816.

Valentijn, A. J. and Gilmore, A. P. 2004. Translocation of full-length Bid to mitochondria during anoikis. *J Biol Chem* 279(31), pp. 32848-32857. doi: 10.1074/jbc.M313375200

Valentijn, A. J., Metcalfe, A. D., Kott, J., Streuli, C. H. and Gilmore, A. P. 2003. Spatial and temporal changes in Bax subcellular localization during anoikis. *J Cell Biol* 162(4), pp. 599-612. doi: 10.1083/jcb.200302154

van Baal, J. O. et al. 2017. The histophysiology and pathophysiology of the peritoneum. *Tissue Cell* 49(1), pp. 95-105. doi: 10.1016/j.tice.2016.11.004

van Grevenstein, W. M., Hofland, L. J., van Rossen, M. E., van Koetsveld, P. M., Jeekel, J. and van Eijck, C. H. 2007. Inflammatory cytokines stimulate the adhesion of colon carcinoma cells to mesothelial monolayers. *Dig Dis Sci* 52(10), pp. 2775-2783. doi: 10.1007/s10620-007-9778-4

van Heek, N. T. et al. 2002. Telomere shortening is nearly universal in pancreatic intraepithelial neoplasia. *Am J Pathol* 161(5), pp. 1541-1547. doi: 10.1016/S0002-9440(10)64432-X

Van Marck, V., Stove, C., Van Den Bossche, K., Stove, V., Paredes, J., Vander Haeghen, Y. and Bracke, M. 2005. P-cadherin promotes cell-cell adhesion and counteracts invasion in human melanoma. *Cancer Res* 65(19), pp. 8774-8783. doi: 10.1158/0008-5472.CAN-04-4414

van Rijn, J. M. et al. 2020. Enhanced Collagen Deposition in the Duodenum of Patients with Hyaline Fibromatosis Syndrome and Protein Losing Enteropathy. *Int J Mol Sci* 21(21), doi: 10.3390/ijms21218200

van Roy, F. 2014. Beyond E-cadherin: roles of other cadherin superfamily members in cancer. *Nat Rev Cancer* 14(2), pp. 121-134. doi: 10.1038/nrc3647

van Stein, R. M., Aalbers, A. G. J., Sonke, G. S. and van Driel, W. J. 2021. Hyperthermic Intraperitoneal Chemotherapy for Ovarian and Colorectal Cancer: A Review. *JAMA Oncol* 7(8), pp. 1231-1238. doi: 10.1001/jamaoncol.2021.0580

Vander Heiden, M. G., Chandel, N. S., Williamson, E. K., Schumacker, P. T. and Thompson, C. B. 1997. Bcl-xL regulates the membrane potential and volume homeostasis of mitochondria. *Cell* 91(5), pp. 627-637. doi: 10.1016/s0092-8674(00)80450-x

Velu, T. J., Beguinot, L., Vass, W. C., Willingham, M. C., Merlino, G. T., Pastan, I. and Lowy, D. R. 1987. Epidermal-growth-factor-dependent transformation by a human EGF receptor proto-oncogene. *Science* 238(4832), pp. 1408-1410. doi: 10.1126/science.3500513

Verbeke, C. 2016. Morphological heterogeneity in ductal adenocarcinoma of the pancreas - Does it matter? *Pancreatology* 16(3), pp. 295-301. doi: 10.1016/j.pan.2016.02.004

Vieira, A. F. and Paredes, J. 2015. P-cadherin and the journey to cancer metastasis. *Mol Cancer* 14, p. 178. doi: 10.1186/s12943-015-0448-4

Vinagre, J. et al. 2016. TERT promoter mutations in pancreatic endocrine tumours are rare and mainly found in tumours from patients with hereditary syndromes. *Sci Rep* 6, p. 29714. doi: 10.1038/srep29714

Vincent, A., Herman, J., Schulick, R., Hruban, R. H. and Goggins, M. 2011. Pancreatic cancer. *Lancet* 378(9791), pp. 607-620. doi: 10.1016/S0140-6736(10)62307-0

Vinogradova, O., Velyvis, A., Velyviene, A., Hu, B., Haas, T., Plow, E. and Qin, J. 2002. A structural mechanism of integrin alpha(IIb)beta(3) "inside-out" activation as regulated by its cytoplasmic face. *Cell* 110(5), pp. 587-597. doi: 10.1016/s0092-8674(02)00906-6

Virdee, K., Parone, P. A. and Tolkovsky, A. M. 2000. Phosphorylation of the pro-apoptotic protein BAD on serine 155, a novel site, contributes to cell survival. *Curr Biol* 10(23), p. R883. doi: 10.1016/s0960-9822(00)00843-5

Viscardi, G. et al. 2019. Atypical haemolytic-uraemic syndrome in patient with metastatic colorectal cancer treated with fluorouracil and oxaliplatin: a case report and a review of literature. *ESMO Open* 4(5), p. e000551. doi: 10.1136/esmoopen-2019-000551

Vlahova, L. et al. 2012. P-cadherin expression in Merkel cell carcinomas is associated with prolonged recurrence-free survival. *Br J Dermatol* 166(5), pp. 1043-1052. doi: 10.1111/j.1365-2133.2012.10853.x

Wang, C., Wu, N., Pei, B., Ma, X. and Yang, W. 2023. Claudin and pancreatic cancer. *Front Oncol* 13, p. 1136227. doi: 10.3389/fonc.2023.1136227

Wang, H. et al. 2014. Mixed lineage kinase domain-like protein MLKL causes necrotic membrane disruption upon phosphorylation by RIP3. *Mol Cell* 54(1), pp. 133-146. doi: 10.1016/j.molcel.2014.03.003

Wang, J. Y. et al. 2021. [Apoptosis of Endothelial Cells Induced by Anti-Platelet Integrin beta3 Antibody]. *Zhongguo Shi Yan Xue Ye Xue Za Zhi* 29(2), pp. 567-573. doi: 10.19746/j.cnki.issn.1009-2137.2021.02.041

Wang, W., Tan, X., Zhou, L., Gao, F. and Dai, X. 2010. Involvement of the expression and redistribution of claudin-23 in pancreatic cancer cell dissociation. *Mol Med Rep* 3(5), pp. 845-850. doi: 10.3892/mmr.2010.334

Wang, W. C. et al. 2018. Survival Mechanisms and Influence Factors of Circulating Tumor Cells. *Biomed Res Int* 2018, p. 6304701. doi: 10.1155/2018/6304701

Wang, X. et al. 2022. Claudin 18.2 is a potential therapeutic target for zolbetuximab in pancreatic ductal adenocarcinoma. *World J Gastrointest Oncol* 14(7), pp. 1252-1264. doi: 10.4251/wjgo.v14.i7.1252

Wang, Y. Z., Cao, M. L., Liu, Y. W., He, Y. Q., Yang, C. X. and Gao, F. 2011. CD44 mediates oligosaccharides of hyaluronan-induced proliferation, tube formation and signal transduction in endothelial cells. *Exp Biol Med (Maywood)* 236(1), pp. 84-90. doi: 10.1258/ebm.2010.010206

Wasnik, A. P., Maturen, K. E., Kaza, R. K., Al-Hawary, M. M. and Francis, I. R. 2015. Primary and secondary disease of the peritoneum and mesentery: review of anatomy and imaging features. *Abdom Imaging* 40(3), pp. 626-642. doi: 10.1007/s00261-014-0232-8

Watanabe, H. 2022. Aggrecan and versican: two brothers close or apart. *Am J Physiol Cell Physiol* 322(5), pp. C967-C976. doi: 10.1152/ajpcell.00081.2022

Watanabe, T. et al. 2012. Production of IL1-beta by ovarian cancer cells induces mesothelial cell beta1-integrin expression facilitating peritoneal dissemination. *J Ovarian Res* 5(1), p. 7. doi: 10.1186/1757-2215-5-7

Weaver, V. M. et al. 2002. beta4 integrin-dependent formation of polarized three-dimensional architecture confers resistance to apoptosis in normal and malignant mammary epithelium. *Cancer Cell* 2(3), pp. 205-216. doi: 10.1016/s1535-6108(02)00125-3

Webb, D. J., Donais, K., Whitmore, L. A., Thomas, S. M., Turner, C. E., Parsons, J. T. and Horwitz, A. F. 2004. FAK-Src signalling through paxillin, ERK and MLCK regulates adhesion disassembly. *Nat Cell Biol* 6(2), pp. 154-161. doi: 10.1038/ncb1094

Weber, G. F., Ashkar, S., Glimcher, M. J. and Cantor, H. 1996. Receptor-ligand interaction between CD44 and osteopontin (Eta-1). *Science* 271(5248), pp. 509-512. doi: 10.1126/science.271.5248.509

Wee, H., Oh, H. M., Jo, J. H. and Jun, C. D. 2009. ICAM-1/LFA-1 interaction contributes to the induction of endothelial cell-cell separation: implication for enhanced leukocyte diapedesis. *Exp Mol Med* 41(5), pp. 341-348. doi: 10.3858/emm.2009.41.5.038

Weidle, U. H., Birzele, F., Kollmorgen, G. and Rueger, R. 2016. Mechanisms and Targets Involved in Dissemination of Ovarian Cancer. *Cancer Genomics Proteomics* 13(6), pp. 407-423. doi: 10.21873/cgp.20004

Wennerberg, K., Rossman, K. L. and Der, C. J. 2005. The Ras superfamily at a glance. *J Cell Sci* 118(Pt 5), pp. 843-846. doi: 10.1242/jcs.01660

Werling, A. M. et al. 2011. Homo- and heterotypic cell-cell contacts in Merkel cells and Merkel cell carcinomas: heterogeneity and indications for cadherin switching. *Histopathology* 58(2), pp. 286-303. doi: 10.1111/j.1365-2559.2011.03748.x

White, D. E., Kurpios, N. A., Zuo, D., Hassell, J. A., Blaess, S., Mueller, U. and Muller, W. J. 2004. Targeted disruption of beta1-integrin in a transgenic mouse model of human breast cancer reveals an essential role in mammary tumor induction. *Cancer Cell* 6(2), pp. 159-170. doi: 10.1016/j.ccr.2004.06.025

Wiedmann, L. et al. 2023. HAPLN1 potentiates peritoneal metastasis in pancreatic cancer. *Nat Commun* 14(1), p. 2353. doi: 10.1038/s41467-023-38064-w

Wight, T. N. 2008. Arterial remodeling in vascular disease: a key role for hyaluronan and versican. *Front Biosci* 13, pp. 4933-4937. doi: 10.2741/3052

Wilson, R. B., Solass, W., Archid, R., Weinreich, F. J., Konigsrainer, A. and Reymond, M. A. 2019. Resistance to anoikis in transcoelomic shedding: the role of glycolytic enzymes. *Pleura Peritoneum* 4(1), p. 20190003. doi: 10.1515/pp-2019-0003

Wittinghofer, A., Scheffzek, K. and Ahmadian, M. R. 1997. The interaction of Ras with GTPase-activating proteins. *FEBS Lett* 410(1), pp. 63-67. doi: 10.1016/s0014-5793(97)00321-9

Witz, C. A., Montoya-Rodriguez, I. A., Cho, S., Centonze, V. E., Bonewald, L. F. and Schenken,

R. S. 2001. Composition of the extracellular matrix of the peritoneum. *J Soc Gynecol Investig* 8(5), pp. 299-304. doi: 10.1016/s1071-5576(01)00122-8

Wolf, M. F., Koerner, U., Klumpp, B. and Schumacher, K. 1987. Inhibition of homotypic aggregation of a human Burkitt-lymphoma cell line. *Int J Cancer* 40(6), pp. 788-791. doi: 10.1002/ijc.2910400614

Wolfenson, H., Lavelin, I. and Geiger, B. 2013. Dynamic regulation of the structure and functions of integrin adhesions. *Dev Cell* 24(5), pp. 447-458. doi: 10.1016/j.devcel.2013.02.012

Wolfgang, C. L., Herman, J. M., Laheru, D. A., Klein, A. P., Erdek, M. A., Fishman, E. K. and Hruban, R. H. 2013. Recent progress in pancreatic cancer. *CA Cancer J Clin* 63(5), pp. 318-348. doi: 10.3322/caac.21190

Wong, J. C. and Lu, D. S. 2008. Staging of pancreatic adenocarcinoma by imaging studies. *Clin Gastroenterol Hepatol* 6(12), pp. 1301-1308. doi: 10.1016/j.cgh.2008.09.014

Wood, L. D. 2013. Pancreatic cancer genomes: toward molecular subtyping and novel approaches to diagnosis and therapy. *Mol Diagn Ther* 17(5), pp. 287-297. doi: 10.1007/s40291-013-0043-6

Woutersen, R. A., Appel, M. J., van Garderen-Hoetmer, A. and Wijnands, M. V. 1999. Dietary fat and carcinogenesis. *Mutat Res* 443(1-2), pp. 111-127. doi: 10.1016/s1383-5742(99)00014-9

Wu, C. 2001. ILK interactions. *J Cell Sci* 114(Pt 14), pp. 2549-2550. doi: 10.1242/jcs.114.14.2549

Wu, Y. Y., Jiang, J. N., Fang, X. D. and Ji, F. J. 2018. STEAP1 Regulates Tumorigenesis and Chemoresistance During Peritoneal Metastasis of Gastric Cancer. *Front Physiol* 9, p. 1132. doi: 10.3389/fphys.2018.01132

Wyckoff, J. B. et al. 2007. Direct visualization of macrophage-assisted tumor cell intravasation in mammary tumors. *Cancer Res* 67(6), pp. 2649-2656. doi: 10.1158/0008-5472.CAN-06-1823

Wycoff, K., Maclean, J., Belle, A., Yu, L., Tran, Y., Roy, C. and Hayden, F. 2015. Anti-infective immunoadhesins from plants. *Plant Biotechnol J* 13(8), pp. 1078-1093. doi: 10.1111/pbi.12441

Wycoff, K. L. et al. 2011. Recombinant anthrax toxin receptor-Fc fusion proteins produced in plants protect rabbits against inhalational anthrax. *Antimicrob Agents Chemother* 55(1), pp. 132-139. doi: 10.1128/AAC.00592-10

Xiang, F. et al. 2017. Omental adipocytes enhance the invasiveness of gastric cancer cells by oleic acid-induced activation of the PI3K-Akt signaling pathway. *Int J Biochem Cell Biol* 84, pp. 14-21. doi: 10.1016/j.biocel.2016.12.002

Xiao, Z. et al. 2014. Molecular mechanism underlying lymphatic metastasis in pancreatic cancer. *Biomed Res Int* 2014, p. 925845. doi: 10.1155/2014/925845

Xie, Y. et al. 2021. Aberrant oligodendroglial LDL receptor orchestrates demyelination in chronic cerebral ischemia. *J Clin Invest* 131(1), doi: 10.1172/JCI128114

Xu, C., Hu, D. M. and Zhu, Q. 2013. eEF1A2 promotes cell migration, invasion and metastasis in pancreatic cancer by upregulating MMP-9 expression through Akt activation. *Clin Exp Metastasis* 30(7), pp. 933-944. doi: 10.1007/s10585-013-9593-6

Xu, F. J. et al. 1997. Heregulin and agonistic anti-p185(c-erbB2) antibodies inhibit proliferation but increase invasiveness of breast cancer cells that overexpress p185(c-erbB2): increased invasiveness may contribute to poor prognosis. *Clin Cancer Res* 3(9), pp. 1629-1634.

Xu, Y., He, Y., Xu, W., Lu, T., Liang, W. and Jin, W. 2019. Promotive effects of capillary morphogenetic protein 2 on glioma cell invasion and the molecular mechanism. *Folia Neuropathol* 57(1), pp. 6-15. doi: 10.5114/fn.2019.83826

Yachida, S. and Iacobuzio-Donahue, C. A. 2009. The pathology and genetics of metastatic pancreatic cancer. *Arch Pathol Lab Med* 133(3), pp. 413-422. doi: 10.1043/1543-2165-133.3.413
10.5858/133.3.413

Yanez-Mo, M. et al. 2003. Peritoneal dialysis and epithelial-to-mesenchymal transition of mesothelial cells. *N Engl J Med* 348(5), pp. 403-413. doi: 10.1056/NEJMoa020809

Yang, J. et al. 2004. Twist, a master regulator of morphogenesis, plays an essential role in tumor metastasis. *Cell* 117(7), pp. 927-939. doi: 10.1016/j.cell.2004.06.006

Yang, J. et al. 2015a. Reciprocal positive regulation between Cx26 and PI3K/Akt pathway confers acquired gefitinib resistance in NSCLC cells via GJIC-independent induction of EMT. *Cell Death Dis* 6(7), p. e1829. doi: 10.1038/cddis.2015.197

Yang, J. C. et al. 2017. TM4SF1 Promotes Metastasis of Pancreatic Cancer via Regulating the Expression of DDR1. *Sci Rep* 7, p. 45895. doi: 10.1038/srep45895

Yang, L. et al. 2011. Gastric cancer stem-like cells possess higher capability of invasion and metastasis in association with a mesenchymal transition phenotype. *Cancer Lett* 310(1), pp. 46-52. doi: 10.1016/j.canlet.2011.06.003

Yang, M., Liu, J., Piao, C., Shao, J. and Du, J. 2015b. ICAM-1 suppresses tumor metastasis by inhibiting macrophage M2 polarization through blockade of efferocytosis. *Cell Death Dis* 6(6), p. e1780. doi: 10.1038/cddis.2015.144

Yang, R., Lu, M., Qian, X., Chen, J., Li, L., Wang, J. and Zhang, Y. 2014. Diagnostic accuracy of EUS and CT of vascular invasion in pancreatic cancer: a systematic review. *J Cancer Res Clin Oncol* 140(12), pp. 2077-2086. doi: 10.1007/s00432-014-1728-x

Yang, Y. M. et al. 2023. Activated Leukocyte Cell Adhesion Molecule (ALCAM), a Potential 'Seed' and 'Soil' Receptor in the Peritoneal Metastasis of Gastrointestinal Cancers. *Int J Mol Sci* 24(1), doi: 10.3390/ijms24010876

Yarema, R. et al. 2019. Hyperthermic intraperitoneal chemotherapy (HIPEC) in combined treatment of locally advanced and intraperitonealy disseminated gastric cancer: A retrospective cooperative Central-Eastern European study. *Cancer Med* 8(6), pp. 2877-2885. doi: 10.1002/cam4.2204

Ye, F., Lagarrigue, F. and Ginsberg, M. H. 2014a. SnapShot: talin and the modular nature of the integrin adhesome. *Cell* 156(6), pp. 1340-1340 e1341. doi: 10.1016/j.cell.2014.02.048

Ye, L., Sanders, A. J., Sun, P. H., Mason, M. D. and Jiang, W. G. 2014b. Capillary morphogenesis gene 2 regulates adhesion and invasiveness of prostate cancer cells. *Oncol Lett* 7(6), pp. 2149-2153. doi: 10.3892/ol.2014.2038

Ye, L., Sun, P. H., Malik, M. F., Mason, M. D. and Jiang, W. G. 2014c. Capillary morphogenesis gene 2 inhibits growth of breast cancer cells and is inversely correlated with the disease progression and prognosis. *J Cancer Res Clin Oncol* 140(6), pp. 957-967. doi: 10.1007/s00432-014-1650-2

Ye, L., Sun, P. H., Sanders, A. J., Martin, T. A., Lane, J., Mason, M. D. and Jiang, W. G. 2014d. Therapeutic potential of capillary morphogenesis gene 2 extracellular vWA domain in tumour-related angiogenesis. *Int J Oncol* 45(4), pp. 1565-1573. doi: 10.3892/ijo.2014.2533

Yilmaz, M. and Christofori, G. 2009. EMT, the cytoskeleton, and cancer cell invasion. *Cancer Metastasis Rev* 28(1-2), pp. 15-33. doi: 10.1007/s10555-008-9169-0

Yin, M. et al. 2016. Tumor-associated macrophages drive spheroid formation during early transcoelomic metastasis of ovarian cancer. *J Clin Invest* 126(11), pp. 4157-4173. doi: 10.1172/JCI87252

Yu, Q., Toole, B. P. and Stamenkovic, I. 1997. Induction of apoptosis of metastatic mammary carcinoma cells in vivo by disruption of tumor cell surface CD44 function. *J Exp Med* 186(12), pp. 1985-1996. doi: 10.1084/jem.186.12.1985

Yu, X., Miyamoto, S. and Mekada, E. 2000. Integrin alpha 2 beta 1-dependent EGF receptor activation at cell-cell contact sites. *J Cell Sci* 113 (Pt 12), pp. 2139-2147. doi: 10.1242/jcs.113.12.2139

Yue, J., Zhang, K. and Chen, J. 2012. Role of integrins in regulating proteases to mediate extracellular matrix remodeling. *Cancer Microenviron* 5(3), pp. 275-283. doi: 10.1007/s12307-012-0101-3

Yurchenco, P. D. 2011. Basement membranes: cell scaffoldings and signaling platforms. *Cold Spring Harb Perspect Biol* 3(2), doi: 10.1101/cshperspect.a004911

Zarkavelis, G. et al. 2019. Genetic mapping of pancreatic cancer by targeted next-generation sequencing in a cohort of patients managed with nab-paclitaxel-based chemotherapy or agents targeting the EGFR axis: a retrospective analysis of the Hellenic Cooperative Oncology Group (HeCOG). *ESMO Open* 4(5), p. e000525. doi: 10.1136/esmoopen-2019-000525

Zawadzki, V., Perschl, A., Rosel, M., Hekele, A. and Zoller, M. 1998. Blockade of metastasis formation by CD44-receptor globulin. *Int J Cancer* 75(6), pp. 919-924. doi: 10.1002/(sici)1097-0215(19980316)75:6<919::aid-ijc15>3.0.co;2-y

Zee, Y. K. et al. 2010. Imaging angiogenesis of genitourinary tumors. *Nat Rev Urol* 7(2), pp. 69-82. doi: 10.1038/nrurol.2009.262

Zeng, C., Toole, B. P., Kinney, S. D., Kuo, J. W. and Stamenkovic, I. 1998. Inhibition of tumor

growth in vivo by hyaluronan oligomers. *Int J Cancer* 77(3), pp. 396-401. doi: 10.1002/(sici)1097-0215(19980729)77:3<396::aid-ijc15>3.0.co;2-6

Zeng, L. et al. 2022. Noncoding RNAs and hyperthermic intraperitoneal chemotherapy in advanced gastric cancer. *Bioengineered* 13(2), pp. 2623-2638. doi: 10.1080/21655979.2021.2021348

Zhang, L., Sanagapalli, S. and Stoita, A. 2018. Challenges in diagnosis of pancreatic cancer. *World J Gastroenterol* 24(19), pp. 2047-2060. doi: 10.3748/wjg.v24.i19.2047

Zhang, P., Goodrich, C., Fu, C. and Dong, C. 2014. Melanoma upregulates ICAM-1 expression on endothelial cells through engagement of tumor CD44 with endothelial E-selectin and activation of a PKCalpha-p38-SP-1 pathway. *FASEB J* 28(11), pp. 4591-4609. doi: 10.1096/fj.11-202747

Zhang, Y., Fang, Y., Ma, L., Xu, J., Lv, C., Deng, L. and Zhu, G. 2022. LINC00857 regulated by ZNF460 enhances the expression of CLDN12 by sponging miR-150-5p and recruiting SRSF1 for alternative splicing to promote epithelial-mesenchymal transformation of pancreatic adenocarcinoma cells. *RNA Biol* 19(1), pp. 548-559. doi: 10.1080/15476286.2021.1992995

Zhang, Z., Vuori, K., Reed, J. C. and Ruoslahti, E. 1995. The alpha 5 beta 1 integrin supports survival of cells on fibronectin and up-regulates Bcl-2 expression. *Proc Natl Acad Sci U S A* 92(13), pp. 6161-6165. doi: 10.1073/pnas.92.13.6161

Zhang, Z. et al. 2015. Anthrax Susceptibility: Human Genetic Polymorphisms Modulating ANTXR2 Expression. *Toxins (Basel)* 8(1), doi: 10.3390/toxins8010001

Zhao, Q., Barclay, M., Hilkens, J., Guo, X., Barrow, H., Rhodes, J. M. and Yu, L. G. 2010. Interaction between circulating galectin-3 and cancer-associated MUC1 enhances tumour cell homotypic aggregation and prevents anoikis. *Mol Cancer* 9, p. 154. doi: 10.1186/1476-4598-9-154

Zhao, X. and Guan, J. L. 2011. Focal adhesion kinase and its signaling pathways in cell migration and angiogenesis. *Adv Drug Deliv Rev* 63(8), pp. 610-615. doi: 10.1016/j.addr.2010.11.001

Zhong, H. et al. 1999. Overexpression of hypoxia-inducible factor 1alpha in common human cancers and their metastases. *Cancer Res* 59(22), pp. 5830-5835.

Zhou, W., Guo, S., Liu, M., Burow, M. E. and Wang, G. 2019. Targeting CXCL12/CXCR4 Axis in Tumor Immunotherapy. *Curr Med Chem* 26(17), pp. 3026-3041. doi: 10.2174/0929867324666170830111531

Zhu, Y., Zhang, H., Chen, N., Hao, J., Jin, H. and Ma, X. 2020. Diagnostic value of various liquid biopsy methods for pancreatic cancer: A systematic review and meta-analysis. *Medicine (Baltimore)* 99(3), p. e18581. doi: 10.1097/MD.0000000000018581

Ziprin, P., Alkhamesi, N. A., Ridgway, P. F., Peck, D. H. and Darzi, A. W. 2004. Tumour-expressed CD43 (sialophorin) mediates tumourmesothelial cell adhesion. *Biol Chem* 385(8), pp. 755-761. doi: 10.1515/BC.2004.092

Ziqian Fang, P. G., Bilal Al-Sarireh, Wen G Jiang, Lin Ye. 2021. Elevated expression level of capillary morphogenesis gene 2 in pancreatic ductal adenocarcinoma cell is associated with distant metastasis and poor prognosis. *British Journal of Surgery* Volume 108(znab282.006),

Zou, J., Xu, L., Ju, Y., Zhang, P., Wang, Y. and Zhang, B. 2014. Cholesterol depletion induces ANTXR2-dependent activation of MMP-2 via ERK1/2 phosphorylation in neuroglioma U251 cell. *Biochem Biophys Res Commun* 452(1), pp. 186-190. doi: 10.1016/j.bbrc.2014.06.001

Appendixes

Supplementary files for Chapter 6

Supplementary Table 6.1 Top 20 proteins upregulated in MiaPaCa-2 cell line with CMG2 overexpression (Change ratio>1.5, ranked by absolute change)

Proteins	MiaPaCa-2 pEF Mean	MiaPaCA-2 CMG2 exp Mean	Ratio	Absolute change	p value
AKAP12	16110.4	34537.37	2.143793	18426.97	1.58E-05
VCL	8285.5	16591.9	2.002522	8306.4	0.00016
MAP1B	9243.567	17395.13	1.881864	8151.567	4.1E-06
SPTAN1	10453.5	17272.43	1.652311	6818.933	8.25E-08
CALD1	2893.033	9688.2	3.348803	6795.167	8.12E-06
BASP1	4807.233	11317.7	2.354306	6510.467	0.001124
SPTBN1	8942	14878.4	1.663878	5936.4	1.54E-06
ACTN1	5132.267	9898.867	1.928751	4766.6	0.000103
MSN	8253.633	12768.1	1.546967	4514.467	1.12E-05
HEL-S-265	1859.067	5019.867	2.700208	3160.8	0.000605
ZYX	2839.533	5603.933	1.97354	2764.4	0.000165
ICAM1	2467.933	4825.1	1.955118	2357.167	0.000197
MYO1B	2074.2	4419.067	2.130492	2344.867	5.37E-07
TARS1	4039.9	6373.267	1.57758	2333.367	4.56E-05
CANX	4032.167	6347.433	1.574199	2315.267	0.002038
NSUN2	3730.433	5826.967	1.562008	2096.533	8.37E-05
AFG3L2	3338.033	5396.4	1.616641	2058.367	5.99E-05
NNMT	246.4333	2281.933	9.25984	2035.5	4.19E-05
CSRP1	1330.633	3202.333	2.406623	1871.7	7.09E-06
CAV1	1809.6	3674.767	2.030707	1865.167	0.001411
NASP	3209.567	5042.9	1.571209	1833.333	7.81E-05
OXCT1	1697.867	3499.1	2.06088	1801.233	4.12E-05
TRIO	2773.867	4557.167	1.642893	1783.3	6.7E-05
CAVIN1	2166.8	3894.467	1.797336	1727.667	0.003761
AKR1B1	2695.333	4377.533	1.624116	1682.2	1.23E-08
RAI14	2119.767	3785.267	1.7857	1665.5	3.7E-06
TUBB6	1003.233	2662.333	2.653753	1659.1	0.000624
ACSL4	2583.967	4185.5	1.619796	1601.533	0.000221
UAP1	1680.4	3237.6	1.926684	1557.2	4.15E-05
SOD2	1244.5	2714.433	2.181144	1469.933	0.00096

Supplementary Table 6.2 Top 30 proteins deregulated in ASPC-1 cell line with CMG2 knockdown (Change ratio< -0.7, ranked by absolute change)

	ASPC-1 ^{sc}	ASPC-1^{CMG2shRNA}			
Proteins	Mean	Mean	Ratio	Absolute change	p value
SORL1	2169.8333	1512.233333	0.696935	-657.6	5.92E-05
SQSTM1	2058.3667	1431.166667	0.695292	-627.2	0.000184
TYMP	1930.4667	1367.966667	0.70862	-562.5	0.010894
CTSH	1759	1200.666667	0.682585	-558.333	0.001146
QPRT	1261.7	815.9	0.646667	-445.8	6E-06
CKAP4	916.26667	495.4	0.540672	-420.867	1.21E-06
CAVIN2	1147.0667	798.1666667	0.695833	-348.9	0.002729
SOD2	910.96667	592.1666667	0.650042	-318.8	0.00149
SFXN3	1024.4667	721.6666667	0.704432	-302.8	0.000212
IGFBP1	979.1	685.6333333	0.700269	-293.467	0.000304
PTGIS	802.5	520.7333333	0.648889	-281.767	0.001446
FHL3	854.56667	588.1666667	0.688263	-266.4	0.000241
KRT80	699.3	442.0666667	0.632156	-257.233	0.001808
OXCT1	500.23333	273.4	0.546545	-226.833	0.002738
UNC13D	636.16667	441.0333333	0.693267	-195.133	0.000583
DEPTOR	476.03333	289.1	0.60731	-186.933	0.001933
FAM83A	587.16667	407.7333333	0.694408	-179.433	0.000629
PFN3	537.23333	373.7	0.695601	-163.533	0.021342
GPX1	401.13333	249.5333333	0.622071	-151.6	0.00023
PODXL	449.4	303.6666667	0.675716	-145.733	0.016279
PLEKHO2	416.6	292.8	0.702832	-123.8	0.000597
SHROOM2	366.5	244.5333333	0.667212	-121.967	0.00175
KRT23	316.33333	203.8666667	0.644468	-112.467	0.000635
KRT15	205.46667	111.7666667	0.543965	-93.7	0.002618
PTGES	271.7	189	0.69562	-82.7	0.000848
TPRG1L	261.9	181.6666667	0.693649	-80.2333	0.005727
KHDRBS1	246.33333	174.2	0.707172	-72.1333	0.003721
ENO2	179.56667	113.8333333	0.633934	-65.7333	0.001513
TPRN	216.23333	151.5333333	0.700786	-64.7	0.001105
SLPI	192.7	128.1666667	0.66511	-64.5333	0.000335
TAF4B	160.8	97.43333333	0.605929	-63.3667	0.004789

Supplementary Table 6.3: Top 30 proteins CMG2 positively correlated proteins in both MiaPaCa-2 and ASPC-1 cell lines, ranked by absolute change

		MiaPaCa-2^{CMG2exp}	ASPC-1^{CMG2shRNA}
Proteins	Absolute change	Ratio	Ratio
VCL	9220.9	2.002522479	0.909131257
MYH9	7761.033333	1.145661177	0.918560604
IQGAP1	5252.133333	1.351471931	0.885811662
ACTN1	4774.766667	1.928751429	0.641812865
FLNB	3928.166667	1.123260668	0.973836799
TPM3	2623.433333	1.416367641	0.923977863
TARS1	2610.833333	1.577580303	0.920695864
ITPR3	2495.566667	1.283789522	0.927757119
MYO1C	2460.8	1.385880445	0.883817981
PGK1	2350.166667	1.260182887	0.979407334
IMMT	2084.566667	1.249552484	0.956506628
TRIO	2048.233333	1.642893194	0.881396147
OXCT1	2028.066667	2.06088032	0.546544946
SOD2	1788.733333	2.181143699	0.65004208
PSAP	1720.1	1.497385706	0.857048434
RAI14	1713.533333	1.785699684	0.933354916
SMC3	1649.366667	1.300520719	0.887891015
STMN1	1602.133333	1.097287641	0.835739988
HADHA	1576.033333	1.091545632	0.829926881
GPD2	1520.366667	1.353680231	0.771104947
L1CAM	1483.9	2.531123572	0.816247323
HK1	1483.666667	1.136633577	0.782584076
NIBAN1	1424.133333	2.023957503	0.860426215
P4HA1	1416.933333	1.660358016	0.839137497
STK10	1372.8	1.988093208	0.888490897
HNRNPUL2	1289.1	1.07595684	0.896550945
ECHS1	1263.366667	1.392549665	0.813960954
VAT1	1249.466667	1.147786828	0.77579758
TUBB3	1224.266667	1.205128534	0.92199569
NUP155	1203.966667	1.519852248	0.939271901

Supplementary Table 6.4: Top 30 proteins CMG2 positively correlated proteins in PANC-1^{CMG2rib} cell line, ranked by absolute change

Protein Name	Mean	Mean	Absolute change	%CFC
mTOR	23390.86	14753.8	-8637.06	-37.13
Bcl-XL	20275.06	12484.27	-7790.79	-38.62
ALK	30861.99	23564.89	-7297.1	-23.89
MKK4	24234.09	17382.7	-6851.39	-28.5
Hsc70	15576.22	9516.31	-6059.91	-39.1
STAT5B	8887.92	5147.43	-3740.49	-42.27
CDK5	11303.67	8767.57	-2536.1	-22.68
Bid	9067.77	6622.06	-2445.71	-27.2
PP1	10935.72	8715.04	-2220.68	-20.56
PP4C	9691.71	7696.73	-1994.98	-20.84
Hsp40	7852.19	5914.06	-1938.13	-24.92
A-Raf	9115.26	7218.24	-1897.02	-21.06
Hsp105	4238.93	2715.42	-1523.51	-36.14
Bcl-xS	7217.77	5792.11	-1425.66	-20.01
NFkappaB p50	6748.55	5384.31	-1364.24	-20.47
STAT6	6512.11	5191.11	-1321	-20.54
Cdc2 p34	3464.34	2483.94	-980.4	-28.53
PAK1	4143.45	3201.84	-941.61	-22.97
MEKK2	4178.46	3272.43	-906.03	-21.93
KAP	3513.89	2778.6	-735.29	-21.18
STI1	960.53	323.48	-637.05	-66.43
Smad2	1069.11	506.14	-562.97	-52.81
IKKg	951.25	423.73	-527.52	-55.6
Cdc25B	2364.02	1855.76	-508.26	-21.75
Abl	1377	880.17	-496.83	-36.28
PITSLRE	2191.88	1731.42	-460.46	-21.26
Lck	666.09	375.82	-290.27	-43.76
ROCK-I	718.51	444.1	-274.41	-38.39
Jun	647.25	430.07	-217.18	-33.77
PKCt	1020.6	815.84	-204.76	-20.32

Supplementary Table 6.5: Top 30 Dephosphorylated proteins in PANC-1 $^{CMG2\ rib}$ cell line (Ranked by absolute change)

Proteins	PANC-1 pEF Abundancy	PANC-1 CMG2 rib Abundancy	Absolute change	CFC%
MEK2	19977.66678	14591.8131	-5385.853678	-27.19154477
PKA Ca/b	14599.56058	11373.96876	-3225.591812	-22.34139764
Kit	13996.08601	11011.76988	-2984.316131	-21.57259457
PKCg	11693.62536	8896.482085	-2797.143277	-24.16207251
WNK1	12836.65899	10391.83812	-2444.820876	-19.30294386
4G10	7017.033129	4602.496196	-2414.536932	-34.61814552
Lck	15050.57931	12649.02545	-2401.553854	-16.22370047
Cortactin	13582.86567	11333.79401	-2249.071668	-16.82338684
ICK	8610.374132	6998.117414	-1612.256718	-18.98293134
PDGFRb	4059.960172	2471.311107	-1588.649065	-39.32315774
ALK	9097.838065	7576.935339	-1520.902726	-16.98191676
Rb	1160.550221	602.4782822	-558.071939	-48.25185564
Akt1 (PKBa)	2815.116382	2262.837469	-552.2789127	-19.87383986
PYK	1819.612541	1271.251177	-548.3613643	-30.35823491
STAT3	1981.615581	1540.454257	-441.1613242	-22.50981073
Tau	1138.150382	781.5162178	-356.6341641	-31.55280272
FAK	899.015517	637.5015135	-261.5140035	-29.31433375
Paxillin 1	724.9835279	603.0104278	-121.9731	-17.08864618
EGFR	644.0221222	535.1506813	-108.8714409	-17.1690542
PAK1/2/3	549.0207026	448.9699211	-100.0507814	-18.4834392
STAT1	487.2981273	393.4076575	-93.89046979	-19.52418382
eIF4E	259.4273649	181.2246516	-78.20271331	-30.36640577
HDAC4/5/9	494.3475514	416.321222	-78.0263294	-16.05139463
Smad2	334.1202388	260.098471	-74.02176772	-22.40167632
Met	342.747493	270.7234963	-72.02399673	-21.26479065
Histone H2A.X	379.6580209	317.4047414	-62.25327955	-16.66294411
Catenin a	173.0371539	120.738923	-52.29823084	-

				30.44549602
PKCt	180.9851389	129.1951194	-51.79001942	-28.84252715
IRS1	164.4847797	117.8188298	-46.66594989	-28.59866847
PKCm (PKD)	280.41518	233.8131603	-46.60201965	-16.88397684

Supplementary Table 6.6: Top 20 proteins down-regulated in MiaPaCa-2 cell line with CMG2 overexpression (Change ratio<0.5, ranked by absolute change)

	MiaPaCa-2 ^{pEF}	MiaPaCA-2 $^{CMG2\ exp}$			
Proteins	Mean	Mean	Ratio	Absolute change	P value
DYNC1H1	26240.03	11703.9	0.446032	-14536.1	6.61E-06
AHNAK2	15062.23	7043.133	0.467602	-8019.1	5E-06
HUWE1	8653.033	3963.767	0.458078	-4689.27	7.89E-07
DSP	7245.767	3323.533	0.458686	-3922.23	8.39E-06
ST13	5202.3	2355.9	0.452857	-2846.4	2.77E-06
MAGED2	4254.267	1874.4	0.440593	-2379.87	1.6E-06
ALDH3A2	3407.933	1284.4	0.376885	-2123.53	5.64E-05
FKBP10	3409.967	1304.8	0.382643	-2105.17	0.000141
DYNC1I2	4099.733	2001.233	0.488137	-2098.5	5.12E-07
NAP1L1	3735.133	1687.333	0.451746	-2047.8	0.000231
PODXL	2074.333	93.9	0.045268	-1980.43	6.69E-05
YA61	2652	1028.767	0.387921	-1623.23	0.000192
DYNC1LI2	2872.333	1424.933	0.496089	-1447.4	4.08E-05
KRT80	1778.1	336.7333	0.189378	-1441.37	1.21E-08
KIF11	2549.667	1148.933	0.450621	-1400.73	3.17E-05
ITGB4	2335.867	981.1667	0.420044	-1354.7	0.000108
APP	2375	1068.567	0.449923	-1306.43	0.000348
derp12	1713.6	574.4	0.335201	-1139.2	0.000203
HMGN5	1494.567	444.8	0.297611	-1049.77	5.21E-07
GOT1	1993.133	966.2	0.484764	-1026.93	1.53E-06

Supplementary Table 6.7: Top 20 proteins deregulated in ASPC-1 cell line with CMG2 knockdown (Change ratio> 1.4, ranked by absolute change)

	ASPC-1 ^{sc}	ASPC-1 $^{CMG2\ shRNA}$			
Proteins	Mean	Mean	Ratio	Absolute change	P value
ANPEP	1872.767	3321.9	1.773793	1449.133	0.000661
KRT9	1295.8	2261.933	1.745588	966.1333	0.028107
PSMD14	988.5667	1465.2	1.482146	476.6333	0.004586
UBXN4	960.8333	1383.567	1.439965	422.7333	0.041325
ALDH1A1	707.0667	1082.933	1.531586	375.8667	0.000448
UMPS	817.2333	1165.467	1.426112	348.2333	0.003448
MTUS1	791.2	1138.333	1.438743	347.1333	0.004422
NCEH1	725.0333	1062.867	1.465956	337.8333	0.001065
MUC13	662.3667	996.1667	1.50395	333.8	0.010542
MUC17	603.3	919.4	1.523952	316.1	0.002278
SCIN	470.8333	771.2667	1.638088	300.4333	0.00203
H1-3	696.1333	980.9	1.409069	284.7667	0.029033
ATAD2	538.9333	820.7333	1.522885	281.8	0.003344
GPC1	408.0667	636.0667	1.558732	228	0.003773
LEO1	337.2	564.4667	1.673982	227.2667	0.020632
SDCBP	367.8	581.1	1.579935	213.3	1.26E-05
NUDT12	377.6	586.0667	1.552083	208.4667	0.006356
MRPL57	372.3	578.6333	1.554213	206.3333	0.011413
IFNGR1	245.6	433.9667	1.766965	188.3667	0.027205
DCD	188.3	365.6667	1.941937	177.3667	0.026108

Supplementary Table 6.8: Top 30 proteins CMG2 inversely correlated proteins in both MiaPaCa-2 and ASPC-1 cell lines, ranked by absolute change

		MiaPaCa-2^{CMG2exp}	ASPC-1^{CMG2sh6}
Proteins	Absolute change	Ratio	Ratio
DSP	-5936.2	0.458686	1.177482
KRT8	-5917.4333	0.576927	1.043344
RRBP1	-4151.5333	0.661973	1.053808
CSE1L	-3501.4	0.71075	1.10814
PKM2	-2978.0667	0.823931	1.055698
TOP2A	-2965.4667	0.684605	1.216842
H2BC21	-2763.9	0.939933	1.243756
TKT	-2428.5333	0.776438	1.103928
SNRNP200	-2376.8333	0.75925	1.038952
GLG1	-2350.4333	0.637166	1.158862
HSPH1	-2248.6333	0.657908	1.0272
SMC2	-2166.4	0.754481	1.137237
EEF2	-2163.7333	0.825645	1.028983
FASN	-2124.2667	0.8124	1.082333
FSCN1	-2039.8	0.626773	1.196099
TGM2	-1977.1333	0.834739	1.230048
TOP2B	-1965.8667	0.772562	1.137029
RECQL	-1949.0667	0.634458	1.073347
NCL	-1926	0.914181	1.050646
MISP	-1639.1667	0.324708	1.208875
EIF5	-1573.6333	0.602729	1.141456
GPI	-1503.8333	0.792277	1.055941
FKBP4	-1485.8333	0.650218	1.166093
PRPF6	-1473.4667	0.731091	1.05546
PARP1	-1340.8	0.958872	1.337441
RRM1	-1262.2	0.523141	1.067632
SCP2	-1245.9667	0.62469	1.081864
IPO7	-1172.1	0.68138	1.036274
CSDE1	-1170.6333	0.746437	1.060064
HMGN5	-1104.3333	0.297611	1.426191

Supplementary Table 6.9: Top 20 proteins CMG2 inversely correlated proteins in PANC-1 cell line

	PANC ^{pEF}	PANC-1 $^{CMG2\ rib}$		
Proteins	Mean	Mean	Absolute change	%CFC
CK1e	21945.03	27741.88	5796.85	26.01
JAK1	11418.72	16021.31	4602.59	39.86
AurKC	12828.67	17373.55	4544.88	35
Akt3	24778.89	28681.36	3902.47	15.38
DUSP2	26445.36	29183.64	2738.28	10
WNK2	3882.46	6217.77	2335.31	59.64
SOCS2	6422.71	8358.89	1936.18	29.73
GCK	3513.01	5318.34	1805.33	50.91
Kit	8310.19	10113.07	1802.88	21.31
Cyclin A	12043.2	13737.05	1693.85	13.7
Calnexin	12693.06	14310	1616.94	12.38
APG2	11306.97	12892.87	1585.9	13.66
WNK1	12374.29	13787.6	1413.31	11.07
GNB2L1	5740.84	7137.46	1396.62	23.93
p107	5374.16	6676.68	1302.52	23.84
VGFR1	11511.75	12810.69	1298.94	10.93
SODD	7264.34	8155.81	891.47	11.92
DUSP10	5165.71	5969.29	803.58	15.19
AurKB	4802.56	5572.05	769.49	15.65
ErbB3	7266.89	8023.96	757.07	10.07

Supplementary Table 6.10: Proteins whose phosphorylation state was inversely correlated with CMG2 in both MiaPaCa-2 and ASPC-1 cell lines

Proteins	Log Fc
Adjusted phosphorylation	
SQSTM1	-1.27146
EIF4G2	-1.11086
NASP	-1.03472
LMNA	-1.02616
PRPF40A	-0.95064
LARP1	-0.81309
BCL9L	-0.80241
MYO1E	-0.79617
TJP2	-0.72122
MLLT1	-0.69298
KMT2B	-0.67552
AHNAK	-0.66761
TCOF1	-0.66346
HMGA1	-0.61555
EPB41L1	-0.55917
FLNA	-0.55567
CANX	-0.54125
EIF4G1	-0.54019
LMNB2	-0.529
MRC2	-0.52237
Un-adjusted phosphorylation	
MISP	-2.60183
KRT8	-2.06839
PKP2	-2.00268
MARCKS	-1.9926
DSP	-1.95896
LARP1	-1.93659
BCL9L	-1.92038
SNX17	-1.91166
EIF4G2	-1.90851
PDXDC1	-1.59443
EIF4G1	-1.59273
EIF4B	-1.58826
DUT	-1.58286
HMGA1	-1.54124
MARCKSL1	-1.44944

ABCA7	-1.43111
IRF2BP2	-1.41328
VILL	-1.38068
HTATSF1	-1.35591
CBX8	-1.33829

Supplementary Table 6.11: Proteins whose phosphorylation state was inversely correlated with CMG2 in PANC-1 cell line

	PANC-1 pEF	PANC-1 CMG2 rib		
Target Protein Name	Abundancy	Abundancy	Absolute change	CFC%
JAK1	176.7062775	435.751245	259.0449675	145.8125102
TrkB	220.1153261	352.521881	132.4065546	59.64419058
MARCKS	105.4150985	163.386594	57.97149525	54.50086786
Cyclin B1	466.2996151	698.300269	232.0006539	49.27754211
PCTK2	7293.934294	10736.2258	3442.291479	46.72601158
CDK6	195.5065246	274.426157	78.91963194	39.92057168
RelB	441.1987446	612.589049	171.3903045	38.4051608
Vimentin	101.8689921	140.817359	38.94836663	37.79438101
CDC7	5305.279986	7316.51713	2011.237148	37.47173334
CDK11A	10629.39766	14429.9872	3800.589515	35.32393365
MDM2	2036.738013	2750.67414	713.9361313	34.62363088
Nek2	9242.00895	12228.0088	2985.999878	31.88842506
Progesterone Receptor	100.069196	131.202963	31.13376697	30.69547627
PAK1	1373.792626	1798.41967	424.6270475	30.49299148
NMDAR2B	80.20190783	102.98583	22.78392169	28.00003708
GSK3a/b	219.9976574	281.482676	61.48501844	27.54132894
PKCe	339.5223012	434.25766	94.73535853	27.495984
Rad17	154.359924	195.315331	40.95540716	26.130205
GATA1	195.5787304	246.22691	50.64817991	25.49638512
eIF4B	233.1765504	293.337449	60.16089894	25.40070023

Supplementary files for Chapter 7

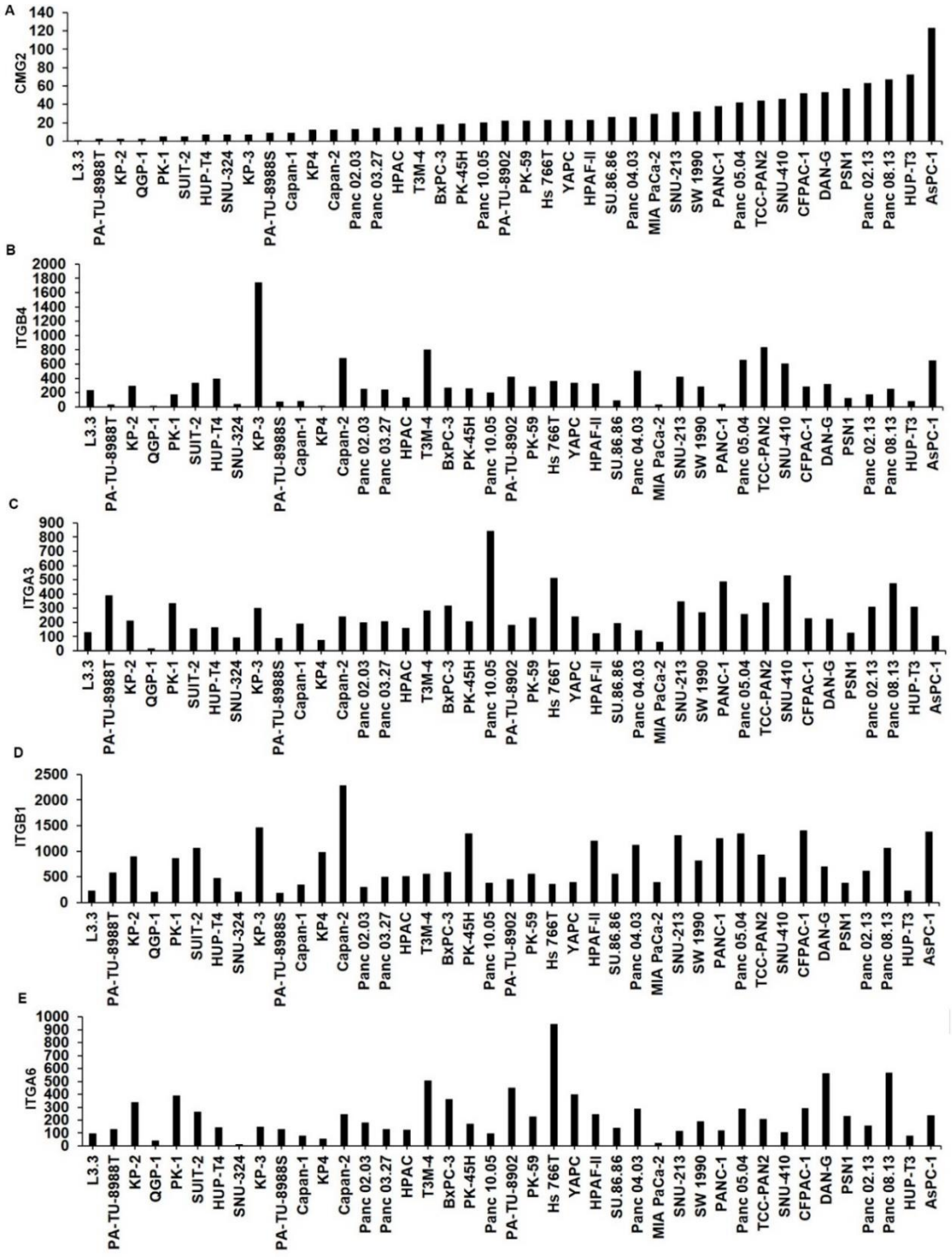

Supplementary Figure 7.1 Cell-cell adhesion molecules expression in pancreatic cancer cell lines with different CMG2 expression. Shown are the expression level of CMG2 (A), ITGB4 (B), ITGA3 (C), ITGB1 (D) and ITGA6 (E) in E-MTAB-2770 cohort.

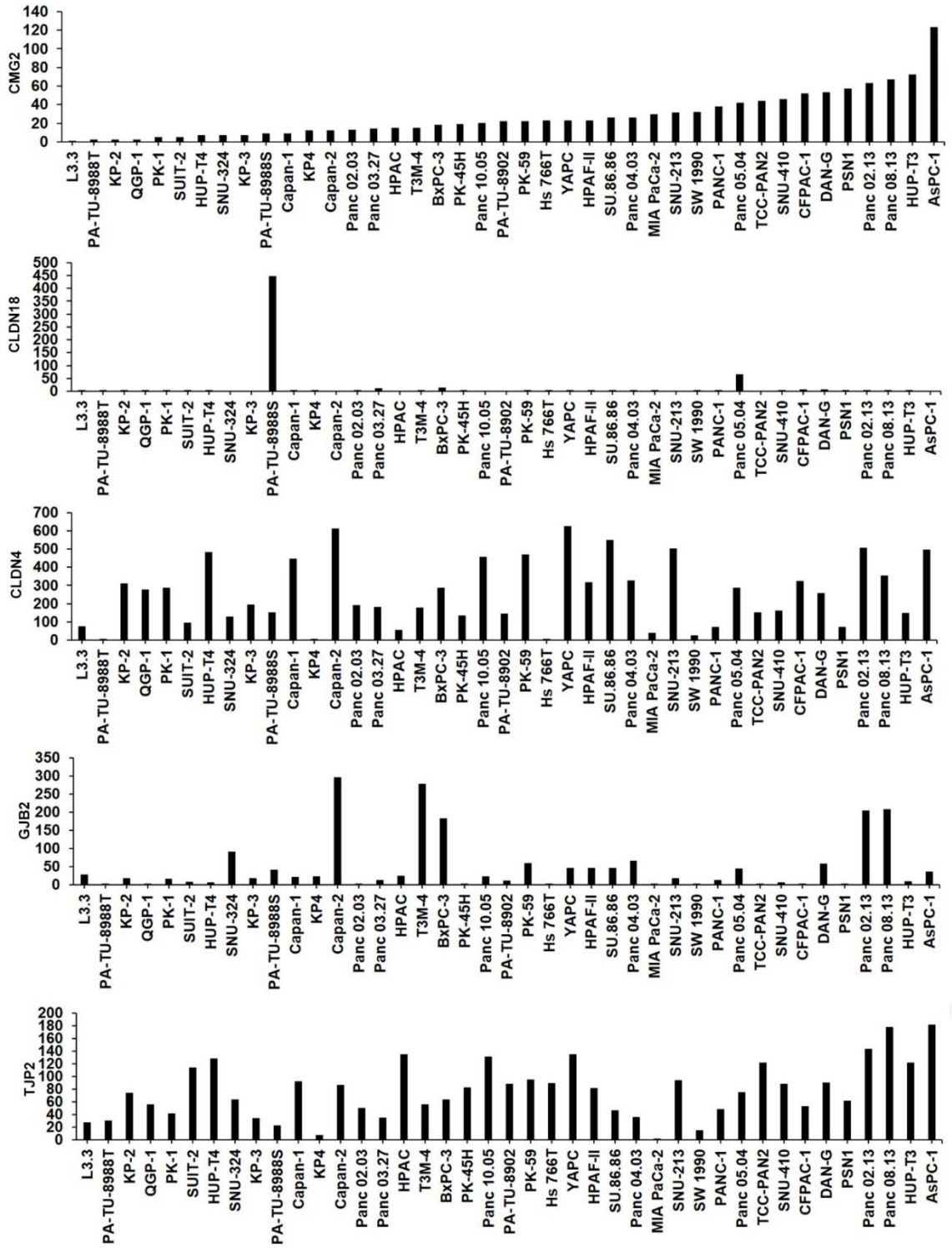

Supplementary Figure 7.2 Cell-cell adhesion molecules expression in pancreatic cancer cell lines with different CMG2 expression. Shown are the expression level of CMG2 (A), CLDN18 (B), CLDN4 (C), GJB2 (D) and TJP2 (E) in E-MTAB-2770 cohort.

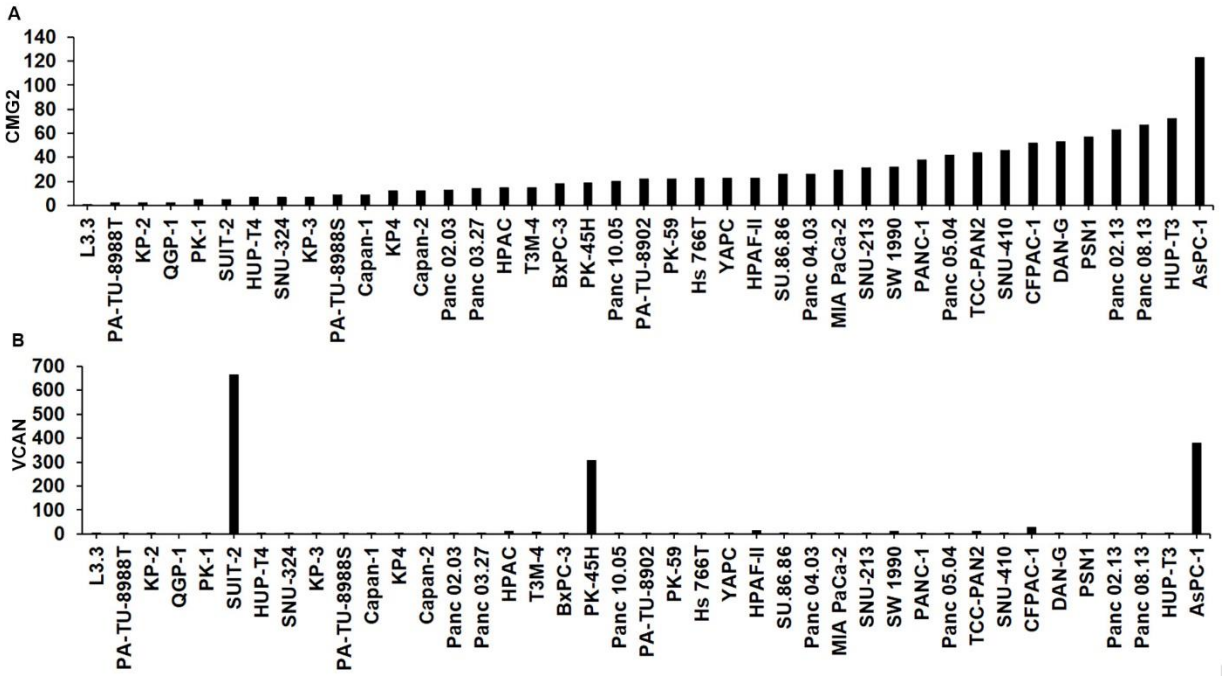

Supplementary Figure 7.3 HA interacting molecules expression in pancreatic cancer cell lines with different CMG2 expression. The expression level of CMG2 (A), and VCAN (B) in the E-MTAB-2770 cohort are shown